CECW-EH-D	Department of the Army U.S. Army Corps of Engineers Washington, DC 20314-1000	EM 1110-2-1502
Engineer Manual 1110-2-1502		20 August 1992
	Engineering and Design COASTAL LITTORAL TRANSPORT	
	Distribution Restriction Statement Approved for public release; distribution is unlimited.	

DEPARTMENT OF THE ARMY
U.S. Army Corps of Engineers
Washington, D.C. 20314-1000

EM 1110-2-1502

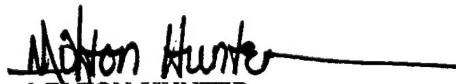Engineer Manual
No. 1110-2-1502

20 August 1992

Engineering and Design
COASTAL LITTORAL TRANSPORT

1. Purpose. This manual provides current guidance, engineering procedures, and case study examples for coastal problems involving nearshore sediment transport processes.

2. Applicability. This manual applies to HQUSACE/OCE elements, major subordinate commands, districts, laboratories, and field operating activities (FOA) having responsibility for design, construction, and operation of civil works projects within the nearshore coastal region.

3. General. This manual describes the forces controlling coastal littoral transport, and presents methods and techniques for determining sediment transport rates. Several case studies are described illustrating application of the methods discussed. The methodologies and examples presented in this manual serve to transfer the technical knowledge obtained from recent research efforts to FOAs.

FOR THE COMMANDER:

MILTON HUNTER
Colonel, Corps of Engineers
Chief of Staff

Engineering and Design
COASTAL LITTORAL TRANSPORT

Table of Contents

Chapter 1
Introduction

1-1. Purpose

This manual assembles into a single source the current practice in coastal engineering with respect to estimating nearshore wave characteristics, longshore currents, and longshore sand transport rates including a section describing littoral budget methodology. This manual draws upon a large number of sources to present techniques for evaluating these nearshore phenomena. The design engineer is expected to adopt general guidance presented in this manual to site-specific projects; deviations from this guidance are acceptable if adequately substantiated.

1-2. Applicability

This manual applies to all HQUSACE elements and USACE Commands having civil works engineering and design responsibilities.

1-3. References

Required and related publications are listed in Appendix A.

1-4. Objective

This manual presents a method for estimating the significant physical parameters and resulting longshore current and sediment transport under natural conditions at coastal sites.

1-5. Background

The beach is the natural buffer between the land and the sea. It is a highly dynamic zone which responds to storms, seasonal variations, and long-term events such as an El Nino, sea level rise, and land subsidence. Its condition is also controlled by the source and supply of beach materials. Problems frequently arise when human activities attempt to fix the location of this dynamic boundary or alter sediment transport processes in its vicinity. Thus, both natural and human-induced actions produce changes in the beach which are addressed in coastal engineering practice.

1-6. Scope

This manual details orthodox methods presently practiced in coastal engineering for estimating longshore sand transport and littoral budgets. Sufficient introductory material and discussion of the methods are provided to enable a person with an engineering background to obtain an understanding of these coastal processes. The manual includes detailed descriptions of applicable methods, techniques, useful data, and worked examples to illustrate typical approaches.

1-7. Overview of Manual

The manual is divided into seven chapters. Chapter 1 provides a manual overview. Chapter 2 presents an introductory discussion of nearshore concepts. Chapter 3 develops a background on waves and presents techniques for estimating the wave climate. Chapter 4 is a discussion of littoral processes. Chapters 5 and 6 present methods for estimating longshore currents and sediment transport, respectively. In Chapter 7, two example littoral budget calculations are presented. There are also five appendixes: a reference list of required and related publications, a list of notation, a glossary of coastal engineering terminology, a table of unit conversions, and a list of computer programs relevant to wave, current, and sand transport problems that are available from the U.S. Army Engineer Waterways Experiment Station's Coastal Engineering Research Center (CERC).

Chapter 2
Definitions and Concepts

2-1. Overview

This chapter gives an integrated overview of major concepts and processes detailed in the chapters that follow. Appendix C is a glossary that can be consulted to review unfamiliar terminology.

2-2. Nearshore Region

a. Processes. The littoral zone is the dynamic interface between the ocean and the land. Bounded on one side by the landward limit of the beach and extending seaward to just beyond the zone of wave breaking, it is the region where wave energy dissipates over a distance of tens to hundreds of meters. Beaches are molded into characteristic forms according to various governing parameters, including rates of wave energy dissipation and momentum transfer, and sediment permeability and fall velocity. A dynamic balance is established between processes and morphology in which the beach, waves, and currents interact. Natural variability in littoral processes, such as in wave height, period, and direction, or the rate that littoral material is supplied to a region, are responsible for beach changes. Modifications to the system such as changing wave conditions, introduction of engineering structures, and altered quantity or type of sediment all cause the dynamic balance to readjust. Rapid and undesired beach changes have been caused by some coastal engineering works. A methodology is provided herein for analyzing the effects of proposed engineering activities on the littoral zone in order to achieve the most desirable solution within project objectives.

b. Littoral materials. The geology of the coast and of the source area of littoral materials ultimately determines the prevalent shape of the shore at a specific locality. Rocky shores are exposed where there is no supply of beach material or the transport out of the region exceeds the sediment input. Gravel beaches, also known as shingle beaches, exist in areas where the only material supplied is coarse, or may develop as a lag deposit in the presence of vigorous wave activity. Some shores are composed of mud and receive such a small amount of incident wave energy that they are termed zero-energy coastlines. However, the focus of this manual is on sandy beaches, those composed of materials in the approximate range of 0.15 mm to 2.0 mm in diameter. About a third of the exposed shorelines of the United States, excluding Alaska, are comprised of unconsolidated materials, and these beaches typically receive the greatest commercial, private, and recreational usage. Primary sources of beach sand are the erosion of upland areas and bluffs and biogenic production. Under some conditions sand may move onshore from submerged deposits. Calcium carbonate sands produced in shallow tropical seas are often moved onshore to create beaches in this manner.

c. Morphologic features. In cross-section the sandy beach profile can be divided into zones according to morphologic features, as shown in Figure 2-1. Beaches are often backed by dunes. Seaward of the dunes is the littoral zone, consisting of the backshore which is rarely submerged; the foreshore, which extends from the limit of uprush of waves at high tide to the backrush of waves at low tide; and the inshore, where energy of spilling and plunging breakers is dissipated. The offshore is separated from the inshore by the location of wave breaking and is included in the littoral zone to the extent that significant littoral processes occur. The backshore is a relatively flat area or consists of flat areas separated by beach scarps. The berm crest separates the berm from the more steeply sloping foreshore.

d. Wave processes. In terms of wave processes, the littoral zone is divided into the offshore and nearshore zones (Figure 2-2). Within the nearshore zone, waves become unstable and begin to break in the breaker zone. Broken waves propagate as bores in the surf zone. The limits of water oscillation on the beach face define the swash zone.

e. Beach profiles. A sandy beach tends toward an equilibrium profile for swell waves. This equilibrium profile, called a summer or swell profile, has been the subject of much field and laboratory investigation and occurs when the depth increases exponentially with distance from shore. Under certain combinations of wave height, period, and sand fall velocity, the profile develops a shore-parallel bar at the location of wave breaking. A trough just shoreward of the bar or under the plunge point of the breaker is also common. If waves reform after initial breaking to break a second time, the nearshore zone may contain multiple bar-trough systems. This profile is called the storm profile or winter profile. The size and location of the bar and trough are related to wave height and period. As a longshore bar grows, its location shifts, as does the wave break point. Material forming the bar is removed
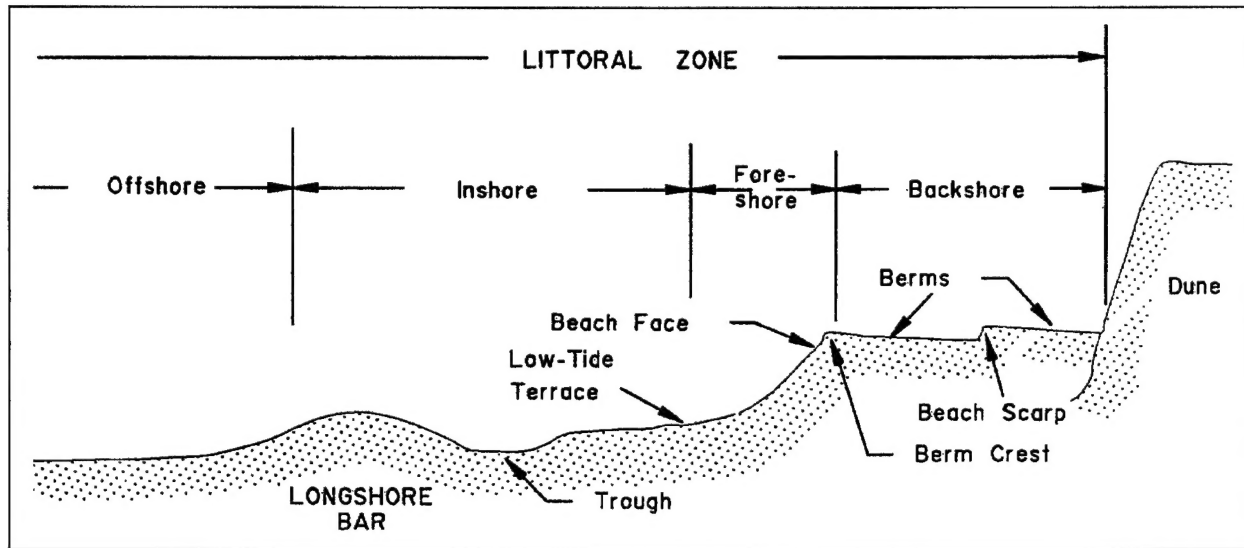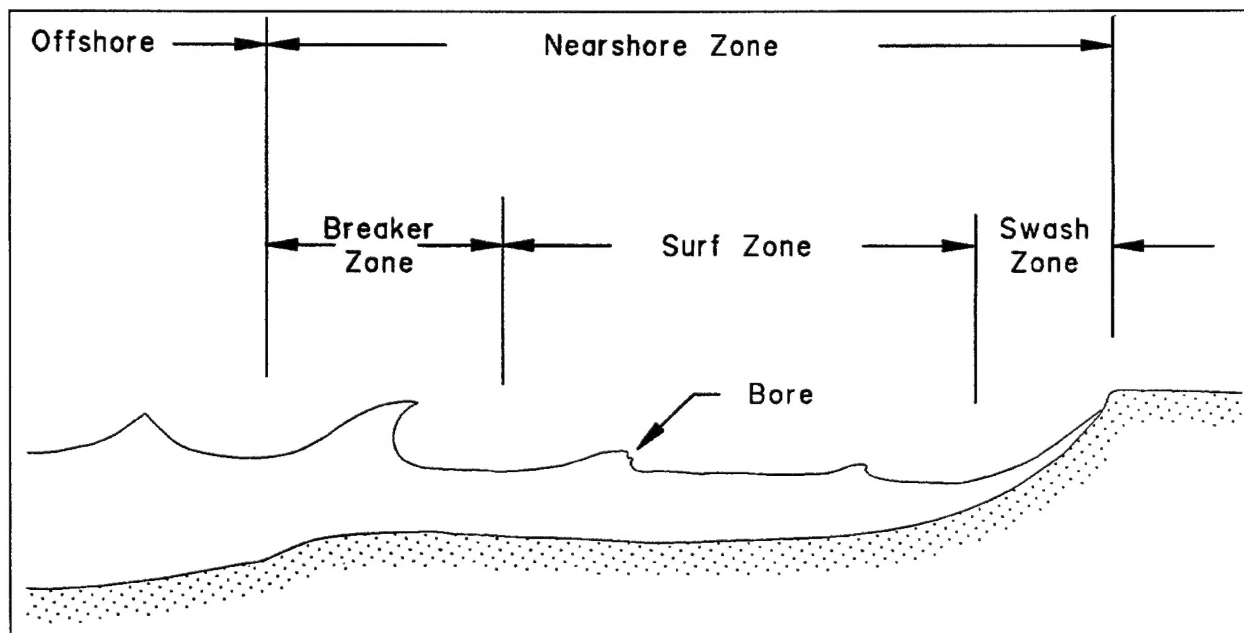
Figure 2-1. Beach profile terminology

Figure 2-2. Nearshore wave processes terminology

from the beach face and berm. Significant longshore transport takes place on the longshore bar. Sand from the bar is returned to the upper profile with the return of swell waves.

f. Geomorphic features. Much of the low-lying sandy coastline in the United States is associated with barrier islands. Barrier islands are shore-parallel, linear features. They have lagoons and back bays and are interrupted by inlets or passes. The ocean beaches have a mild slope which causes waves to break offshore, dissipating their energy over a wide surf zone. Another type of linear feature is a spit, which usually grows in the direction of longshore transport from a more stable land form.

g. Cuspate features. A variety of cuspate features are observed in the littoral zone, including beach cusps, crescentic bars, and cuspate forelands. Beach cusps are an alongshore series of horns separated by embayments in the swash zone. Beach cusps point seaward and their spacings may range from 1 to 60 meters. Crescentic bars lie seaward of the low-water position with the concave sides facing the beach and are spaced at 100 meters (m) to 2000 meters. Cuspate forelands are found in elongate water bodies and on outer coasts facing crescentic bars. A cell circulation pattern with a single rip current can develop within these cuspate features (Figure 2-3a). At other times several rip currents may be present within the outer crescentic bar, cresting a segmented linear inner bar (Figure 2-3b). The inner bars and shoals align with approaching wave crests. If waves change to arrive at an oblique angle to the beach, the shoals, rip currents, and troughs also rotate and may form sand waves or transverse bars (Figure 2-4).

h. Plan-view response. If alongshore-moving material encounters a relatively impermeable littoral barrier, an accumulation forms, called a fillet. The shoreline tends to become oriented with incident wave crests to establish a uniform longshore transport rate. An embayment downdrift of a promontory that partially blocks transport develops a spiral shape in response to the wave refraction and diffraction at the promontory. Beaches completely confined by littoral barriers and of relatively short along-coast extent are termed pocket beaches.

i. Wave parameters. Waves are the single most important forcing mechanism in nearshore physical processes. Waves in the littoral zone are very complex
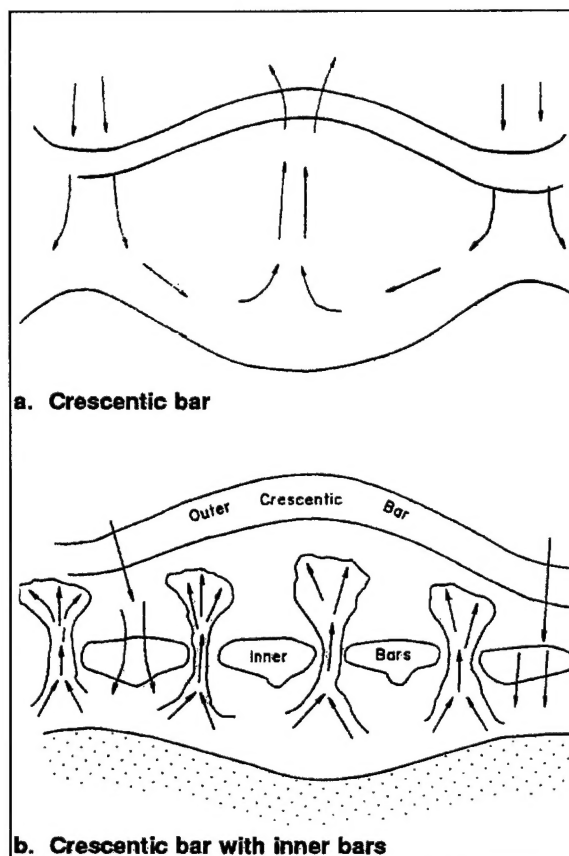
Figure 2-3. Cell circulation patterns due to various morphologies

and a number of theories involving different levels of approximation have been developed. The most commonly used is linear wave theory, which characterizes a single wave by its height, length, and period. Wave height is the vertical distance between crest and trough, and amplitude is that between the still-water level and the crest or trough. Wavelength of a single wave is the horizontal distance between adjacent wave forms, often taken as the point of zero downcrossing (where the water surface intersects the still-water line). Wave period is the length of time for adjacent wave forms to pass a fixed point. Wave frequency is the inverse of period. Linear waves are symmetrical about the still-water level, and the wave height is assumed small with respect to the length. Neither of these assumptions is valid in the littoral zone. Nevertheless, many quantities derived using linear wave theory in shallow water are useful in nearshore process calculations. In linear wave theory, wavelength can be computed from knowledge of the wave period and water depth. Thus the true

a. Shore-normal wave approach

b. Oblique wave approach
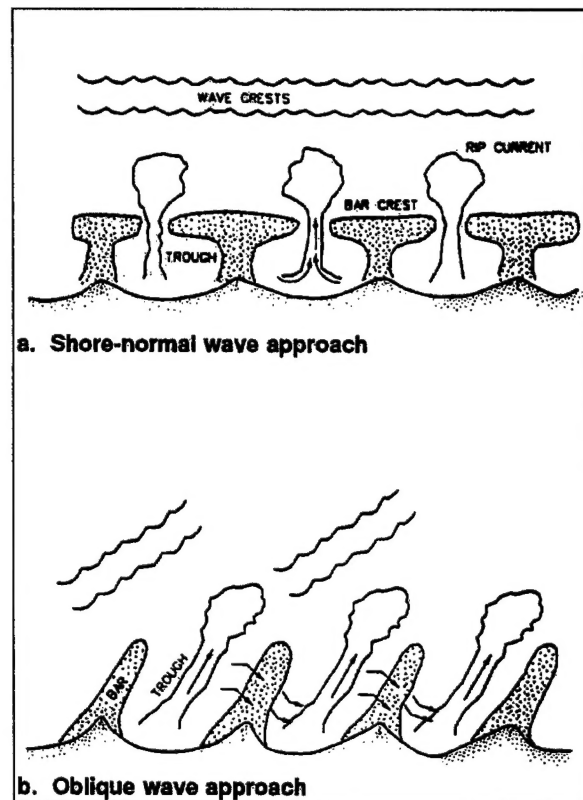
Figure 2-4. Inner bars and troughs as a function of wave direction

fundamental variables are wave height, wave period, and water depth.

2-3. Littoral Zone Dynamics

Water circulation in the littoral zone results from a combination of oceanographic currents, tidal currents, wave-induced currents, and wind-induced currents. Sediment will move in the direction of the current, and circulation currents caused by breaking waves are typically the most important to littoral transport. Therefore, the discussion of circulation is limited to that generated by waves. When waves propagate into the surf zone and break, their momentum is transferred in part to changing the water level and generation of currents. The shore-normal gradient in the momentum flux is balanced by a displacement of the mean free surface, termed wave setup and setdown.

   a. Longshore current. If waves break at an oblique angle to the shoreline, a longshore current is generated by the gradient of momentum flux in the surf zone. A

gradient in breaker height may be created by a particular wave transformation pattern or by wave blocking by some structure or land mass. The result is a differential setup which drives a current in the direction of the lower wave height. The longshore current is primarily confined to the surf zone with a maximum value near the midsurf position.

   b. Sand transport. Sand transport in the nearshore may be as bed load or suspended load. The relative importance of these modes varies depending on the sediment and wave conditions. Suspended load is that part maintained above the bed by fluid turbulence. Bed load is that part maintained in a dispersive state by grain-to-grain collisions. The longshore sand transport rate is computed using an empirical relationship between volumetric transport rate and the longshore component of wave energy flux evaluated at the breaker zone. Wave energy flux is calculated in terms of wave height and period. Transport rates are expressed as cubic meters or cubic yards per day or year.

2-4. Variability in Sediment Transport

Sediment transport rates often vary significantly at a location. This variation can be on a time scale of days, individual storms, seasons, years, or decades. Storms cause variability in beach width by modifying the nearshore profile and by transporting sand from the beach or dunes to the offshore. Depending on their track, storms may also generate currents which reverse the direction of longshore transport. Longshore transport magnitude and direction may vary along the coastline because of wave transformations or a change in local shoreline angle. At a particular coastal location, transport may be to the right (by convention, the orientation is looking seaward) during one part of the year and to the left during the remainder of the year. Annual net transport is the difference between the left and right transports. Gross transport is the sum of the magnitudes of left and right transports. A longshore gradient in net longshore transport rate results in a loss or gain of sand volume in the section of coast. A change in sand volume over a period of many years is reflected in a change of average berm width, since the shape of the beach profile tends to remain constant.

2-5. Sediment Budget

A sediment budget is a mass balance of sediment for a specified reach of shoreline. It is an accounting of sediment movement into and out of the reach and the

resulting gains or losses in sediment volume. If there is a gradient in the rates of sediment transport entering or leaving the cell, then the volumes of sand entering and leaving the reach do not balance and there must be a change in sand volume within the reach. Sediment can also be lost or gained from the offshore and backshore, such as gains from river discharges and losses from dredge material placement out of the littoral zone. The time interval of the budget analysis is arbitrary. However, most budget analyses are performed to understand the long-term change of the shoreline. For these studies the time interval must be long enough to average out seasonal variations.

Chapter 3
Waves

3-1. Introduction

Waves are the dominant force controlling littoral processes on open coasts. Determination of appropriate wave conditions is necessary before estimates of currents and sediment transport can be undertaken. Waves are the major factor in determining the geometry and composition of beaches and significantly enter into the planning and design of coastal structures. Waves generally derive their energy from storms over the open ocean. A significant amount of this energy may be dissipated before the waves reach the design site. An understanding of surface waves must precede a description of water motions in the nearshore. This chapter provides information necessary for the reader to assimilate and apply guidance presented in succeeding chapters; it is not intended to be a complete reference on waves. Additional information concerning obtaining, interpreting, and applying wave and water level information can be found in EM 1110-2-1414. This chapter defines terms and explains concepts used for littoral transport estimates, presents an overview of linear wave theory, discusses methods for determining deep water wave conditions, and explains propagation of these deep water waves to the nearshore. Chapter 2 of the Shore Protection Manual (SPM) (1984) provides a thorough introduction to the linear theory of surface water waves.

3-2. Description of Waves

a. Wave energy. Energy in the nearshore zone occurs over a broad range of frequencies. An approximate distribution of this energy is shown in Figure 3-1. The waves addressed in this chapter fall within the gravity wave band. However, studies have suggested that infragravity waves also play a significant role in littoral processes (e.g., Komar and Holman 1986). A number of terms commonly associated with the description of surface water waves are defined in Figure 3-2.

b. Linear wave theory.

(1) Waves in the ocean often appear confused, with constantly changing crests and troughs on the water surface. This is particularly true when waves are under the influence of the wind. However, it is often assumed that waves are simple periodic, so that each wave is exactly the same as all others. Simple periodic waves

may either be linear or nonlinear. There are a number of periodic wave theories, but the most commonly employed is linear wave theory (LWT), also known as Airy wave theory. Regions of validity for various wave theories are shown in Figure 3-3. In LWT, the free surface is assumed to be a simple sinusoid and the amplitude of the crest a_c equals the amplitude of the trough a_t. Linearized free surface boundary conditions are applied at the still-water level (SWL), also referred to as the mean water line (MWL), rather than at the actual surface. For this condition to be satisfied, the wave height to wavelength ratio must be very small. In spite of these restrictions, LWT is often applied for large waves with reasonable success in littoral processes descriptions. Sinusoidal waves are characterized by the wave height H, wave period T, and water depth d.

(2) The wavelength is related to the water depth and wave period through the dispersion equation. This is a transcendental relationship and solutions may not be obtained explicitly for arbitrary water depths. Therefore, it is common to consider the deep and shallow water limits in the hyperbolic tangent function to develop simplifications. These are summarized in Table 3-1. Solutions to the dispersion equation for arbitrary depths are tabulated in Appendix C in the Shore Protection Manual (1984). Solutions may also be easily determined on microcomputers using the half-interval method, Newton-Raphson or Padé approximates. A FORTRAN subroutine based on Padé approximates (Hunt 1979) is given in Table 3-2. A simple approximation which provides reasonable accuracy in shallow and intermediate water depths is

$$L = (2\pi d L_0)^{\frac{1}{2}} \left(1 - \frac{\pi d}{3L_0} \right) \qquad (3\text{-}1)$$

in which L is the wave length, $\pi = 3.14159...$, and L_0 is the deep water wavelength given in Table 3-1. The relative error for this relationship is less than 2% for $d/L_0 < 0.3$.

(3) As waves approach the nearshore, the crests become higher and steeper, and the troughs become longer and flatter. The assumptions of LWT are no longer valid. Nonlinear wave theories provide a better description of the waves. The nonlinearities are important in nearshore processes. For example, steep waves exert a larger on-shore bottom stress which is significant in the development of an equilibrium beach profile.
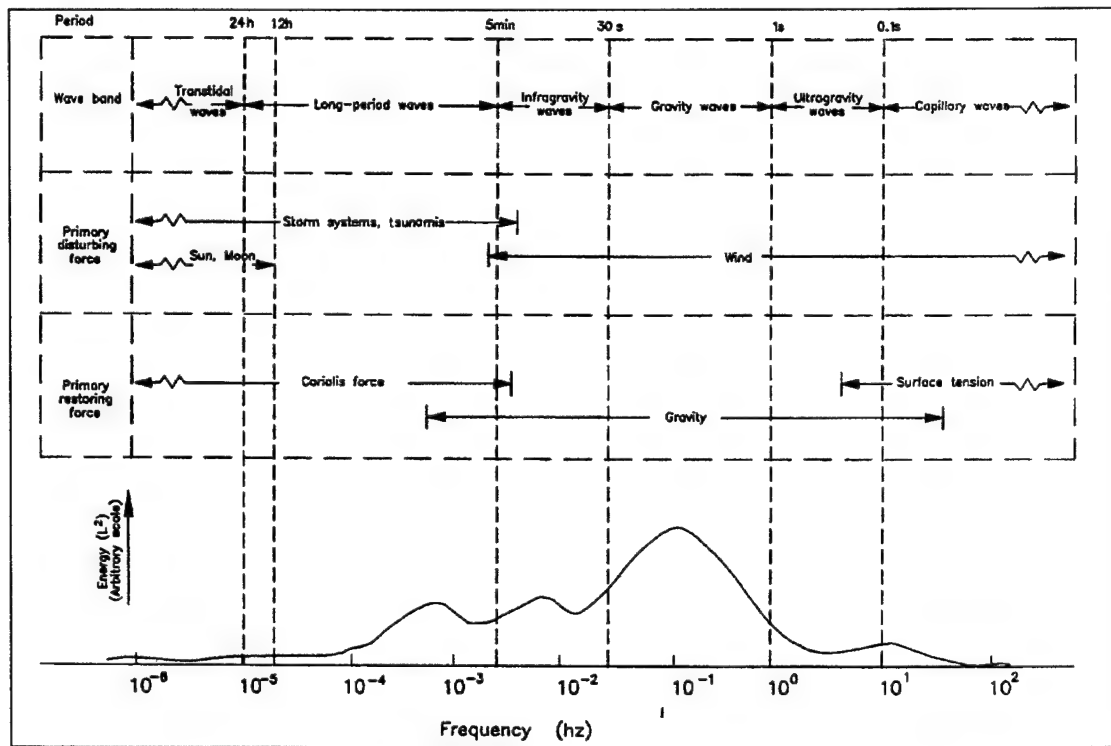
Figure 3-1. Approximate distribution of ocean surface wave energy (after Kinsman 1965)
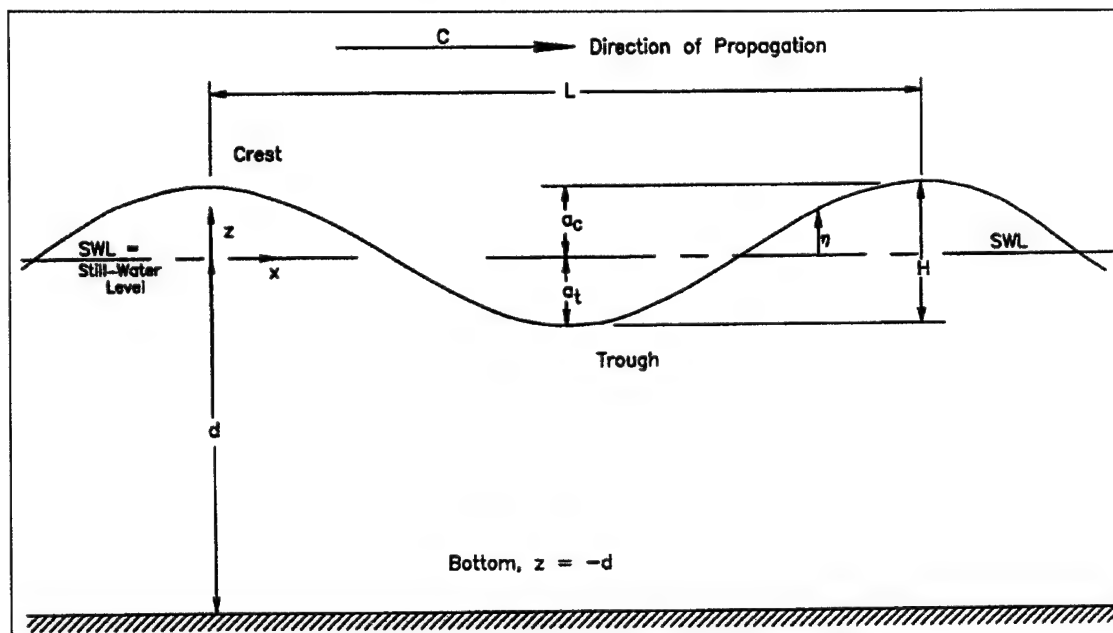
Figure 3-2. Definitions of surface waves
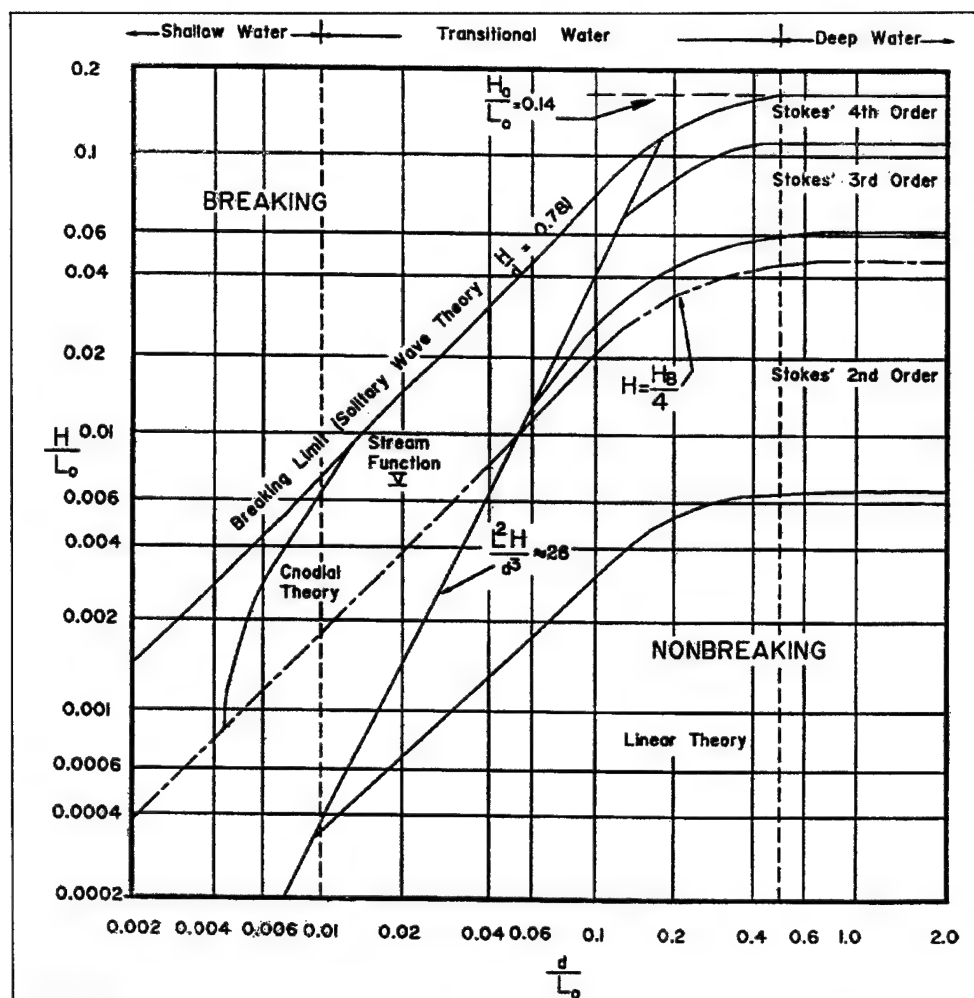
Figure 3-3. Regions of validity for various wave theories (after LeMehaute 1969)

In spite of this, most models for estimating longshore currents and sediment transport are based on LWT. In fact, many of the published models use shallow water LWT. Therefore, no discussion of nonlinear waves is given. Appendix A provides a list of references which address this topic. A review of nonlinear wave theories is given by Dean and Dalrymple (1983).

c. Short term wave statistics.

(1) Wave heights measured over a duration of several hours will show a variation, even if the spectrum does not change with time. If the waves have a narrow banded spectrum (small variation in wave period), then the wave heights are Rayleigh distributed (Longuet-Higgins 1952). The Rayleigh distribution is given by

$$P(H) = 1 - \exp\left(\frac{-H^2}{H_{rms}^2}\right) \qquad (3\text{-}2)$$

where $P(H)$ is the probability of wave height H occurring, and H_{rms} is the root mean square *(rms)* wave height defined by

Table 3-1
Linear Wave Theory Relationships

		Shallow Water ($d/L < 1/25$)	Intermediate Water ($1/25 < d/L < 1/2$)	Deep Water ($d/L > 1/2$)
Wave profile	n	same as →	$\frac{H}{2} \cos \Theta$	← same as
Wavelength	L	$(gd)^{1/2} T$	$\frac{gT^2}{2\pi} \tanh kd$	$\frac{gT^2}{2\pi}$
Wave speed	C	$(gd)^{1/2}$	$\frac{gT}{2\pi} \tanh kd$	$\frac{gT}{2\pi}$
Group speed	C_g	$(gd)^{1/2}$	$\left(1 + \frac{2kd}{\sinh 2kd}\right) \frac{C}{2}$	$\frac{gT}{4\pi}$
Horizontal component of particle velocity	u	$\frac{H}{2}(g/d)^{1/2} \cos \Theta$	$\frac{H}{2} \frac{gk}{\omega} \frac{\cosh k(d+z)}{\cosh kd} \cos \Theta$	$\frac{\pi H}{T} e^{ks} \cos \Theta$
Vertical component of particle velocity	w	$\frac{H\pi}{T}(1+z/d) \sin \Theta$	$\frac{H}{2} \frac{gk}{\omega} \frac{\sinh k(d+z)}{\cosh kd} \sin \Theta$	$\frac{\pi H}{T} e^{kz} \sin \Theta$
Subsurface pressure	p	$\rho g(n-z)$	$\rho g \left(n \frac{\cosh k(d+z)}{\cosh kd} - z \right)$	$\rho g(n\, e^{kz} - z)$

Note:

Θ = phase angle = $2\pi \left(\frac{X}{L} - \frac{t}{T} \right)$

k = wave number = $\frac{2\pi}{L}$

ω = frequency (in radians) = $\frac{2\pi}{T}$

Table 3-2
FORTRAN Subroutine to Estimate Wavelength Using Padé Approximates (Hunt 1979)

```
      SUBROUTINE PADÉ (DEPTH, PERIOD, GRAVITY, LENGTH)
C     This subroutine gives a solution to the linear wave theory
C     dispersion equation using Pade' approximates.
C     DEPTH                      STILL WATER DEPTH
C     PERIOD                     WAVE PERIOD
C     GRAVITY                    ACCELERATION DUE TO GRAVITY
C     LENGTH                     WAVELENGTH

      REAL LENGTH, C(6)

      DATA C/0.666, 0.355, 0.1608465608, 0.0632098765,
                    0.0217540484, 0.0065407983/

      PI=4.*ATAN(1.)
      Y=DEPTH*(2.*PI/PERIOD)**2/GRAVITY
      SUM=0.
      DO 100 I=1,6
100   SUM=SUM+C(I)*Y**I
      LENGTH=2.*PI*DEPTH/SQRT(Y**2+Y/(1.+SUM))
      RETURN
      END
```

$$H_{rms} = \left(\frac{1}{N}\sum_{n=1}^{N} H_n^2\right)^{\frac{1}{2}} \qquad (3\text{-}3)$$

H_{rms} characterizes the distribution of the waves. However, other statistically representative waves are often used in engineering practice. The average of the highest n waves in the distribution is termed $H_{1/n}$. The case where $n = 3$ is termed the significant wave height and approximately corresponds to the wave height that a trained observer would visually determine. $H_{1/3}$ is often denoted as H_s. The relationship between H_{rms} and other statistically representative waves is summarized in Table 3-3.

Table 3-3
Statistically Representative Waves Based on Rayleigh Wave Height Relationships

Wave Height	Notation	H/H_{rms}
Mode	--	0.707
Median	--	0.833
Mean	$\overline{H} = H_1$	0.886
Root-mean-square	H_{rms}	1.000
Significant	$H_s = H_{1/3}$	1.416
Average of tenth-highest waves	$H_{1/10}$	1.800
Average of hundredth-highest waves	$H_{1/100}$	2.359

(2) The largest wave H_{max} in a wave record is approximately (Goda 1985)

$$\frac{H_{max}}{H_s} = \left(\frac{\ln N}{2}\right)^{\frac{1}{2}} + e\,(8\ln N)^{\frac{1}{2}} \qquad (3\text{-}4)$$

in which N is the number of waves and e is Euler's constant ($e \sim 0.5722$). The Rayleigh distribution is particularly suited to a narrow banded spectrum, so the peak frequency f_p may be used to determine the number of waves in the record. The peak frequency is the frequency corresponding to the maximum energy in the spectrum. Assuming the waves are stationary (i.e., the wave spectrum does not change with time), then $N = $

D/T_p where D is the duration of the record or storm and T_p is the peak period. The maximum expected wave height is shown in Figure 3-4 for different peak periods for a fully developed spectrum having a Rayleigh distribution of heights. The maximum expected wave height may be useful for estimating extreme runup, overtopping, and wave forces.

(3) Waves are usually recorded as a digital time series of the free surface elevation. There are two common techniques for recovering the significant wave height and period from these records, zero downcrossing and spectral analysis.

(4) The significant wave height can be estimated from a digital record by direct computation of $H_{1/3}$. Individual waves are between successive points where the free surface passes down through the mean elevation. The height for each of these zero downcrossing waves is then determined. These heights are ranked and the average of the highest one-third is $H_{1/3}$. The significant wave period can be determined in a similar manner. The mean period is calculated as the average of all of the wave periods.

(5) In the spectral approach, the significant wave height in deep water is defined as four times the standard deviation of the record of sea surface elevations. The significant wave height determined in this manner is the zero moment wave height, denoted as H_{m0}, to clearly identify that it was obtained by the spectral approach. The exact value of H_{m0} depends on wave steepness and relative depth as indicated in Figure 3-5. In the spectral approach, the significant wave period T_p is often taken as the period corresponding with the peak energy, and the finite depth wavelength of waves at the spectral peak is denoted as L_p. The mean period is calculated from the square root of the ratio of the zeroeth to the second moment of the spectrum.

(6) Both of these methods provide reasonable results and both are commonly used. Since the two approaches yield slightly different results, it should be made clear which approach is being used to estimate the significant wave height, significant period, and mean period.

d. Long-term wave statistics. Extreme wave heights are an important parameter in many coastal designs. Often the extreme wave heights are limited by the water depth. For deeper water or low energy sites, extreme values are usually described in terms of significant wave height as a function of the return period. Extreme values of other height statistics, such as $H_{1/10}$, can be
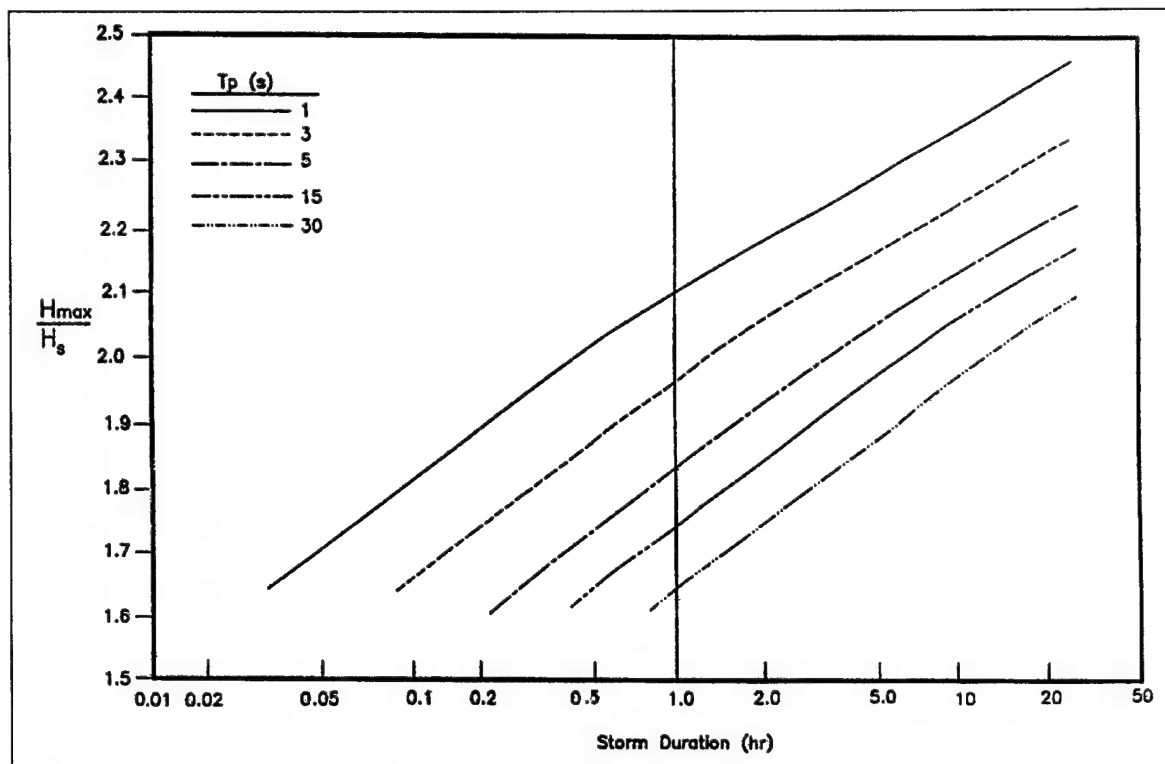
Figure 3-4. Expected maximum wave height
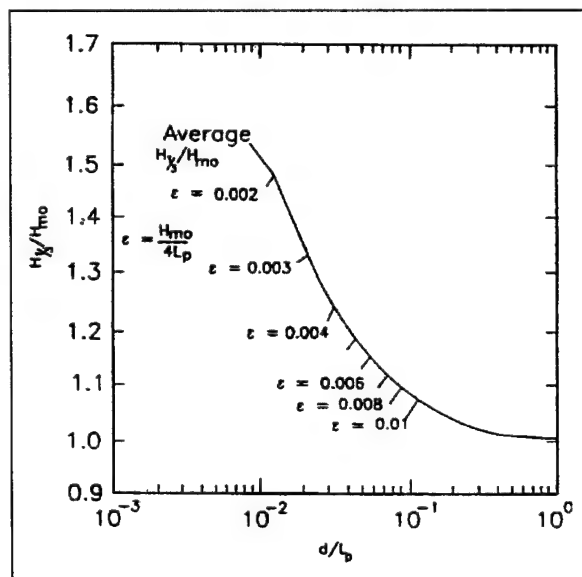
Figure 3-5. Variation in the relationship between $H_{1/3}$ and H_{mo} (after Thompson and Vincent 1985)

obtained from the significant height data and a model for the distribution of the individual wave heights. Consideration of different statistical populations may be required. The basic approaches for predicting extreme wave conditions are the extrapolation of a long-term distribution of significant wave heights, and extreme value analysis with annual maxima or with peak significant wave heights of major storms above a certain threshold. For a detailed description of these methods, the reader is directed to Chapter 5 of EM 1110-2-1414. Brief descriptions of the methods are given below.

(1) The first approach, extrapolation of a long-term distribution of significant wave heights, is relatively easy to apply. However, care must be taken concerning any statistical dependency among successive observations. A method for correcting for statistical dependency is given by Nolte (1973). The long-term distribution for wave height is usually represented by the cumulative probability distribution of the data. It is also often fit with a model distribution function. There is no strong theoretical basis for a particular model. Several models are widely used because of their success at describing

measured waves; these models are further discussed in EM 1110-2-1414.

(2) Applying extreme value analysis with annual maxima or peak significant wave heights of major storms above a certain threshold is more detailed than the first approach. In general, a probability value is assigned to each extreme data point, and the data are ordered according to wave height. These points are then plotted on an extreme value probability paper or construct paper using a wave height relationship for the abscissa and ordinate scales. A straight line is drawn through the points to represent the trend. The line can then be extrapolated to locate a design value corresponding to a chosen return period or encounter probability. The return period is the average time interval between successive events of the design wave being equaled or exceeded. The encounter probability is the probability that the design wave is equaled or exceeded during a prescribed time period. The computer program WAVDIS1 can be used to estimate the parameters of three commonly used extremal probability distributions; WAVDIS2 is an alternate version of WAVDIS1 that estimates parameters by the method of moments. The computer program FWAVOCUR is used to determine the expected frequency of extreme wave conditions over a specified period of time. These computer programs are available through the MACE program and are briefly outlined in Appendix E.

3-3. Wave Data

There are a number of sources for obtaining wave data. These include ship observations, NOAA buoys, Littoral Environment Observations (LEO), and the Wave Information Studies (WIS). A listing of publications which contain extensive summaries of meteorological and oceanographic data is given in Table 3-4. In addition to wave and water level data, the sources listed can include wind speed and direction, air and sea temperatures and other information required for wave and water level studies. Access to coastal wave and water level data is described in Table 3-5. The telephone numbers provided in Table 3-5 are for the points of contact for the programs. The points of contact for each program will instruct potential users on how to access the systems. In addition, information may be available from the Coast Guard, port and harbor authorities, and local universities. Several of these sources are summarized in Table 3-6.

a. WIS data.

(1) The Wave Information Study (WIS) was initiated by the Corps of Engineers to produce a wave climate for U.S. coastal waters. The study was divided into three main phases (Corson et al. 1982).

Phase I (Deep Ocean) are numerical hindcasts of deep water wave data from historical synoptic surface pressure charts and shipboard observations of wind velocity. Spatial grids are on the order of 2 degrees and the time increments are greater than 6 hours. The primary wave processes are air-sea and wave interactions.

Phase II (Shelf Zone) are numerical hindcasts using the same meterological information as in Phase I, but at a finer scale to better resolve the sheltering effects of the continental geometry. Phase I data serve as the boundary conditions at the seaward edge of the Phase II grid. The grid size is 0.5 degree and the time step is 3 to 6 hours. The wave processes are air-sea and wave-wave interactions.

Phase III (Nearshore Zone) is the transformation of the Phase II wave data into shallow water.

(2) Phases I, II, and III have been completed for the Atlantic and Pacific coasts. The Gulf of Mexico hindcast with a 2-degree grid (Phase I) was omitted since it is a relatively small water body compared to the Atlantic and Pacific Oceans. The Great Lakes were hindcast with a 16-km (10-mile) grid.

(3) Phase II wave estimates are provided for 71 stations along the Atlantic coast, 53 stations along the Pacific coast of California, Oregon, and Washington, and 50 stations along the Gulf coast. Hindcasts were conducted at 3-hour intervals. Tables are provided for each station which summarize the percent occurrence of wave height and period by direction. Tables are also given for the mean and largest significant wave heights by month for the 20-year hindcast.

(4) Phase III transformations from Phase II wave information are available for the Atlantic coast and Pacific coast north of Pt. Conception, California. The coastal reaches are shown in Figures 3-6 and 3-7. A Phase II hindcast was conducted for the region south of Pt. Conception to the Mexican border (Figure 3-8). Wave information on the Great Lakes is available at

Table 3-4
Summary Sources of Meteorological and Oceanographic Data

Changery, M.J. 1978 (December). "National Wind Data Index: Final Report," National Climatic Data Center, Asheville, NC 28801.

Hatch, W.L. 1983 (July). "Selective Guide to Climatic Data Sources," Key to Meteorological Records Documentation No. 4.11, National Climatic Data Center, Asheville, NC 28801.

National Oceanic and Atmospheric Administration. 1985 (May). "Index of Tide Stations: United States of America and Miscellaneous Other Stations," National Ocean Service, Tidal Datum Section, Rockville, MD 20852.

National Oceanic and Atmospheric Administration. 1985 (November). "National Ocean Service Products and Services Handbook," NOS, Sea and Lake Levels Branch, Rockville, MD 20852.

US Army Engineer Waterways Experiment Station. 1985 (October). "WES Engineering Computer Programs Library Catalog," Vicksburg, MS 39180-6199.

US Department of Commerce. 1977. "Climatic Atlas of the Outer Continental Shelf Waters and Coastal Regions of Alaska," Research Unit No. 347, National Climatic Data Center, Asheville, NC 28801.

US Department of Commerce, National Climatic Data Center. 1986 (April). "Climatic Summaries for NDBC Data Buoys," National Data Buoy Center, NSTL Station, MS 39529.

US Navy, Naval Oceanography Command. 1983 (October). "US Navy Hindcast, Spectral, Ocean Wave Model Climatic Atlas: North Atlantic Ocean," NAVAIR 50-1C-538, Naval Oceanography Command, NSTL Station, MS 39529.

Table 3-5
Sources of Coastal Wave and Water Level Data

Source	Type of Information
OL-A USAF Environmental Technical Applications Center (MAC) Federal Building Asheville, NC 28801 (704) 259-0218 (Non-Department of Defense users should contact the National Climatic Data Center at the above address.) (704) 259-0682	Global, meteorological, and oceanographic data and data products.
National Oceanographic Data Center User Service (Code OC21) 1825 Connecticut Ave., NW Washington, DC 20235 (202) 673-5549	Variety of oceanographic data.
Coastal Engineering Information and Analysis Center USAEWES 3909 Halls Ferry Rd. Vicksburg, MS 39180-6199 (601) 634-2012	Coastal Engineering Information Management (CEIMS) LEO Retrieval System, gage data from the Corps Coastal Field Data Collection Program and other sources.
Coastal Oceanography Branch USAEWES 3909 Halls Ferry Rd. Vicksburg, MS 39180-6199 (601) 634-2028	State-of-the-art computer programs for wave growth and transformation, WIS hindcast wave parameters, and two-dimensional spectra.

(Continued)

Table 3-5. (Concluded)

Source	Type of Information
Corps Computer Programs Library USAEWES IM-RS 3909 Halls Ferry Rd. Vicksburg, MS 39180-6199 (601) 634-2300	Documented computer programs for wave measurement analysis and wave growth and transformation.
Automated Coastal Engineering Group USAEWES 3909 Halls Ferry Rd. Vicksburg, MS 39180-6199 (601) 634-2017	Wave and tide analysis programs.
National Geophysical Data Center NOAA E/GC 3 325 Broadway Boulder, CO 80303 (303) 497-6388	Digital bathymetric data for United States coasts, including Alaska, Hawaii, and Puerto Rico.
California Coastal Data Information Program Scripps Institute of Oceanography Mail Code A022 University of California, San Diego LaJolla, CA 92093 (619) 534-3033	United States west coast gage network and gage at CERC's FRF in North Carolina.
Field Coastal Data Network Coastal & Oceanographic Engineering Department 336 Weil Hall University of Florida Gainesville, FL 32611 (904) 392-1051	Coastal Florida wave gage network.
Navy/NOAA Oceanographic Data Distribution system operated by: Science Applications International Corporation 205 Montecito Avenue Monterey, CA 93940 (408) 375-3063	Global forecast wave and weather data.
NOAA National Ocean Service Tidal Datums and Information Section 6001 Executive Blvd. Rockville, MD 20852 (301) 443-8467	Tidal table, tidal current tables, and digital data for selected locations.
Alaska Coastal Data Collection Program Plan Formulation Section US Army Engineer District, Alaska Pouch 898 Anchorage, AK 99506-0898 (907) 753-2620	Wind and wave data for coastal Alaska.

Table 3-6
Additional Sources of Meteorological and Oceanographic Data

The Sea State Engineering Analysis System (SEAS) enables Corps users to access WIS data and form a variety of summaries. SEAS is a user-friendly system which consists of a data base of hindcast wave parameters, a retrieval system, and a library of statistical routines to produce desired summaries.

An interactive system developed at Scripps Institute of Oceanography (SIO) is available for accessing parameters from the SIO-based network of wave gages. The network includes primarily west coast gages, many of which are supported by the Corps' Coastal Field Data Collection Program.

A system similar to SIO's interactive system is operated by the University of Florida for wave gages along the Florida coast.

Global forecast wave and weather information is available through the Navy/NOAA Oceanographic Data Distribution System (NODDS). The forecast wave data are calculated using the Navy's Global Spectral Ocean Wave Model. NODDS is operated by Science Applications International Corporation under contract to the Jet Propulsion Laboratory.

CEIMS is a computerized system being developed by CERC. It will provide indexes to a wide variety of coastal data. It will also provide direct access to selected data sets and processing programs.

An interactive environmental data reference service is described in Blumenthal and O'Quinn (1981).

stations 16 km (10 miles) apart as shown in Figure 3-9. Gulf Coast stations are shown in Figure 3-10. The Phase III results bring the hindcast waves into the near-shore. If these data are available at a design site, they should be included in the design wave selection. WIS reports are listed in Table 3-7.

b. LEO data.

(1) The Corps of Engineers program for collection of wave observations from shore is the Littoral Environment Observation (LEO) program. The LEO program was established to provide data on coastal phenomena at low cost. Volunteer observers obtain daily estimates which include the breaker height, wave period, direction of wave approach, wind speed, wind direction, current speed, and current direction. Wave height and direction are visual estimates. Other parameters are estimated with simple equipment. The skill of individual observers significantly influences the validity of the observations from shore.

(2) The locations of active LEO sites are shown in Figure 3-11. Generally, LEO data are tabulated annually as scatter diagrams of the percent occurrence of waves in different wave height-wave period categories. To be statistically descriptive of a site, observations must be recorded for at least 20 days of each month for a period of at least 3 years. Additional information on the LEO program is given in Schneider (1981), and Sherlock and Szuwalski (1987).

c. NOAA buoy data. Since 1972 the National Oceanic and Atmospheric Administration (NOAA) has maintained a number of oceanographic buoys throughout United States coastal waters. Table 3-8 gives locations of the NOAA buoys and years of information through 1988. Further updates or actual buoy data can be obtained from the National Oceanographic Data Center. Available information includes wind direction and speed, sea level pressure, air temperature, sea surface temperature, significant wave height, dominant wave period, and peak gust data (US Department of Commerce 1990).

d. Ship observations.

(1) Wave observations have been collected by observers aboard ships in passage for many areas of the world over many years. The observations include average wave height, period, and direction of the sea waves (locally generated) and the swell waves (generated elsewhere and propagated to the area). In modern observations, the sea direction is assumed to coincide with the wind direction.

(2) The reliability of shipboard observations must be considered. Individual observations are highly variable, and the accuracy of reported wave heights is lower for high energy conditions. There are a limited number of high energy observations because ships tend to avoid storms, and measurements made under these conditions are less reliable. A cumulative distribution of shipboard

**Figure 3-6. Atlantic coast locations of WIS Phase II and III information
(Sheet 1 of 3)**

Figure 3-6. (Sheet 2 of 3)
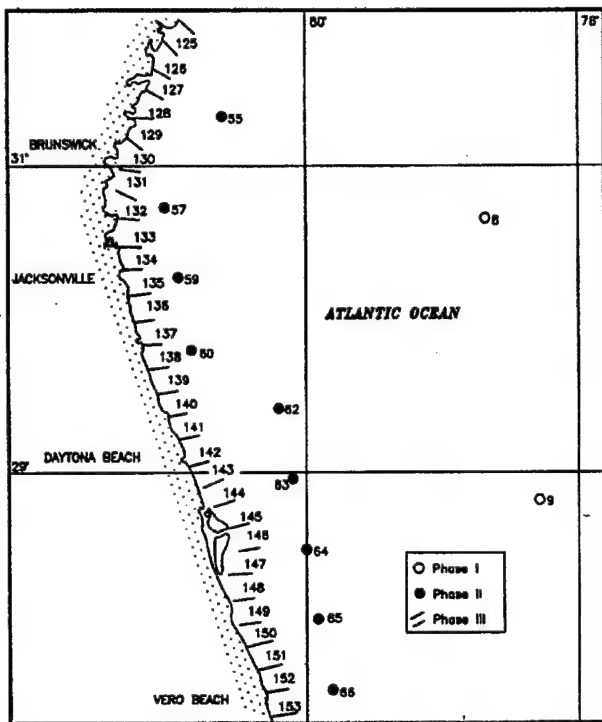
Figure 3-6. (Sheet 3 of 3)
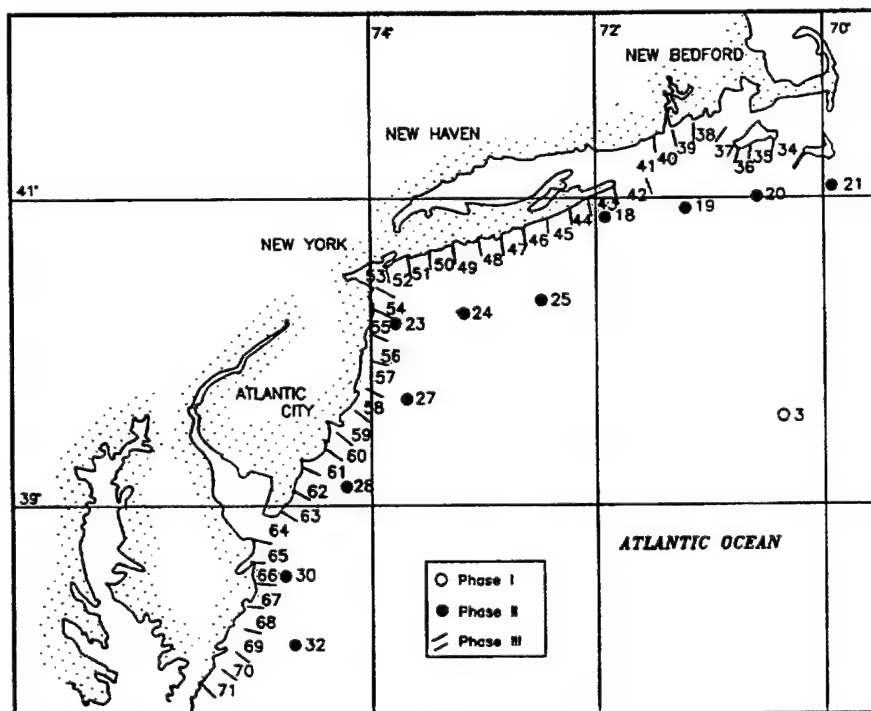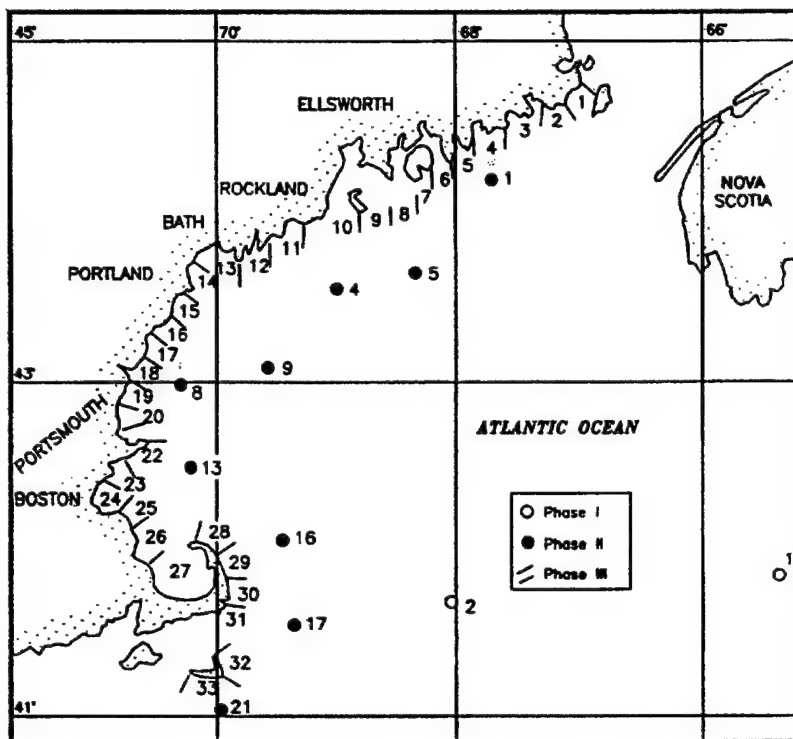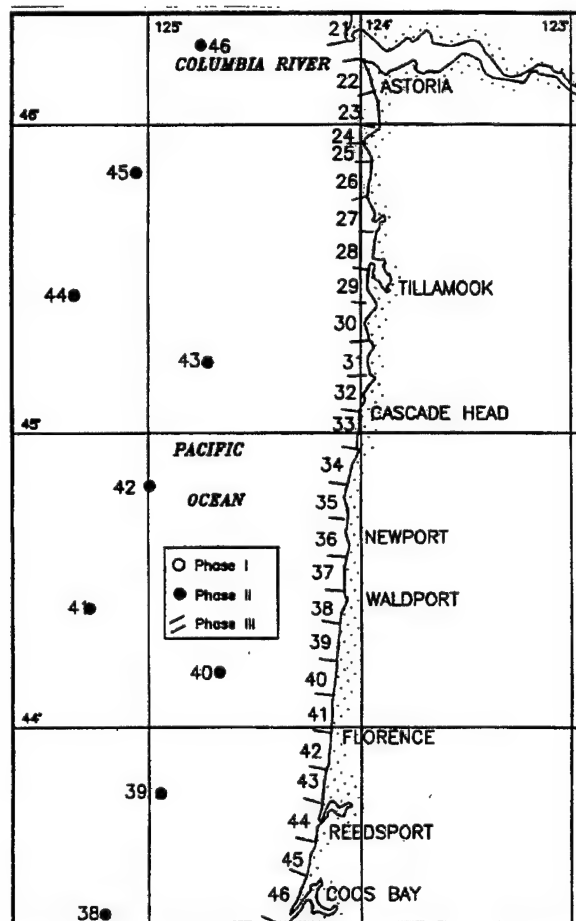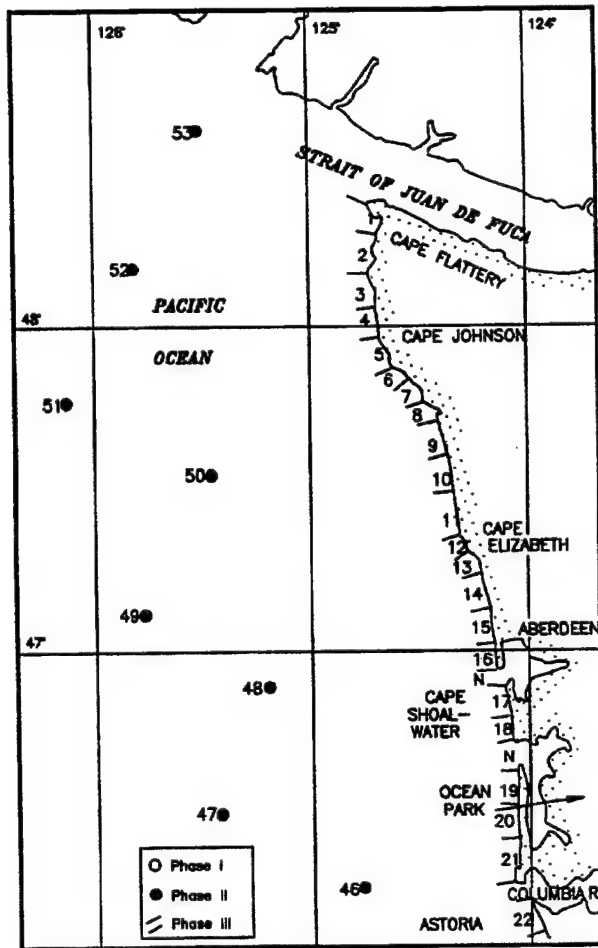
Figure 3-7. Pacific coast locations of WIS Phase II and III information (Sheet 1 of 3)
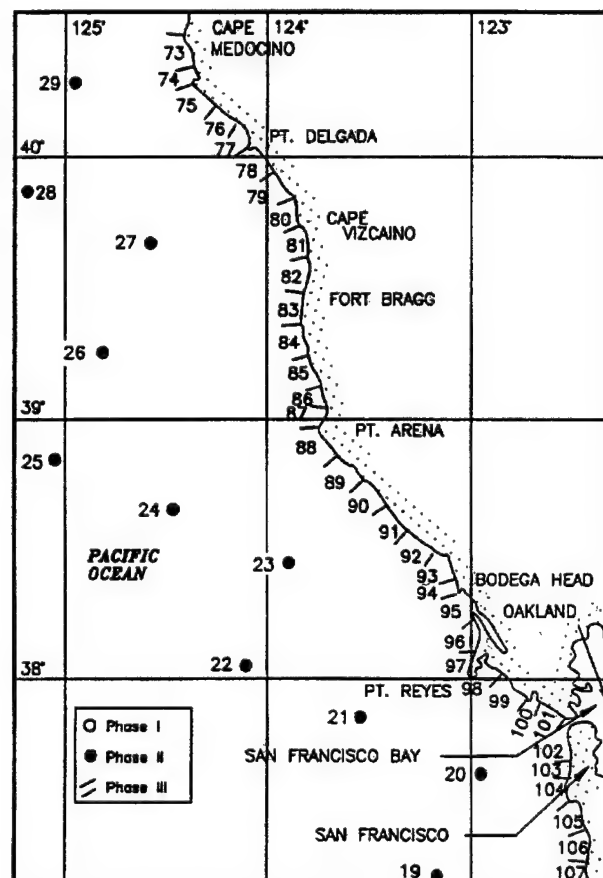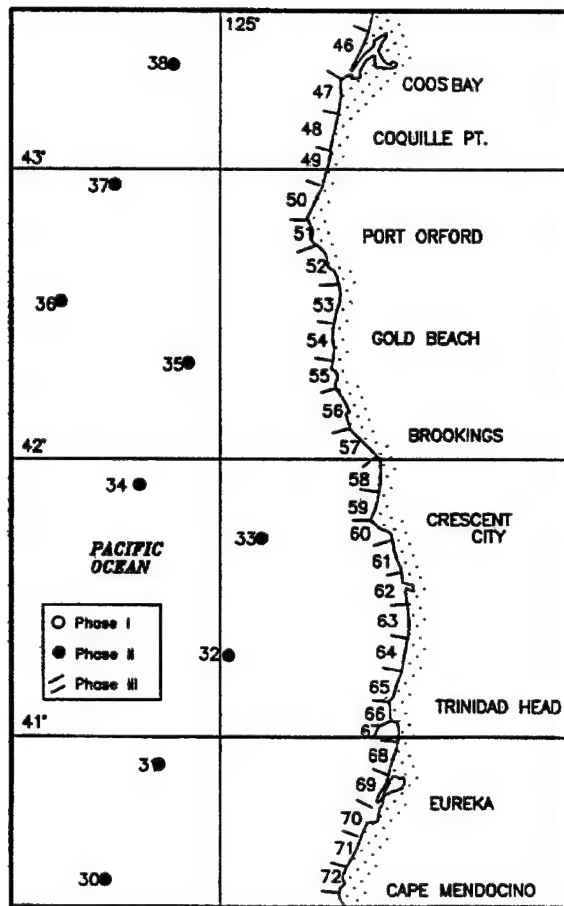
Figure 3-7. (Sheet 2 of 3)
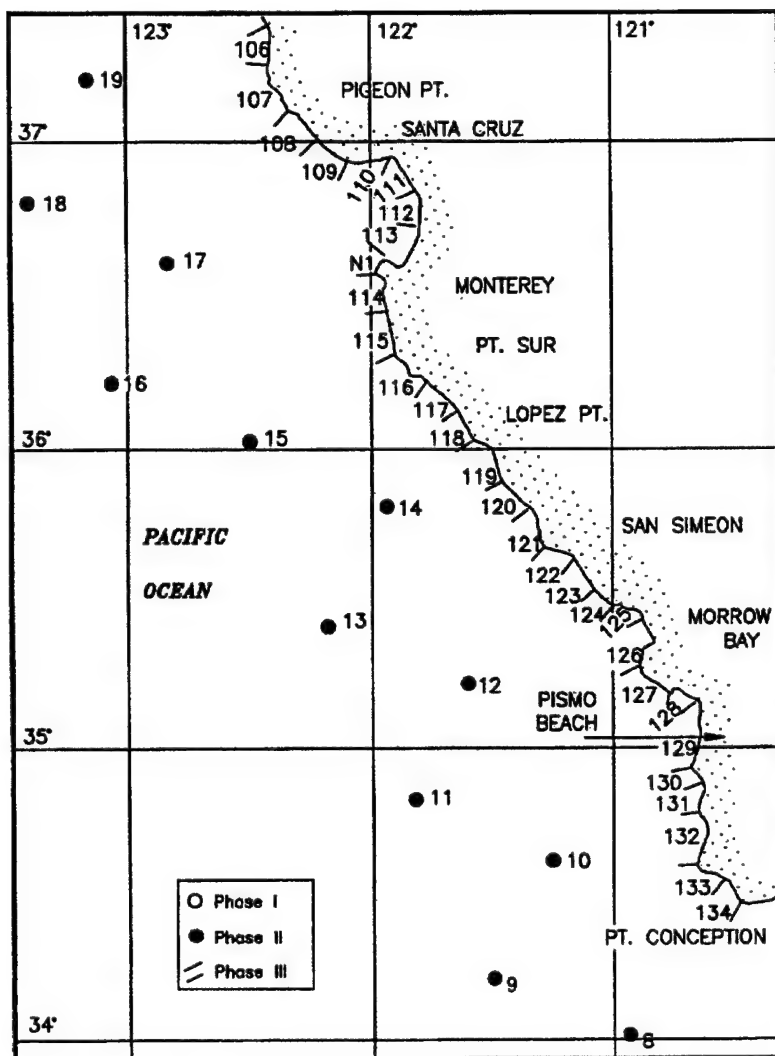
Figure 3-7. (Sheet 3 of 3)
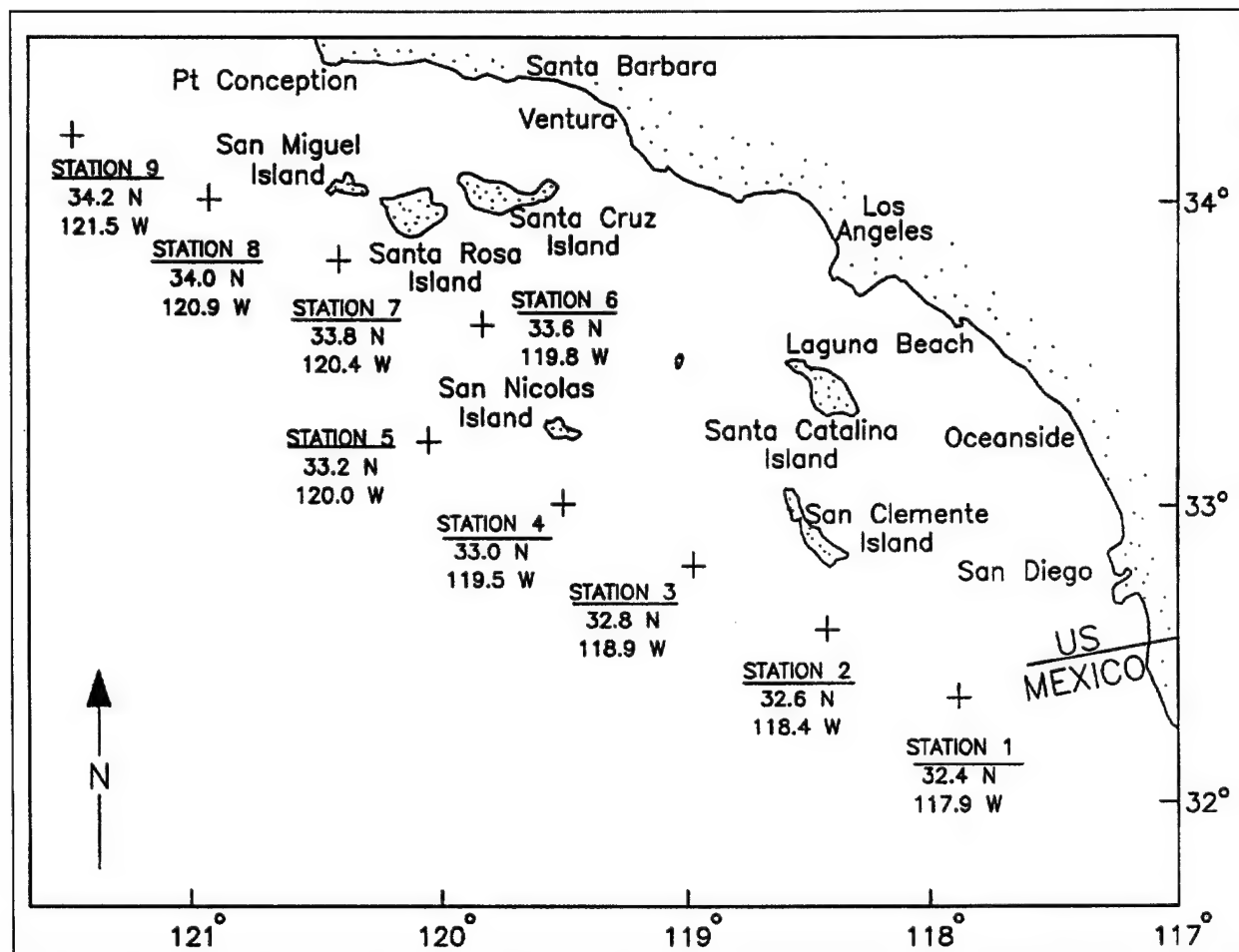
Figure 3-8. WIS Phase II locations for Southern California Bight

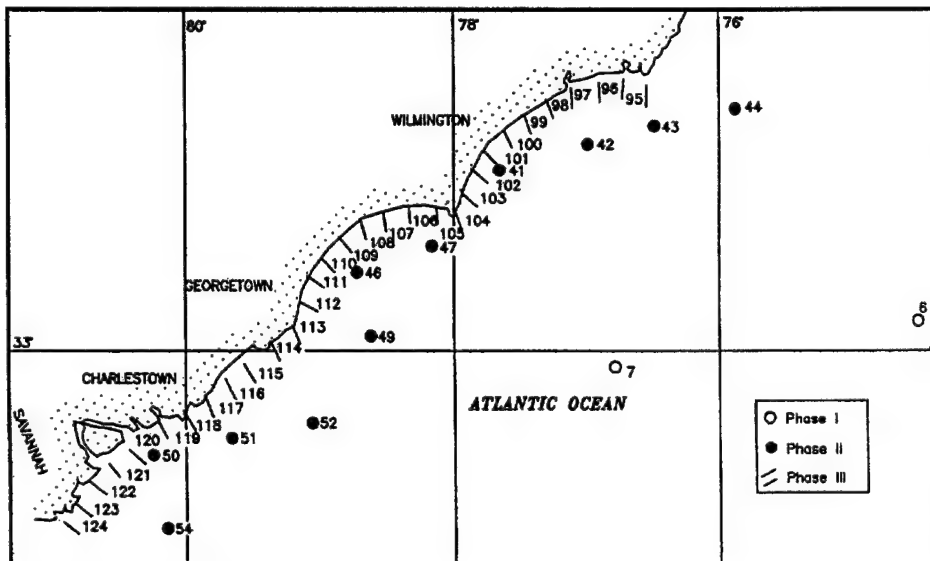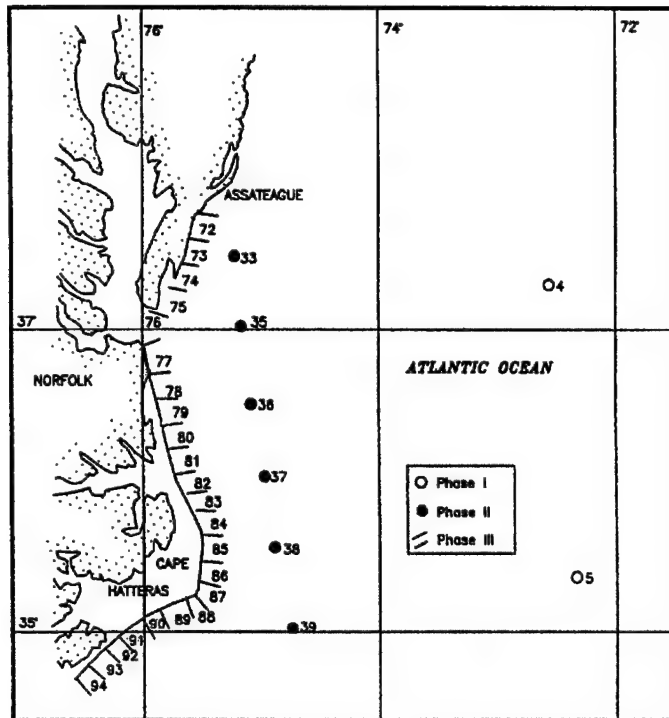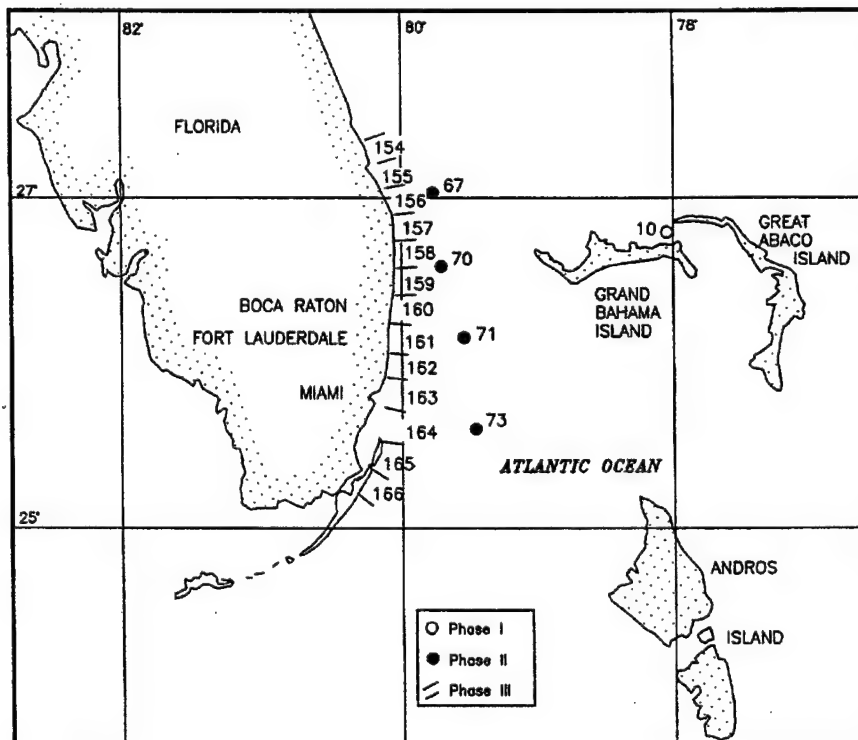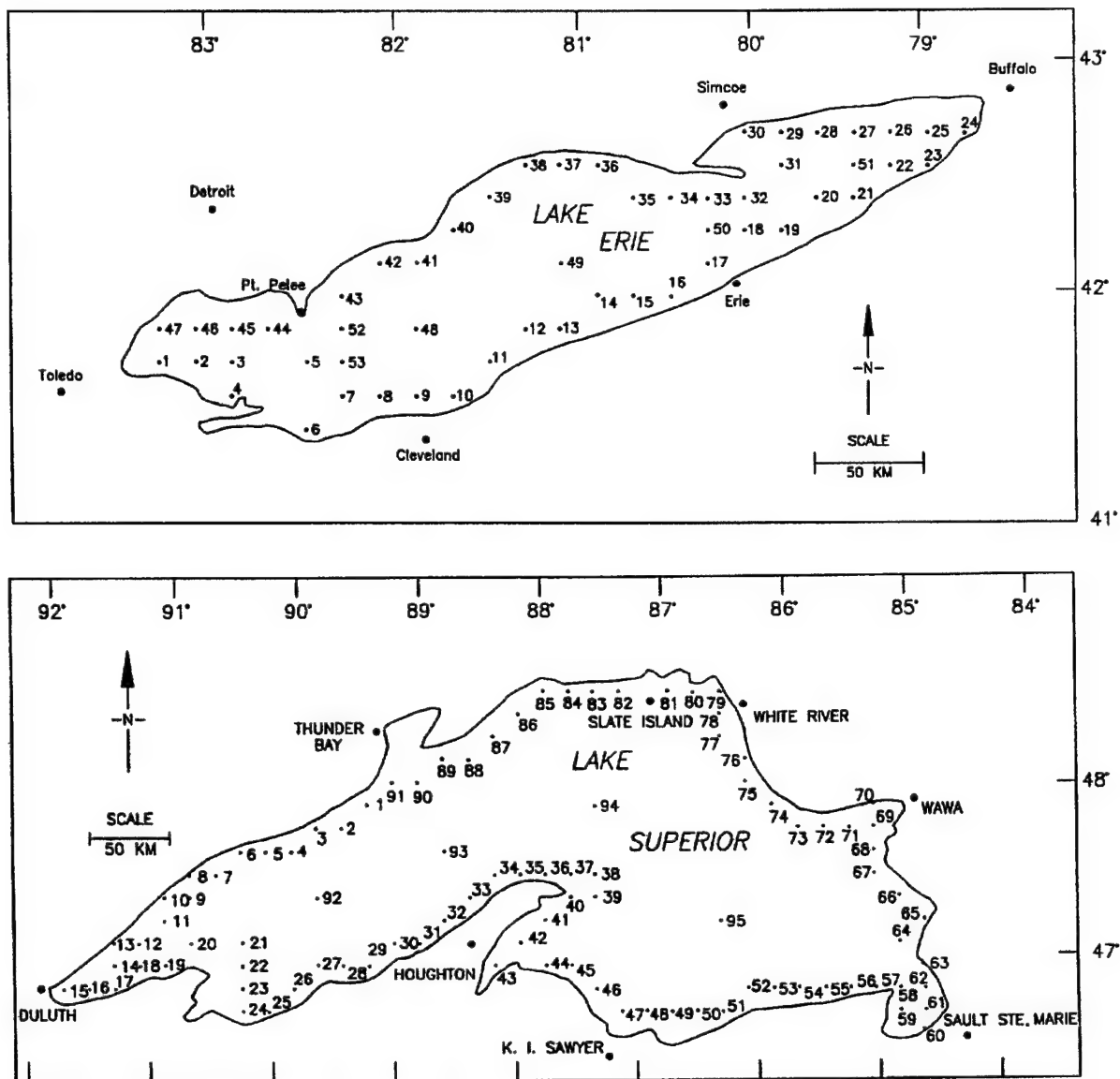Figure 3-9. Great Lakes hindcast stations (Sheet 1 of 3)
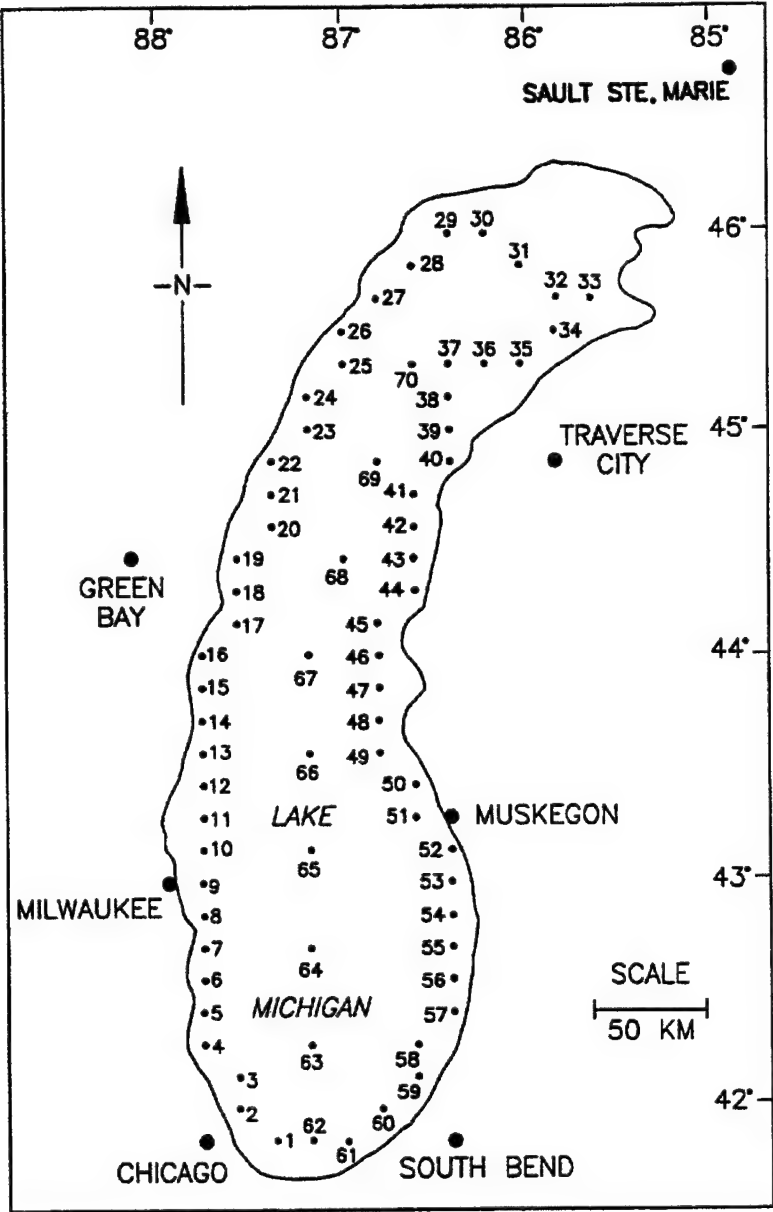
Figure 3-9. (Sheet 2 of 3)
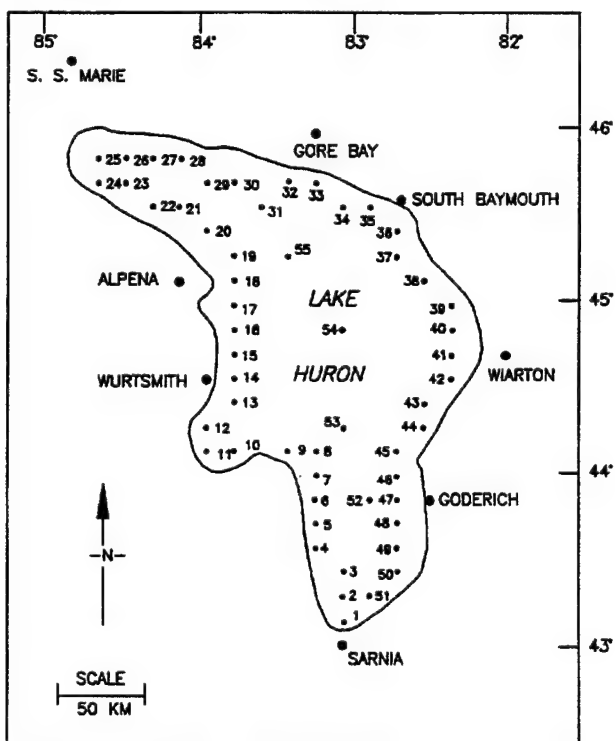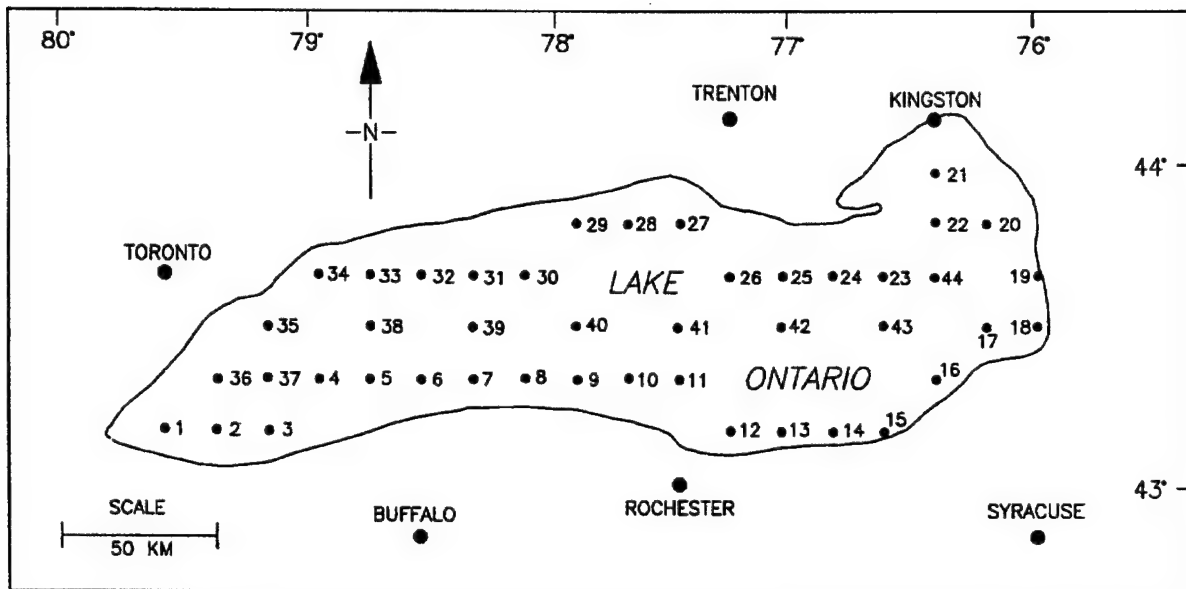
Figure 3-9. (Sheet 3 of 3)
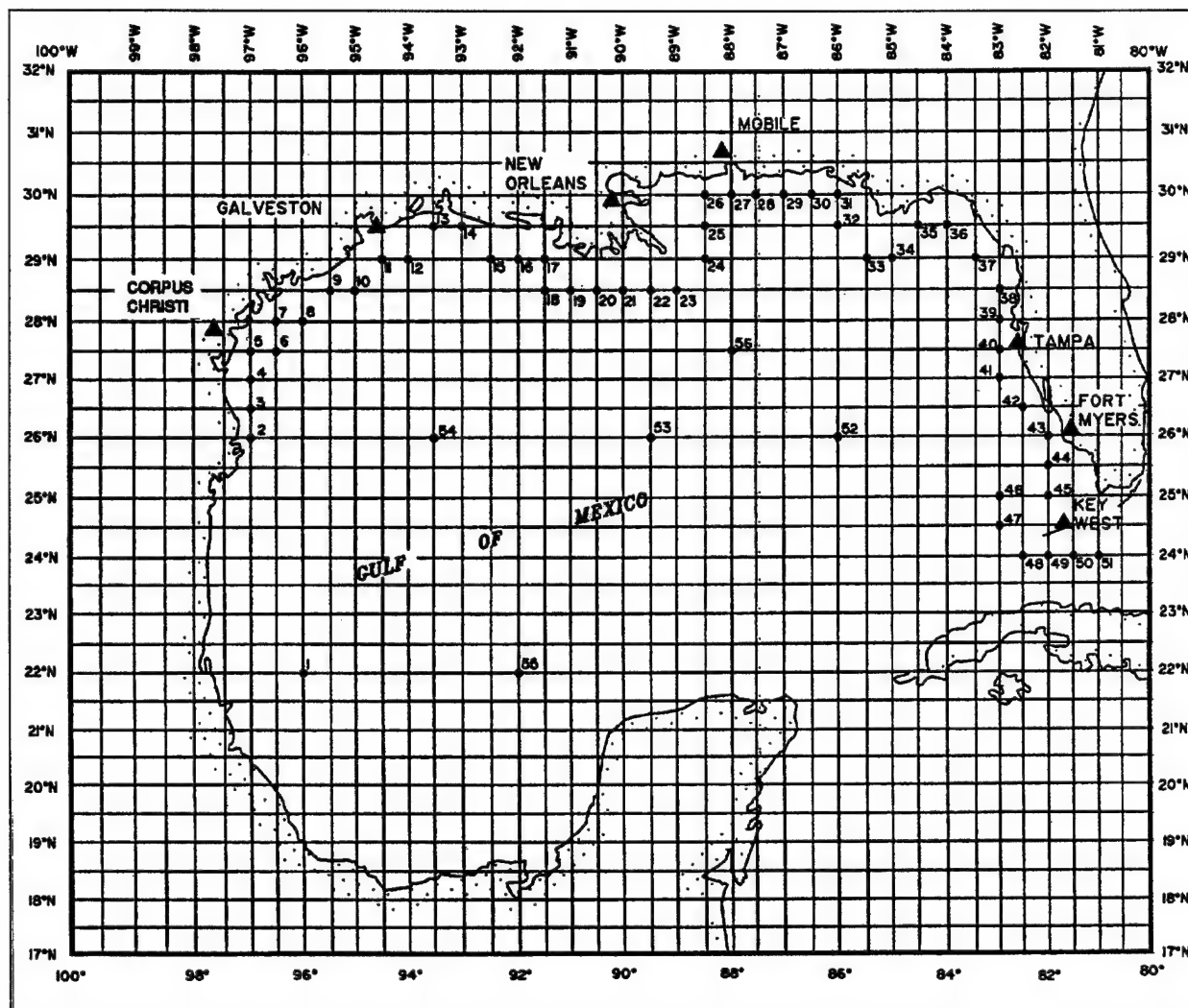
Figure 3-10. Gulf coast locations of WIS phase II information

Table 3-7
Wave Information Studies (WIS) Reports

Bibliographic Information

Atlantic and Pacific Coasts Reports

Corson, W. D., Resio, D. T., and Vincent, C. L. 1980 (July). "Wave Information Study of U.S. Coastlines; Surface Pressure Field Recon-struction for Wave Hindcasting Purposes," TR HL-80-11, Report 1.

Corson, W. D., Resio, D. T., Brooks, R. M., Ebersole, B. A., Jensen, R. E., Ragsdale, D. S., and Tracy, B. A. 1981 (January). "Atlantic Coast Hindcast, Deepwater Significant Wave Information," WIS Report 2.

Corson, W. D., and Resio, D. T. 1981 (May). "Comparisons of Hindcast and Measured Deepwater Significant Wave Heights," WIS Report 3.

Resio, D. T., Vincent, C. L., and Corson, W. D. 1982 (May). "Objective Specification of Atlantic Ocean Windfields from Historical Data," WIS Report 4.

Resio, D. T. 1982 (March). "The Estimation of Wind-Wave Generation in a Discrete Spectral Model," WIS Report 5.

Corson, W. D., Resio, D. T., Brooks, R. M., Ebersole, B. A., Jensen, R. E., Ragsdale, D. S., and Tracy, B. A. 1982 (March). "Atlantic Coast Hindcast Phase II, Significant Wave Information," WIS Report 6.

Ebersole, B. A. 1982 (April). "Atlantic Coast Water-Level Climate," WIS Report 7.

Jensen, R. E. 1983 (September). "Methodology for the Calculation of a Shallow Water Wave Climate," WIS Report 8.

Jensen, R. E. 1983 (January). "Atlantic Coast Hindcast, Shallow-Water Significant Wave Information," WIS Report 9.

Ragsdale, D. S. 1983 (August). "Sea-State Engineering Analysis System: Users Manual," WIS Report 10.

Tracy, B. A. 1982 (May). "Theory and Calculation of the Nonlinear Energy Transfer Between Sea Waves in Deep Water," WIS Report 11.

Resio, D. T., and Tracy, B. A. 1983 (January). "A Numerical Model for Wind-Wave Prediction in Deepwater," WIS Report 12.

Brooks, R. M., and Corson, W. D. 1984 (September). "Summary of Archived Atlantic Coast Wave Information Study, Pressure, Wind, Wave, and Water Level Data," WIS Report 13.

Corson, W. D., Abel, C. E., Brooks, R. M., Farrar, P. D., Groves, B. J., Jensen, R. E., Payne, J. B., Ragsdale, D. S., and Tracy, B. A. 1986 (March). "Pacific Coast Hindcast, Deepwater Wave Information," WIS Report 14.

Corson, W. D., and Tracy, B. A. 1985 (May). "Atlantic Coast Hindcast, Phase II Wave Information: Additional Extremal Estimates," WIS Report 15.

Corson, W. D., Abel, C. E., Brooks, R. M., Farrar, P. D., Groves, B. J., Payne, J. B., McAneny, D. S., and Tracy, B. A. 1987 (May). "Pacif-ic Coast Hindcast Phase II Wave Information," WIS Report 16.

Jensen, R. E., Hubertz, J. M., and Payne, J. B. 1989 (Mar). "Pacific Coast Hindcast, Phase III North Wave Information," WIS Report 17.

Hubertz, J. M., and Brooks, R. M. 1989 (Mar). "Gulf of Mexico Hindcast Wave Information," WIS Report 18.

Abel, C. E., Tracy, B. A., Vincent, C. L., and Jensen, R. E. 1989 (Apr). "Hurricane Hindcast Methodology and Wave Statistics for Atlantic and Gulf Hurricanes from 1956-1975," WIS Report 19.

Jensen, R. E., Hubertz, J. M., Thompson, E. F., Reinhard, R. D., Groves, B., Brown, W. A., Payne, J. B., Brooks, R. M., and McAneny, D. S. (In preparation). "Southern California Hindcast Wave Information," WIS Report 20.

Tracy, B. A., and Hubertz, J. M. (In preparation). "Hindcast Hurricane Swell for the Coast of Southern California," WIS Report 21.

(Continued)

Table 3-7. (Concluded)

Bibliographic Information

Great Lakes Reports

Resio, D. T., and Vincent, C. L. 1976 (January). "Design Wave Information for the Great Lakes; Report 1: Lake Erie," TR H-76-1.

Resio, D. T., and Vincent, C. L. 1976 (March). "Design Wave Information for the Great Lakes; Report 2: Lake Ontario," TR H-76-1.

Resio, D. T., and Vincent, C. L. 1976 (June). "Estimation of Winds Over Great Lakes," MP H-76-12.

Resio, D. T., and Vincent, C. L. 1976 (November). "Design Wave Information for the Great Lakes; Report 3: Lake Michigan," TR H-76-1.

Resio, D. T., and Vincent, C. L. 1977 (March). "Seasonal Variations in Great Lakes Design Wave Heights: Lake Erie," MP H-76-21.

Resio, D. T., and Vincent, C. L. 1977 (August). "A Numerical Hindcast Model for Wave Spectra on Water Bodies with Irregular Shoreline Geometry," Report 1, MP H-77-9.

Resio, D. T., and Vincent, C. L. 1977 (September). "Design Wave Information for the Great Lakes; Report 4: Lake Huron," TR H-76-1.

Resio, D. T., and Vincent, C. L. 1978 (June). "Design Wave Information for the Great Lakes; Report 5: Lake Superior," TR H-76-1.

Resio, D. T., and Vincent, C. L. 1978 (December). "A Numerical Hindcast Model for Wave Spectra on Water Bodies with Irregular Shoreline Geometry," Report 2, MP H-77-9.

Note:
All reports listed above were published by and are available from the US Army Engineer Waterways Experiment Station, Coastal Engineering Research Center, 3909 Halls Ferry Road, Vicksburg, MS 39180-6199

observed wave heights should be considered reliable up to about the one percent level of occurrence or the point at which 20 observations are represented, whichever criterion is more restrictive.

(3) Wave period is difficult to estimate aboard a moving ship, and only the overall mean period should be used. Wave directions are also somewhat difficult to estimate and should be assumed to have a resolution of 45 degrees or coarser.

3-4. Wave Hindcasting

WIS results may not be available for a specific time period of interest or wave measurements may not be available at the design site of sufficient quality or quantity to allow direct determination of the design wave. However, reasonable weather data are often available so this information may be used to hindcast waves. Waves that are generated by a storm are a function of the wind speed U, the duration of the storm t, and how large an area the storm covers, or fetch length F. Table 3-9 is a qualitative description of the sea state as a function of the wind speed and typical wave conditions. These descriptions are for a fully arisen sea state that requires a minimum duration to develop. These values should not be used for design, but rather to

appreciate various sea states.

a. Predictive methods.

(1) There are a variety of techniques and computer models available for predicting sea states as a function of storm conditions. The more complex models can provide estimates of wave height, wave period, and direction as well as the frequency distribution of energy. These types of models were used to generate the WIS results. However, there are cases where neither the time available nor the cost justifies using a complex numerical method. In these situations, simplified methods may be appropriate. The wave hindcasting method outlined in this manual follows the technique described in more detail in the Shore Protection Manual (1984). In this simplified technique, the significant wave height and period are estimated from the wind stress, storm duration, and fetch length.

(2) Unfortunately, there are a variety of locations (i.e., over land, over water, or different elevations) and techniques for presenting wind measurements. If measured wind speeds are provided, care must be taken to convert to the appropriate wind speeds for wave hindcasting. These corrections are given in the Shore Protection Manual (1984) in Chapter 3, Section IV. A
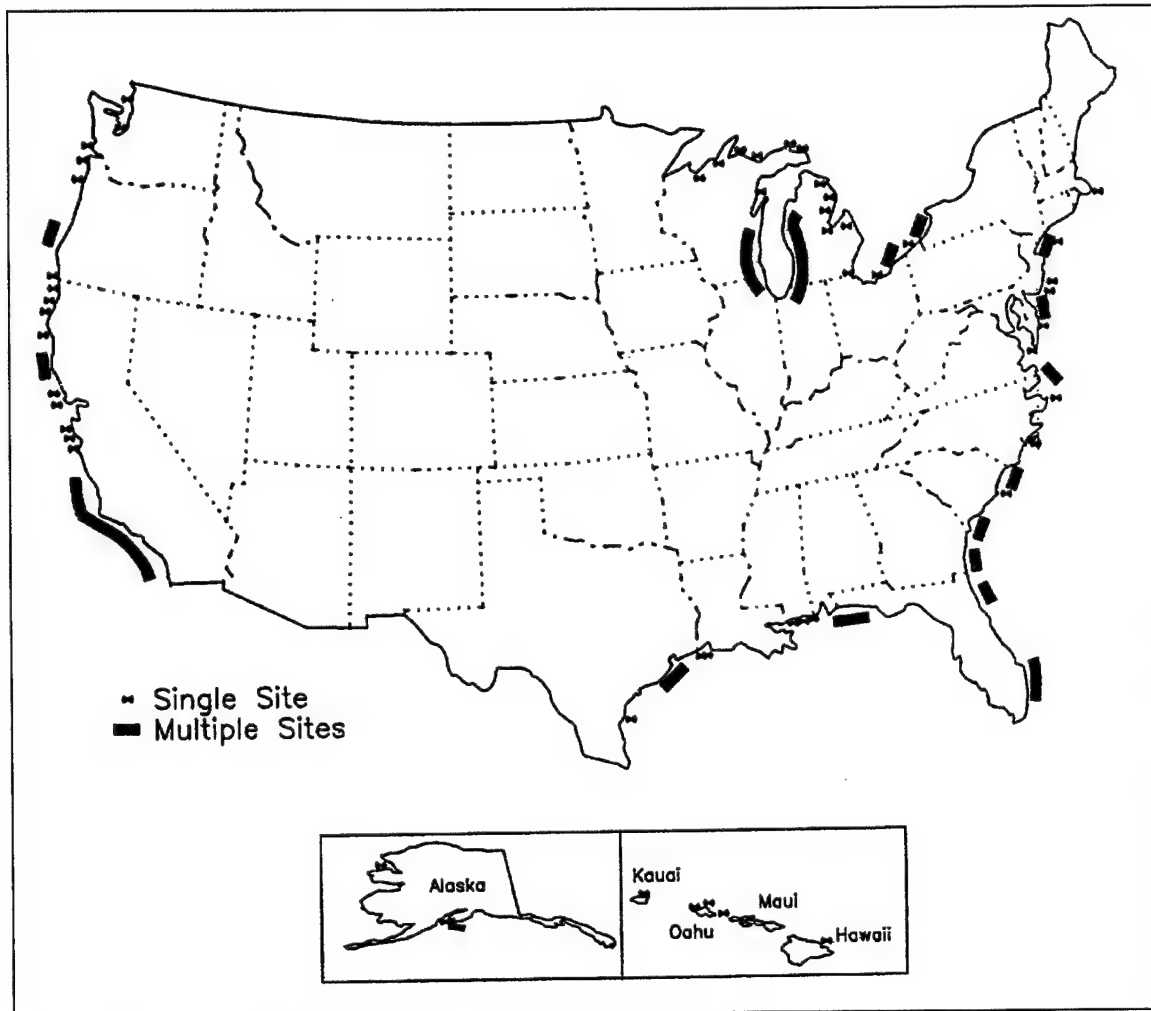
Figure 3-11. Leo sites

Table 3-8
NOAA Buoy Locations and Years (US Department of Commerce 1990)

Station No.	Latitude, °N	Longitude, °W	Years	Station No.	Latitude, °N	Longitude, °W	Years
	Great Lakes				*Gulf of Mexico* (Cont'd)		
45006	47.3	90.0	81-88	42001	29.6	93.5	81-84
45001	48.0	87.6	79-88	42008	28.7	85.3	80-84
45004	47.2	86.5	80-88	42002	26.0	93.5	76-88
45002	45.3	86.3	79-88	42001	25.9	89.7	75-88
45007	42.7	87.1	81-88	42003	26.0	85.9	76-88
45003	42.7	87.1	80-88				
45008	44.3	82.4	81-88		*Pacific*		
45005	41.7	82.5	80-88				
				46016	63.3	170.3	81-84
	Atlantic			46017	60.3	172.3	81-84
				46001	56.3	148.2	72-88
44007	43.5	70.1	82-88	46003	51.9	155.7	76-88
44005	42.7	68.3	78-88	46004	51.0	136.0	76-88
44013	42.4	70.8	84-88	46005	46.1	131.0	76-88
44003	40.8	68.5	77-84	46010	46.2	124.2	79-88
44011	41.1	66.6	84-88	46029	46.2	124.2	84-87
44002	40.1	73.0	75-80	46006	40.7	137.7	77-88
44008	40.5	69.4	82-88	46002	42.5	130.3	75-88
44012	38.8	74.6	84-88	46027	41.8	124.4	83-88
44004	38.5	70.7	77-88	46022	40.8	124.5	82-88
44001	38.7	73.6	75-79	46014	39.2	124.0	81-88
44009	38.5	74.6	84-88	46013	38.2	123.3	81-88
CHLV2	36.9	75.7	84-88	46026	37.8	122.7	82-88
41001	34.9	72.9	72-88	46012	37.4	122.7	80-88
41002	32.3	75.3	74-88	46028	35.8	121.7	83-88
41004	32.6	78.7	78-82	46011	34.9	120.9	80-88
41005	31.7	79.7	79-82	46023	34.3	120.7	82-88
41003	30.3	80.4	77-82	46024	33.8	119.5	82-84
41006	29.3	77.3	82-88	46025	33.6	119.0	82-88
				51001	23.4	162.3	81-88
	Gulf of Mexico			51003	19.2	160.8	84-88
				51002	17.2	157.8	84-88
42009	29.3	87.5	80-86	51004	17.5	152.6	84-88
42007	30.1	88.9	81-88				

common way to estimate the wind speed is from surface synoptic charts. These are available from the US Weather Service. An example synoptic chart is given in Figure 3-12. The pressure isobars are typically contoured at either 3 or 4 millibar (mb) intervals. This particular chart has a contour interval of 4 mb. Since the pressure is usually around 1000 mb, it is only necessary to record the last two digits of the pressure on the isobars. The pressure gradients indicated by the isobars are primarily due to density differences in the air. This pressure gradient is nearly in equilibrium with the Coriolis force produced by the rotation of the earth. The geostrophic wind is defined by assuming that an equilibrium or exact balance exists. The geostrophic wind blows approximately parallel to the isobars with low pressure to the left when looking in the direction of the wind in the northern hemisphere. In the southern hemisphere, the low pressure is on the right. The geostrophic wind is usually the best simple estimate of the wind speed. Figure 3-13 may be used to determine the geostrophic wind speed. The geostrophic wind speed depends on the latitude, the average pressure gradient across the fetch, and the isobar spacing on the synoptic chart.

(3) Once the geostrophic wind speed is known, several correction factors should be applied. The first of these, R_T, accounts for the air-sea temperature difference. This correction is given in Figure 3-14. If no temperature data are available, then use $R_T = 0.9$ for $T_a > T_s$, $R_T = 1.0$ for $T_a = T_s$, and $R_T = 1.1$ for $T_a < T_s$. The wave prediction curves are based on the wind speed measured at a 10-meter elevation. A correction must be applied to the geostrophic wind speed U_g to correct it

Table 3-9
Qualitative Sea State Descriptions (Meyers, Holm, and McAllister 1969)

Sea State	Description	Beaufort Wind Force	Description	U(kts)	H_s(ft)	T_p(s)
0	Sea like a mirror.	0	Calm	0	0	
1	Ripples with the appearance of scales are formed, but without foam crests.	1	Light airs	2.0	0.08	0.7
	Small wavelets, still short but more pronounced; crests have a glassy appearance, but do not break.	2	Light breeze	5.0	0.29	2.0
	Large wavelets, crests being to break. Foam of glassy appearance. Perhaps scattered white horses.	3	Gentle breeze	8.5	1.0	3.4
2				10.0	1.4	4.0
				12.0	2.2	4.8
	Small waves, becoming larger; fairly frequent white horses.	4	Moderate breeze	13.5	2.9	5.4
3				14.0	3.3	5.6
		5		16.0	4.6	6.5
	Moderate waves, taking a more pronounced long form; many white horses are formed (chance of some spray).		Fresh breeze	18.0	6.1	7.2
4				19.0	6.9	7.7
				20.0	8.0	8.1
5	Large waves begin to form; the white foam crests are more extensive everywhere (probably some spray).	6	Strong breeze	24.0	12.0	9.7
				24.5	13.0	9.9
6				26.0	15.0	10.5
	Sea heaps up and white foam from breaking waves begins to be blown in streaks along the direction of the wind (spindrift begins to be seen).	7	Moderate gale	28.0	18.0	11.3
				30.0	22.0	12.1
				30.5	23.0	12.4
				32.0	26.0	12.9
7	Moderately high waves of greater length; edges of crests break into spindrift. The foam is blown in well-marked streaks along the direction of the wind. Spray affects visibility.	8	Fresh gale	34.0	30.0	13.6
				36.0	35.0	10.3
				37.0	37.0	14.9
				38.0	40.0	15.4
				40.0	45.0	16.1
8	High waves. Dense streaks of foam along the directions of the wind. Sea begins to roll. Visibility affected.	9	Strong gale	42.0	50.0	17.0
				44.0	58.0	17.7
				46.0	64.0	18.6
		10	Whole gale	48.0	71.0	19.4
	Very high waves with long overhanging crests. The resulting foam is in great patches and is blown in dense white streaks along the direction of the wind. On the whole, the surface of the sea takes a white appearance. The rolling of the sea becomes heavy and shocklike. Visibility is affected.			50.0	78.0	20.2
				51.5	83.0	20.8
				52.0	87.0	21.0
				54.0	95.0	21.8
	Exceptional high waves (small and medium-sized ships might for a long time be lost to view behind the waves).	11	Storm	56.0	103.0	22.6
9	The sea is completely covered with long white patches of foam lying along the direction of the wind. Everywhere the edges of the wave crests are blown in froth. Visibility affected.			59.5	116.0	24.0
	Air filled with foam and spray. Sea completely white with driving spray; visibility very seriously affected.	12	Hurricane	>64.0	>128.0	(26)

Figure 3-12. Simplified surface synoptic chart (pressure contours in millibars)
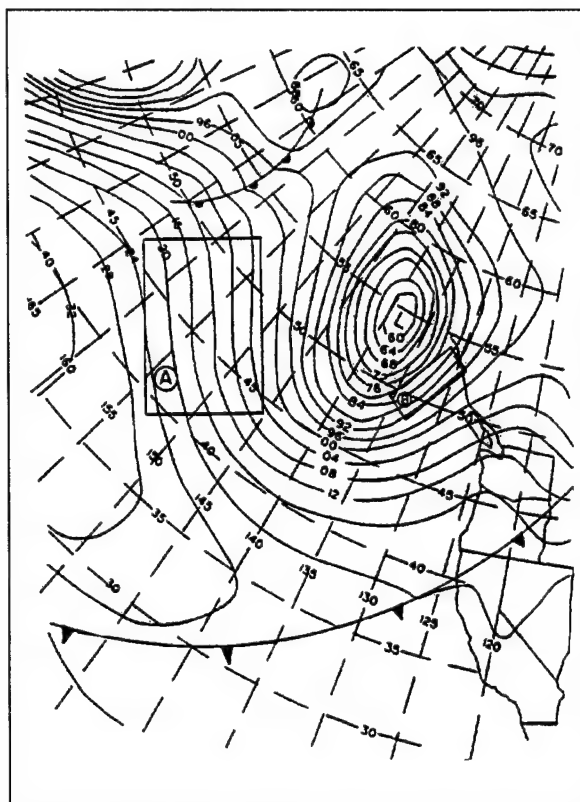
to the 10-meter wind speed U. This correction factor R_G is given in Figure 3-15. The temperature corrected 10-meter wind speed is given by

$$U = R_T R_G U_g \qquad (3-5)$$

Wave growth formula diagrams are expressed in terms of a wind stress factor U_A. Wind speed is converted to a wind stress factor by

$$U_A = 0.71 \ U^{1.23} \quad (U \text{ in m/sec}) \qquad (3-6)$$

(4) The fetch is the region over which the wind speed and direction are relatively constant. Results are best when variation of direction of the wind speed (assumed parallel to the isobars) does not exceed ±15 degrees. Direction deviations of 30 degrees should not be exceeded. Variations in the wind speed should not exceed ±2.5 meters/second from the mean. Since the wind speed is related to the isobar spacing, this implies that the spacing should be nearly constant across the

fetch. Using these rules, several fetches have been identified on the synoptic chart in Figure 3-12. Frequently, the discontinuity at a weather front will also limit a fetch. The fetch length is simply determined by measuring the length of the fetch and noting that 5 degrees of latitude = 300 nautical miles (nmi) = 555 kilometers.

(5) Estimates of the duration of the wind are also needed for wave prediction. Complete synoptic weather charts are prepared at only 6-hour intervals. Thus, interpolation to determine the duration may be necessary. Linear interpolation is adequate in most cases.

(6) With the estimates of the wind stress factor, wind duration, and fetch length available, the deep water significant wave height and peak spectral period may be determined from Figure 3-16, or with the Automated Coastal Engineering System (ACES) program "Windspeed Adjustment and Wave Growth" (see Appendix E). For a given wind speed, the wave height can either be limited by the fetch length or the duration of the storm.

*************** EXAMPLE 3-1 ****************

GIVEN: The wind stress factor is 20 m/sec (66 ft/sec), the fetch length is 90 km (49 nmi), and the storm duration is 5 hours.

FIND: Determine the significant wave height and peak spectral period.

SOLUTION: From Figure 3-16, two possible wave conditions can be estimated.

1) $U_A = 20$ m/sec (66 ft/sec) and $F = 90$ km (49 nmi) yield

$H_s = 3.0$ m (9.8 ft) and $T_P = 7.6$ sec

2) $U_A = 20$ m/sec (66 ft/sec) and $t = 5$ hours yield

$H_s = 2.5$ m (8.2 ft) and $T_P = 6.6$ sec

The smaller of these two should be selected. Since the duration yields the smaller wave, this wave is termed duration limited. If the duration had been greater than 6.5 hours, then the wave would have been fetch limited.

************** END EXAMPLE 3-1 **************
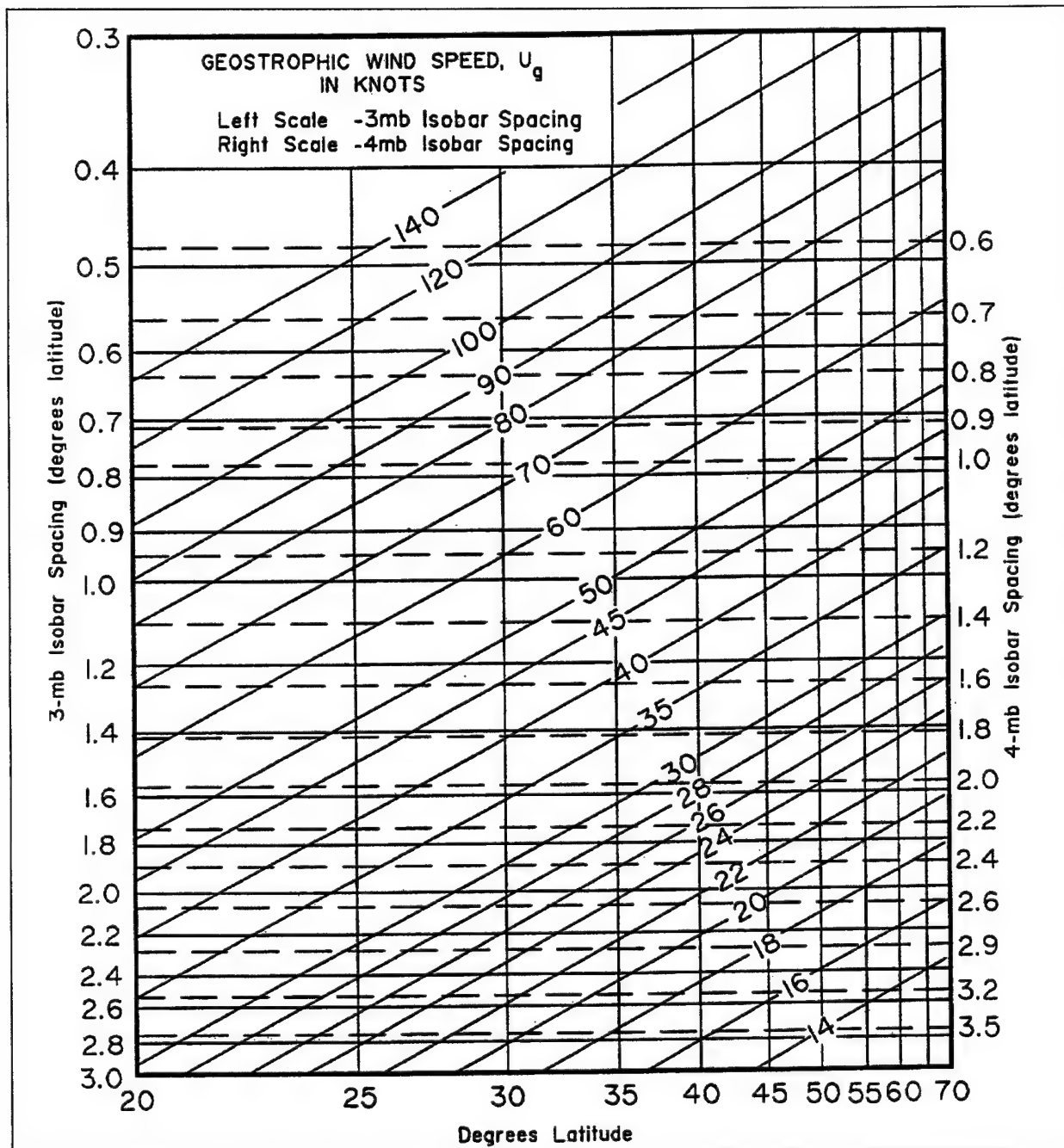
Figure 3-13. Geostrophic wind scale
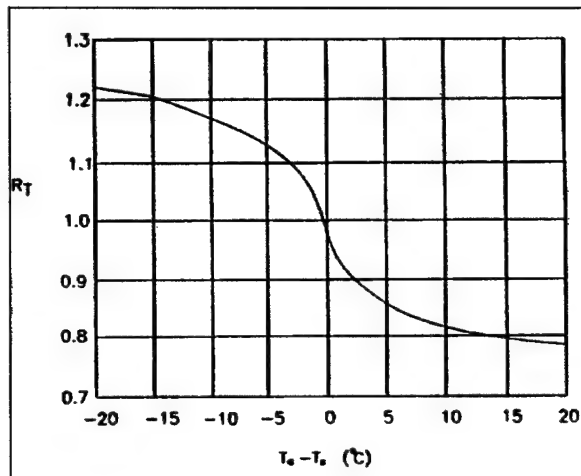
Figure 3-14. Correction factor for the air-sea temperature difference, $(T_a - T_s)$°C (after Resio and Vincent 1977)
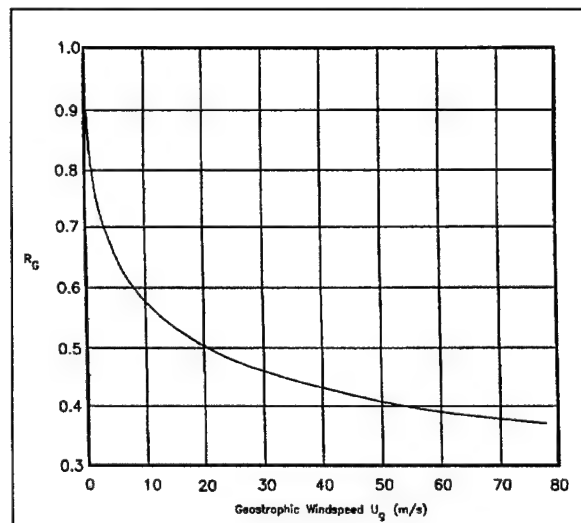
Figure 3-15. Correction factor to convert the geostrophic wind speed to the 10-meter elevation wind speed

*************** EXAMPLE 3-2 *****************

GIVEN: An examination of a series of synoptic charts indicated that the conditions in Figure 3-12 persisted for 10 hour. The air and sea temperature were reported at 9 °C and 11 °C, respectively.

FIND: Estimate the wave height and period generated by these weather conditions at approximately 54 °N 130 °W.

SOLUTION: This problem can be divided into four steps: delineate a fetch, calculate the geostrophic wind, calculate the wind stress, and estimate the wave conditions.

1) Fetch - The appropriate fetch for this location is fetch B in Figure 3-12. Noting that 5° latitude = 555 km (300 nmi), the fetch length is

$$F = 600 \text{ km (328 nmi)}$$

2) Geostrophic Wind - The fetch width w and pressure change Δp are

$$w = 1.9 \text{ °lat}$$
$$\Delta p = 12 \text{ mb}$$

The isobar spacing s on this synoptic chart is

$$s = 4 \text{ mb}$$

The pressure gradient across the fetch is

$$p_g = \frac{w(\text{°lat})}{\Delta p(mb)} \ s(mb) = \frac{1.9}{12} \ 4 = 0.63 \text{ °lat}$$

The center of the fetch is at 52 °N. Figure 3-13 gives

$$U_g = 75 \text{ knots} = 38.6 \text{ m/sec}$$

3) Wind Stress - The air-sea temperature difference is

$$T_a - T_s = 9 - 11 = -2 \text{ °C}$$

Figure 3-14 yields

$$R_T = 1.07$$

For $U_g = 38.6$ m/sec, Figure 3-14 gives

$$R_G = 0.44$$

The corrected wind speed is determined from Equation 3-5
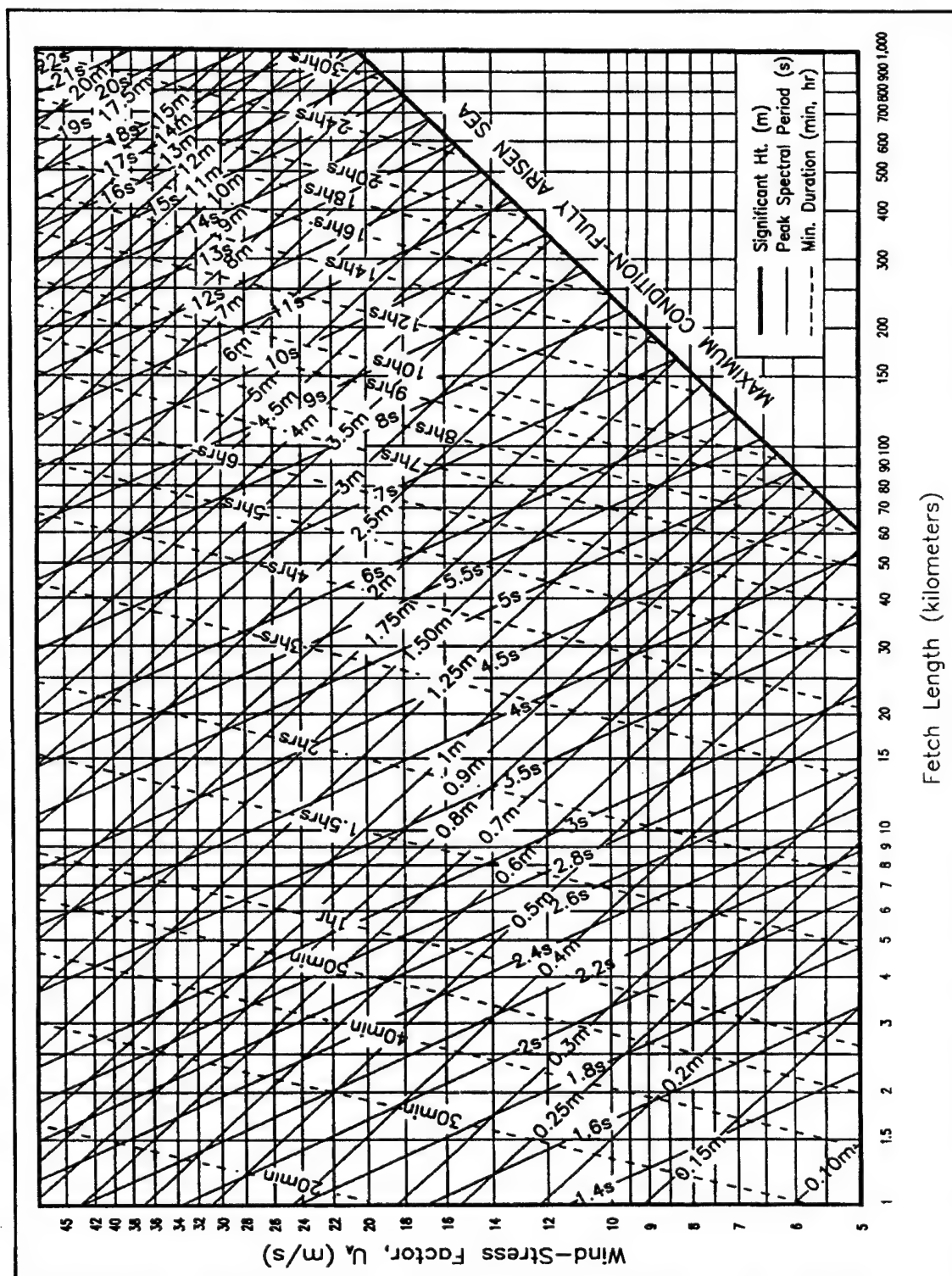
Figure 3-16. Nomograms of deepwater significant wave prediction as a function of the wind stress factor, fetch length, and wind duration

$U = R_T\,R_G\,U_g = (1.07)(0.44)(38.6) =$
18.2 m/sec (59.7 ft/sec)

This is converted to a wind stress using Equation 3-6

$U_A = 0.71\ U^{1.23} = 0.71\ (18.2)^{1.23} = 25.2$
m/sec (82.7 ft/sec)

4) Wave Prediction - For U_A = 25.2 m/sec (82.7 ft/sec), F = 600 km (328 nmi) and t = 10 hours, the significant wave height and peak period are estimated from Figure 3-15.

H_s = 5.4 m (17.7 ft) T_P = 10.3 sec

************** END EXAMPLE 3-2 **************

3-5. Wave Transformations

As waves propagate from the deep water generation area to the design site, they undergo a number of transformations. The local waves in the generation area are referred to as seas. Local seas are typically steeper and short crested. As they propagate, they become more regular and transform into longer period, lower wave height swell. Long period waves propagate faster than short period waves. After traveling several thousand kilometers, this transformation yields a more peaked spectrum (narrow frequency range) for swell waves. Figure 3-17 may be used to estimate swell period as a function of travel distance. Use of these curves requires the wave period leaving the fetch, T_F (seconds), the minimum fetch, F_{min} (nmi), and the travel distance, D (nmi). In the case of a fetch limited storm, the minimum fetch corresponds to the actual fetch. For a duration limited storm, F_{min} corresponds to the fetch length at the duration limit. These curves should be used only as an indicator of wave period increase with travel distance.

**************** EXAMPLE 3-3 ***************

GIVEN: A storm with F_{min} = 740 km (400 nmi) generates waves with T_F = 10 s.

FIND: Estimate the swell conditions for a travel distance of 3700 km (2000 nmi).

SOLUTION: The conditions for this example are shown on Figure 3-17. The decayed wave period is

$T_D/T_F = 1.28$; $T_D = 12.8$ s

************* END EXAMPLE 3-3 **************

a. Nearshore. As the waves approach the shoreline, they will be modified by interactions with the bottom. These modifications are shoaling, refraction, diffraction, dissipation, and breaking. The local wave height H is given by

$$H = K_s\,K_R\,K_D\,K_F\,H_O \qquad (3\text{-}7)$$

where K_S is the shoaling coefficient, K_R is the refraction coefficient, K_D is the diffraction coefficient, K_F is the dissipation coefficient, and H_0 is the deep water wave height.

(1) Shoaling is the change in wave height required for the conservation of wave energy flux to balance the change in the group velocity as the waves enter shallower water. The linear wave theory shoaling coefficient K_s is given by

$$K_S = \tanh(kd)\left(1 + \frac{2kd}{\sinh(2kd)}\right)^{-\frac{1}{2}} \qquad (3\text{-}8)$$

in which k is the wave number (= $2\pi/L$) . Tabulated values of the shoaling coefficient are given in Appendix C of the Shore Protection Manual (1984).

(2) Refraction is the bending of wave crests due to phase speed differences associated with different water depths. Refraction is a site specific wave transformation. If the bottom contours are straight and parallel, and the waves are normally incident to the shoreline, then no refraction occurs. If the contours are straight and parallel (this does not require a planar slope) and the waves approach at an angle, then analytical estimates of wave refraction are available. Combined refraction and shoaling coefficients for monochromatic waves are given in Figure 3-18 for straight and parallel bottom contours. Figure 3-18 also gives the angle of the wave crest to contour (local wave angle), α.

(3) Refraction of random seas depends on the peakedness of the spectrum. Even if the predominant wave direction is normal to the coastline, there will be refraction. This is due to the refraction of waves with directions other than the predominant direction. This effect decreases for narrow spectra. Refraction coefficients K_R for random seas on a coast with straight and parallel depth contours given a predominant deepwater
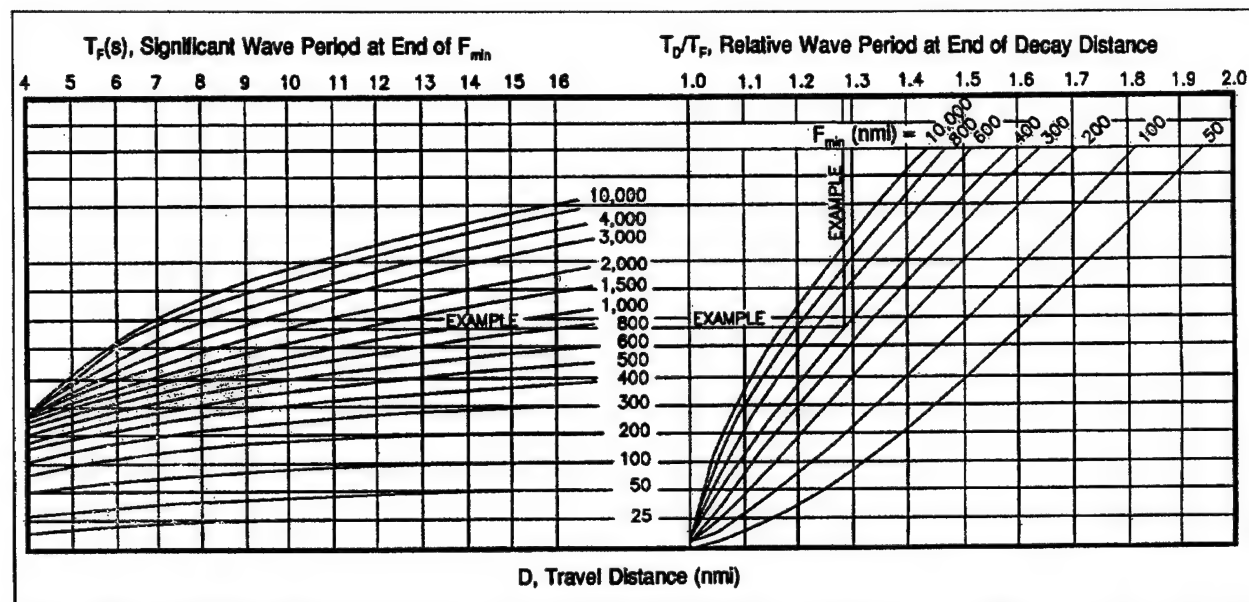
Figure 3-17. Wave period decay curves

direction $(\alpha_0)_P$ are given in Figure 3-19. The refraction angle of the predominant direction α_P is given in Figure 3-20. Several numerical shoaling and refraction models are listed in Appendix E.

(4) If the bottom contours cannot be approximated as straight and parallel, then graphical or numerical techniques must be employed to determine the refraction coefficient. The graphical template method is described in detail in the Shore Protection Manual (1984) in Chapter 2, Section III. This method may be used to construct wave rays to determine local refraction coefficients.

(5) Diffraction is the lateral transfer of wave energy due to variations in wave height along the crest. Diffraction is also a site specific wave transformation. Waves may be diffracted by surface piercing structures such as headlands, jetties, and breakwaters, or by bottom topography such as shoals and reefs. If these types of features exist near the design site, then diffraction effects must be considered. Graphical results for diffraction around the end of surface piercing structures are presented in the Shore Protection Manual (1984) for monochromatic waves and constant depth (Chapter 2). Similar graphs for random seas are presented in Chapter 7.

(6) Models of combined refraction and diffraction

have been developed based on the parabolic equation method (Berkoff 1972). A review of these models is given in Liu, et al. (1986). This approach is generally limited to mild bottom slopes. However, this method represents a significant improvement in the determination of nearshore waves. The computer model RCPWAVE is based on this formulation (Ebersole, Cialone, and Prater 1986) (see Appendix E for a brief description). These combined refraction-diffraction models are not routinely employed on smaller projects.

(7) Dissipation is the loss of wave energy as the waves propagate shoreward. This is the result of viscosity, turbulence, bottom friction, percolation in the bottom, and wave-induced motion of the seabed. The importance of this wave dissipation is site specific. Along the Pacific coast of the continental United States, where the continental shelf is narrow, this loss of wave energy tends to be rather small. On coastlines with wide continental shelves, this dissipation may be significant. Numerical wave propagation models, such as those used in the WIS program, can incorporate this effect.

(8) Wave breaking is one of the most important wave transformations in the determination of nearshore
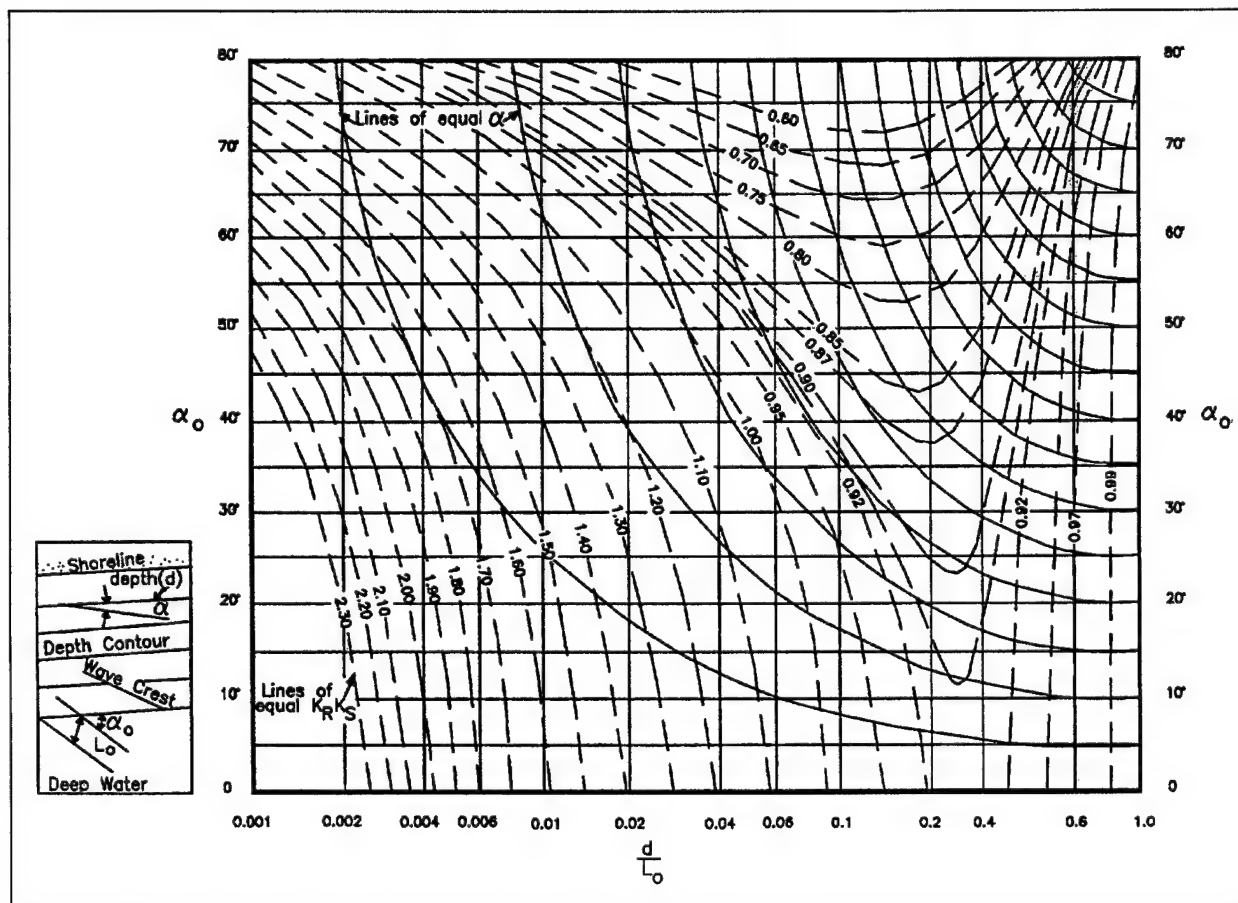
Figure 3-18. Change in monochromatic wave height and direction due to refraction and shoaling for straight and parallel bottom contours
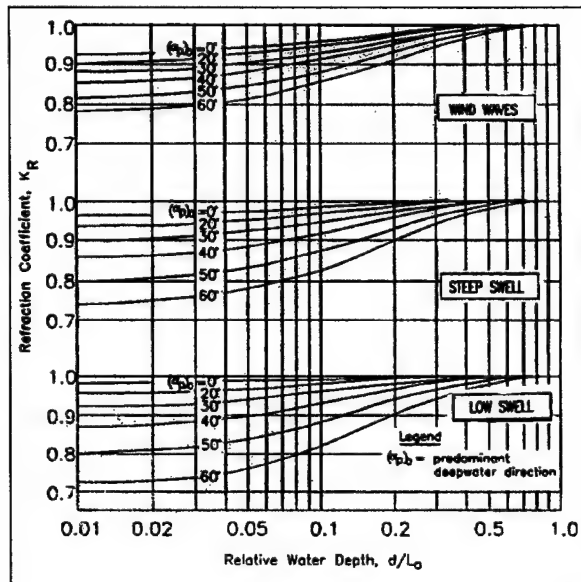
Figure 3-19. Refraction coefficients from random sea waves on a coast with straight and parallel bottom contours (Goda 1985)

currents and sediment transport. Unfortunately, wave breaking is not well understood. Models developed from the work of Longuet-Higgins and Cokelet (1976) show promise for quantifying the kinematics in near-breaking waves. However, these models have not evolved to a level that they can be used in routine design. Other models have been developed on the basis of momentum or energy flux (Peregrine and Svendsen 1978; Thornton and Guza 1983; Dally, Dean, and Dalrymple 1984). The Dally model is incorporated in RCPWAVE.

(9) The use of empirical curves remains a common method for estimating breaking wave conditions. Figures 3-21 and 3-22 provide a means of estimating the breaking wave height H_b and breaking depth d_b as a function of the wave steepness H_0'/L_0, where H_0' is the unrefracted deepwater wave height, and bottom slope m. Since refraction is site specific, this is a contrived method to remove this dependency. The deep water wave is shoaled and refracted onshore. It is then shoaled back out to sea without refraction to yield H_0'. This procedure enables curves for nearshore processes to be represented by the unrefracted deep water wave height.

(10) Breaking waves are often classified as spilling, plunging, or surging. Figure 3-21 shows the conditions for which these types of breakers occur. Profiles of these breaker types are given in Figure 3-23.
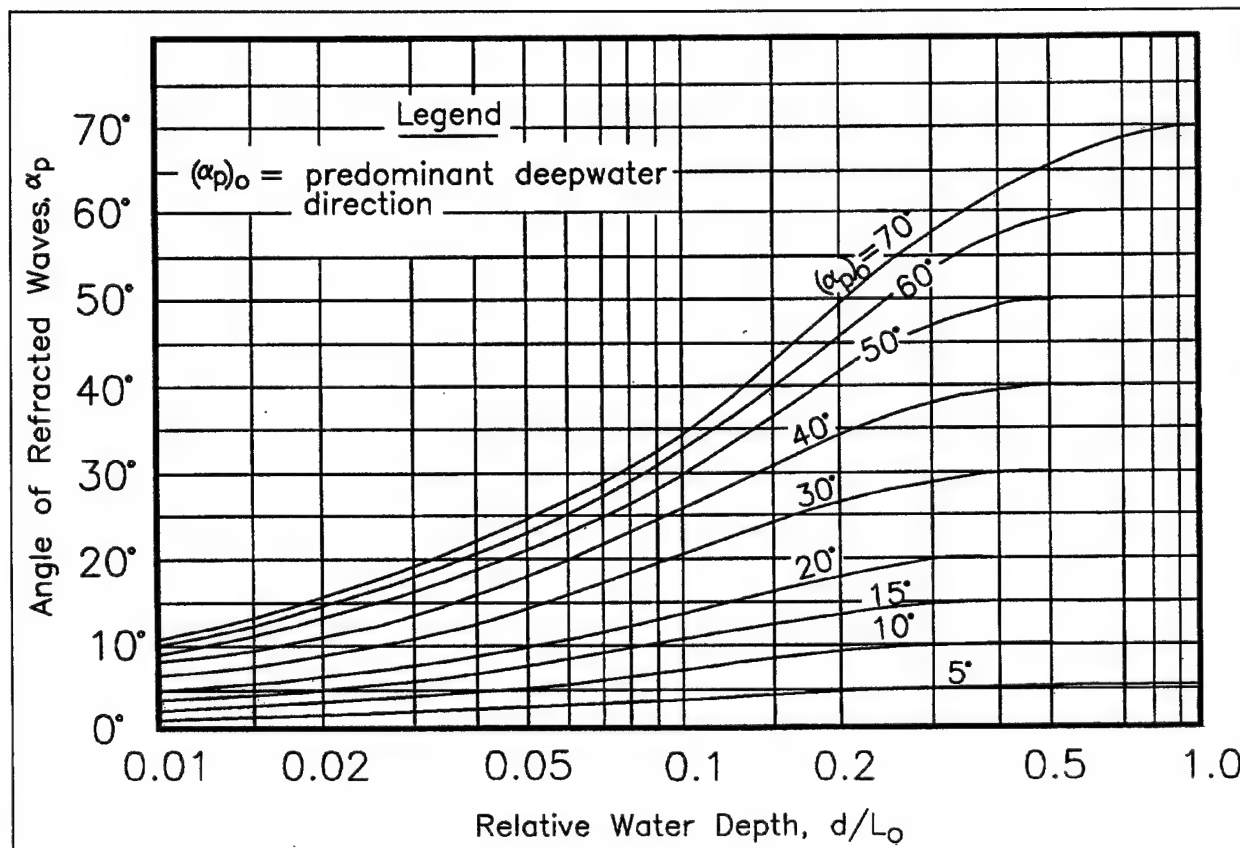
Figure 3-20. Variation of predominant wave direction for random sea waves on a coast with straight and parallel bottom contours (Goda 1985)
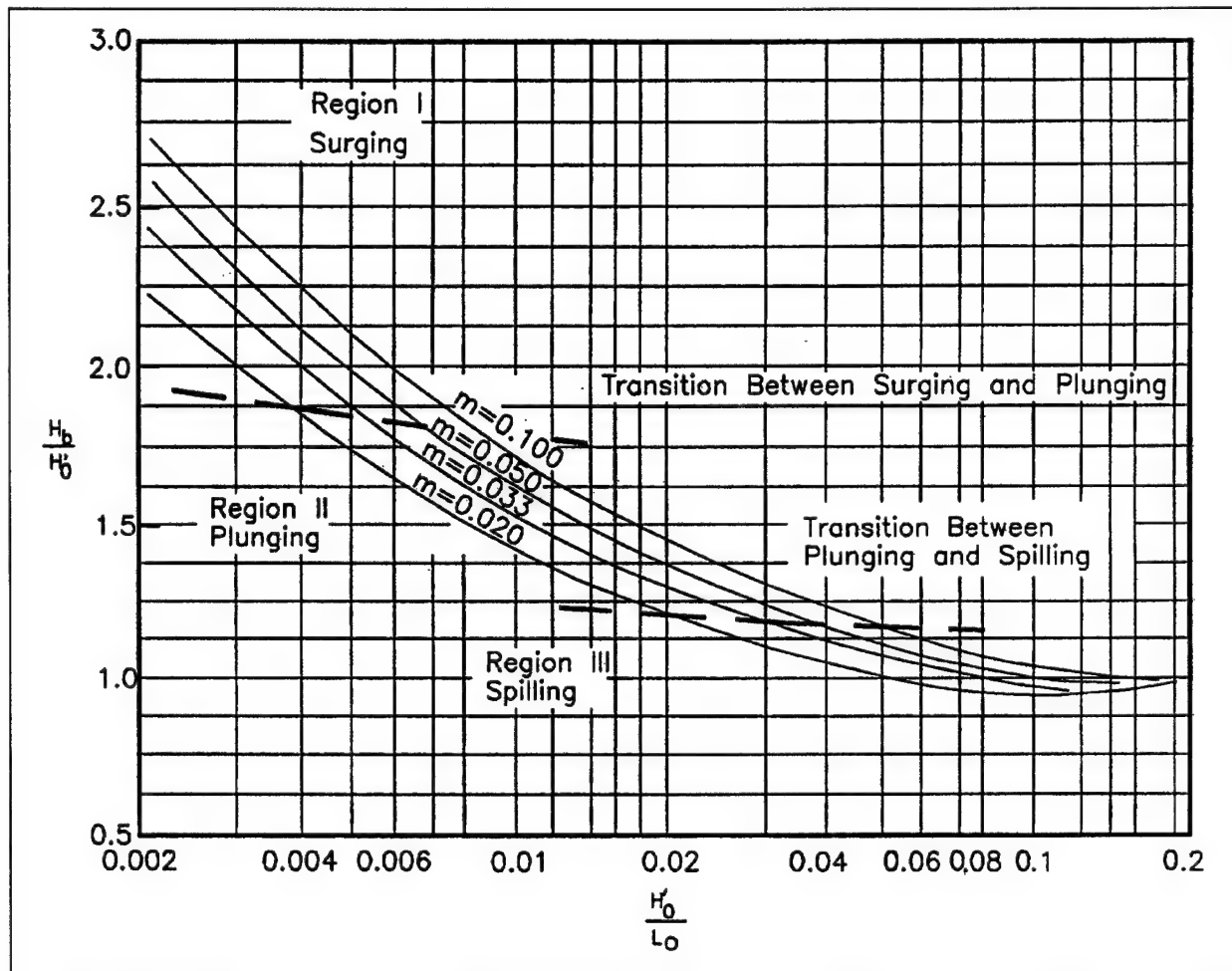
Figure 3-21. Breaker height dependency on wave steepness and bottom slope
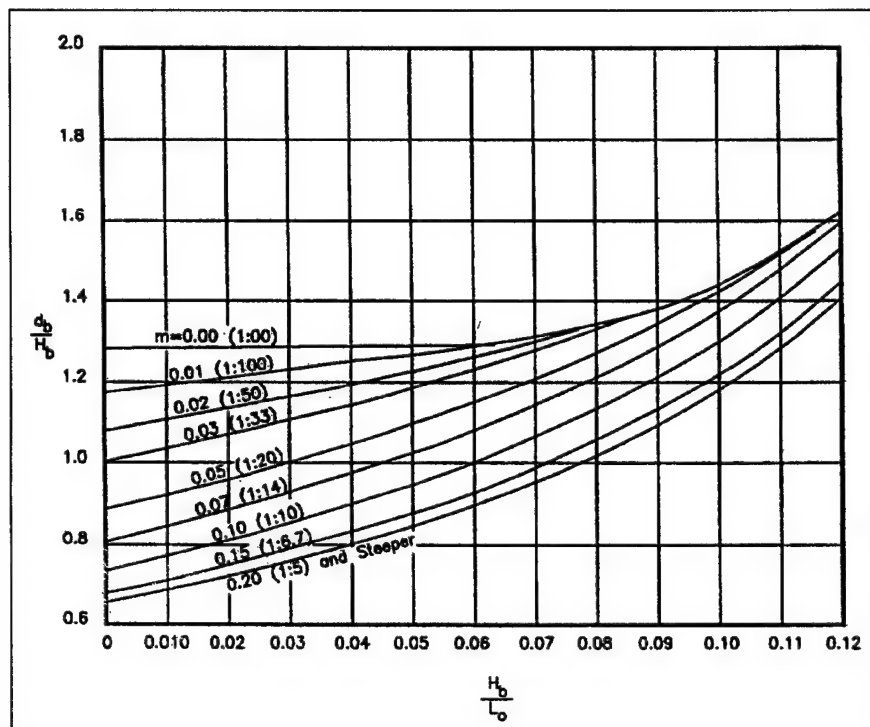
Figure 3-22. Breaker depth dependency on wave steepness and bottom slope
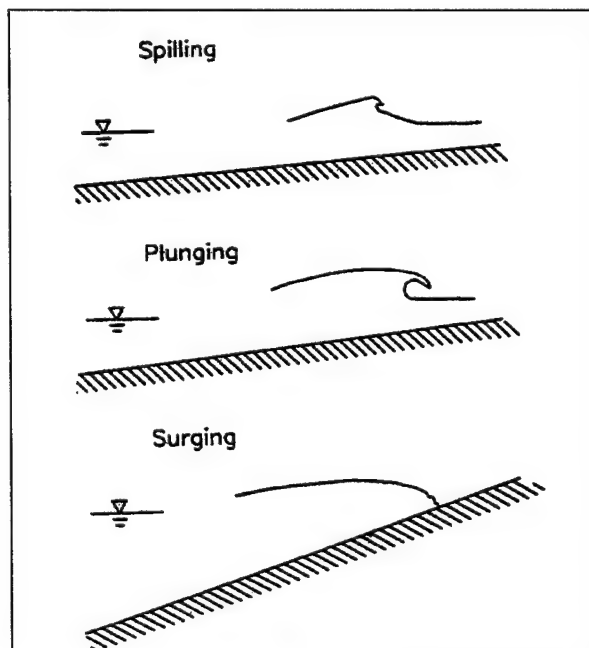
Figure 3-23. Breaking wave profiles

Chapter 4
Littoral Processes

4-1. Littoral Materials

a. Sources.

(1) The responses of a specific beach depend mainly on the composition and grain sizes of the sediment and on the nature and intensity of the nearshore waves and currents. The sediment may consist of any material that is available in significant quantities and is of a suitable grain size. Most beaches in temperate regions are composed principally of quartz and feldspar grains. These are derived ultimately from the weathering of granitic-type rocks that are abundant on the continents. In addition to the quartz and feldspar ("light minerals"), beach sands generally also contain small amounts of "heavy minerals" such as hornblende, garnet, and magnetite, also derived from the original source rocks. The light versus heavy minerals are defined on the basis of their specific gravities and are listed in Table 4-1. More often they are distinguished in the beach sands by color since the quartz and feldspars are tan, cream, or transparent, whereas the heavy minerals are generally dark (black, red, dark green, etc.). Individual sand grains may consist of more than one mineral type, possibly incorporating both light and heavy minerals. This composite nature becomes more important as the grain size increases, such that most pebbles are small rock fragments.

(2) Shells may represent an important fraction of the beach materials, especially in the tropics where biological productivity is high and chemical weathering of rocks tends to be intense. Shell material may also be abundant because the supply of terrigenous sands is either very low or of the wrong grain size for the particular beach. For example, the shell content of beaches along the southern Atlantic coast of the United States shows a general increase from north to south because of increasing biological productivity and decreasing supply of quartz-feldspar sand to the south. Shells and the derived sands are composed of the minerals calcite or aragonite, whose specific gravities are not much different from quartz and feldspar (Table 4-1). The littoral sediments of volcanic islands commonly consist entirely of fragments of basalt lavas or individual minerals derived from the lavas. Well known are the green-sand and black-sand beaches of Hawaii; the green sands contain a high percentage of the mineral olivine derived

Table 4-1
Density of Typical Beach Materials

	Specific Gravity (dimensionless)	Color
Light Minerals:		
Quartz	2.65	Colorless, white
Feldspars	2.65-2.76	Colorless, white, light brown
Calcite	2.71	White, yellow, brown, pink
Aragonite	2.93	White, yellow, brown, pink
Heavy Minerals:		
Hornblende	3.0-3.4	Dark green, brown, black
Epidote	3.3-3.6	Green to black
Garnet	3.6-4.3	Red, pink, reddish brown, green
Augite	3.3-3.5	Dark green
Tourmaline	3.0-3.2	Blue, pink, brown, black
Magnetite	5.2	Opaque black
Ilmenite	4.7-4.8	Opaque black

from volcanic rocks, and the black-sand beaches consist of fresh microcrystalline lava and volcanic glass.

b. Size.

(1) The grain sizes of beach sediments range from large cobbles to fine sand. Terms such as cobbles, pebbles, and sand refer to specific ranges of grain sizes. Figure 4-1 shows the Wentworth Classification where sand encompasses the diameter range 0.0625 to 2 mm, but its category is further subdivided into very fine sand to very coarse sand. The size limits are based on a geometric series involving exponents of 2. For example, the limits for sand are $2^{-4} = 0.0625$ mm and $2^1 = 2$ mm. Geologists use the exponents as a measure of grain size, defining the phi (ϕ) scale as

$$D = 2^{-\phi} \qquad (4\text{-}1a)$$

or

$$\phi = -\log_2 D = -3.3219 \log_{10} D \qquad (4\text{-}1b)$$

where the grain diameter D is in millimeters. By this scale, the limits of the sand range are $\phi = -1$ and 4; note that the higher the value of ϕ, the smaller the grain size so that negative values of ϕ represent the coarsest sizes.

Figure 4-1. Wentworth and φ grain size scales

by the geology. The importance of source is obvious. Rocks such as granite tend to weather and break down into their constituent minerals. These form the sand-sized grains of quartz, feldspars, and heavy minerals. These small grains can be transported by rivers for thousands of miles from their original sources prior to being delivered to a beach. Coarser pebbles and cobbles are derived from the physical fragmentation of source rocks and will have the same compositions and densities as the original rocks. Beaches consisting of pebbles and cobbles are generally close to the rock sources.

(4) The beach environment will preferentially select the grain sizes that are appropriate for its particular wave energy level and slope. There is a general tendency for the high-energy beaches (those with the largest waves) to have the coarsest sediments. However, a simple correlation between grain size and energy level for all beaches cannot be made. This is apparent when one recognizes that medium-sand beaches may be found in lakes with very small waves, as well as on high-energy ocean beaches. Headlands often have small pocket beaches of cobbles and boulders, while nearby beaches between headlands are composed of sand. This may be due in part to the higher energy levels on the headland beaches, but also of importance is the general offshore slope upon which the beaches are formed and on the slope of the beach itself.

(5) A sample of beach sediment could contain a distribution of grain sizes that might range, for example, from sand through pebbles. If there is a single mode of sizes within the distribution, then the overall distribution can be characterized by statistical parameters such as the median and mean diameters and the standard deviation which describes the degree of sorting of the sediment. Calculations of these statistical parameters are described in the SPM (1984). Many beach sediments are bimodal, consisting of a sand mode and a separate pebble or cobble fraction. In such cases, separate statistical parameters should be determined for the individual modes.

Figure 4-1 gives the limits for the entire list of grain-size terms for the Wentworth Classification.

(2) The term gravel has common usage which roughly corresponds to combined granules, pebbles, and cobbles of the Wentworth Classification, and it will be used in that sense here. Gravel has a more specific designation in the Unified Soils Classification where it denotes sizes between 4.76 mm (-2.25φ) and 76 mm (-6.25φ) (SPM 1984).

(3) There are three main factors that control grain sizes of sediments found on a particular beach: (a) the source(s) of the sediment, (b) the wave energy level, and (c) the general offshore slope as governed primarily

(6) The distribution of grain sizes affects the porosity and permeability of the beach sediments. Porosity relates to the volume fraction of pore spaces between the solid grains and depends more on the distribution of grain sizes and their packing arrangement than on the absolute sizes of the particles. For most beach sands the porosity, n, is approximately $n = 0.4$. That is, 40 percent of the bulk sediment volume is pore space whereas the remaining 60 percent consists of solid

sediment grains. Permeability depends in part on the porosity, but it is a distinct property of the bulk sediment and also depends on the sediment size. Although the porosities of a gravel beach and a sand beach may be effectively the same, the permeability of the gravel beach will be much greater. Accordingly, the water from the wave runup on a gravel beach will tend to percolate down into the beach face, whereas the percolation into a sand beach is comparatively minor.

4-2. Beach Morphology and Littoral Processes

a. Beach face slope.

(1) The overall slope of the beach face tends to increase with sediment grain size. This dependence is illustrated in Figure 4-2 which relates the slope of the beach face to the median grain size of sediments collected at the midtide level. The slope of the beach face under the action of wave swash is governed by the asymmetry of the intensity of the onshore swash versus the strength of the offshore backwash. Because of the asymmetry of the incident waves, friction, and water percolation into the beach, the return backwash tends to be weaker than the shoreward uprush. This flow asymmetry moves sediment onshore until a slope is built up in which gravity supports the backwash and offshore sediment transport. When the same amount of sediment is transported landward as is moved seaward, the beach-face slope becomes constant and is in a state of dynamic equilibrium. This final slope will depend on the amount of water lost through percolation into the beach. This rate of percolation is governed principally by the grain size of the beach sediments and, as noted above, is much greater for a gravel beach than for a fine sand beach. The result is that the return backwash on a gravel beach is much reduced in strength, and its slope is accordingly much greater than that for beaches composed of fine sand.

(2) Separate trends are seen in Figure 4-2 for high-energy versus low-energy beaches, a division in the data sets between U.S. west and east coast beaches. For a specific grain size, the low-energy beaches have greater beach face slopes than the high-energy beaches. Also included in Figure 4-2 is a series of data points from Halfmoon Bay, California. This bay is partially sheltered by a headland (see Figure 4-3) which produces a gradient of wave energy and beach face sand sizes along the shore. The wave energy is lowest close to the headland and progressively increases as sheltering of the headland is lost. There is a corresponding change in grain sizes, tabulated in Figure 4-3, with the finest sand

found close to the headland where the beach has maximum protection from the waves. The sheltered beach has the lowest slope, due to the combined effects of finer grain sizes and the lower wave energy level. As plotted in Figure 4-2, the measurements from Halfmoon Bay are seen to progressively shift from the curve for low-energy beaches to that for high-energy beaches due to the longshore gradient of wave energy.

b. Profile shape. On most coastlines there are seasonal variations in wave energy, and this produces a change in the slope of the beach and in the overall form of profile. This shift is illustrated schematically in Figure 4-4, characterized in terms of a storm profile versus a swell profile. The terms winter profile and summer profile are also commonly used to denote this change, reflecting its seasonality on many coasts. However, the response is to high-energy, irregular storm waves versus low, regular swell waves, and the shifts illustrated in Figure 4-4 can occur irrespective of season. A specific example of profile response to an individual storm is illustrated in Figure 4-5, based on data obtained at the Coastal Engineering Research Center (CERC) Field Research Facility (FRF) at Duck, North Carolina. Four distinct storms occurred at about a weekly interval, causing a bar to move offshore a total of 172 m (564 ft). The first three storms had a negligible effect on the profile above MSL. Only storm 4, which coincided with a high spring tide and generated the highest waves, caused the upper beach to erode and produced a landward displacement of the MSL line on the profile. As illustrated in Figure 4-4, the high wave energies of many storms combine to cut back the beach face and eliminate most or all of the berm, transporting the eroded sand seaward where it is deposited in the form of offshore bars. The return of low regular waves reverses the process, moving the sand shoreward where it accumulates as a new berm. The slope of the high-energy storm profile is less than that of the low-energy swell profile. This change agrees with the data trends established in Figure 4-2, where it is also seen that seasonal measurements from the Fort Ord and "landing barge" beach sites specifically document changes in beach face slopes while maintaining the same median grain size.

c. Beach profile state.

(1) Empirically based equations or criteria have been developed to predict the beach profile state, or more directly, erosion and accretion, in terms of simple environmental parameters such as wave height, wave period, wave steepness, grain size, and sediment fall speed.
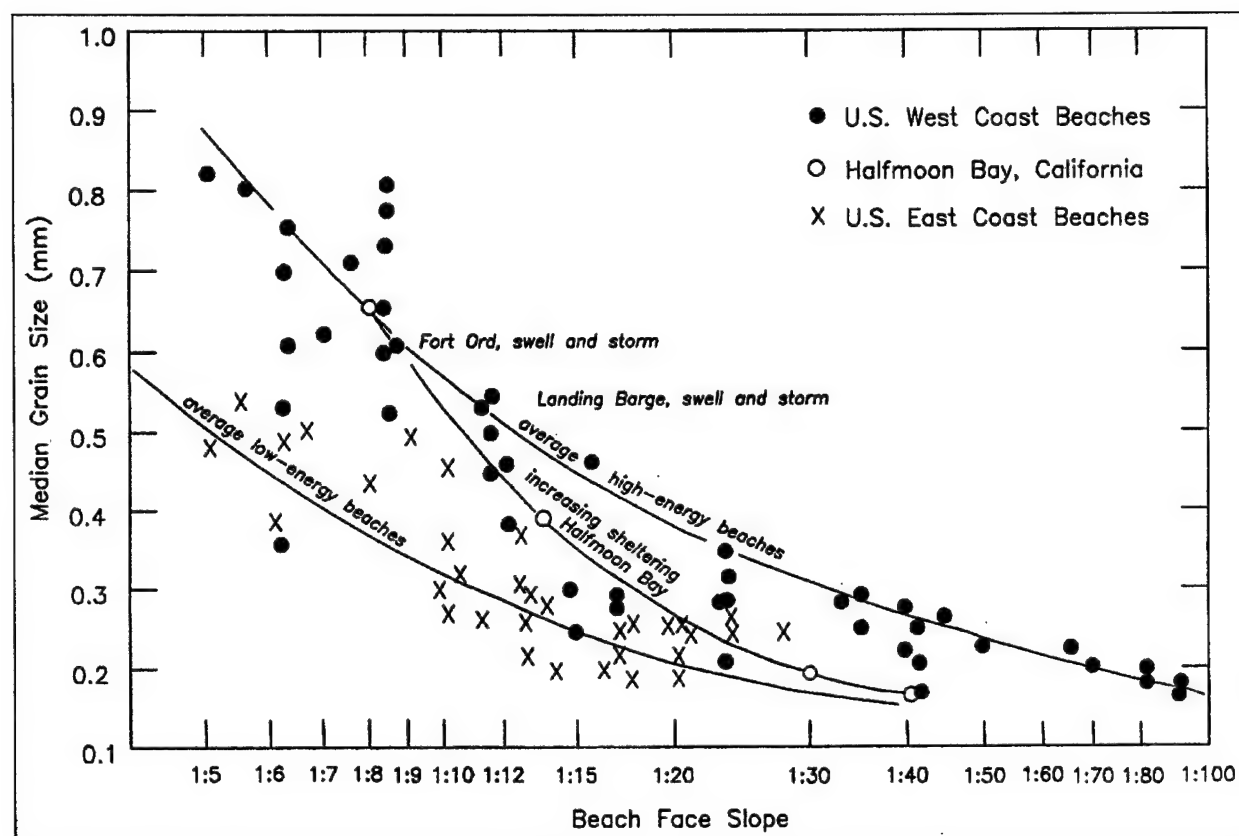
Figure 4-2. Beach face slope dependency on grain size and wave energy

Kriebel, Dally, and Dean (1987), Larson and Kraus (1989), and Kraus, Larson, and Kriebel (1991) have reviewed and compared many of these expressions. An important conclusion from these and similar studies is that experience with profile change in small-scale laboratory experiments cannot be transferred directly to the field situation because of "scale effects," meaning that the absolute sizes of the sand grains and wave height control beach state.

(2) Prediction of beach profile state has practical application to estimate, for example, the stability of natural beaches and beach fills. An important question to be answered is whether beach material of certain grain size will erode or accrete by cross-shore sediment transport under waves of certain characteristics. The subject concerns change in profile state of engineering significance such as that produced by storms and predominant summer and winter wave conditions; the many small changes in the profile that occur hourly and daily

are not expected to be predictable without detailed modeling of the many processes involved.

(3) The term "erosion" describes removal of material from the visible beach by wave action, often to produce a gentle slope in the surf zone and one or more large longshore bars in the offshore. The term "accretion" describes sand accumulation in the form of one or more berms on the visible beach and, typically, a steep profile in the surf zone. Although the terms erosion and accretion commonly refer to the response of the visible beach, material is not necessarily lost from or gained by the system but only displaced and rearranged along the beach profile extending from the dune crest to a water depth where no significant net sediment movement occurs. Surveys of wide longshore and cross-shore extent are required to determine if a beach has experienced a net loss or gain of material. Discussion is restricted to beach profile change produced by waves normally or near-normally incident to an open coast.
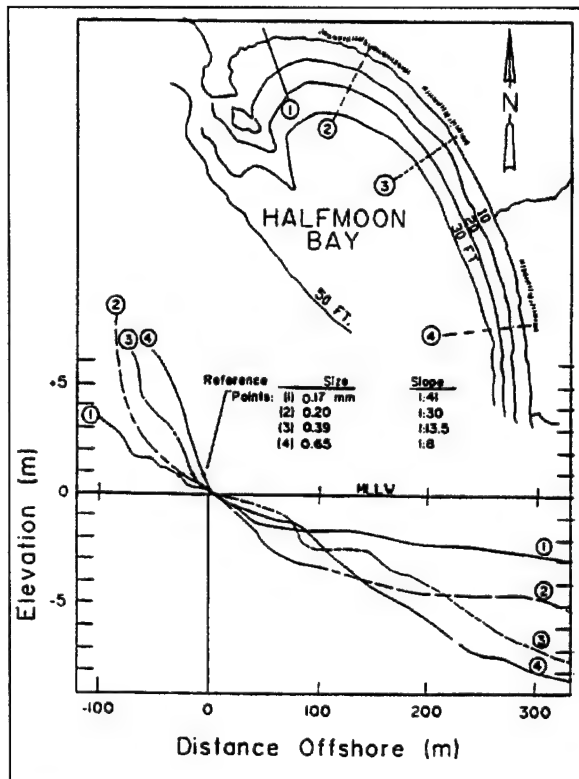
Figure 4-3. Systematic changes in the beach face slope along the length of Halfmoon Bay, California (after Bascom 1951)

(4) Laboratory and field measurements have indicated that the following variables determine in great part whether a beach will erode or accrete: deepwater wave height, H_o; wave period, T; and sediment particle fall speed, w (obtained from knowledge of the median grain diameter d_{50} and water temperature). The three quantities H_o, T, and w can be arranged in several ways in the form of two nondimensional ratios. The two nondimensional ratios used here are

$$\text{deepwater wave steepness} \quad S_o = \frac{H_o}{L_o} \quad (4\text{-}2a)$$

$$\text{deepwater fall speed parameter} \quad N_o = \frac{H_o}{w\,T} \quad (4\text{-}2b)$$

in which $L_o = gT^2/2\pi$ is the wavelength in deep water and g is the acceleration due to gravity ($g = 9.81$ m/sec^2 = 32.2 ft/sec^2). In metric units, $L_o = 1.56\,T^2$ (m) whereas in American Customary units, $L_o = 5.12\,T^2$ (ft), for which T is given in seconds.

(5) For predominantly quartz sand beaches, a sieve-determined median diameter may be an adequate description of grain size. However, the sediment particle fall speed w provides a more general representation of "hydraulic" grain size and can account for the effect
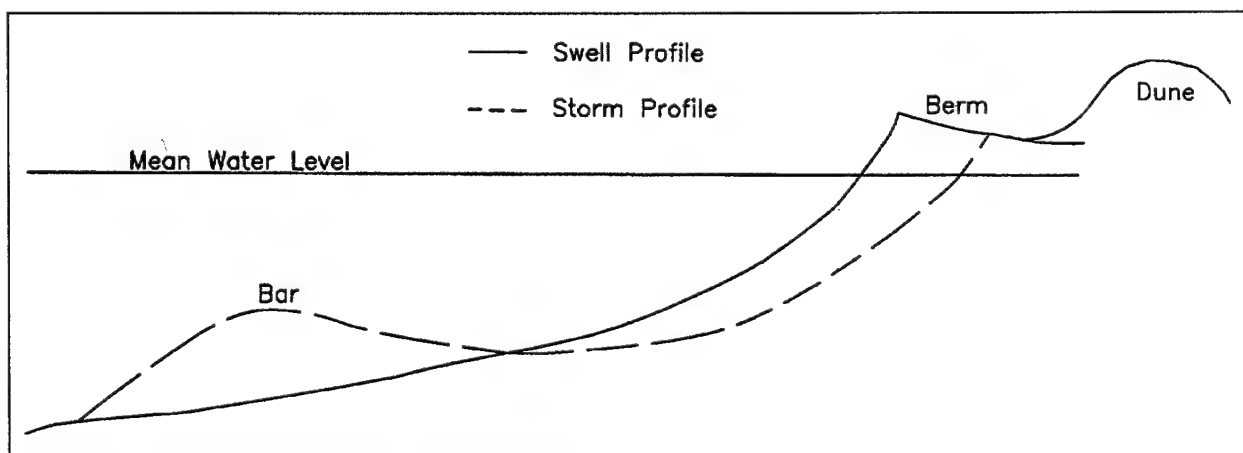
Figure 4-4. Idealized swell and storm beach profiles
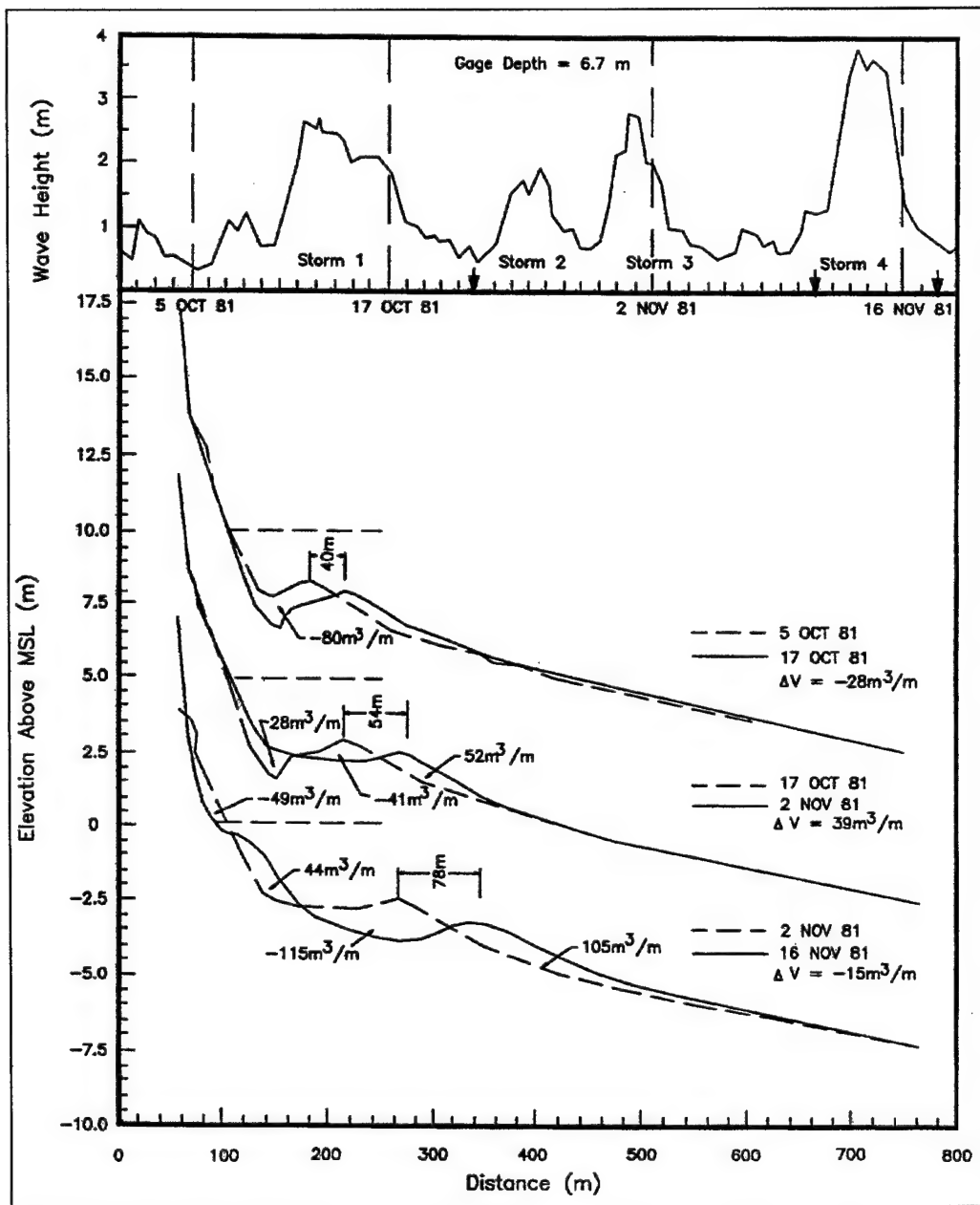
Figure 4-5. Effects of four storms on the beach profile measured near Duck, North Carolina (from SPM 1984)

of water temperature (water viscosity) for which, as an example, lower temperatures would tend to keep sand in suspension. Sand fall speed may be calculated by Equations 4-7 to 4-9 of the SPM (1984). A listing of fall speed values based on those equations is given in Table 4-2.

Table 4-2
Short Table of Fall Speed Values (m/sec) (Quartz Grains)

Water Temperature Deg C	Grain Size, mm					
	0.15	0.20	0.25	0.30	0.35	0.40
10	0.016	0.023	0.029	0.035	0.042	0.048
15	0.017	0.024	0.030	0.037	0.043	0.050
20	0.018	0.025	0.032	0.039	0.046	0.053
25	0.019	0.026	0.034	0.041	0.049	0.055

(6) Kraus, Larson, and Kriebel (1991) recommend two criteria for predicting erosion and accretion of the beach profile. These criteria were originally evaluated based on two sets of laboratory data (labeled CE and CRIEPI) involving quartz sand, wave and beach dimensions of prototype scale, and monochromatic waves (Larson and Kraus 1989). The criteria were further evaluated using a field data set of 100 erosion and accretion events compiled from the literature describing 31 beaches around the world.

(7) The prototype-scale laboratory tests provide accurate data obtained under controlled conditions and are superior to field observations in that possible factors not necessarily related to the beach sediment and normally incident waves, such as wave direction, lateral boundary conditions, tide and long-period surf beat, are absent. The disadvantage of laboratory tests performed with monochromatic waves is that the appropriate equivalent statistical wave (for example, root-mean-square wave height, mean wave height, significant wave height, etc.) is not known without reference to field data. In comparison of erosion and accretion predictors based on the laboratory and field data, the empirical factors in these criteria retained the same approximate value if the mean wave height was used in the evaluation. Under the standard assumption of a narrow-banded wave spectrum, for which a single dominant peak in wave height is present, the mean wave height $\bar{H}$ is proportional to the significant wave height as $\bar{H} = 0.626 H_s$ (see Table 3-3), and the criteria presented here for field application were modified to allow use of significant wave height. Also, the period associated with the peak in the spectrum should be used in field applications. If knowledge of the spectral peak period is lacking, the period associated with the significant wave height should be used.

(8) *Criterion 1*: This criterion (Larson and Kraus 1989) is expressed as $S_o = M N_o^3$, in which the empirical factor $M = 0.00070$ for mean wave height (or for monochromatic-wave laboratory experiments of large scale), and $M = 0.00027$ for significant wave height in field applications. This criterion is shown as the diagonal line drawn ($M = 0.0007$) in Figure 4-6 together with the data from the monochromatic-wave laboratory tank experiments. Wave steepness and fall speed parameter combinations producing a prominent berm (accretion) are labeled with open symbols, and combinations giving a prominent bar (erosion) are labeled with filled symbols. The diagonal line separates regions occupied by erosion and accretion.

(9) Figure 4-7a shows the same criterion ($M = 0.00027$) plotted against the field data set (using significant wave height), in which open and filled symbols again represent accretionary and erosional events, respectively. The different symbol shapes, denoting beach location, are explained in Figure 4-7b. Although there is some crossing of accretionary and erosional events about the solid diagonal line, the criterion distinguishes the main body of the data for the two beach responses. The dashed lines represent predictions obtained with one-half and double the value of the empirical coefficient and provide a measure of reliability of the prediction. Criterion 1 may be summarized as follows for field applications:

If $S_o > 0.00014 N_o^3$, then ACCRETION is highly probable

If $S_o > 0.00027 N_o^3$, then ACCRETION is probable

(4-3)

If $S_o \leq 0.00027 N_o^3$, then EROSION is probable

If $S_o < 0.00054 N_o^3$, then EROSION is highly probable

(10) *Criterion 2*: Observing the trend in the data in Figures 4-6 and 4-7a, a vertical line expressed by the simple equation $N_o = 2.0$ (Figure 4-6, laboratory data, mean wave height) and $N_o = 3.2$ (Figure 4-7a, field data, significant wave height) well separates accretionary and erosional events. By including an error estimate formed by decreasing and increasing the empirical coefficient by 25 percent, the following criterion is obtained for field use:
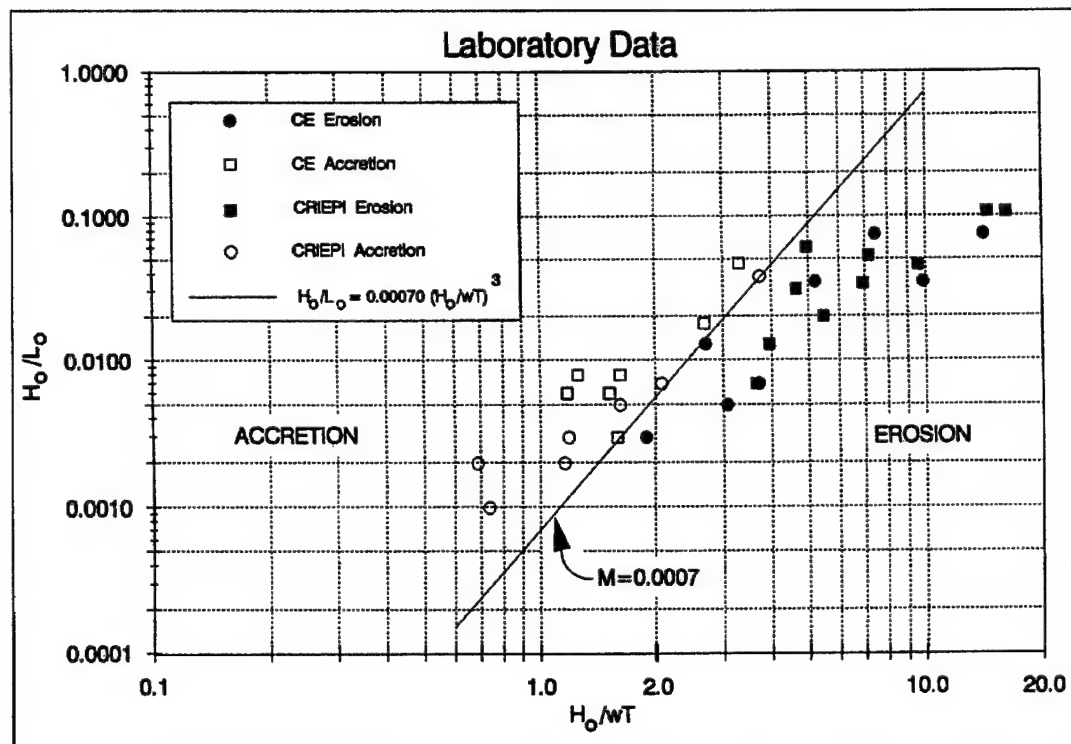
Figure 4-6. Criterion for determining erosion and accretion: large tank data, monochromatic waves (Larson and Kraus 1989)

If $N_o < 2.4$, then ACCRETION is highly probable
If $N_o < 3.2$, then ACCRETION is probable
If $N_o \geq 3.2$, then EROSION is probable
If $N_o > 4.0$, then EROSION is highly probable

$$(4\text{-}4)$$

The parameter N_o was popularized by Dean (1973) in an article devoted to prediction of erosion and accretion and is sometimes called the "Dean number." Wright et al. (1984) used average values of N_o to explain changes in beach state between and including episodes of erosion and accretion. Based on six-and-a-half years of daily observations at three beaches in Australia, Wright et al. found that accretion tended to occur if $N_o < 2.3$ and erosion if $N_o > 5.4$, in general agreement with Equation 4-4.

(11) The predictive capability of the erosion/accretion criteria can be degraded in three ways.

First, the wave height, wave period, and sediment fall speed may be incorrectly estimated. The error bands described above were developed by assuming a 10 percent error in each of these quantities (Kraus, Larson, and Kriebel 1991). Second, factors not directly related to H, T, and average w, such as the tide, surf beat and associated large runup, and variable grain size across the profile, can produce beach change. Third, longshore variability may mask beach change induced by cross-shore transport. Longshore variability includes variations in the incident waves produced by an irregular offshore bathymetry, variations in dune size and composition, three-dimensional circulation patterns containing rip currents, and combined effects of oblique wave incidence and littoral controls such as jetties and groins. The third condition indicates that the criteria are most applicable to straight stretches of beach distant from inlets, jetties, groins, and other coastal structures.

0.1000

ACCRETION

H_o/L_o

0.0100

0.0010

$H_o/L_o = 0.00027 (H_o/wT)^3$

EROSION

$H_o/wT = 3.2$

0.0010

0.0001

0.2   1.0   3.2   10.0   20.0

H_o/wT
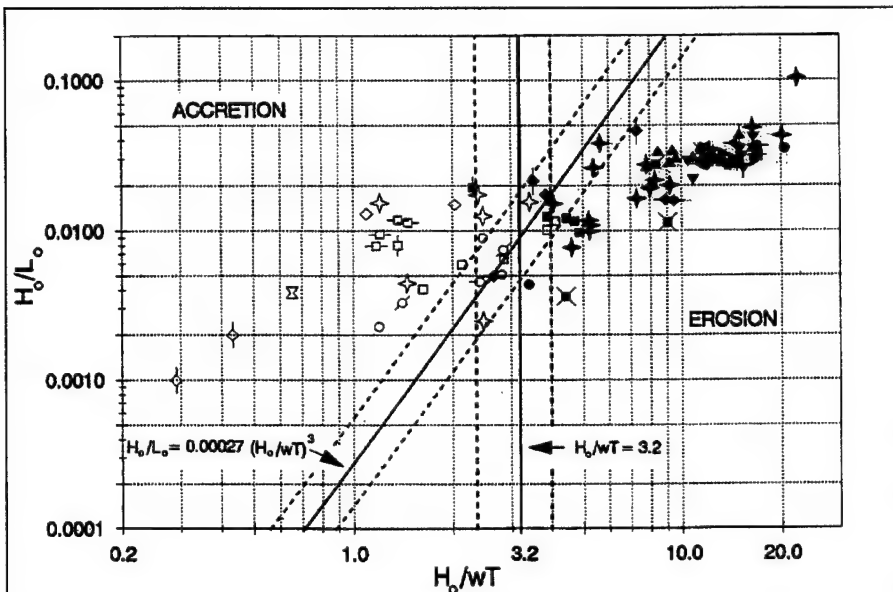
a. Field data, significant wave height (Kraus, Larson, and Kriebel 1991)

Erosion
    Accretion

▲   Long Beach Island, NJ
▼   Atlantic City, NJ
▲   Ludlam Beach, NJ
↓   Misquamicut Beach, RI
◀   Jones Beach, NY
◀   Nauset Beach, MA
▶   Westhampton Beach, NY
●   ○   Fort Walton, FL
◆   ◇   Stevensville, MI
◆   South Beach, OR
✕   Bethany Beach, DE
      ♂   Clearwater, FL
             Naka, Japan:
      ⊡   North site
      ▯   Central site
      ▢   South site
■   ⊙   Manasquan, NJ
✕   Torrey Pines, CA
◆   ◇   Sandy Hook, NJ
■   Ocean City, MD
✦   ✧   Sunamura, 1980 (12 Beaches)
      ⊠   New River Inlet, NC
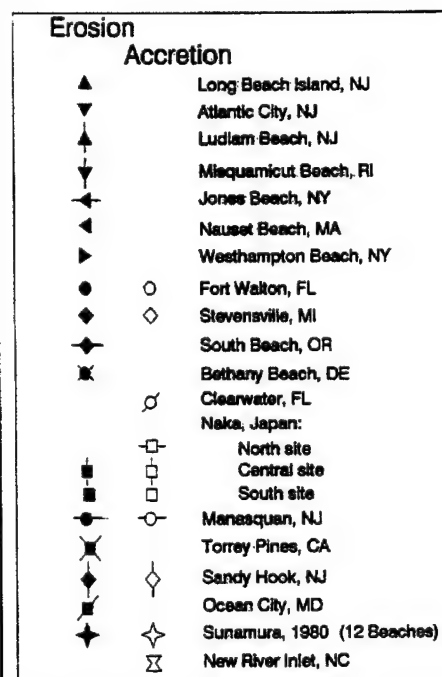
b. Beach location symbols for Figure 4-7a

Figure 4-7. Criterion for distinguishing erosion and accretion

(12) It is noted in Figures 4-6 and 4-7a that the two criteria do not cover exactly the same domains, and regions exist in the vicinities of the upper and lower ends of the diagonal line where the criteria will give conflicting results. For example, at the upper end of the diagonal, there are values of wave steepness and fall speed parameter such that Criterion 1 predicts accretion to be highly probable, whereas Criterion 2 predicts erosion highly probable. This region corresponds to steep waves and relatively large grain size (or high fall speed). The available field data do not provide guidance as to which prediction is correct. Because Figure 4-6 indicates a trend that better supports Criterion 1, at present Criterion 1 is recommended over Criterion 2 in situations of conflicting predictions.

(13) A program implementing and automating evaluation of Criteria 1 and 2 is available for use on IBM-compatible personal computers (PCs) (Kraus 1991). The program allows input of wave height and period in deep water or in finite depth water and shoals the wave by linear-wave theory to determine its height in deep water. The sand fall speed is also calculated and output as a function of water temperature and median grain size.

*************** EXAMPLE 4-1 ****************

PROBLEM: Determine, using the criteria presented, whether a beach of specified (quartz) sand grain size will experience erosion or accretion, given a wave condition and two sand sizes. Assume that the water temperature is 20° C.

GIVEN: [A] $d_{50} = 0.2$ mm   [B] $d_{50} = 0.4$ mm
              $H_o = 1$ m $H_o = 1$ m
              $T = 7$ sec $T = 7$ sec

SOLUTION:

a) Calculate L_o (metric units)

$L_o = 1.56T^2 = 1.56(7)^2 = 76.5$ m; $S_o = H_o/L_o = 1/76.5$
$= \underline{0.013}$

b) Read w from Table 4-2

[A] $w = \underline{0.025 \text{ m/sec}}$

$N_o = H_o/wT = 1/(0.025*7) = 5.7$; $N_o^3 = \underline{185.2}$

[B] $w = \underline{0.053 \text{ m/sec}}$

$N_o = H_o/wT = 1/(0.053*7) = 2.7$; $N_o^3 = \underline{19.7}$

c) Evaluate criteria for each situation

[A]

Criterion 1:

$S_o = \underline{0.013} < 0.00054\ N_o^3 = 0.00054*185.2$

$= 0.10$

indicates erosion highly probable

Criterion 2:

$N_o = 5.7 > 4.0$

indicates erosion highly probable

[B]

Criterion 1:

$S_o = \underline{0.013} > 0.00014\ N_o^3 = 0.00014*19.7$

$= 0.0028$

indicates accretion highly probable

Criterion 2:

$N_o = 2.7 < 3.2$

indicates accretion probable

The two criteria have shown that the finer sand size beach will erode and the coarser sand beach will accrete under the given wave condition.

************** END EXAMPLE 4-1 **************

d. Dissipative vs. reflective beaches.

(1) A more comprehensive classification of beaches than storm versus swell profiles describes them in terms of dissipative versus reflective systems (Wright and Short 1983). These two beach states are contrasted in Figure 4-8. In addition to differing in the nature of the beach profiles, dissipative and reflective beaches differ in the type of wave breaking, the importance of surf bores, and in the nature of the nearshore circulation. On dissipative beaches the waves break by spilling and continue as bores across the wide surf zone which has a fairly uniform and gentle slope, with only subtle long-shore bars. On a fully reflective beach, waves break by plunging or by surging, and the surf zone is narrow so that breaking is immediately followed by intense wave swash. A pronounced step is generally found at the base of the steep beach face, with the offshore bottom slope being significantly less.

(2) Dissipative beaches typically have spilling breakers which continuously break across the surf zone. For this type of breaking wave, a smoother cross-shore profile for the longshore current and the longshore transport would be observed. Reflective beach profiles dissipate more energy at the breakline; hence, the longshore current and sediment transport would be concentrated in this region. The impact that short cross-shore structures such as groins have on the littoral system is, therefore, a function of the beach type. A short structure may have a more significant impact on a dissipative profile than a reflective profile.

(3) The storm (erosive) and swell (accretive) profiles of Figure 4-4 may correspond respectively to dissipative and reflective beach systems. Therefore, some beaches will show seasonal shifts from reflective to dissipative, or shifts during individual storms. However, a beach composed of coarse sediments might always be reflective, whereas a fine sand beach is dissipative irrespective of the wave conditions. Wright and Short (1983) have recognized a series of intermediate states which are characterized by the geometry of the offshore bars, longshore rhythmicity, and the importance of rip currents in the nearshore water circulation. A particular beach might pass through all or part of this sequence during and following a major storm. A particular beach

may also tend to shift from dissipative toward reflective as the tide level increases. This is due to the concave-up nature of most beach profiles so that the effective slope is steeper at high tide than during low tides, causing a change in surf zone processes indicative of dissipative versus reflective conditions.

(4) Wright and Short (1983) have established that the extremes in the beach state, dissipative versus reflective, depend on a scaling parameter that is equivalent to the Irribarren number or surf similarity parameter, I, where

$$I = \frac{m}{\left(\dfrac{H_b}{L_o}\right)^{\frac{1}{2}}} \qquad (4\text{-}5)$$

in which m is the beach slope, H_b is the breaker height, and L_0 is the deep-water wavelength. The beach will be strongly reflective if $1 < I < 2.5$, whereas values for purely dissipative beaches are typically $0.1 < I < 0.3$.

(5) A basic attribute of the dissipative beach system is that effectively all of the arriving wave energy is dissipated in the nearshore. In contrast, on a reflective system a significant portion of the wave energy is reflected back to sea. The wave bores on a dissipative beach continuously lose energy as they cross the wide surf zone and have little energy left when they reach the shore. Measurements of wave runup on dissipative beaches have shown that little energy remains at the periods of the incident waves (Guza and Thornton 1982, Holman and Sallenger 1985). Instead, most of the energy of the runup on the beach face occurs at longer periods, typically on the order of 30 to 120 seconds, termed infragravity motions. It has been observed that dissipative beaches are more conducive to the formation of infragravity edge waves. These low frequency waves concentrate wave energy on the upper beach profile and may be associated with increased erosion and sediment transport. So again, short structures would have a larger impact on dissipative beaches. Figure 4-9 contains data from a dissipative beach in California and shows that as the significant wave height of the incident waves increases, there is not the expected increase in runup
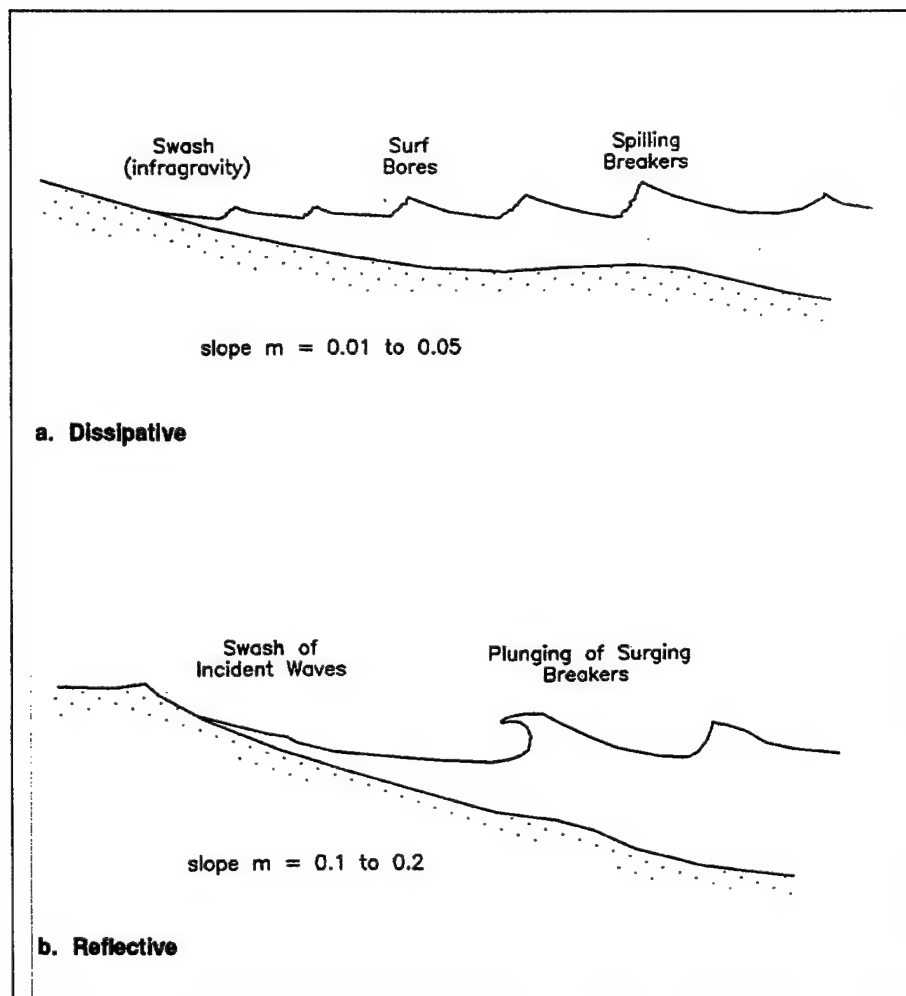
Figure 4-8. Examples of beach states

energy at incident wave periods. This is because, on dissipative beaches, an increase in heights of incoming waves causes them to break farther offshore, producing a greater distance of bore travel and decay so there is little change in runup energy of the bores at the shoreline.

4-3. Littoral Budget

a. Introduction. Beach erosion results if more sand leaves a coastal site than reaches it. This represents a deficit in what is commonly termed the budget of littoral sediments, and is an application of the principle of continuity or conservation of mass to the littoral sediments. In practice, the analysis evaluates the various sediment volume contributions (credits) and losses (debits), and equates these to the net gain or loss for a given sedimentary compartment or stretch of coast. This balance of sediment volumes is reflected in local beach erosion or deposition, depending on whether the balance is in the "red" or "black."
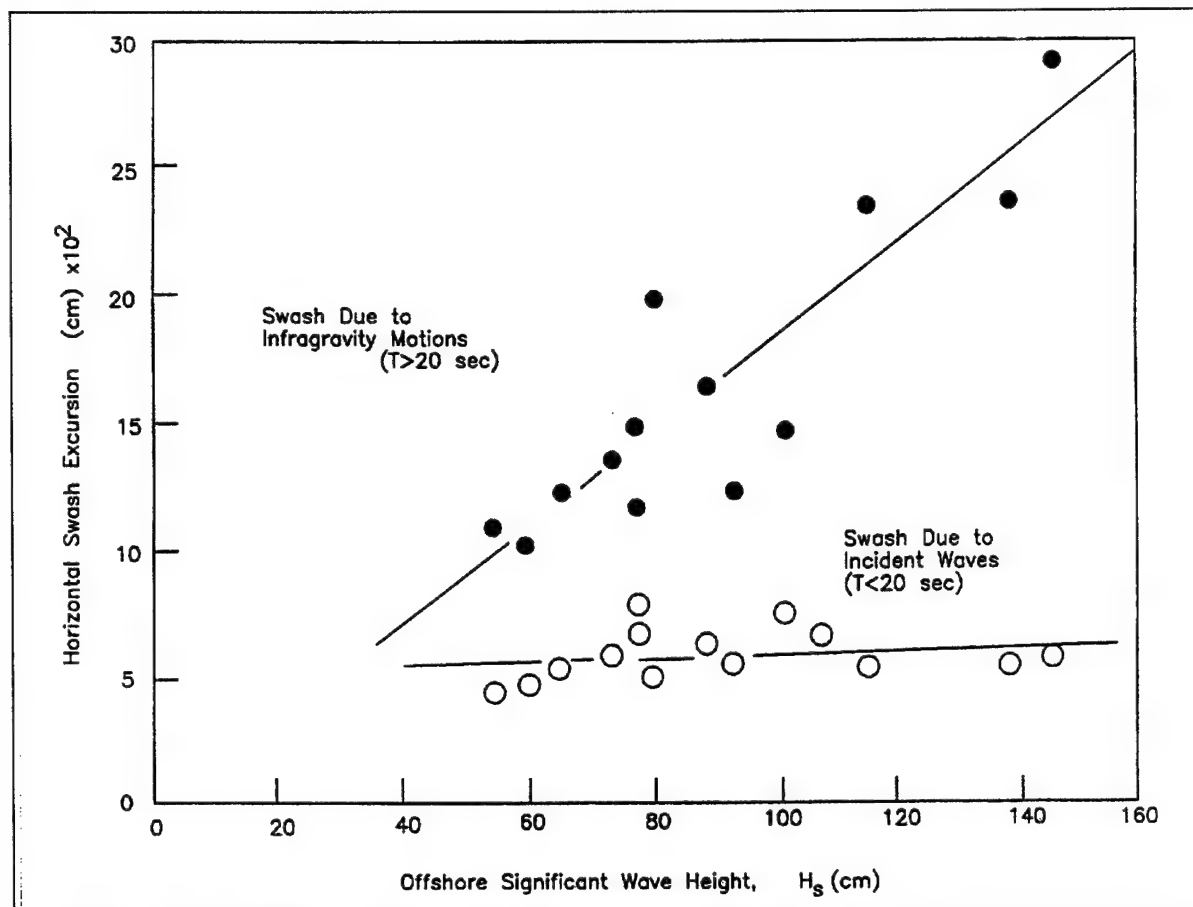
Figure 4-9. Dependency of the horizontal swash excursion on offshore wave height for wind and infragravity frequency bands (Guza and Thornton 1982)

b. Sources and sinks.

(1) There are many potential gains and losses of beach sediments that can play a role in the budget. In general, sand supply from rivers, sea cliff erosion, and longshore sediment transport into the area constitute the major natural sources. Natural losses can include sand blowing inland to form dunes, offshore transport to deeper water, and the longshore transport that carries littoral sediments out of the study area. Beach nourishment represents a human-induced gain in the budget, one that is designed to shift the balance to the surplus, replacing erosion with deposition. Sand mining is a human-induced deficit in the budget. Figure 4-10,

summarizes the various possible losses and gains in a littoral budget.

(2) An application of the budget of sediments requires a quantitative evaluation of the various gains and losses. This includes assessments of the annual discharge of sediments from rivers entering the study area, the amount of sand blown inland to form dunes, the littoral drift, and so on. These quantities are then balanced to evaluate the resulting erosion (negative balance) or deposition (positive balance). Detailed discussions of how these gains and losses can be evaluated are given in the SPM (1984), and two examples

LAND   OCEAN

Cliff, Dune, and
Backshore Erosion   Offshore Slope
                                            (source or sink?)

Beach Replenishment   Submarine Canyon

Rivers

Dune and Backshore
Storage   Dredging
                        Littoral Zone
Winds
(supply and deflation)

                                            Calcium Carbonate
                                            (production and loss)

Inlets and Lagoons,
Including Overwash

Mining

Longshore Currents,
Tidal Currents, and
Longshore Winds
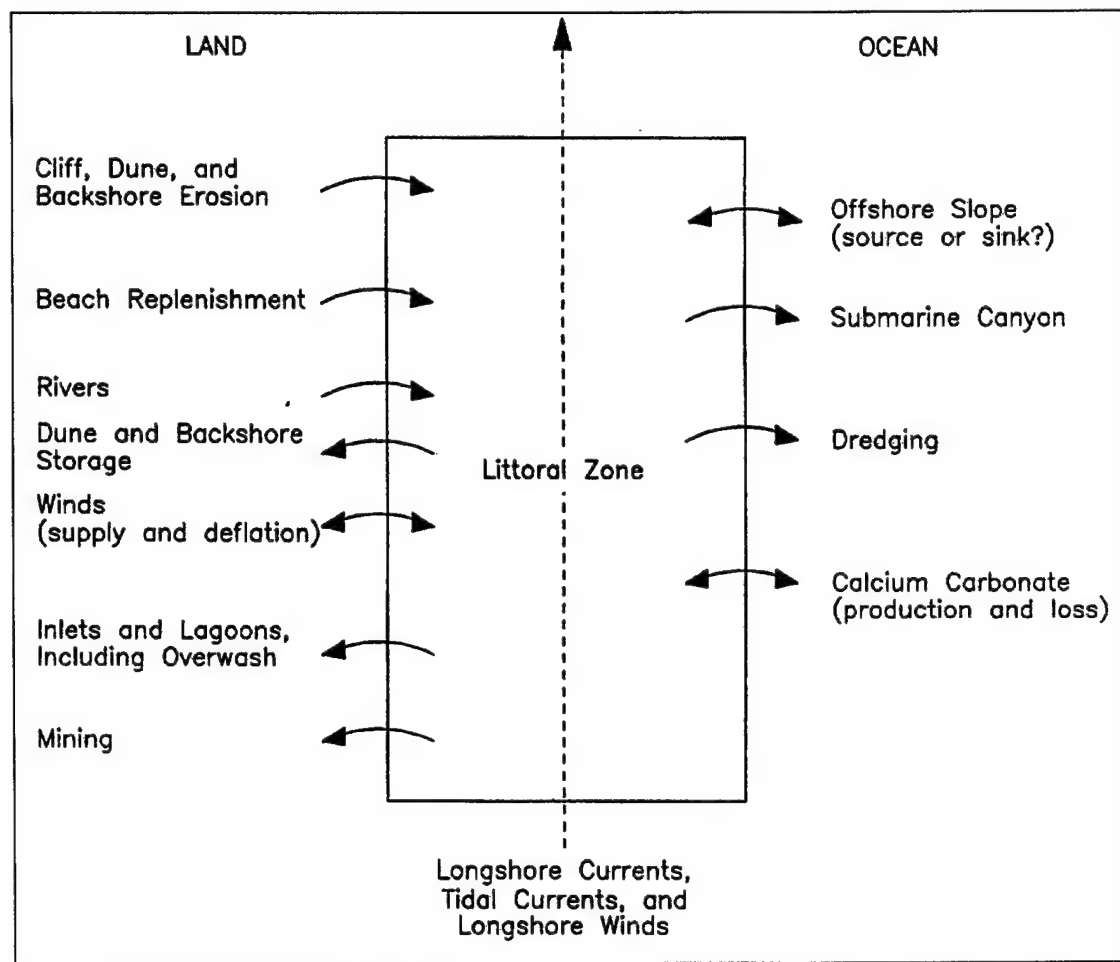
Figure 4-10. Materials budget for the littoral zone (SPM 1984)

are presented in Chapter 7. In practice it is often diffi-
cult to make reasonable estimates for some of these
quantities. Evaluation of the losses or gains from the
offshore is particularly difficult. Generally, the best
known component in the budget is the balance itself, the
rate of erosion or deposition on the beach. Knowing
that balance, it is sometimes possible to work backwards
to arrive at reasonable estimates for the multiple inputs
and outflows of sand.

c. *Littoral cells.* In some coastal areas there are
natural compartments or littoral cells that help define the

stretch of beach to which the budget of sediments is
evaluated. Headlands and long jetties are particularly
useful in this regard, if they block longshore sediment
transport. A good example of this is the coast of south-
ern California which is divided into a series of sedimen-
tation cells (Figure 4-11). In each cell the mechanisms
that add and remove sand are balanced. Rivers and cliff
erosion are the principal sources of sediments for the
beaches in the cells, and the chief losses are the series
of submarine canyons which bisect the continental shelf
and intercept the sand as it moves southward along the
coast. In general, it is best to form a sediment budget
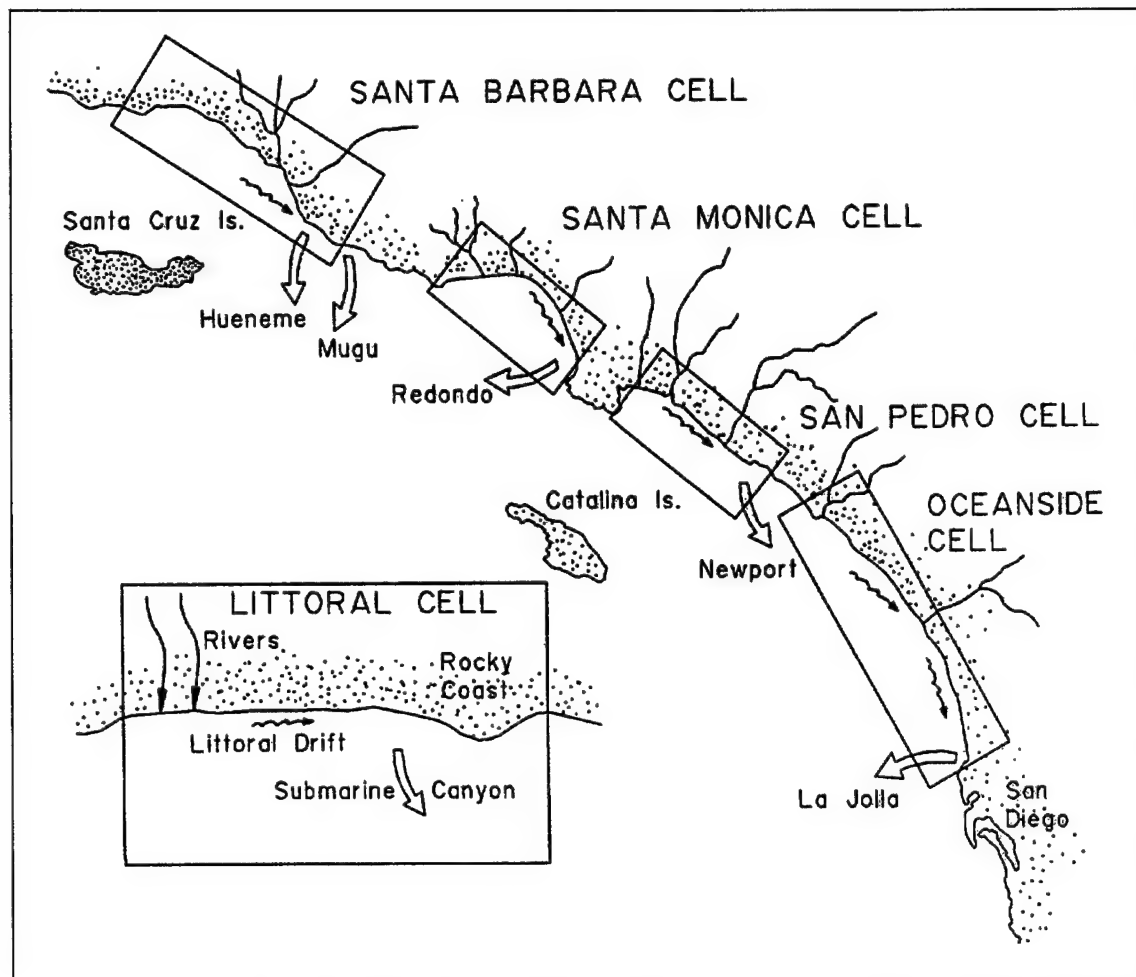
Figure 4-11. Southern California littoral cells (after Inman and Frautschy 1966)

over a region where lateral sediment exchanges can be well estimated, such as regions bounded by headlands, inlets, and jetties.

d. Applications. The budget of littoral sediments is particularly useful in assessing the possible impacts of engineering activities on the coast. For example, once a budget has been developed for the natural conditions at the study site, it is possible to make quantitative evaluations of the effects of a proposed dam on a river that would cut off one of the sources. Similarly, one can assess the impacts of sand mining on the beach, the

placement of a protection structure to halt sea cliff retreat (the erosion of which supplies sand to the beach), or the construction of a jetty which interrupts longshore sand movements into the study area.

4-4. Beach Nourishment

a. Beach nourishment involves the placement of substantial quantities of compatible sand to advance the shoreline seaward and is usually undertaken to reverse a trend of beach recession. The wider beach following nourishment is better able to act as a buffer, providing

protection to upland structures from storm waves and inundation. Another direct benefit is the recreational value of the enlarged beach. An indirect benefit is in serving as a feeder beach for down-coast locations needing a continuous supply of sand.

b. It is important to establish any beach nourishment project within the overall budget of sediments for the area. Such an understanding will aid in recognizing probable rates of beach fill losses, and lead to a better assessment of the lifetime of the project. Beach nourishment can result in a seaward extension of the shoreline and an unnatural increase in sand relative to the original contours. This leads to profile adjustments and the immediate offshore transport of sand, and also movements in the longshore direction that can carry sand out of the nourished area. Models for these processes have been summarized by Dean (1983) and can be used to predict the fate of the nourished sediments.

Chapter 5
Nearshore Currents

5-1. Introduction

When waves reach the coast and break on a beach, they generate nearshore currents which combine with the direct action of waves to transport beach sediments. This chapter reviews the patterns of observed nearshore current systems and discusses their modes of generation and prediction of their associated velocities. The transport of sediments produced by nearshore currents and waves is described in Chapter 6.

5-2. Significance and Patterns

a. Wave-generated currents tend to dominate water movements in the nearshore of open coastlines and are therefore important in the movement of sediments and dispersal of discharges, such as sediment introduced at river mouths. Nearshore currents combine with wave orbital motions to transport beach sediments. For example, sediments mobilized by breaking waves are often transported by nearshore currents. Therefore, currents give direction to the movement of beach sediments and mold the nearshore topography. The beach topography in turn becomes an important factor in controlling the currents.

b. Two principal horizontal current patterns can be distinguished which span the range of observed flow field types. When waves break with their crests at significant angles to the average trend of the shoreline, the generated longshore current flows parallel to the shore and is confined largely to the nearshore between the breakers and the shoreline (Figure 5-1a). The other pattern, Figure 5-1b, occurs when waves break effectively parallel to the shoreline; the generated currents then take the form of a cell circulation with seaward flowing rip currents. In many cases, especially with small breaker angles, the observed currents take on the combined aspects of these two patterns, Figure 5-1c, being driven in part by oblique breakers, but also turning seaward as rip currents. Different processes generate these contrasting nearshore current systems; therefore, their analyses also differ.

5-3. Mean Longshore Currents Produced by Oblique Wave Approach

a. Best understood of the nearshore currents are those of Figure 5-1a, where the flow is due to oblique breakers. Observations on natural beaches and in
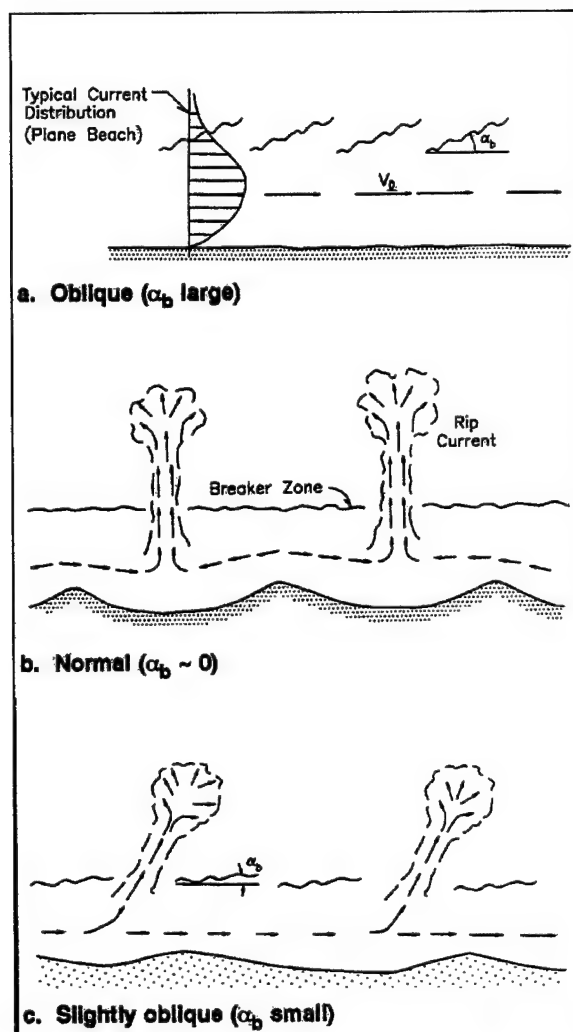
Figure 5-1. Observed horizontal circulation patterns as a function of wave approach

laboratory wave basins show that this current is largely confined to the surf zone and rapidly decreases in magnitude seaward of the breakers. It has been established that this longshore current is generated by the momentum flux (radiation stress) of the waves breaking obliquely to the shore. The longshore current may be modified by wind-driven currents and tides.

b. Several theories have been proposed to account for this wave-generated longshore current, but modern analyses originated with the papers by Bowen (1969a), Longuet-Higgins (1970a,b) and Thornton (1970). Each employed the concept of radiation stress to describe the flux of momentum associated with the waves, which is the driving force of the longshore current. That

generating force is opposed by the frictional drag be-
tween the bottom and the resulting current. There is
also a process of horizontal mixing which acts to
smooth the cross-shore profile of current magnitude.
The analysis of Longuet-Higgins leads to solutions
which can be used in the simplest applications.

c. In some applications it is adequate to evaluate
only a mean longshore current, that which occurs ap-
proximately at the midsurf position, halfway between
the shoreline and the outer breakers. The analysis of
Longuet-Higgins (1970a) for the current on a plane
beach yields a relationship that is equivalent to

$$V_\ell = k \frac{m}{f_w} \sqrt{gH_b} \ \sin(2\alpha_b) \qquad (5\text{-}1)$$

for the magnitude of the longshore current V_ℓ, where k
is a dimensionless proportionality coefficient that must
be established empirically, m is the average beach slope,
f_w is a frictional drag coefficient, H_b is the breaking
wave height, and α_b is the angle of wave breaking with
respect to the longshore trend of the shoreline. Field
data are shown in Figure 5-2 that support the simplified
relationship

$$V_\ell = 0.58 \ \sqrt{gH_{br}} \ \sin(2\alpha_b) \qquad (5\text{-}2a)$$

where H_{br} is the rms wave height at breaking. If the
significant wave height at breaking H_{bs} is used, the
relationship is

$$V_\ell = 0.49 \ \sqrt{gH_{bs}} \ \sin(2\alpha_b) \qquad (5\text{-}2b)$$

Excellent agreement is also found with nearly all labora-
tory data (Komar 1975). Comparisons with longshore
current measurements, therefore, imply that the ratio
m/f_w in the theoretically derived Equation 5-1 is
approximately constant (Komar and Inman 1970; Komar
1979). This is reasonable to a first approximation in
that as the grain size of the beach sediment increases,
the beach slope m increases (see Figure 4-2), as does
the frictional drag coefficient, f_w .
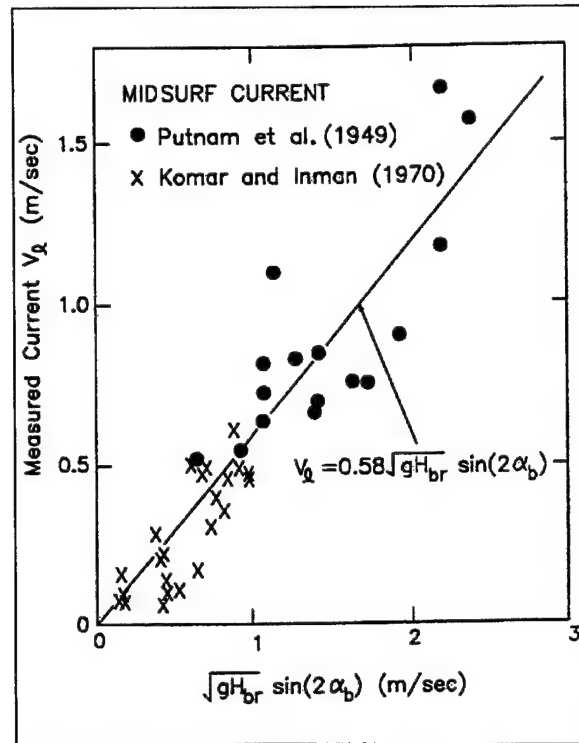
Figure 5-2. Field measurements of longshore current

************** EXAMPLE 5-1 ***************

GIVEN: Breaking waves on a beach have a signif-
             icant wave height of 0.65 m, and break at
             an angle 13.5°. The beach slope is
             $m = 0.139$.

FIND: Calculate a mean longshore current repre-
             sentative of approximately the midsurf
             position.

SOLUTION: Using $H_{bs} = 0.65 \ m$ (2.1 ft) , $g = 9.8$
             m/sec^2 (32.2 ft/sec^2), and $\alpha_b = 13.5°$,
             Equation (5-2b) gives

$$V_\ell = 0.49\sqrt{gH_{bs}} \ \sin(2\alpha_b)$$

$$V_\ell = 0.49\sqrt{9.8(0.65)} \ \sin[2(13.5)]$$

$$V_\ell = 0.56 \ m/\text{sec} \ (1.8 \ \text{ft/sec})$$

The measurements used in this example are part of a data set presented in Figure 5-2. The actual measured longshore current (0.61 *m*/sec (2.0 ft/sec)) compares well with the predicted current.

************* END EXAMPLE 5-1 *************

5-4. Cross-Shore Distribution of Longshore Currents

a. Equations 5-1 and 5-2 predict the magnitude of the longshore current at the midsurf position on an approximately uniformly sloping or mildly concave upward beach bottom. Many applications require calculation or knowledge of the complete velocity distribution, i.e., the profile of the longshore current across the surf zone. For the well-studied and simple situation of a uniformly sloping beach, mathematical solutions are available to predict the distribution of the current across the shore. The main characteristic of the distribution is that it is unipeaked, typically reaching the single maximum in the mid- to outer half of the surf zone, with a relatively sharp decrease in magnitude of the flow seaward of the main breaker line, as shown in Figure 5-1a. The longshore current velocity decreases more gradually toward the shore, and at the shoreline the current becomes effectively zero.

b. Often, however, the beach bottom exhibits one or more longshore bars and accompanying troughs. Larger waves may break on an outer bar, reform in the deeper trough, and break again at the next bar or on the foreshore. For this not uncommon situation, the distribution is multipeaked, with local maxima located seaward of bars where breaking occurs. On a barred beach, a "midsurf longshore current velocity" may not be representative of the longshore current in the surf zone, requiring calculation of the current distribution for an accurate result. For situations with complex surf zone bathymetry, numerical models must be used to calculate the distribution.

c. Recently, a numerical model called NMLONG (Numerical Model of the LONGshore current) has become available that calculates the distribution of the longshore current for almost arbitrary wave and beach conditions (Kraus and Larson 1991, Larson and Kraus 1991). The model runs on a personal computer and has a convenient menu and graphical interface. The main assumption underlying the model is uniformity of waves and bathymetry alongshore, but the beach bottom can be irregular across the shore. NMLONG calculates both

the wave and wind-induced longshore current and the wave height distribution for multiple bar and trough bathymetry and arbitrary offshore (input) wave conditions, and provides a plot of the results. Figure 5-3 gives an example NMLONG calculation and comparison to the field measurements of the current and breaking waves reported by Kraus and Sasaki (1979). Waves broke on the outer bar, reformed in the broad trough, then broke again near to shore. Options in NMLONG to calculate random breaking waves and nonlinear bottom friction were used in the simulation. Reasonable agreement is found for this realistic simulation. As with all numerical models, proper use of NMLONG requires careful reading of the related documentation.
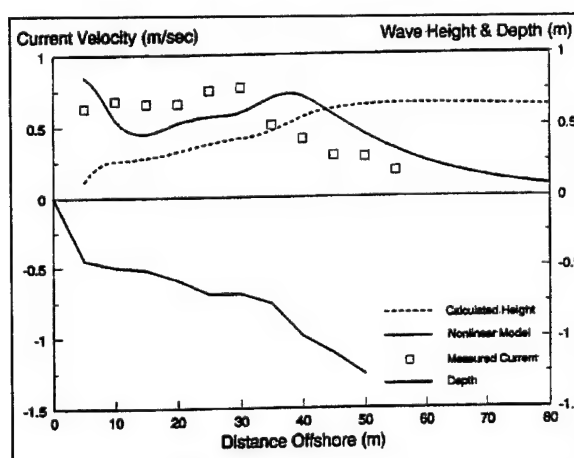
Figure 5-3. Example NMLONG simulation for multiple barred beach

5-5. Cell Circulation and Currents Due to Longshore Variations in Wave Breaker Heights

a. When waves break with their crests effectively parallel to the shoreline, a cell circulation is established, Figure 5-1b, which consists of a shoreward mass transport, longshore currents, and narrow seaward-flowing rip currents that extend through the breaker zone and spread out into rip heads (Shepard and Inman 1950). Rip currents are strong, narrow flows, and are the most visible feature of nearshore circulation systems. Rip currents are fed by longshore-directed surf zone currents which increase from zero at a point between two neighboring rips, to a maximum just before turning seaward to form a rip current.

b. Examples have been noted which provide clear evidence that cell circulation can be generated by

longshore variations in wave breaker height. The rip currents at Scripps Beach, La Jolla, California, are situated in longshore positions where the breaker heights are lowest, Figure 5-4, which are in turn governed by wave refraction over offshore submarine canyons. The longshore currents of the cells flow away from locations where the wave breakers are highest, converge on longshore positions where the breakers are lowest, and then turn seaward as rip currents.

c. This association of cell circulation with longshore variations in wave breaker height has been explained by Bowen (1969b). His analysis showed that the higher the breaking waves, the greater the setup of water in the surf zone above the level of the sea. The existence of longshore variations in breaker heights, therefore, gives rise to a longshore gradient in the water level elevation, with the levels highest shoreward of the larger breakers and lowest shoreward of the small breakers. This longshore gradient in the setup gives rise to the flow of a longshore current toward the position of

lowest breakers and setup, where the flow then turns seaward as a rip current.

d. A cell circulation can also be formed in the protected zone of a headland or in the sheltered area of a jetty or detached breakwater, again due to longshore variations in breaker height. The rip current is usually positioned close to the headland or jetty, where the wave heights are lowest. This situation has been investigated by Gourley (1974, 1976) in a series of wave basin experiments, and theoretically by Sasaki (1975) and Mei and Liu (1977). The experimental arrangement of Gourley is shown in Figure 5-5, where the sheltered area behind a breakwater produced a longshore variation in wave breaker height and setup. These gradients induced a longshore current which became part of an eddy behind the breakwater.

e. The longshore current speed can be increased or decreased by the longshore variation in breaker height, depending on the relative directions of the current and breaker height decay. Experiments in a wave basin with a cuspate shoreline yielded a near balance between the two current-producing mechanisms, so that the resultant current was zero even though waves broke at an angle to the shoreline and a longshore gradient in wave height persisted (Komar 1971, 1975). These laboratory experiments illustrate a limitation of surf zone sediment transport formulae that depend primarily on breaker angle to predict current speed and resulting transport rates. The shoreline change numerical model GENESIS uses a transport formula that evaluates currents generated both by waves breaking at an angle to the shoreline and longshore variations in wave height (see paragraph 6-11).
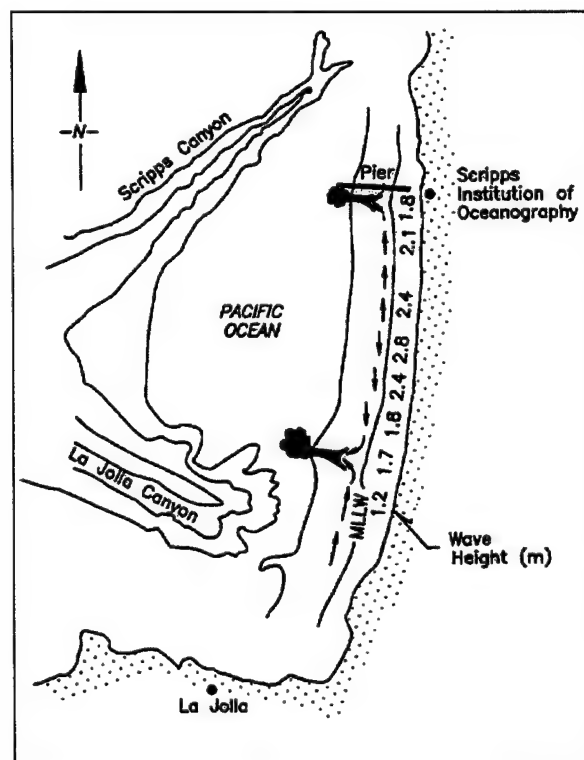
Figure 5-4. Rip current at Scripps Beach, California (After Shepard and Inman 1950)
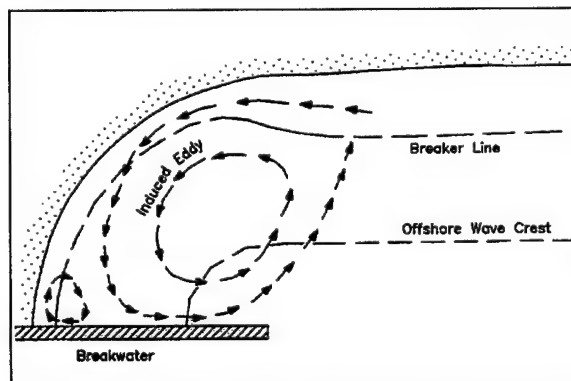
Figure 5-5. Cell circulation due to longshore variation in wave height (after Gourley 1976)

f. Irregularities in the bathymetry of the beach can also induce, or at least maintain, a cell circulation. This was documented by Sonu (1972) at Seagrove, Florida, and later numerically modeled by Noda (1974). The nearshore bathymetry at Seagrove consisted of shoals and seaward trending troughs, alternating along the length of the beach. The shoreward currents in a circulation cell typically occur over shoals, while the rip currents are positioned over troughs. Measurements at Seagrove established that wave setup was higher over the shoals than over the troughs, but breaker heights were found to be uniform in the longshore. It was demonstrated by Sonu that the variation in the setup was instead produced by a difference in breaker types; over the shoals the waves broke by spilling, while over the troughs they were of the plunging type. Since spilling waves continuously dissipate their energy as they move through the surf zone, these waves formed a setup with a constant gradient, whereas shoreward of the plunging waves the setup was irregular. Water flowed "downhill" from the higher to lower setup region, thereby creating the observed circulation pattern.

g. A close association like that at Seagrove between beach topography and the nearshore cell circulation is typical of many beaches. However, it is probable that in many cases the cell circulation was established first, and that its currents remolded the beach bathymetry into the observed series of shoals and troughs. Observations such as those of Sonu (1972) at Seagrove indicate that once the morphology of the beach has been modified, it can then control the patterns of nearshore currents, permitting the currents to persist even after the original bathymetry-molding mechanism has disappeared.

h. Circulation cells can exist on long, straight beaches with a smooth, regular bathymetry. Therefore, mechanisms must exist which produce longshore variations in wave height or otherwise induce circulation without topographic controls. One suggestion has been that the normal wind waves reaching a beach interact with waves, termed edge waves, trapped in the nearshore (Bowen 1969b; Bowen and Inman 1971). Edge waves are trapped by the seaward slope of the beach and are, in a sense, held there by wave refraction. When reflected from the shoreline at a small angle, they first travel seaward but refract as they propagate, eventually turning back toward the shore to be reflected once more to repeat the process (Holman 1983; Komar and Holman 1986). Bowen (1969b) and Bowen and Inman (1969) demonstrated that edge waves can add to or subtract from the incident waves to produce a regular variation in wave breaker height along the length of the

beach, and thus a regular spacing of a series of rip currents. It is necessary that the edge wave period is a harmonic of the incident waves so that they interact constructively to produce large breakers in some areas, and interact in opposition in other areas to form small breakers. Bowen and Inman demonstrated the basic validity of this mechanism in a series of wave basin experiments. However, since it is difficult on natural beaches to detect the presence of edge waves having the same period as the incident waves, the cell-generating mechanism has not been firmly established under field conditions.

i. An alternate hypothesis for the generation of cell circulation on a regular beach involves instability models (Hino 1974; Leblond and Tang 1974; Miller and Barcilon 1978). These models consider the existence of perturbations of the wave setup which give rise to a regular pattern of longshore variations in surf zone water levels. Analyses of the momentum and energy conservation equations yield cell circulation currents when coupling between the currents and waves is included. This establishes criteria for the development of most likely rip current spacings. However, instability models have not been adequately tested with field data.

j. A number of mechanisms have been proposed to explain observed cell circulation systems in the nearshore. It is possible that any one or a combination could account for the flow on a given beach. It is difficult to adequately test the validities and relative contributions of the theoretical models. Circulation cells are three-dimensional and therefore require an extensive deployment of instruments. Theoretical analyses generally involve complex numerical models which include many simplifying assumptions. The currents produce sediment transport which modifies the beach bathymetry, which in turn alters the current patterns. Therefore, circulation cells are dynamic and ever-changing.

5-6. Patterns of Nearshore Currents, Sediment Transport, and Beach Topography

The waves reaching a beach can mobilize sediment, but it is the pattern of superimposed nearshore currents that gives direction to the resulting sediment movements. The result is that the nearshore current system, though generally hydraulically weaker than breaking waves, often determines the evolution of the beach topography.

a. Normal wave approach. The importance of nearshore currents in molding beach topography is most apparent for the cell circulation with strong rip currents.

The rip currents generally transport sand offshore to beyond the breaker zone, and hollow out embayments in the beach berm. The magnitudes of the longshore currents feeding the rip currents progressively increase as the current approaches a rip, reaching its highest velocity just before turning seaward. This results in increasing quantities of beach sand being carried by the current and produces erosion which forms the embayment and leaves a cusp at the position where the longshore currents diverge (Figure 5-6). A series of rip currents can produce a series of embayments separated by cuspate projections. On typical ocean beaches these have spacings of tens to hundreds of meters. In general, the rip currents along a beach differ in their intensities and, therefore, hollow out embayments of different sizes. This can give rise to an extremely irregular beach topography with a complex pattern of bars, troughs, and shoreline embayments.

   b. Small angle of wave approach. Rip currents are usually ephemeral, changing spacings and positions with
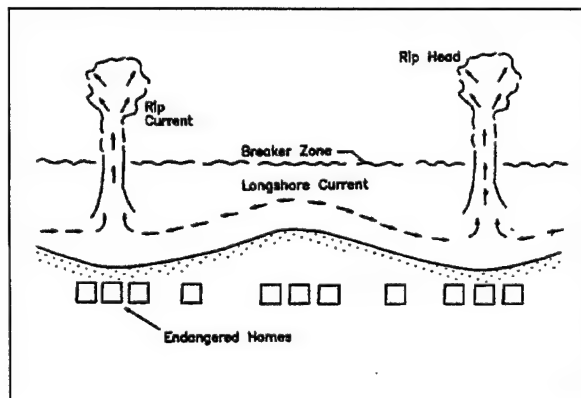
Figure 5-6. Local erosion caused by rip currents due to normal wave approach

varying wave conditions. If rip currents are present with some oblique wave approach (Figure 5-1c), they tend to migrate slowly alongshore. In such cases, the rips have insufficient time to erode significant embayments or otherwise affect the beach topography. At times rip currents do become fixed in position, in part by the longshore troughs and embayment they have eroded, and have been observed to persist for several months (Komar 1983). In such circumstances, they may continue to enlarge the embayments cut into the beach berm, so that the erosion reaches the coastal properties backing the beach. The embayment then becomes the focus of property losses as waves pass through the deeper water of the embayment and wash directly against the property. It has been shown that such embayments along the barrier islands of the eastern United States can threaten coastal structures and often control locations of barrier island washovers (Dolan 1971). They have similarly been found to control areas of maximum erosion on west-coast beaches (Komar 1983) and in Australia (Wright and Short 1983).

   c. Large angle of wave approach. The longshore currents generated by waves breaking obliquely to the shoreline, Figure 5-1a, may flow along an extended length of beach. Strong longshore currents tend to erase any beach topography irregularities that were produced by rip currents and the cell circulation. The cuspate shoreline is smoothed into a more linear form, and the offshore bars and troughs tend to be continuous along the length of the beach. Therefore, the topography seen at a beach provides immediate evidence as to the nature of the dominant nearshore currents. It also indicates whether the incident waves are strongly oblique or nearly parallel to the coastal trend, as well as the patterns of sediment transport in the nearshore.

Chapter 6
Sediment Transport Processes

6-1. Introduction

a. The breaking waves and surf in the nearshore combine with the various horizontal and vertical patterns of nearshore currents to transport beach sediments. Sometimes this transport results only in a local rearrangement of sand into bars and troughs, or into a series of rhythmic embayments cut into the beach. At other times there are extensive longshore displacements of sediments, possibly moving hundreds of thousands of cubic meters of sand along the coast each year. The objective of this chapter is to examine techniques that have been developed to evaluate this sediment transport rate. This transport is among the most important nearshore processes that control the beach morphology and determine whether shores erode, accrete, or remain stable. An understanding of longshore sediment transport is essential to sound coastal engineering design practice.

b. The currents associated with the nearshore cell circulation generally act to produce only a local rearrangement of beach sediments. The rip currents of the circulation can be important in the cross-shore transport of sand, but there is minimal along-coast displacements of beach sediments. More important to the longshore movements of sediments are waves breaking obliquely to the coast and the longshore currents they generate which may flow along an extended length of beach (Chapter 5). The resulting along-coast movement of beach sediment is referred to as littoral transport or as the longshore sediment transport, whereas the actual volumes of sand involved in the transport are termed the littoral drift. This longshore movement of beach sediments is of particular importance in that the transport can either be interrupted by the construction of jetties and breakwaters, structures which block all or a portion of the longshore sediment transport, or can be captured by inlets and submarine canyons. In the case of a jetty, the result is a buildup of the beach along the updrift side of the structure together with erosion in its downdrift direction (Figure 6-1), an impact that not only poses problems to the adjacent communities, but can often threaten the usefulness of the adjacent navigable waterways (channels, harbors, etc.).

c. In studies of coastal erosion or the design of harbor structures, it is important to have an ability to assess directions of the longshore sediment transport and

to evaluate quantities of that transport as a function of the wave and current conditions. This need has led to numerous research efforts, both on natural beaches and in laboratory wave basins. Research has gone beyond simple empirical attempts to predict total quantities of the littoral drift, and many investigations have focused on the physics of the transport processes.

6-2. Indicators of Longshore Transport Direction

a. Definitions.

(1) On most coasts, waves reach the beach from different quadrants, producing day-to-day and seasonal reversals in transport direction. At a particular beach site, transport may be to the right (looking seaward) during part of the year and to the left during the remainder of the year. If the left and right transports are denoted respectively by Q_L and Q_R with each being a positive quantity, then the net annual transport is $Q_N = Q_R - Q_L$, in effect the net resultant of the daily movements where contrasting directions are taken into account. The net annual transport can range from essentially zero to a very large volume, estimated at a million cubic meters of sand for some coastal sites. The gross longshore transport is defined as $Q_G = Q_R + Q_L$, the sum of the daily quantities of littoral transport irrespective of direction. Accordingly, it is possible to have a very large gross longshore transport at a beach site, while the net annual transport is effectively zero. These two contrasting assessments of longshore sediment movements have different engineering applications. For example, the gross longshore transport is used to predict shoaling rates in navigation channels and uncontrolled inlets, whereas the net longshore transport relates to the deposition versus erosion rates of beaches on opposite sides of jetties or breakwaters.

(2) Multiple lines of evidence have been used to discern directions of longshore sediment transport. Most of these are related to the net transport, the long-term resultant of many individual transport events. Blockage by structures such as jetties can provide the clearest indication of the long-term net transport direction (Figure 6-1). Sand entrapment by groins is similar, but generally involves smaller volumes and responds to the shorter term reversals in transport directions; therefore, groins do not always provide a positive indication of the net annual transport direction. Other indicators of transport direction include the deflection of streams or tidal inlets by the longshore sand movements, shoreline
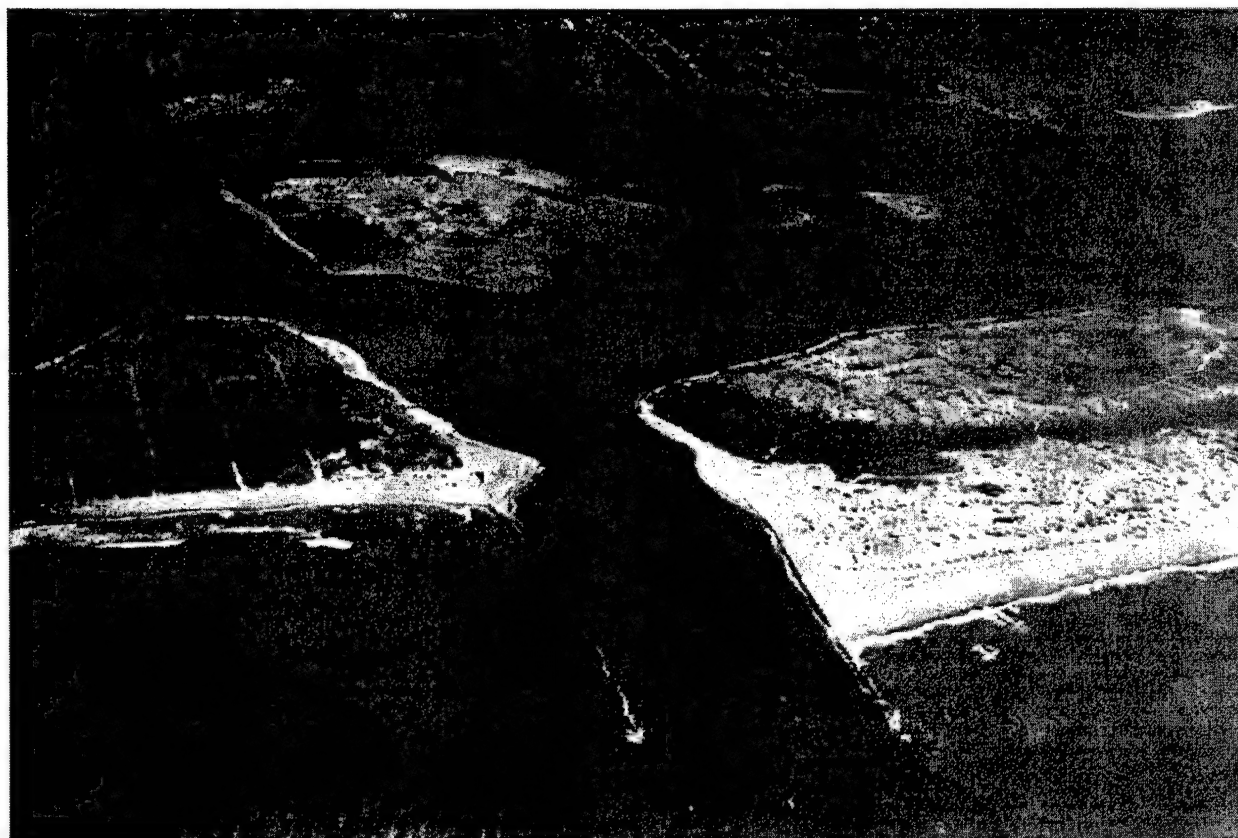
Figure 6-1. Impoundment of longshore transport at South Lake Worth Inlet, Florida

displacements at headlands similar to that at jetties, and the longshore growth of sand spits.

b. Geomorphic and sedimentological indicators.

(1) Grain sizes and compositions of the beach sediments have also been used to determine transport direction as well as sources of the sediments. It is often believed that a longshore decrease in the grain size of beach sediment provides an indication of the direction of the net transport. This is sometimes the case, but grain size changes can also be the product of along-coast variations in wave energy levels that have no relation to sediment transport directions. The use of unique heavy minerals contained within the sand to deduce transport paths is illustrated by the analyses of Trask (1952, 1955). By using the heavy mineral augite as a tracer of longshore sand movements, Trask demonstrated that the sand filling the harbor at Santa Barbara, California, originates at a distance of more than 160 km up the coast, derived from volcanic rocks in the Morro

Bay area north of Santa Barbara. Noting the progressive dilution of the augite content of the beach sand by addition of sand from other sources, Bowen and Inman (1966) were able to compute littoral drift rates along the California coast as well as establish the direction of the net transport.

(2) Many of the geomorphic and sedimentological indicators of longshore sediment transport directions are not absolute, and too strong a reliance on them can lead to misinterpretations. It is best to examine all potential evidence that might relate to transport direction, and consider their relative reliabilities.

6-3. Measurements of Longshore Sediment Transport Rates

a. Some of the qualitative indicators of longshore transport direction can also be used to obtain estimates of the quantities involved in the process. Repeated surveys over a number of years and analyses of aerial

photographs of the longshore growth of sand spits have been used to establish approximate rates of sediment transport. For the estimates to be reasonable, it is necessary that such surveys span a decade or longer, so the results represent a long-term net sediment transport rate. The blockage of the longshore sediment transport by jetties and breakwaters and the resulting growth and erosion patterns of the adjacent beaches have yielded reasonable evaluations of the net transport rates at many coastal sites. In most cases, such an estimate has been the integrated transport over several years, evaluated during and immediately after jetty construction. Johnson (1956, 1957) compiled data of this type for many shorelines and found net transport rates up to approximately one million cubic meters of sand per year. The patterns of littoral drift for a portion of the east coast of the United States are shown in Figure 6-2, and Table 6-1 lists representative net longshore transport rates for selected U.S. coasts (SPM 1984). Transport rate magnitudes are clearly related to the general wave climate as energetic (west coast), intermediate (east coast and parts of the Gulf of Mexico), and low (Great Lakes and west coast of Florida).

b. Sand bypassing plants have been constructed at some jetties and breakwaters as a practical measure to reduce the accretion/erosion patterns adjacent to the structures. The first measurements obtained relating sand transport rates to causative wave conditions were collected by Watts (1953a) at Lake Worth Inlet, Florida, using measured quantities of sand pumped past the jetties. The best correlation was obtained using month-long net sand volumes. A number of subsequent studies have similarly employed sand blockage by jetties and breakwaters to obtain data relating transport rates to wave conditions. Caldwell (1956) estimated the longshore sand transport from erosion rates of the beach downdrift of the jetties at Anaheim Bay, California. Bruno and Gable (1976), Bruno, Dean, and Gable (1980), and Bruno et al. (1981) measured transport rates by repeatedly surveying the accumulating blocked sand at Channel Islands Harbor, California; Dean et al. (1982) measured sand accumulations in the spit growing across the breakwater opening at Santa Barbara, California; and Dean et al. (1987) collected data from the sand bypassing plant at Rudee Inlet, Virginia. All of these studies yielded measurements of longshore sediment transport rates that are used in correlations with wave parameters. However, errors are introduced with the use of jetties and breakwaters to measure sediment transport rates, the foremost being the local effects of the structure on waves and currents, and the long-term nature of the determinations. In some cases it takes a month or
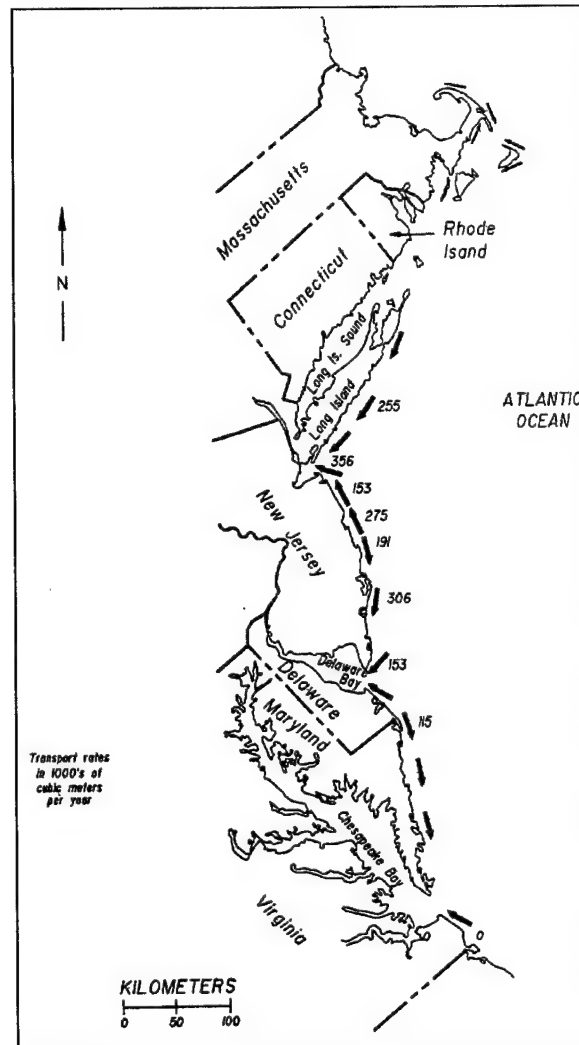
Figure 6-2. Annual net longshore transport rates and directions along the east coast of the United States (Komar 1977)

longer of sand accumulation to make the transport measurement meaningful, an interval during which waves and currents are continuously changing. Nevertheless, rates determined by impoundment and erosion are very valuable as they are closely related to gross quantities involved in the design of projects, such as the amount of sediment required to be bypassed at an inlet.

c. Short-term measurements of longshore sand transport rates have been obtained using sand tracers, a technique which involves tagging the natural beach sediment with a coating of fluorescent dye or inducing low level radioactivity. Tracers are injected into the surf zone,

Table 6-1
Longshore Transport Rates From U.S. Coasts[1] (SPM 1984)

Location	Predominant Direction of Transport	Longshore[2] Transport (cu m/yr)	Date of Record	Reference	
Atlantic Coast					
Suffolk County, N.Y.	W	153,000	1946-55	New York District	(1955)
Sandy Hook, N.J.	N	377,000	1885-1933	New York District	(1954)
Sandy Hook, N.J.	N	333,000	1933-51	New York District	(1954)
Asbury Park, N.J.	N	153,000	1922-25	New York District	(1954)
Shark River, N.J.	N	229,000	1947-53	New York District	(1954)
Manasquan, N.J.	N	275,000	1930-31	New York District	(1954)
Barnegat Inlet, N.J.	S	191,000	1939-41	New York District	(1954)
Absecon Inlet, N.J.	S	306,000	1935-46	New York District	(1954)
Ocean City, N.J.	S	306,000	1935-46	U.S. Congress	(1953a)
Cold Spring Inlet, N.J.	S	153,000	--	U.S. Congress	(1953b)
Ocean City, Md.	S	115,000	1934-36	Baltimore District	(1948)
Atlantic Beach, N.C.	E	22,500	1850-1908	U.S. Congress	(1948)
Hillsboro Inlet, Fla.	S	57,000	1850-1908	U.S. Army	(1955b)
Palm Beach, Fla.	S	115,000 to 175,000	1925-30	BEB	(1947)
Gulf of Mexico					
Pinellas County, Fla.	S	38,000	1922-50	U.S. Congress	(1954a)
Perdido Pass, Ala.	W	153,000	1934-53	Mobile District	(1954)
Pacific Coast					
Santa Barbara, Calif.	E	214,000	1932-51	Johnson	(1953)
Oxnard Plain Shore, Calif.	S	765,000	1938-48	U.S. Congress	(1953c)
Port Hueneme, Calif.	S	382,000	--	U.S. Congress	(1954b)
Santa Monica, Calif.	S	206,000	1936-40	U.S. Army	(1948b)
El Segundo, Calif.	S	124,000	1936-40	U.S. Army	(1948b)
Redondo Beach, Calif.	S	23,000	--	U.S. Army	(1948b)
Anaheim Bay, Calif.	E	115,000	1937-48	U.S. Congress	(1954c)
Camp Pendleton, Calif.	S	76,000	1950-52	Los Angeles District	(1953)
Great Lakes					
Milwaukee County, Wis.	S	6,000	1894-1912	U.S. Congress	(1946)
Racine County, Wis.	S	31,000	1912-1949	U.S. Congress	(1953d)
Kenosha, Wis.	S	11,000	1872-1909	U.S. Congress	(1953b)
Ill. State Line to Waukegan	S	69,000	--	U.S. Congress	(1953e)
Waukegan to Evanston, Ill.	S	44,000	--	U.S. Congress	(1953e)
South of Evanston, Ill.	S	31,000	--	U.S. Congress	(1953e)
Hawaii					
Waikiki Beach	-	8,000	--	U.S. Congress	(1953f)

Notes:
[1] Method of measurement is by accretion except for Absecon Inlet and Ocean City, New Jersey, and Anaheim Bay, California, which were measured by erosion, and Waikiki Beach, Hawaii, which was measured according to suspended load samples.
[2] Transport rates are estimated net transport rates, Q_N. In some cases, these approximate the gross transport rates, Q_G.
(from Wiegel 1964, Johnson 1957)

and the beach material is sampled on a grid to determine the subsequent tracer distribution. The longshore displacement of the center of mass of the tracer on the beach between injection and sampling provides a measure of the mean transport distance, and the sand advection velocity is obtained by dividing this distance by the elapsed time. The time between tracer injection and sampling is usually an hour to a few hours, so the measurement is basically the instantaneous longshore sand transport under a fixed set of wave conditions. The technique, therefore, provides measurements that are particularly suitable for correlations with causative waves and longshore currents, as enter in time-dependent numerical models of longshore transport rates and beach change, but is not particularly useful in determining long-term net transport rates and directions. Studies that have used sand tracers to determine sand transport rates include Komar and Inman (1970), Knoth and Nummedal (1977), Duane and James (1980), Inman et al. (1980), and Kraus et al. (1982).

d. Other techniques that have been used to measure sediment movements on beaches include various sand traps, pumps, and optical devices. However, such sampling schemes may relate to specific modes of transport, either the bedload or suspension transport, rather than yielding total quantities of littoral sediment transport. The results of studies relating to the modes of sediment transport will be discussed in paragraph 6-9.

e. In engineering applications, the longshore sediment transport rate is generally expressed as the volume transport rate, Q_ℓ , having units such as cubic meters per day or cubic yards per year. This is the total volume and includes about 40 percent void space between the particles as well as the 60 percent solid grains. Another representation of the longshore sediment transport rate is an immersed weight transport rate, I_ℓ , related to the volume transport rate by

$$I_\ell = (\rho_s - \rho)g(1 - n)Q_\ell \qquad (6\text{-}1)$$

where ρ_s is the mass density of the sediment grains, ρ is the mass density of water, g is the acceleration due to gravity, and n is the in-place sediment porosity ($n \approx 0.4$). The parameter n is a pore-space factor such that $(1\text{-}n)Q_\ell$ is the volume transport of solid sand alone, eliminating pore spaces included in the Q_ℓ volume transport rate. One advantage of using I_ℓ is that this immersed weight transport rate accounts for the density

of the sediment grains. The factor ρ_s - ρ accounts for the buoyancy of the particles in water.

6-4. Energy Flux Method for Predicting Potential Sediment Transport Rates

a. The potential longshore sediment transport rate, dependent on an available quantity of littoral material, is most commonly correlated with the so-called longshore component of wave energy flux or power,

$$P_\ell = (EC_g)_b \, \sin\alpha_b \, \cos\alpha_b \qquad (6\text{-}2a)$$

$$E_b = \frac{\rho g H_b^2}{8} \qquad (6\text{-}2b)$$

$$C_{gb} = \sqrt{gd_b} \qquad (6\text{-}2c)$$

where E_b is the wave energy evaluated at the breaker line and C_{gb} is the wave group velocity at the breaker line, so that $(EC_g)_b$ is the wave energy flux or power of the breaking waves, and α_b is again the wave breaker angle. The rationale for using P_ℓ to represent the wave conditions generally involves a derivation where $(EC_g)_b$, the wave energy flux per unit wave crest length, is converted to a unit shoreline basis by the inclusion of the $\cos\alpha_b$ factor, and then multiplication by $\sin\alpha_b$ to yield the longshore component, assumed to be that portion of the wave power available for transporting sediments in the longshore direction. The immersed weight transport rate I_ℓ has the same units as P_ℓ, so that the relationship

$$I_\ell = KP_\ell \qquad (6\text{-}3)$$

is homogeneous, that is, the empirical proportionality coefficient K is dimensionless. This is another advantage in using I_ℓ rather than the Q_ℓ volume transport rate.

b. Field data relating I_ℓ and P_ℓ are plotted in Figure 6-3 where the calculations of the wave power are based on the rms wave height at breaking, H_{br} . It is
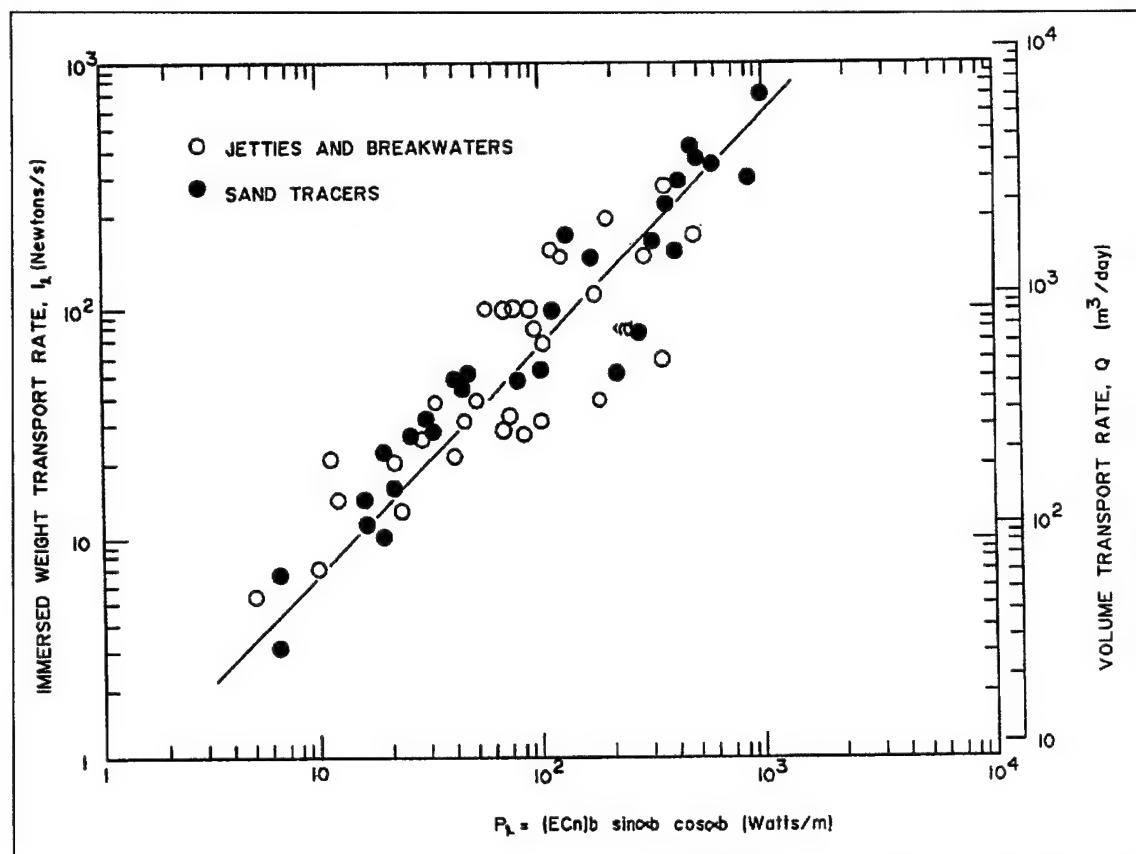
Figure 6-3. Field data relating I_ℓ and P_ℓ (after Komar 1988)

seen that the measurements involving sand accumulation at jetties and breakwaters are consistent with those obtained using sand tracers. Figure 6-3 includes more data than presented in the SPM (1984); therefore, the solid line in the figure yielding the coefficient $K = 0.70$ is more representative of the transport rate data set and supersedes the coefficient presented in the SPM ($K = 0.77$). Equation 6-3 then becomes

$$I_\ell = 0.70P_\ell = 0.70(EC_g)_b \sin\alpha_b \cos\alpha_b \qquad \text{(6-4a)}$$

$$I_\ell = 0.70\left(\frac{\rho g H_{br}^2}{8}\right)(g H_{br})^{\frac{1}{2}} \sin\alpha_b \cos\alpha_b \qquad \text{(6-4b)}$$

$$I_\ell = 0.088\rho g^{\frac{3}{2}} H_{br}^{\frac{5}{2}} \sin\alpha_b \cos\alpha_b \qquad \text{(6-4c)}$$

$$I_\ell = 0.044\rho g^{\frac{3}{2}} H_{br}^{\frac{5}{2}} \sin(2\alpha_b) \qquad \text{(6-4d)}$$

It has been assumed that the breaker index $\kappa = 1.0$ in the evaluation $C_{gb} = (g d_b)^{1/2} = (g H_b/\kappa)^{1/2}$. The sediment transport data are too scattered to incorporate possible variations in κ . By using Equation 6-1, the above relationships for I_ℓ can be converted to a volume transport rate:

$$Q_\ell = \frac{0.70}{(\rho_s - \rho)g(1 - n)} P_\ell \qquad (6\text{-}5a)$$

Taking $\rho_s = 2650$ kg/m^3 for quartz-density sand, $\rho = 1025$ kg/m^3 for salt water, $g = 9.8$ m/sec^2, and $n = 0.4$, and a unit conversion factor 1 day = 86,400 sec, this relationship becomes

$$Q_\ell = 6.3 \, P_\ell \qquad (6\text{-}5b)$$

where the units for P_ℓ must be watts/meter or, equivalently, newtons/second (N/sec), and the calculations will yield Q_ℓ with units m^3/day. A similar conversion of Equation 6-4d gives

$$Q_\ell = (1.2 \times 10^4) H_{br}^{\frac{5}{2}} \sin(2\alpha_b) \qquad (6\text{-}5c)$$

where the units for the rms wave breaker height must be meters and Q_ℓ is again expressed in m^3/day. In American Customary units, the relationship becomes

$$Q_\ell = (2.3 \times 10^4) \, H_{br}^{\frac{5}{2}} \sin(2\alpha_b) \qquad (6\text{-}5d)$$

where $\rho_s = 5.14$ slug/ft^3, $\rho = 1.99$ slug/ft^3 for salt water, $g = 32.2$ ft/sec^2, the wave height is measured in feet, and Q_ℓ is expressed in ft^3/day. The I_ℓ relationships of Equations 6-4a through 6-4d can be applied to calculate transport rates for sands of any density, but the Q_ℓ relations given in Equations 6-5a through 6-5d can only be used for quartz-density sand. In both Equations 6-4a through 6-4d and 6-5a through 6-5d, the correlations are based on the rms wave height, H_{br}, the height which corresponds to the correct assessment of wave energy as evaluated from the spectrum. This correlation was obtained by determining the empirical factor K as 0.70 in Equation 6-5a, and enters into the proportionality coefficients. The proportionality coefficients must be changed if the calculations are in terms of the

significant wave height, H_{bs}. Since from Table 3-3 $H_{bs}/H_{br} \approx 1.41$ (Longuet-Higgins 1952), the calculated wave power differs by $(1.41)^{5/2} = 2.4$. The relationships then become

$$I_\ell = 0.30P_\ell = 0.30\left(\frac{\rho g H_{bs}^2}{8}\right)$$
$$\left[(gH_{bs})^{\frac{1}{2}}\right] \sin\alpha_b \, \cos\alpha_b \qquad (6\text{-}6a)$$

$$I_\ell = 0.036\rho g^{\frac{3}{2}} H_{bs}^{\frac{5}{2}} \sin\alpha_b \, \cos\alpha_b \qquad (6\text{-}6b)$$

$$I_\ell = 0.018\rho g^{\frac{3}{2}} H_{bs}^{\frac{5}{2}} \sin(2\alpha_b) \qquad (6\text{-}6c)$$

Using metric units with Q_ℓ expressed in m^3/day, P_ℓ in watts/meter (or newtons/second), and H_{bs} in meters,

$$Q_\ell = 2.6P_\ell$$
$$= 2.6\left(\frac{\rho g H_{bs}^2}{8}\right)\left[(gH_{bs})^{\frac{1}{2}}\right]\sin\alpha_b \, \cos\alpha_b \qquad (6\text{-}7a)$$

$$Q_\ell = (5.1 \times 10^3) H_{bs}^{\frac{5}{2}} \sin(2\alpha_b) \qquad (6\text{-}7b)$$

The equivalent equation for American Customary units is

$$Q_\ell = (9.7 \times 10^3) \, H_{bs}^{\frac{5}{2}} \sin(2\alpha_b) \qquad (6\text{-}7c)$$

where H_{bs} is in feet and Q_ℓ is ft^3/day.

*************** EXAMPLE 6-1 ****************

GIVEN: Waves having a significant wave height of 2.3 m (7.5 ft) break on a sand beach at an angle 4.5°.

FIND: Calculate the potential immersed-weight and volumetric longshore sand transport rates.

SOLUTION: Since the wave height is given as a significant wave height, the potential sand transport rates are calculated with Equations 6-6c and 6-7b. With H_{bs} = 2.3 m (7.5 ft), ρ = 1025 kg/m³ (1.99 slug/ft³), g = 9.8 m/sec² (32.2 ft/sec²) and α_b = 4.5°, these respective equations give

$$I_\ell = 0.018 \rho g^{3/2} H_{bs}^{5/2} \sin(2\alpha_b)$$

$$I_\ell = 0.018(1025)(9.8)^{3/2}(2.3)^{5/2} \sin [(2\,(4.5°)]$$

$$I_\ell = 875 \ N/\text{sec} \ (157 \ \text{lb/sec})$$

This potential immersed-weight transport rate could be converted to a potential volumetric rate by using Equation 6-1, or Equation 6-7b can be used.

$$Q_\ell = 5.1 \times 10^3 \ H_{bs}^{5/2} \sin(2\alpha_b)$$

$$Q_\ell = 6.4 \times 10^3 \ \text{m}^3/\text{day} \ (8.4 \times 10^3 \ \text{yd}^3/\text{day})$$

************* END EXAMPLE 6-1 *************

*************** EXAMPLE 6-2 ****************

GIVEN: Spectral analysis of wave measurements at an offshore buoy in deep water yield a wave energy density of 2.1 x 10³ N/m (144 lb/ft), with a single peak centered at a period 9.4 sec. At the measurement site the waves make an angle of 7.5° with the trend of the coast, but after undergoing refraction, the waves break on a sandy beach with an angle of 3.0°.

FIND: Calculate the potential volumetric longshore sand transport rate along the beach.

SOLUTION: The group speed of the waves in deep water is given in Table 3-1 as

$$C_{go} = gT/4\pi = 9.8 \ (9.4) \ / \ (4\pi)$$
$$= 7.3 \ \text{m/sec} \ (24.0 \ \text{ft/sec})$$

The energy flux per unit shoreline length of the waves in deep water is

$$(EC_g)_o \cos\alpha_o = (2.1 \times 10^3)(7.3)\cos(7.5°)$$

$$= 1.5 \times 10^4 \ N/\text{sec} \ (3.4 \times 10^3 \ \text{lb/sec})$$

The inclusion of the $\cos\alpha_o$ factor accounts for wave refraction as the waves approach the beach so that this energy flux can be assumed constant during the shoaling processes (bottom friction and other energy losses are assumed to be negligible). The conservation of wave energy flux allows the substitution

$$(EC_g)_b \cos\alpha_b = (EC_g)_o \cos\alpha_o$$

Equation 6-2 for the longshore component of the energy flux at the shoreline then becomes

$$P_\ell = (EC_g)_b \ \sin\alpha_b \ \cos\alpha_b$$

$$= [(EC_g)_o \cos\alpha_o]\sin\alpha_b$$

$$= (1.5 \times 10^4) \ \sin(3.0°)$$

$$= 800 \ N/\text{sec} \ (180 \ \text{lb/sec})$$

Spectra yield wave parameters equivalent to rms conditions, and therefore Equation 6-5b is the appropriate choice for the calculation of the potential volumetric sand transport rate. This gives

$$Q_\ell = 6.3 \ P_\ell = 6.3(8.0 \times 10^2) = 5.0 \times 10^3 \ \text{m}^3/\text{day} \ (6.5 \times 10^3 \ \text{yd}^3/\text{day})$$

************* END EXAMPLE 6-2 *************

6-5. Estimating Potential Sand Transport Rates Using WIS Data

a. Introduction. Potential longshore sand transport rates can be calculated using Wave Information Study (WIS) Phase III hindcast wave estimates (see Chapter 3). First, refraction and shoaling of incident linear waves are calculated using Snell's law and the conservation of wave energy flux. The shallow-water wave breaking criterion then defines wave properties at the break point, and potential longshore sand transport rates are calculated by means of the energy flux method.

b. Wave transformation procedure. To calculate the potential longshore sand transport rate using Equations 6-5c (metric units) or 6-5d (American Customary units), the breaking wave height and incident angle with respect to the shoreline are required. WIS hindcast estimates, however, are given for water depths greater than or equal to 10 m (Jensen 1983a, 1983b). A transformation of the WIS hindcast wave estimates to breaking conditions is therefore necessary. Refraction and shoaling of incident waves provided by WIS can be accomplished using linear wave theory. Two assumptions in the present treatment are that offshore depth contours are straight and parallel to the trend of the shoreline and that no wave energy dissipation occurs prior to breaking. The governing equations are given below, where subscripts 1 and 2 denote values at locations 1 and 2. Wave direction is obtained through Snell's law:

$$\frac{\sin\alpha_1}{L_1} = \frac{\sin\alpha_2}{L_2} \tag{6-8}$$

The wave height is obtained by invoking the conservation of wave energy flux directed onshore,

$$E_1 C_{g1}\cos\,\alpha_1 = E_2 C_{g2}\cos\,\alpha_2 \tag{6-9}$$

where the wave energy is given by Equation 6-2b and wave group speed is given in Table 3-1 as

$$C_g = \frac{L}{2T}\left[1 + \frac{4\pi d}{L\,\sinh\left(\frac{4\pi d}{L}\right)}\right] \tag{6-10}$$

Wavelength can be determined through a Padé approximation (Table 3-2) or Newton-Raphson iteration using the relationship presented in Table 3-1:

$$L = \frac{gT^2}{2\pi}\,\tanh\left(\frac{2\pi d}{L}\right) \tag{6-11}$$

The Automated Coastal Engineering System (ACES) provides a program, "Linear Wave Theory with Snell's Law," that performs similar calculations, shoaling waves from an offshore depth to an inshore depth using Snell's law (see Appendix E).

c. Wave conditions.

(1) As discussed in Chapter 3, WIS hindcast wave estimates are compiled at deep water (Phase I), intermediate water (Phase II), and a 10-m depth (Phase III). The FORTRAN program WISTRT (see Appendix E) and examples presented herein use Phase III WIS data; however, the concepts are equally applicable to wave estimates obtained from Phase I and Phase II stations. WIS hindcast wave estimates are presented in 30-deg wave angle bands. Angles reported for WIS Phase III stations, α_{WIS}, are defined with respect to shoreline orientation and are measured counter-clockwise from the shoreline (i.e., $\alpha^o \leq \alpha_{WIS} \leq 180°$). For calculation of longshore sand transport, a right-handed coordinate system is more convenient, in which waves approaching normal to the shoreline are given an angle of 0 deg. Looking seaward, waves approaching from the right are associated with negative angles, and wave approaching from the left are associated with positive angles such that positive transport is directed to the right. Conversion of WIS angles to angles associated with transport calculations, α, may be accomplished by means of the following relationship:

$$\alpha = \alpha_{WIS} - 90^o \tag{6-12}$$

An example of a typical WIS Phase II wave statistics summary is given in Table 6-2. Percent occurrence multiplied by 1000 is listed for specific wave height and period bands. The header gives the record length (20 years), angle band, water depth, and shoreline orientation angle. Because of the sensitivity of the calculated

Table 6-2
Percent Occurrence by Angle Band, WIS Atlantic Coast Phase III Station 54

Station 54 20 Years   Wave Approach Angle (Degrees) = 60.0-89.9
Shoreline Angle = 4.0 Degrees Azimuth
Water Depth = 10.00 Meters
Percent Occurrence (X1000) of Height and Period by Direction

Height (Meters)	0.0-2.9	3.0-3.9	4.0-4.9	5.0-5.9	6.0-6.9	7.0-7.9	Period (Seconds) 8.0-8.9	9.0-9.9	10.0-10.9	11.0-Longer	Total
0.00 - 0.49	634	744	.	.	593	2861	2286	992	278	455	8843
0.50 - 0.99	.	571	1309	148	37	718	631	277	311	106	4108
1.00 - 1.49	.	.	111	693	147	164	131	30	70	58	1404
1.50 - 1.99	.	.	.	34	256	159	71	6	11	25	562
2.00 - 2.49	.	.	.	.	29	285	80	5	1	25	425
2.50 - 2.99	.	.	.	.	.	51	92	5	1	1	150
3.00 - 3.49	.	.	.	.	.	.	6	10	5	.	21
3.50 - 3.99	.	.	.	.	.	.	.	8	.	.	8
4.00 - 4.49	.	.	.	.	.	.	.	.	.	.	0
4.50 - 4.99	.	.	.	.	.	.	.	.	.	.	0
5.00 - Greater											
Total	634	1315	1420	875	1062	4238	3297	1333	677	670	

Average HS(M) = 0.61   Largest HS(M) = 3.70   Angle Class % = 15.5

longshore sand transport rate to shoreline orientation, this quantity should be verified using a nautical chart. The last line in the table gives the average and largest significant wave height, together with the angle class percent. A representative wave period for the given average significant wave height may be determined by calculating a weighted average of all the wave periods given across the bottom of the table in the row labeled "total." Similarly, a representative period for each of the wave height bands can be calculated. The central angle of the angle band given in Table 6-2 (75 deg) converted to the transport coordinate system using Equation 6-12 is -15 deg.

(2) Data given in WIS statistical tables may be used in several ways to calculate the potential longshore sand transport rate. Two examples using the data in Table 6-2 will be given. In Example 6-3, the potential longshore sand transport rate is estimated with average significant wave height. In Example 6-4, wave data are more accurately represented by calculating a representative wave period for each of the given wave height bands.

*************** EXAMPLE 6-3 *************

FIND: Calculate the potential longshore sand transport rate using average significant wave height and a weighted period for the data given in Table 6-2.

SOLUTION: The data in Table 6-2 are used to calculate an average period T_{avg} = 7.2 sec, and angle associated with transport calculations α = -15 deg. Using values of $(H_s)_{avg}$ = 0.61 m at a depth of 10 m, with percent occurrence = 15.5, the program WISTRT gives

H_b = 0.87 m (2.85 ft)

α_b = -5.6 deg

Q_ℓ = -50,800 m^3/year (66,400 yd^3/year) (directed to the left)

*************** END EXAMPLE 6-3 ***********

*** EXAMPLE 6-4 ***

<u>FIND</u>: Calculate the potential longshore transport rate using each of the eight wave height bands given in Table 6-2.

<u>SOLUTION</u>:

	Program Input					Program Output		
Wave Condition	$(H_s)_{avg}$ m	T_{avg} sec	α deg	Depth m	Percent Occurrence %	H_b m	α deg	Q m³/year
1	0.25	7.5	-15.0	10.0	8.843	0.43	-3.9	-3,500
2	0.75	6.5	-15.0	10.0	4.108	1.00	-6.2	-21,100
3	1.25	6.6	-15.0	10.0	1.404	1.53	-7.6	-25,500
4	1.75	7.3	-15.0	10.0	0.562	2.09	-8.5	-24,700
5	2.25	7.9	-15.0	10.0	0.425	2.62	-9.3	-36,000
6	2.75	8.2	-15.0	10.0	0.150	3.12	-10.1	-21,200
7	3.25	9.5	-15.0	10.0	0.021	3.66	-10.7	-4,700
8	3.75	9.5	-15.0	10.0	0.008	4.13	-11.3	-2,500
								-139,200

Q = -139,200 m^3/year (directed to the left)

*** END EXAMPLE 6-4 ***

The ACES program "Longshore Sediment Transport" also provides a method for calculation of potential longshore sediment transport rates under the action of waves (see Appendix E).

6-6. Calculations of Littoral Transport Rates from Longshore Currents

a. Early workers such as Grant (1943) stressed that sand transport in the nearshore results from the combined effects of waves and currents, the waves placing sand in motion, and the longshore currents producing a net sand advection. Such a model was given a mathematical framework by Bagnold (1963), and applied specifically to the evaluation of longshore sediment transport on beaches by Inman and Bagnold (1963). Their analysis yielded,

$$I_\ell = K'(EC_g)_b \frac{V_\ell}{u_m}$$ (6-13)

where V_ℓ is the longshore current velocity, in practice measured at the mid-surf position, u_m is the maximum horizontal component of the orbital velocity of the waves evaluated at the breaker zone, and the proportionality coefficient K' is dimensionless. The sand transport field measurements of Komar and Inman (1970) and Kraus et al. (1982) are shown in Figure 6-4 and yield $K' = 0.25$. Taking $E_b = (\rho g H_b^2)/8$ for the wave energy, $u_m = (2E_b/\rho d_b)^{1/2} = 0.5\kappa^{1/2}(gH_b)^{1/2}$ according to linear wave theory, and $\kappa = 1$, the relationship of Equation 6-13 reduces to

$$I_\ell = 0.062 \, \rho g(H_{br})^2 V_\ell$$ (6-14a)

$$I_\ell = 0.031 \, \rho g(H_{bs})^2 V_\ell$$ (6-14b)

for which the breaker heights are the rms and significant wave height, respectively. Using Equation 6-1 to convert from I_ℓ to the volume transport rate, Q_ℓ
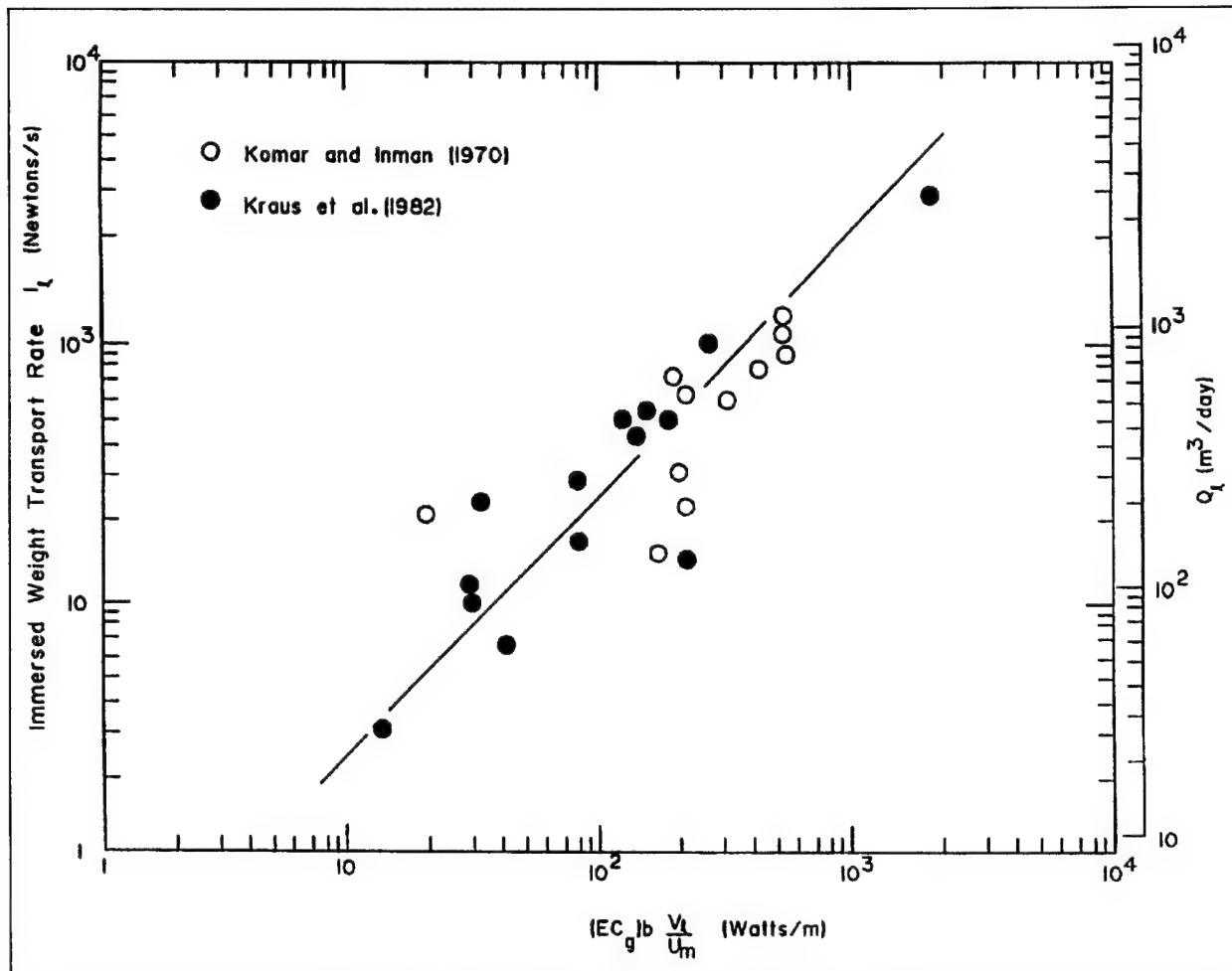
Figure 6-4. Comparison of Bagnold model with measured sediment transport rates

$$Q_\ell = 0.062 (H_{br})^2 V_\ell \qquad (6\text{-}15a)$$

$$Q_\ell = 0.031 (H_{bs})^2 V_\ell \qquad (6\text{-}15b)$$

for quartz density sands, similar to a relationship first derived by Kraus et al. (1982). These relationships are dimensionally homogeneous and can be used with any consistent set of units. The equivalence of the coefficients in the respective I_ℓ and Q_ℓ relationships is fortuitous, and results from $(\rho_s-\rho)(1-n)/\rho \approx 1$ for quartz sand in water with $n = 0.4$.

b. Equations 6-14 and 6-15 have several advantages over the P_ℓ based sediment transport relationships. From a practical standpoint, it is often easier and more accurate to measure the longshore current V_ℓ than it is to determine the breaker angle α_b needed in the P_ℓ formulation. Equation 6-13 was derived by Bagnold (1963) on the basis of considerations of the physical processes of sand transport, and accordingly should be viewed as more fundamental than the empirical correlations with P_ℓ. In the derivation of Equations 6-13 through 6-15, the origin of the longshore current V_ℓ is not specified, so it could be due to an oblique wave approach, tidal currents, part of the cell circulation with rip currents, or generated by local winds (Komar and Inman 1970). If the longshore current is generated solely by waves breaking obliquely to the shore, then

the velocity as given by Equation 5-2a and Equation 6-14a becomes

$$I_\ell = 0.62 \rho g (H_{br})^2 V_\ell \qquad (6\text{-}16a)$$

$$I_\ell = 0.62 \rho g (H_{br})^2 \left[0.58 \sqrt{g H_{br}} \ \sin(2\alpha_b) \right] \qquad (6\text{-}16b)$$

and with some algebraic modification,

$$I_\ell = 0.036 \rho g^{\frac{3}{2}} H_{br}^{\frac{5}{2}} \ \sin(2\alpha_b) \qquad (6\text{-}16c)$$

which is nearly the same as the energy flux littoral transport formula, Equation 6-4d. The difference in the coefficients, 0.036 versus 0.044, results because the 0.036 value combines three empirical coefficients, K and K' for the sand transport relationships, and the 0.58 coefficient for the longshore current formula, Equation 5-2. The implication of this result is that any of the P_ℓ relationships for sediment transport on beaches are suitable only for the specific case where the longshore current and the resulting sediment transport are produced solely by waves breaking at an angle to the shoreline (Komar and Inman 1970).

*************** EXAMPLE 6-5 ****************

GIVEN: Breaking waves in the sheltered zone of a breakwater have an rms height 1.8 m (5.9 ft), and although they break effectively parallel to the shore, there is a persistent longshore current flowing toward the structure with mean velocity 0.25 m/sec (0.82 ft/sec) as measured at approximately the mid-surf position.

FIND: Calculate the resulting volumetric longshore transport of sand moving toward the breakwater.

SOLUTION: Since $\alpha_b = 0$, it is apparent that the P_ℓ approach to evaluating potential longshore sand transport rates is inappropriate and that the Bagnold model is required. With

H_{br} = 1.8 m (5.9 ft) and V_ℓ = 0.25 m/sec (0.82 ft/sec) , Equation 6-15a gives

$$Q_\ell = 0.062 (H_{br})^2 V_\ell$$

$$= 0.062 (1.8)^2 (0.25)$$

$$= 0.050 \text{ m}^3/\text{sec} = 4.3 \times 10^3 \text{ m}^3/\text{day (5.6}$$
$$\times 10^3 \text{ yd}^3/\text{day)}$$

************* END EXAMPLE 6-5 *************

6-7. Transport Dependence on Sediment Grain Size and Beach Morphology

a. It is clear that sediment transport rates on beaches should depend on environmental factors such as the grain diameter or settling velocity of the sediment, and possibly on factors such as the beach slope or wave steepness. Accordingly, it would be expected that the proportionality coefficients K in Equation 6-3 and K' in Equation 6-13 would both decrease as the grain size increases. Unfortunately, examinations of such dependencies for the available field data are hampered by problems with large random scatter within any one data set, and by systematic differences between separate studies that have employed diverse measurement techniques.

b. Data summaries by Bruno, Dean, and Gable (1980), Bruno et al. (1981), and Dean et al. (1982, 1987) suggested that K of Equation 6-3 does decrease from approximately 1.6 to 0.3 as the median diameter D_{50} of the beach sand increases from 0.2 mm to 1.0 mm, which is a very strong dependence. However, Komar (1988) has reviewed the same data and noted that the trend was established mainly by two K values, that of Bruno and Gable (1976) from the Channel Islands Harbor, California, and of Moore and Cole (1960) from Cape Thompson, Alaska, data where the estimates for K are uncertain. The very high $K = 1.6$ value that had been used for the Bruno and Gable data was based on measurements collected by the Littoral Environmental Observation (LEO) program; when those visual observations are replaced by data obtained from wave gauges, the coefficient is reduced to $K = 0.80$. The revised graphs of K and K' versus D_{50} indicate that it is not possible to establish trends with confidence (Komar 1988). Similar results were obtained with data from sandy beaches in comparisons between K and K' and beach slopes and with the deep water wave steepness.

c. The field data relating longshore transport rates to wave parameters included in Figures 6-3 and 6-4 are limited to sand beaches with D_{50} covering only the narrow range 0.2 to 1 mm. Within that grain-size range, at the present time K and K' can be taken as constants in a pragmatic sense, as can be the derivative proportionality coefficients in the various sand transport relationships. Limited measurements are available from gravel beaches that do support the belief that K and K' will have lower values for coarse-grained beaches. Hattori and Suzuki (1979) measured particle advection rates on a beach where D_{50} = 2 cm, and a reanalysis of their results suggests $K \approx 0.2$ in Equation 6-3 (Komar 1988). Measurements from beaches where D_{50} = 4 cm yield $K \approx 0.01$ to 0.04 (Komar 1988). Although the inclusion of these data from gravel beaches does support the expected decrease in K with increasing D_{50}, the results are sufficiently uncertain and limited in number that they should be used in applications only as an approximate guide.

d. Although it is apparent that K and K' should depend on environmental factors such as D_{50}, the anticipated trends cannot be established with confidence using the existing field data. More success is achieved with laboratory wave basin data on longshore sand transport (Kamphuis et al. 1986). Those results might be employed for guidance of expected trends in field applications.

6-8. Applications of Sediment Transport Relationships and Their Uncertainties

a. The equations presented above relate the total longshore sand transport rate to wave and nearshore current parameters. Because wave conditions change from day to day, the transport rate and its direction will also change. The daily measurements of the wave conditions can provide daily estimates of sand movement, and these can be summed algebraically to determine the annual gross littoral transport or summed vectorily to evaluate the net transport (quantity and direction), as described in paragraph 6-5. However, it is important to recognize the uncertainties and variabilities involved in these respective estimates. It is apparent from the scatter of the data in Figure 6-3 that even if one has absolute confidence in the value of P_ℓ for the wave conditions, the resulting estimate of the transport could potentially range by a factor of 2 to 3. As a percentage, this uncertainty is more significant to the estimated net transport than to the gross transport, since the magnitude of the latter will be much greater than the net transport. On coasts where there is a variability in wave approach,

the resultant of the net transport could be smaller than the uncertainty of the daily estimates, and the resultant direction could even be incorrect. In such cases, it is important to compare the estimated transport directions and quantities with direct field evidence. This evidence could be the amount of sand captured by groins or jetties, or the estimated littoral drift as one component in the total budget of sediments.

b. The accuracy of wave data used to calculate potential transport rates also leads to uncertainty in predictions. Wave measurements and observations have associated uncertainties based on instrumentation accuracy and observer bias. Given that there are breaking wave height and wave angle uncertainty values ΔH_b and $\Delta\alpha_b$, respectively, an associated longshore transport uncertainty ΔQ_ℓ can be calculated. From Equations 6-5c, 6-5d, 6-7c and 6-7d, we see that $Q_\ell \sim H_b^{5/2} \sin 2\alpha_b$. An estimate of the uncertainty in the longshore transport rate can be evaluated by including the uncertainties in breaking wave height and angle:

$$Q_\ell \pm \Delta Q_\ell \sim (H_b \pm \Delta H_b)^{5/2} \atop \sin 2(\alpha_b \pm \Delta\alpha_b) \qquad (6\text{-}17)$$

Assuming that the wave angle at breaking is small, and using the first two terms of a Taylor series expansion of Equation 6-17, the uncertainty in the longshore transport rate is estimated as

$$\Delta Q_\ell \sim \pm Q_\ell \left(\frac{\Delta\alpha_b}{\alpha_b} + \frac{5}{2}\frac{\Delta H_{sb}}{H_{sb}} \right) \qquad (6\text{-}18)$$

c. A 15 percent uncertainty in wave height and 15 percent uncertainty in wave angle result in 37.5 and 15 percent uncertainty contributions for height and angle, respectively, totaling a 52.5 percent uncertainty in Q_ℓ.

6-9. Modes of Sediment Transport

a. A distinction is made between two modes of sediment transport, suspended sediment transport carried above the bottom by the turbulent eddies of the water, and bed-load sediment transport where the grains remain close to the bed and move by rolling and saltating. Although this distinction may be made conceptually, it

is difficult to separately measure these two modes of transport on beaches. Considerable uncertainty remains and differences of opinion exist on their relative contributions to the total transport rate.

b. The data included in Figures 6-3 and 6-4 were collected by blocking littoral drift at a jetty or breakwater and by using sand tracers. Those measurement approaches are believed to come closest to yielding total quantities of longshore sediment transport, the bed load plus suspended load transport. Other measurement techniques are designed to separately determine either the bed load or suspended load. It is far easier to measure suspended load transport, and this has been the focus of numerous studies. One approach has been to pump water containing suspended sand from the surf zone, a technique which has the advantage that large quantities can be processed, leading to some confidence that the samples are representative of sediment concentrations found in the surf (Watts 1953b; Fairchild 1972, 1977; Coakley and Skafel 1982). The disadvantages of the approach are that one cannot investigate time variations in sediment concentrations at different phases of

wave motions, and the sampling has often been undertaken from piers which may disturb the water and sediment motion. Another method for measuring suspension concentrations is with traps, usually consisting of a vertical array of three or four sample collectors, and so can be used to examine the vertical distribution of suspended sediments and can be positioned at any location across the surf zone (Hom-ma, Horikawa, and Kajima 1965; Kana 1977, 1978; Inman et al. 1980; Kraus, Gingerich, and Rosati 1988). Figure 6-5 shows vertical distributions of the longshore sediment flux (transport rate per unit area) through the water column obtained in a 5-min sampling interval by traps arranged across the surf zone (Kraus, Gingerich, and Rosati 1989). The steep decrease in transport with elevation above the bed is apparent; such considerations are important in groin and weir design. The sharp decrease in transport at the trap located seaward of the breaker line indicates that the main portion of longshore sediment transport takes place in the surf and swash zones.

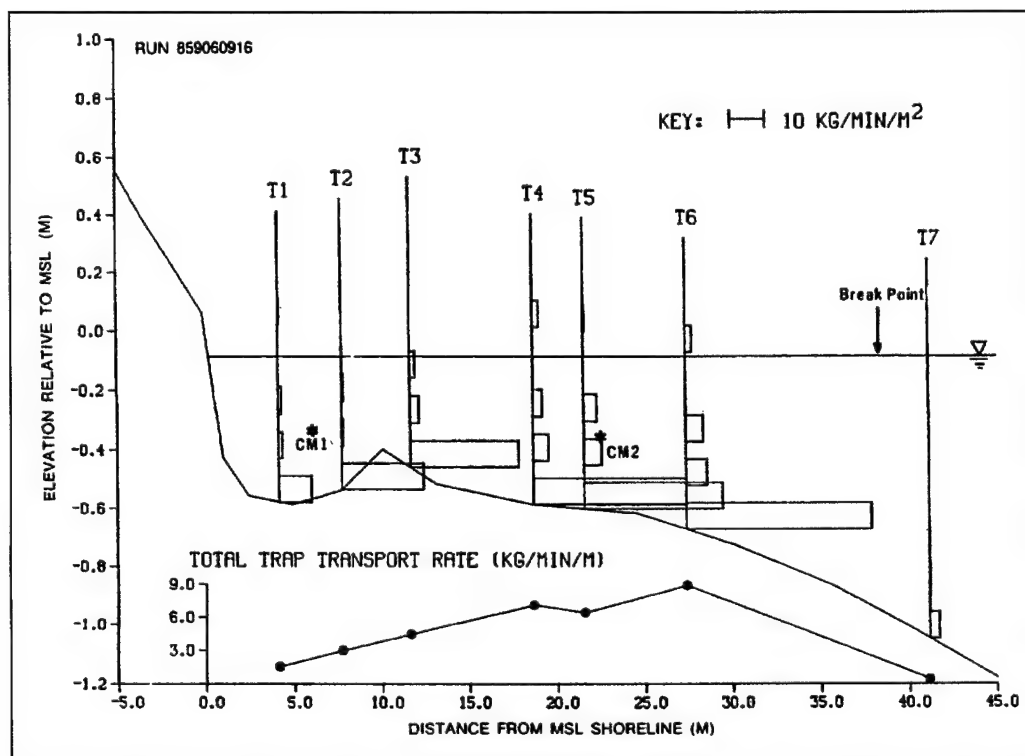*c.* Recent studies have turned to the use of optical and acoustic techniques for measuring suspension

Figure 6-5. Cross-shore distribution of the longshore sand transport rate measured with traps (Kraus, Gingerich, and Rosati 1989)

concentrations in the nearshore (Brenninkmeyer 1976; Thornton and Morris 1977; Katoh, Tanaka, and Irie 1984; Downing 1984; Sternberg, Shi, and Downing 1984; Beach and Sternberg 1987; Hanes et al. 1988). The advantage of these approaches is that they yield continuous measurements of the instantaneous concentrations of suspended sediments, and arrays of instruments can be employed to document variations across the width of the surf zone and vertically in the water column. In contrast to these techniques for measuring suspended transport, the only method presently suitable for measuring the bed load is bed-load traps, but there are questions as to sampling efficiency when used in the nearshore because of the potential for scour (Thornton 1972; Rosati and Kraus 1989).

d. Much has been learned about the patterns of sediment transport on beaches, especially for the suspended load. It has been demonstrated that suspension concentrations decrease exponentially with height above the bottom (Kraus, Gingerich, and Rosati 1988, 1989). The highest concentrations typically are found in the breaker and swash zones, with lower concentrations at midsurf positions. On reflective beaches, individual suspension events are correlated with the incident breaking wave period. In contrast, on dissipative beaches the long-period infragravity water motions have been found to account for significant sediment suspension, the suspension concentrations being 3 to 4 times larger than those associated with the short-period incident waves (Beach and Sternberg 1987).

e. Although much has been learned about suspension transport in the nearshore, the relative roles of suspension versus bed-load transport on beaches are still uncertain (Komar 1990). Critical to the argument has been measurements of suspended loads close to the bed where concentrations are highest, and establishing at what level the suspended load gives way to bed-load transport. Other problems are the lack of a satisfactory method for measuring bed load alone, and the large uncertainties involved in measurements of suspension transport versus the total longshore sediment transport.

6-10. Cross-Shore Profiles of Longshore Transport Rates

a. The relationships given above yield the total longshore sediment transport. Some applications require evaluations of the cross-shore distribution of the transport. For example, it is central to the effective design of groins, jetties, and weirs. In addition, equations for the prediction of the details of the transport within the

nearshore are required in many computer simulation models.

b. The collection of field data on cross-shore distributions of sand transport rates is difficult. The earliest approach was to use sand tracers. Zenkovitch (1960) determined distributions by averaging a large number of observations and found three maxima for the sand transport, two over longshore bars and a third in the swash zone. Kraus et al. (1982) provide an example of the use of sand tracers to investigate profiles of the longshore transport, employing tracers with four distinct colors injected on a line crossing the surf zone. Thornton (1972) used sediment traps on a Florida beach to obtain measurements of the transport distribution. His data show a maximum transport on the seaward side of the longshore bar where the waves were breaking, with decreasing rates of transport both shoreward and seaward of the breaker zone. Kraus and Dean (1987) and Kraus, Gingerich, and Rosati (1989) give general examples of vertical and cross-shore distributions of longshore sediment flux measured with portable traps (Figure 6-5). An interesting approach is that of Bodge and Dean (1987) who utilized a short-term sediment impoundment scheme consisting of the rapid deployment of a low profile, shore-perpendicular barrier. Beach profile changes in the vicinity of the barrier were determined from repeated surveys over short intervals of time. A series of laboratory experiments were completed, and field measurements were undertaken at the CERC Field Research Facility at Duck, North Carolina. One profile from the field experiments is shown in Figure 6-6, indicating the presence of a maximum in the outer surf zone just shoreward of the breaker zone, and a second maximum in the swash zone. The relative significance of the peaks was found by Bodge and Dean (1987) to be a function of the breaker type. As the wave conditions varied from spilling to collapsing, the outer peak near the breaker zone decreased while that in the swash zone increased. Longshore transport in the swash zone was found to represent some 5 percent of the total transport with spilling breakers, increasing to over 60 percent for collapsing breakers. The longshore transport seaward of the breakpoint was found to represent about 10 to 20 percent of the total transport.

c. Stresses exerted by waves vary in the crossshore direction, generally decreasing from the breaker zone to the shoreline, but not necessarily in a uniform manner due to the presence of bars and troughs on the beach profile. The longshore current also has a characteristic profile (Figure 5-3), and since sand transport is a result of the combined waves and currents, its distribution will
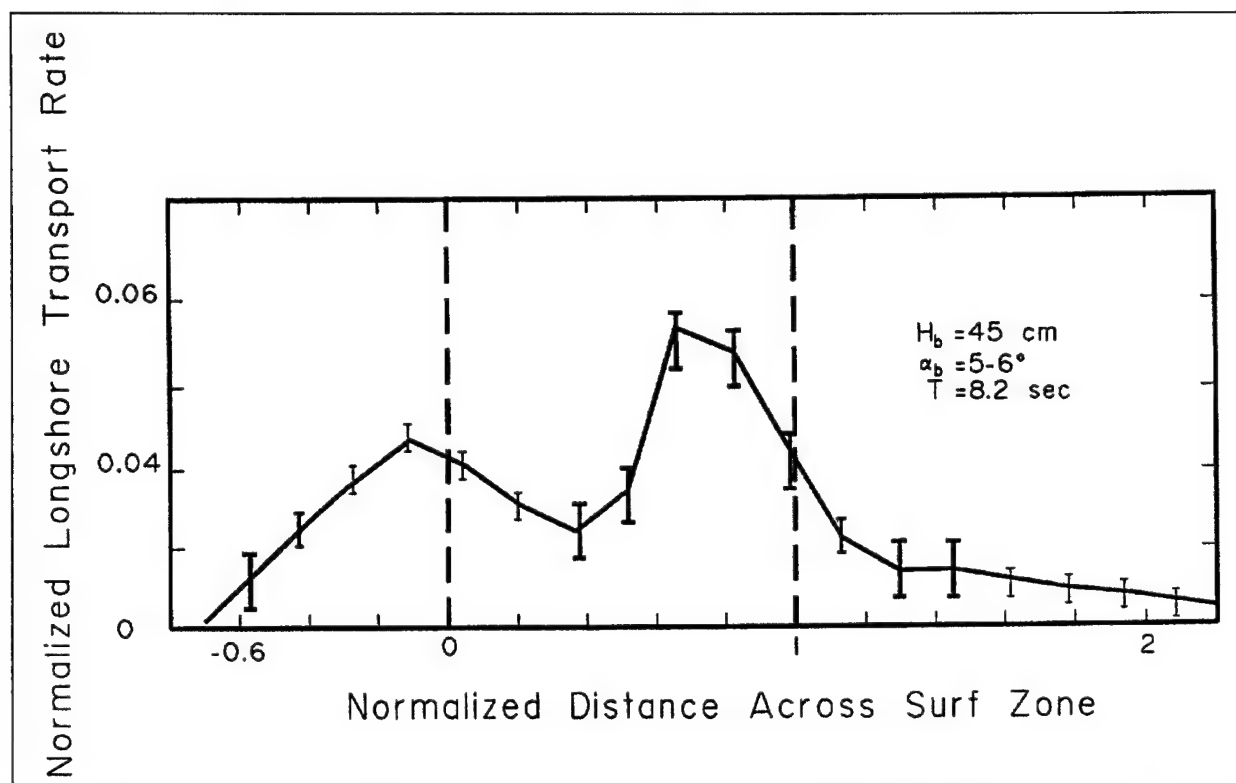
Figure 6-6. Measured cross-shore distribution of longshore transport rate at Duck, North Carolina (after Bodge and Dean 1987)

be the product of their distributions. Komar (1977) utilized the Bagnold (1963) model to derive a theoretical distribution of the longshore sand transport as the product of the local wave stress and the local current velocity. Based on the Bagnold model, the local immersed weight transport rate per unit cross-shore distance, $i(x)$, was taken to be proportional to the product of the local stress $\tau(x)$ produced by the wave orbital motions, and the local longshore current, $V_\ell(x)$. Taking the wave stress as $\tau = 0.5f_w\rho u_m^2$ where f_w is the drag coefficient for oscillatory wave motions (Jonsson 1966, Kamphuis 1975) and u_m is the local maximum wave orbital velocity, the derivation leads to the relationship,

$$i(x) = \frac{\pi k_1}{4}(0.5f_w)\,\rho\kappa^2\;d(x)V_\ell(x) \qquad (6\text{-}19)$$

where $d(x)$ is the local water depth. The quantity k_1 is a dimensionless proportionality coefficient which was

calibrated by integrating $i(x)$ across the surf zone and equating it to the total transport I_ℓ from Equation 6-4. The longshore current distribution, $V_\ell(x)$, was calculated from the solution of Longuet-Higgins (1970b) with its empirical coefficients based on Equation 5-1 so that the current magnitude at the midsurf position agreed with Equation 5-2. The resulting solution for $i(x)$ is an analytical expression having only one free parameter which depends on the degree of horizontal eddy mixing and determines the longshore current profile in the Longuet--Higgins solution. The magnitudes of the $V_\ell(x)$ and $i(x)$ distributions are governed by the wave breaker height and breaker angle. An example of a sand transport distribution calculated by this approach is shown in Figure 6-7 for the case of $H_b = 2.0$ m and $\alpha_b = 15°$, and a beach slope $m = 0.01$; the sand transport has been converted from an $i(x)$ distribution to a $q_\ell(x)$ volume transport distribution. The significance of these distributions is that $V_\ell(x)$ at the midsurf position agrees with Equation 5-2 and thus with the measurements of longshore currents, and if the $q_\ell(x)$ distribution is integrated
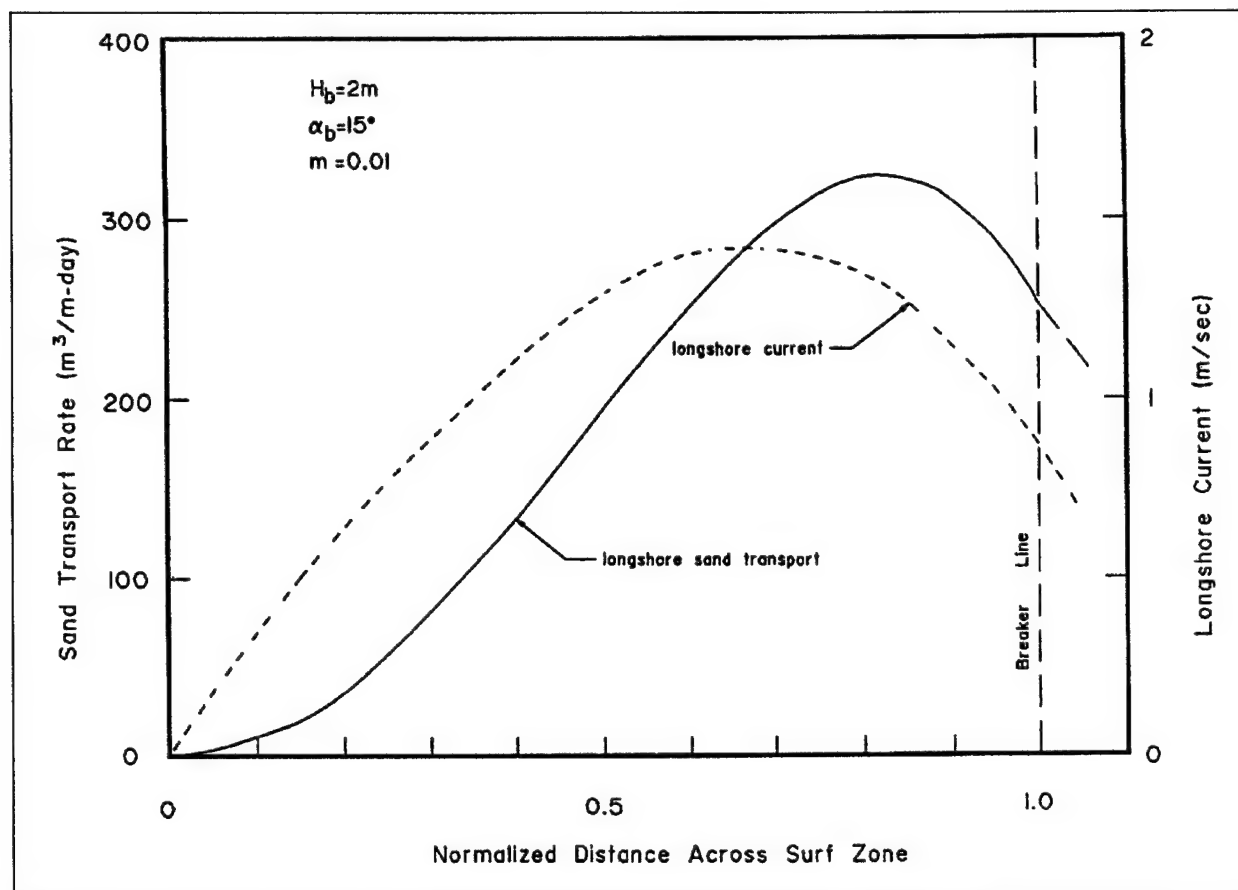
Figure 6-7. Calculated cross-shore distribution of longshore transport

across the surf zone, it yields the correct total longshore sand transport for those wave conditions.

6-11. Shoreline Change Numerical Models

a. Mathematical modeling of shoreline change is a useful engineering technique for understanding and predicting the evolution of the plan and profile shapes of sandy beaches. In particular, mathematical models provide a concise, quantitative means of describing systematic trends in shoreline evolution commonly observed at groins, jetties, breakwaters, revetments, seawalls and coastal engineering activities such as beach nourishment and sand mining. The responses of these complex shoreline processes may be rapidly and economically examined by adapting analytical or numerical solutions to the mathematical models which describe the shoreline response. However, the complexity of nearshore processes and the limitations of the models require careful interpretation of results.

b. The equations for fully describing nearshore waves, circulation, and shoreline evolution must be three-dimensional and time-dependant. Development of these equations is still an area of active research and general models are not available for routine engineering design. Models are available which average the equations over depth and the incident wave period. These types of models are often referred to as radiation stress models because the gradients in the radiation stresses (wave momentum) are the principle driving forces. These models provide insight into wave transformations and circulation for complicated bathymetry and in the vicinity of nearshore structures. However, they are less useful for making long-term shoreline evolution calculations because they are computationally intensive. These models also involve poorly known empirical coefficients such as those related to bottom friction, turbulent mixing, and sediment transport. Integrating the calculated local distributions of sediment transport over the cross-shore and for long time periods may lead to erroneous

results because small local inaccuracies will be amplified over a long simulation.

c. The Large Scale Sediment Processes Committee at the Nearshore Processes Workshop in St. Petersburg in 1989 recommended that long-term simulations are more reasonably formulated on the basis of bulk transport models such as Equation 6-5. These models have fewer coefficients and provide no details for the sediment transport profile. However, they have been calibrated to include the integrated effect of all of the local processes on the total transport.

d. The shoreline change models developed from bulk transport models are often referred to as line models. One-line models assume that the beach profile is a constant shape (Komar 1973, Kraus and Harikai 1983). The computer model GENESIS (GENEralized model for SImulating Shoreline change) is a sophisticated one-line model developed at CERC (Hanson and Kraus 1989; Gravens, Kraus, and Hanson 1991). N-line models allow the cross-shore profile to change (Perlin and Dean 1983, Scheffner and Rosati 1987, Kobayashi and Han 1988). The geometry of the cross-shore profile is typically related to the wave conditions and sediment size through empirical relationships.

e. One-line models have been used successfully in numerous projects to calculate longshore sand transport rates and long-term shoreline changes. In this type of model the profile is displaced parallel to itself in the cross-shore direction. The profile may include bars and other features but is assumed to always maintain the same shape. This assumption is best satisfied if the profile is in equilibrium. The formulation of the one-line model is based on the conservation equation of sediment in a control volume or shoreline reach. It is assumed that there is an offshore closure depth, D_C, at which there are no significant changes in the profile, and the upper end of the active profile is at the berm crest elevation, D_B. The constant profile shape moves in the cross-shore direction between these two limits. This implies that the sediment transport is uniformly distributed over the active portion of the profile. The incremental volume of sediment in a reach is simply $(D_B + D_C)\Delta x \Delta y$, where Δx is the cross-shore displacement of the profile and Δy is the reach length. Conservation of sediment volume may be written as

$$\frac{\Delta x}{\Delta t} + \frac{1}{D_B + D_C}\left(\frac{\Delta Q_\ell}{\Delta y} \pm q\right) = 0 \qquad (6\text{-}20)$$

in which Q_ℓ is the longshore transport rate, q is a line source or sink of sediment along the reach, and t is time (Figure 6-8). As examples, line sources of sediment may be rivers and coastal cliffs, and sinks may be produced by sand mining.

f. The longshore transport rate is evaluated using equations similar to 6-5 or 6-15. These require measurement or calculation of the breaking wave angle relative to the beach. The local wave angle relative to the beach is the difference between the wave angle relative to a model baseline and the shoreline angle relative to the model baseline (Figure 6-9),

$$\alpha_b = \alpha_{bg} - \alpha_{sg} = \alpha_{bg} - \tan^{-1}\left(\frac{dy}{dx}\right) \qquad (6\text{-}21)$$

where y is the shoreline position, and x is the distance alongshore.

g. If the angle of the shoreline is small with respect to the x axis and simple relationships describe the waves, analytical solutions for shoreline change may be developed. Larson, Hanson, and Kraus (1987) present a number of those analytical solutions. Figure 6-10 shows the shoreline evolution as a function of dimensionless time t' resulting from a trapezoidal beach fill. Figure 6-11 shows the development of a fillet as a function of t' on the updrift side of a groin. For more complex conditions, numerical models such as GENESIS must be used. Complexities include time-varying wave conditions, large shoreline angles, variable longshore wave height (for example due to diffraction), multiple structures, etc. As a result, numerical models must be used in engineering studies involving design.

h. As discussed by Hanson and Kraus (1989), the empirical predictive formula for the longshore sand transport rate used in GENESIS is
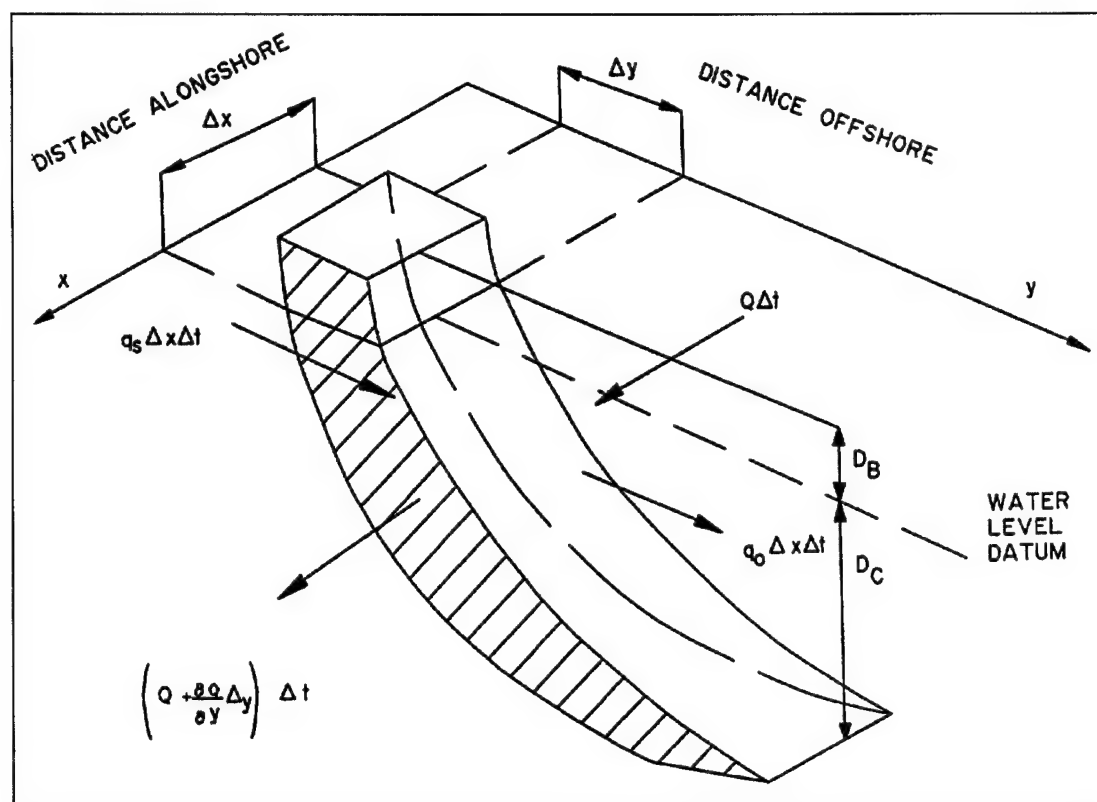
Figure 6-8. Elemental volume on equilibrium beach profile

$$Q_t = H_{bs}^2 C_{gb} \left(a_1 \ sin2\alpha_b - a_2 \ cos\alpha_b \frac{dH_{bs}}{dx} \right) \qquad (6\text{-}22)$$

The nondimensional parameters a_1 and a_2 are given by

$$a_1 = \frac{K_1}{16(\frac{\rho_s}{\rho} - 1)(1 - n)(1.416)^{5/2}} \qquad (6\text{-}23)$$

and

$$a_2 = \frac{K_2}{8(\frac{\rho_s}{\rho} - 1)(1 - n) \ m \ (1.416)^{7/2}} \qquad (6\text{-}24)$$

where K_1 and K_2 are empirical coefficients, treated as calibration parameters, and m is the average bottom slope from the shoreline to the depth of active longshore sand transport. The factors involving 1.416 are used to convert from significant wave height, the statistical wave height required by GENESIS, to rms wave height.

i. The first term in Equation 6-22 corresponds to Equation 6-5, and accounts for longshore sand transport produced by obliquely incident breaking waves. The second term in Equation 6-22 is used to describe the effect of another generating mechanism for longshore sand transport, the longshore gradient in breaking wave height. The contribution arising from the longshore gradient in wave height is usually much smaller than that from oblique wave incidence in an open-coast situation. However, in the vicinity of structures, where diffraction produces a substantial change in breaking wave height over a considerable length of beach, inclusion of the second term provides an improved modeling result, accounting for the diffraction current.
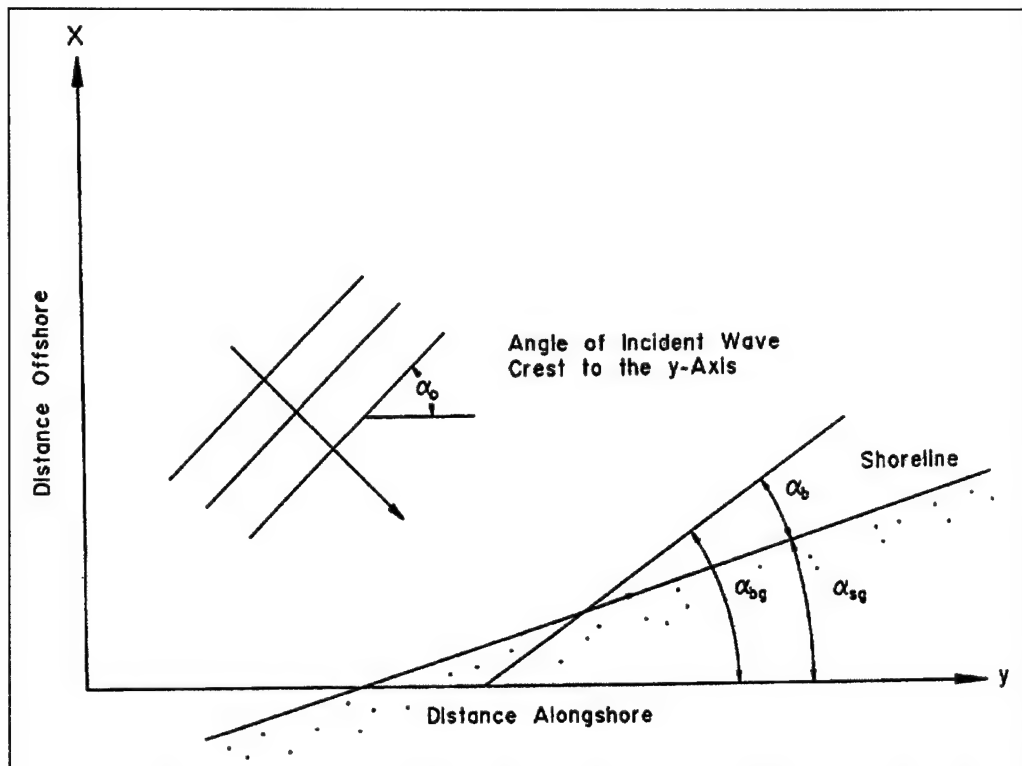
Figure 6-9. Definition of local breaker angle

j. The boundary conditions at the ends of a study area in a shoreline change modeling project must be specified. There are three common boundary conditions: no sand transport ($Q_\ell = 0$), free sand transport ($dQ_\ell/dy = 0$), and partial sand transport ($Q_\ell \neq 0$). The locations of the study area ends should be selected with these options in mind. Large headlands or jetties which completely block the longshore transport are good choices for model boundaries. At these locations $Q_\ell = 0$. Points where the position of the shoreline has not changed for many years are also good locations for boundaries. At these points, the gradient in longshore transport is small so that a free transport condition can be specified ($dQ_\ell/dx = 0$). At some locations, the longshore transport rate is known and can be used as a boundary condition (i.e., artificial sand bypassing at a jetty). If none of these "good" locations exist, engineering judgment must be used. In all cases, results should be verified and calibrated using known shoreline positions and wave conditions for the longest period possible. The modeler also attempts to use wave data applicable to the period between the dates of the calibration shorelines. The GENESIS technical reference (Hanson and Kraus 1989) provides full discussion on the operation of shoreline change numerical simulation models.
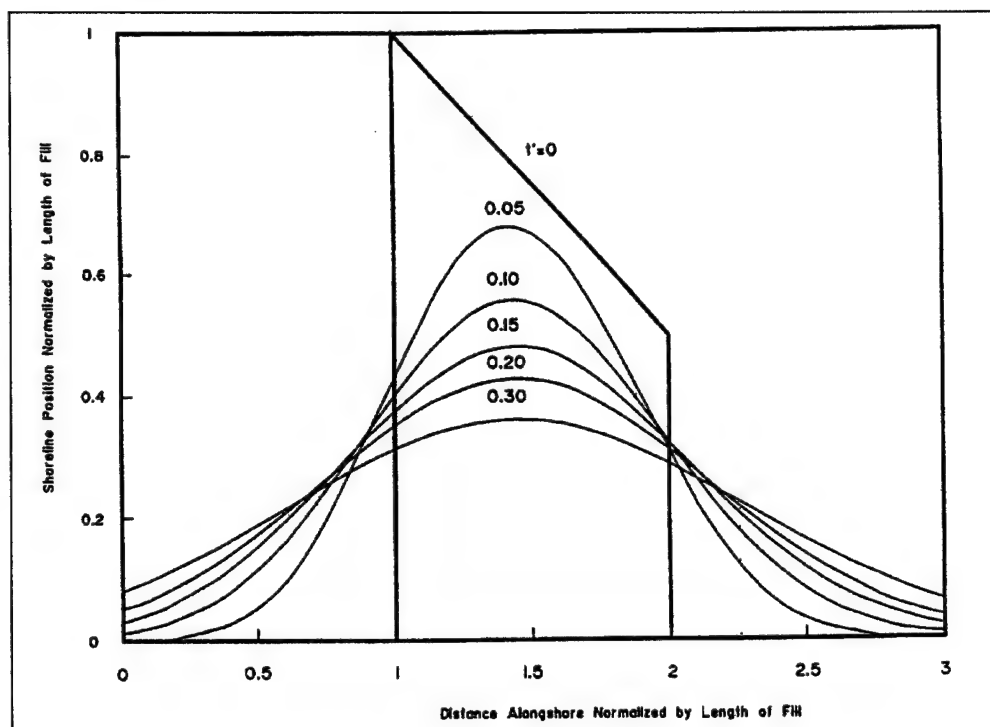
Figure 6-10. Shoreline evolution of an initially trapezoidal beach form (Larson, Hanson, and Kraus 1987)
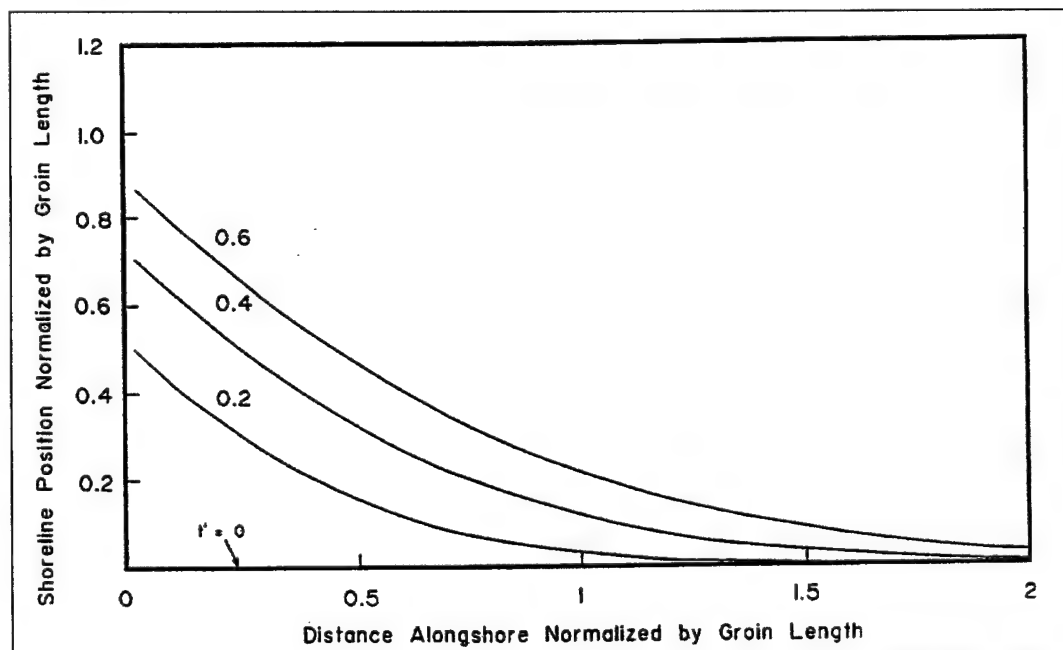
Figure 6-11. Updrift fillet development for a groin which completely blocks the longshore transport (Larson, Hanson, and Kraus 1987)

Chapter 7
Examples Demonstrating Methodology

7-1. Introduction

a. Two littoral budget analyses are presented in this Chapter. The first is an east coast example for a stretch of coast near Asbury Park, New Jersey. This analysis is a condensation of the budget developed by Gravens, Scheffner, and Hubertz (1989). The motivation for this littoral budget was to examine the shadowing effect of Long Island on the local wave climate of the study reach. The second example is for Oceanside, California, and is a condensation of the sediment budget analysis conducted by Kraus et al. In preparation, also discussed by Simpson, Kadib, and Kraus (1991). This analysis was developed to determine the impacts of various management alternatives.

b. The level of detail is quite different for the two littoral budgets presented. The appropriate level of analysis is a function of the intended uses of the littoral budget, and the actual level of analysis may depend also on the available resources to complete the project. However, both include the essential components of a budget analysis. These begin with a site description, background, and examination of previous analyses. An examination of past and present conditions and the results of other studies should be completed before initiating a new budget analysis.

c. Next is the determination of the longshore sediment transport rate. This requires data on wave conditions over as long a time period as possible. These waves are propagated to and transformed in the surf zone. Appropriate sediment transport equations must be selected and incorporated in a shoreline change model. This model must be calibrated and sensitivities to boundary conditions examined. Ideally, historical shoreline positions and wave conditions are available for the same period of time to allow this calibration.

d. The actual determination of the budget can then be completed. Usually there are poorly quantified components remaining in the analysis, such as offshore gains and losses. These must be estimated using any available data, engineering judgment, and the requirement that the budget close. Although a significant effort goes into the development of a littoral budget, it must be remembered that it is an estimate and can easily be in error by a factor of two. The budget is calibrated with shoreline positions over a number of years and

indicates long-term average rates of change. It may not be indicative of the changes in any one year.

7-2. East Coast Example: Asbury Park to Manasquan Inlet, New Jersey

The sediment budget of the New Jersey coast from Asbury Park south to Manasquan Inlet was studied by Gravens, Scheffner, and Hubertz (1989) and is discussed here because several features of that study provide guidance for similar calculations at other localities. To solve the budget, the authors employed WIS information to calculate sediment transport at specific locations, shoreline movement information from photo and map analyses in determining sand volume changes, knowledge of processes important to the area based on previous studies, and engineering judgment regarding adjustments to transport rates.

a. Site description. The study area is between Asbury Park and Manasquan, New Jersey. It is a sandy stretch of coastline 8.5 miles long (Figure 7-1) with 25- to 150-ft-wide beaches. This reach has 81 groins, two structurally stabilized tidal inlets, and intermittent sections of sheet pile and wood bulkheads. There is no coastal dune in the study area.

b. Background. Correct nearshore wave data are essential for calculating sand transport rates. These transport rates are used to estimate or verify shoreline changes. The purpose of the sediment budget analysis by Gravens, Scheffner, and Hubertz (1989) was to confirm that wave shadowing by Long Island to the north was properly represented in the wave hindcast time series for subsequent shoreline change simulation. Wave shadowing was confirmed by the agreement of historical transport rates with those calculated using WIS data and the energy flux method.

c. Previous analyses. The historical average transport rates were calculated from differences in survey measurements made from Mantoloking (approximately 5 miles south of Manasquan Inlet) northward to Sandy Hook, New Jersey, at various times from 1838 to 1935, and reported by Caldwell (1966). Sandy Hook accumulated sand at the northern boundary at the average rate of 493,000 cu yd/year for that period, and the loss of sand from that location was considered zero. Thus the northward transport rate at Sandy Hook was established at 493,000 cu yd/year. Caldwell estimated that the northward transport was uniform along the study area, based on an earlier study that showed wave energy approaching from the southeast quadrant was uniform
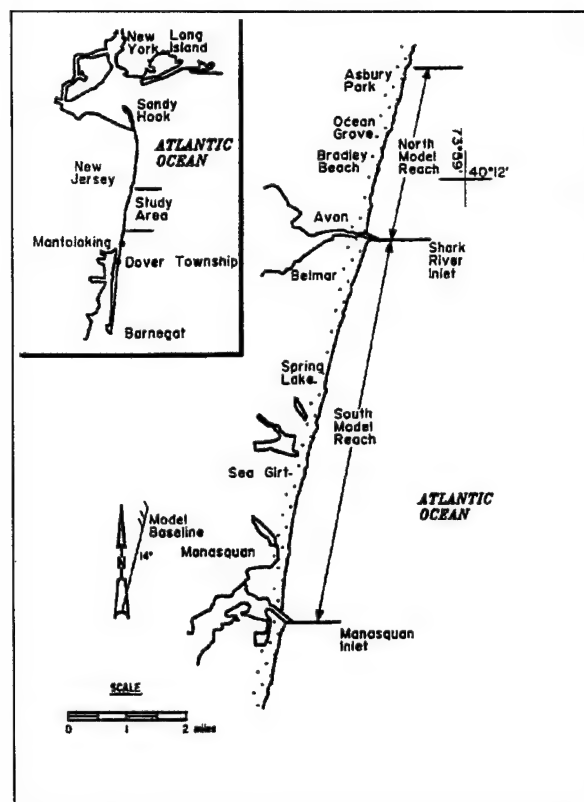
Figure 7-1. Location of Asbury Park to Manasquan study area

over the New Jersey coast. However, wave energy from the northeast quadrant is diminished at Sandy Hook because of sheltering by Long Island, but farther south along the coast there is no sheltering effect. The result of these patterns is a nodal point of net littoral transport at Dover Township, 35 miles south of Sandy Hook. Evidence showed the 493,000 cu yd/year accumulation at Sandy Hook came from the beach face in that 35-mile distance. Measured erosion averaged 723,000 cu yd/year, but about one-third of that volume was material finer than sand and, once eroded, was lost from the system.

(1) The study area was divided into four segments based on locations where transport rates were known or could be inferred: (a) Mantoloking to Manasquan, (b) Manasquan to Asbury Park, (c) Asbury Park to base of Sandy Hook, and (d) base of Sandy Hook to tip of Sandy Hook. At the south end of the study area, Caldwell reasoned that net transport into the segment Mantoloking to Manasquan was zero, but measured differences in surveys indicated net transport out of the reach to be

74,000 cu yd/year. With the sand transport rates established at the two ends of the study area and sand volume changes measured for all the reaches, the sediment budget could then be solved, as illustrated in Figure 7-2. In this figure the control volume represents a reach of the littoral stream, and a quantity eroded from the shore face is considered as flux into the control volume.

d. Wave conditions. Wave summary statistics are available from WIS hindcasts at five stations located in 33-ft water depth along the study reach (Figure 7-3). Percent occurrence statistics are tabulated by period band and height increment for angle bands of 30°. Table 7-1 lists statistics for Station 54, located near Sandy Hook, as an example. The angles reported for these WIS Phase III stations are oriented to the shoreline trend and are measured counter-clockwise from the shoreline. Transport calculations required that central angles of the given angle bands be referenced to shore-normal. By convention, waves approaching shore at positive angles cause transport to the right when looking seaward from shore, and waves of negative angles cause leftward transport.

e. Description of Transport Algorithm. Wave input was developed for a program to calculate wave transformation by linear wave theory and assumption of straight and parallel contours and longshore sand transport by the CERC formula. The CERC formula is based on the energy flux method, an empirical correlation between transport rate and the longshore component of wave power evaluated at the breaker zone (Equations 6-1 and 6-2). A program to calculate wave transformation to breaking and resulting sand transport was developed by Gravens (1988, 1989).

f. Model calibration. The input and calculated results are listed in Table 7-2. To investigate alongshore variation in transport, average height and weighted average period were calculated for each angle band at each hindcast station. Transport rates calculated for reaches corresponding to the wave hindcast stations were compared with those determined from survey measurements reported by Caldwell.

(1) This first effort at using WIS summary statistics yielded an alongshore trend in transport rates which agreed with that of the Caldwell study, but magnitudes differed greatly. Upon closer examination of representative shoreline orientations for each calculation reach, small differences were found between angles used in the Phase III transformations and the shoreline angles measured from a small-scale map. The decision was made

Average Annual Volume (x 1000 cu yd)
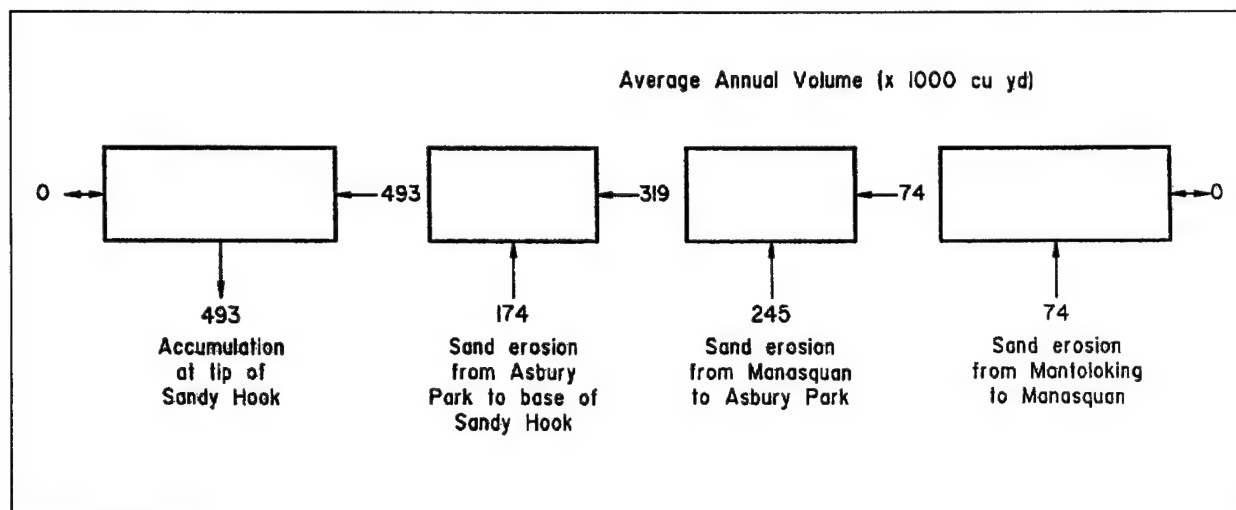
Figure 7-2. Sediment budget from Sandy Hook to Manasquan, New Jersey, 1838 - 1935 (after Caldwell, 1966) (cu yd/year)
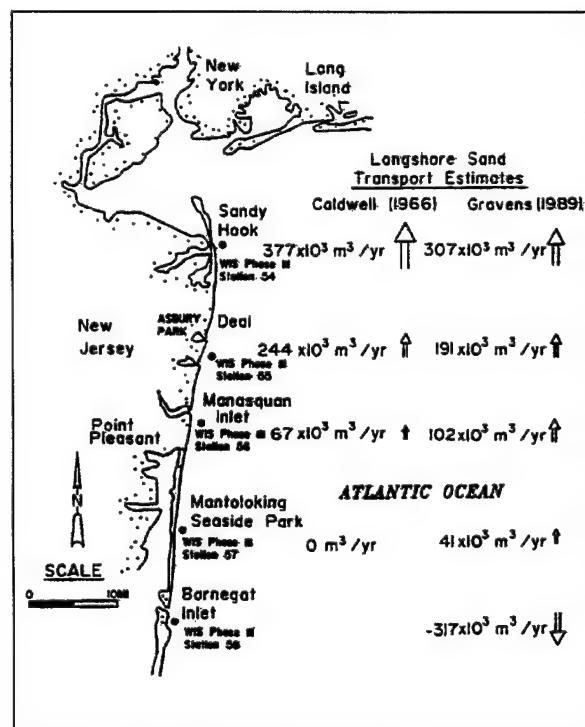
Figure 7-3. Potential longshore sand transport rates (Gravens, Scheffner, and Hubertz 1989)

to apply corrections to the angles in the WIS statistics and recalculate transport rates. Table 7-3 illustrates the difference in transport rates made by a systematic 8-deg change at Station 54. The proper alongshore trend was again reproduced by recalculating transports for the five stations, and results showed an improvement in transport rates with respect to historical averages.

g. *Sediment budget.* Because of the success of the preliminary calculations, a more refined discretization of the WIS Phase II data was undertaken. Within each angle band, distributions of height and period are tabulated by height categories of 0.5-m increments and period categories of 1 sec. The median height and the weighted average period within each height category were then input to the longshore transport routine. Twenty-eight height-period-direction combinations were required to represent the wave climate effective in transporting sand alongshore (Table 7-4). Calculated left and right transport rates for the reaches yield net rates that correspond well with average historical rates, and both are shown on Figure 7-3. This analysis established confidence that the WIS time series could be utilized as input to the shoreline change model, GENESIS, and would permit accurate shoreline change simulation. The sediment budget studies showed that shadowing of the waves by the large land mass to the north was accounted for properly.

Table 7-1
Percent Occurrence by Period and Angle Band for WIS Phase III Station 54

Station 54 20 Years   Wave Approach Angle (Degrees) = 0.0-29.9
Shoreline Angle* = 4.0 Degrees Azimuth
Water Depth = 10.00 Meters
Percent Occurrence (X1000) of Height and Period by Direction

| Height (Meters) | Period (Seconds) | | | | | | | | | | Total |
	0.0-2.9	3.0-3.9	4.0-4.9	5.0-5.9	6.0-6.9	7.0-7.9	8.0-8.9	9.0-9.9	10.0-10.9	11.0-Longer	
0.00 - 0.49	2888	5985	4065	2347	588	869	313	11	6	.	17072
0.50 - 0.99	.	313	1976	1213	388	179	47	5	6	1	4128
1.00 - 1.49	.	.	17	77	100	6	.	.	1	.	201
1.50 - 1.99	.	.	.	.	10	1	.	.	.	.	11
2.00 - 2.49	.	.	.	.	.	.	.	.	.	.	0
2.50 - 2.99	.	.	.	.	.	.	.	.	.	.	0
3.00 - 3.49	.	.	.	.	.	.	.	.	.	.	0
3.50 - 3.99	.	.	.	.	.	.	.	.	.	.	0
4.00 - 4.49	.	.	.	.	.	.	.	.	.	.	0
4.50 - 4.99	.	.	.	.	.	.	.	.	.	.	0
5.00 - Greater	.	.	.	.	.	.	.	.	.	.	0
Total	2888	6298	6058	3637	1086	1055	360	16	13	1	

Average HS(M) = 0.32   Largest HS(M) = 1.85   Angle Class % = 21.4

Station 54 20 Years   Wave Approach Angle (Degrees) = 30.0-59.9
Shoreline Angle* = 4.0 Degrees Azimuth
Water Depth = 10.00 Meters
Percent Occurrence (X1000) of Height and Period by Direction

Height (Meters)	0.0-2.9	3.0-3.9	4.0-4.9	5.0-5.9	6.0-6.9	7.0-7.9	8.0-8.9	9.0-9.9	10.0-10.9	11.0-Longer	Total
0.00 - 0.49	944	1254	.	.	3237	7493	3879	302	494	465	18059
0.50 - 0.99	.	821	1651	340	130	1481	795	80	205	8	5511
1.00 - 1.49	.	.	114	665	316	485	248	53	37	.	1918
1.50 - 1.99	.	.	.	25	154	309	109	20	10	1	628
2.00 - 2.49	.	.	.	.	27	90	51	10	.	.	178
2.50 - 2.99	.	.	.	.	.	3	11	11	1	.	26
3.00 - 3.49	.	.	.	.	.	.	.	3	.	.	3
3.50 - 3.99	.	.	.	.	.	.	.	.	.	.	0
4.00 - 4.49	.	.	.	.	.	.	.	.	.	.	0
4.50 - 4.99	.	.	.	.	.	.	.	.	.	.	0
5.00 - Greater	.	.	.	.	.	.	.	.	.	.	0
Total	944	2075	1765	1030	3864	9861	5093	479	747	465	

Average HS(M) = 0.47   Largest HS(M) = 3.05   Angle Class % = 26.3

(Continued)

(Sheet 1 of 3)

Table 7-1
(Continued)

Station 54 20 Years   Wave Approach Angle (Degrees) = 60.0-89.9
Shoreline Angle* = 4.0 Degrees Azimuth
Water Depth = 10.00 Meters
Percent Occurrence (X1000) of Height and Period by Direction

Height (Meters)	Period (Seconds)										
	0.0-2.9	3.0-3.9	4.0-4.9	5.0-5.9	6.0-6.9	7.0-7.9	8.0-8.9	9.0-9.9	10.0-10.9	11.0-Longer	Total
0.00 - 0.49	634	744	.	.	593	2861	2286	992	278	455	8843
0.50 - 0.99	.	571	1309	148	37	718	631	277	311	106	4108
1.00 - 1.49	.	.	111	693	147	164	131	30	70	58	1404
1.50 - 1.99	.	.	.	34	256	159	71	6	11	25	562
2.00 - 2.49	.	.	.	.	29	285	80	5	1	25	425
2.50 - 2.99	.	.	.	.	.	51	92	5	1	1	150
3.00 - 3.49	.	.	.	.	.	.	6	10	5	.	21
3.50 - 3.99	.	.	.	.	.	.	.	8	.	.	8
4.00 - 4.49	.	.	.	.	.	.	.	.	.	.	0
4.50 - 4.99	.	.	.	.	.	.	.	.	.	.	0
5.00 - Greater	.	.	.	.	.	.	.	.	.	.	0
Total	634	1315	1420	875	1062	4238	3297	1333	677	670	

Average HS(M) = 0.61   Largest HS(M) = 3.70   Angle Class % = 15.5

Station 54 20 Years   Wave Approach Angle (Degrees) = 90.0-119.9
Shoreline Angle* = 4.0 Degrees Azimuth
Water Depth = 10.00 Meters
Percent Occurrence (X1000) of Height and Period by Direction

Height (Meters)	0.0-2.9	3.0-3.9	4.0-4.9	5.0-5.9	6.0-6.9	7.0-7.9	8.0-8.9	9.0-9.9	10.0-10.9	11.0-Longer	Total
0.00 - 0.49	908	1839	1471	1617	1358	1795	961	123	78	432	10582
0.50 - 0.99	.	116	956	1018	236	1651	1247	210	333	1156	6923
1.00 - 1.49	.	.	17	349	316	586	545	102	85	313	2313
1.50 - 1.99	.	.	.	8	123	381	217	44	15	131	919
2.00 - 2.49	.	.	.	.	13	154	138	6	6	23	340
2.50 - 2.99	.	.	.	.	.	15	49	3	1	15	83
3.00 - 3.49	.	.	.	.	.	.	1	1	.	3	5
3.50 - 3.99	.	.	.	.	.	.	.	1	.	1	2
4.00 - 4.49	.	.	.	.	.	.	.	.	.	.	0
4.50 - 4.99	.	.	.	.	.	.	.	.	.	.	0
5.00 - Greater	.	.	.	.	.	.	.	.	.	.	0
Total	908	1955	2444	2992	2046	4582	3158	490	518	2074	

Average HS(M) = 0.61   Largest HS(M) = 3.68   Angle Class % = 21.2

(Continued)

Table 7-1
(Concluded)

Station 54 20 Years   Wave Approach Angle (Degrees) = 120.0-149.9
Shoreline Angle* = 4.0 Degrees Azimuth
Water Depth = 10.00 Meters
Percent Occurrence (X1000) of Height and Period by Direction

Height (Meters)	Period (Seconds)										Total
	0.0-2.9	3.0-3.9	4.0-4.9	5.0-5.9	6.0-6.9	7.0-7.9	8.0-8.9	9.0-9.9	10.0-10.9	11.0-Longer	
0.00 - 0.49	10	.	.	.	.	.	.	.	.	.	10
0.50 - 0.99	.	.	.	.	.	.	.	.	.	.	0
1.00 - 1.49	.	.	.	.	.	.	.	.	.	.	0
1.50 - 1.99	.	.	.	.	.	.	.	.	.	.	0
2.00 - 2.49	.	.	.	.	.	.	.	.	.	.	0
2.50 - 2.99	.	.	.	.	.	.	.	.	.	.	0
3.00 - 3.49	.	.	.	.	.	.	.	.	.	.	0
3.50 - 3.99	.	.	.	.	.	.	.	.	.	.	0
4.00 - 4.49	.	.	.	.	.	.	.	.	.	.	0
4.50 - 4.99	.	.	.	.	.	.	.	.	.	.	0
5.00 - Greater	.	.	.	.	.	.	.	.	.	.	0
Total	10	0	0	0	0	0	0	0	0	0	

Average HS(M) = 0.01   Largest HS(M) = 0.01   Angle Class % = 0.0

Station 54 20 Years   Wave Approach Angle (Degrees) = 150.0-179.9
Shoreline Angle* = 4.0 Degrees Azimuth
Water Depth = 10.00 Meters
Percent Occurrence (X1000) of Height and Period by Direction

Height (Meters)	0.0-2.9	3.0-3.9	4.0-4.9	5.0-5.9	6.0-6.9	7.0-7.9	8.0-8.9	9.0-9.9	10.0-10.9	11.0-Longer	Total
0.00 - 0.49	.	.	.	.	.	.	.	.	.	.	0
0.50 - 0.99	.	.	.	.	.	.	.	.	.	.	0
1.00 - 1.49	.	.	.	.	.	.	.	.	.	.	0
1.50 - 1.99	.	.	.	.	.	.	.	.	.	.	0
2.00 - 2.49	.	.	.	.	.	.	.	.	.	.	0
2.50 - 2.99	.	.	.	.	.	.	.	.	.	.	0
3.00 - 3.49	.	.	.	.	.	.	.	.	.	.	0
3.50 - 3.99	.	.	.	.	.	.	.	.	.	.	0
4.00 - 4.49	.	.	.	.	.	.	.	.	.	.	0
4.50 - 4.99	.	.	.	.	.	.	.	.	.	.	0
5.00 - Greater	.	.	.	.	.	.	.	.	.	.	0
Total	0	0	0	0	0	0	0	0	0	0	

Average HS(M) = 0   Largest HS(M) = 0   Angle Class % = 0

(Sheet 3 of 3)

Table 7-2
Wave Conditions and Estimated Longshore Sediment Transport

Central Angle deg	Wave Height m	Period sec	Percent Occurrence	Breaking Wave Height, m	Breaking Wave Angle, deg	Longshore Transport Rate m³/year
75	0.32	4.3	21.412	0.24	14.7	7,100
45	0.47	6.9	26.323	0.62	13.2	83,000
15	0.61	7.2	15.521	0.87	5.6	50,500
-15	0.61	6.9	21.167	0.86	-5.6	-67,100
-45	0.01	1.5	0.010	0.12	-18.1	-0

Gross Northerly Longshore Sediment Transport Rate: 140,600 m³/year
Gross Southerly Longshore Sediment Transport Rate: -67,100 m³/year
Net Longshore Sediment Transport Rate (North): 73,500 m³/year

Table 7-3
Input Wave Data (10-m Depth), Breaking Wave Conditions, and Estimated Longshore Sediment Transport Rate (Adjusted Shoreline Angle) for Asbury Park to Manasquan Inlet, New Jersey

Central Angle deg	Wave Height m	Period sec	Percent Occurrence	Breaking Wave Height, m	Breaking Wave Angle, deg	Longshore Transport Rate, m³/year
83	0.32	4.3	21.412	0.18	12.9	2,900
53	0.47	6.9	26.323	0.58	14.5	76,900
23	0.61	7.2	15.521	0.85	8.4	72,000
-7	0.61	6.9	21.167	0.86	-2.7	-32,600
-37	0.01	1.5	0.010	0.12	-15.3	-0

Gross Northerly Longshore Sediment Transport Rate: 151,800 m³/year
Gross Southerly Longshore Sediment Transport Rate: -32,600 m³/year
Net Longshore Sediment Transport Rate (North): 119,200 m³/year

7-3. West Coast Example: Oceanside, California

a. Site description. The Oceanside littoral cell is located along the southern California coast just north of San Diego (Figure 7-4). It is about 57 miles long, extending from Dana Point at the north end to Point La Jolla at the south end. Oceanside Harbor and its entrance jetties are located near the center of the cell and locally interrupt littoral processes. Notable beach erosion at Oceanside began when the first boat basin was constructed in 1942, and the erosion became severe after the harbor was expanded and the jetties were extended. A summary of the harbor development is given in Figure 7-5. Therefore, the shoreline change modeling effort in the sediment budget analysis focused on shorelines adjacent to the harbor and extending 4 miles north and south of the harbor, as discussed herein.

(1) Primary sources of sediment in the Oceanside littoral cell are rivers and beach nourishment. The long-term net direction of sand transport through the cell is believed to be from northwest to southeast. However, seasonality in transport direction is strong. Sand is typically transported to the north from May to October as the result of waves originating from southern hemisphere storms. At other times of the year, the transport is typically to the south. Dana Point, the northwest boundary of the cell, is a nearly complete littoral barrier (Everts, Bertolotti, and Anderson 1989). It extends

Table 7-4
Input Wave Data (10-m Depth), Breaking Wave Conditions, and Estimated Longshore Sediment Transport Rate (28 Wave Conditions), Asbury Park to Manesquan Inlet, New Jersey

Angle Band	Central Angle deg	Wave Height m	Period sec	Percent Occurrence	Breaking Wave Height, m	Breaking Wave Angle, deg	Longshore Transport Rate, m³/year
1	83	0.25	4.1	17.072	0.14	12.0	1,300
.	.	0.75	5.1	4.128	0.39	17.0	5,200
.	.	1.25	6.0	0.201	0.64	20.1	1,000
.	.	1.75	6.6	0.011	1.87	22.6	100
2	53	0.25	7.2	18.059	0.35	11.1	11,900
.	.	0.75	6.1	5.511	1.81	17.9	45,300
.	.	1.25	6.7	1.918	1.28	21.8	58,400
.	.	1.75	7.5	0.628	1.75	24.7	46,100
.	.	2.25	7.7	0.178	2.18	27.4	24,300
.	.	2.75	8.9	0.026	2.99	31.3	8,500
.	.	3.25	9.5	0.003	3.08	31.8	1,100
3	23	0.25	7.5	8.843	0.42	5.9	4,900
.	.	0.75	6.5	4.108	0.98	9.3	29,700
.	.	1.25	6.6	1.404	1.50	11.3	35,800
.	.	1.75	7.3	0.562	1.92	12.4	28,900
.	.	2.25	7.9	0.425	2.57	14.0	50,500
.	.	2.75	8.2	0.150	3.06	15.1	29,600
.	.	3.25	9.5	0.021	3.59	16.1	6,500
.	.	3.75	9.5	0.008	4.05	17.0	3,500
4	-7	0.25	5.8	10.582	0.39	-1.9	-1,700
.	.	0.75	7.8	6.923	1.05	-2.8	18,500
.	.	1.25	8.1	2.313	1.56	-3.4	-19,800
.	.	1.75	8.4	0.919	2.16	-4.0	-20,800
.	.	2.25	8.3	0.340	2.66	-4.4	-14,200
.	.	2.75	9.0	0.083	3.18	-4.7	-5,900
.	.	3.25	10.8	0.005	3.72	-5.0	-600
.	.	3.75	10.8	0.002	3.96	-5.1	-300
5	-37	0.25	1.5	0.010	0.28	-22.9	-0

Gross Northerly Longshore Sediment Transport Rate: 392,600 m³/year
Gross Southerly Longshore Sediment Transport Rate: -81,800 m³/year
Net Longshore Sediment Transport Rate (North): 310,800 m³/year

900 ft seaward from Dana Strand Beach and then continues submerged an additional 2,500 ft to depths of 40 to 60 ft. This rocky underwater protrusion is believed to permit only small quantities of sand to move around the headland. Scripps and La Jolla Submarine Canyons, located at the southeast end of the cell, are the ultimate repositories of sediment transported alongshore in the Oceanside littoral cell. There is no indication that sand bypasses these canyons and the Point La Jolla headland into the Mission Bay region. These canyons are important sediment sinks because they extend close to shore (Inman 1976). Point La Jolla has been considered a complete littoral barrier by a number of investigators (Shepard 1950; Inman 1953; Everts and Dill 1988).
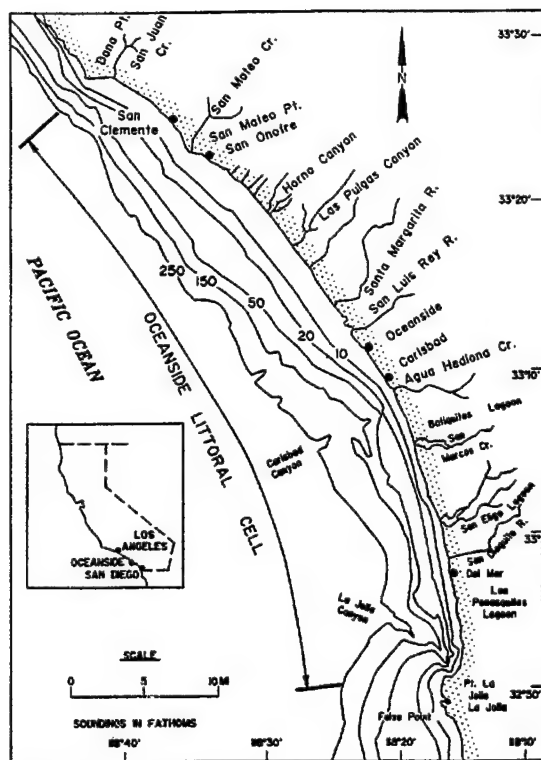
Figure 7-4. Oceanside littoral cell

(2) The Santa Margarita and San Luis Rey Rivers were once major sources of beach sediment for the Oceanside littoral cell. Neither has provided significant nourishment to the beaches in recent years, due in part to sand impoundment at flood control systems in their upper watersheds, but perhaps also due as much to a lack of extreme rainfall and subsequent large flood flows (Griggs 1987). Estimates of riverine sediment discharges into the coastal zone of the Oceanside littoral cell have been made by several investigators since the 1970s (Inman 1976; California Department of Navigation and Ocean Development (DNOD) 1977; Brownlie and Taylor 1981; Inman and Jenkins 1983; Simons, Li, & Assoc. 1988). The most detailed analysis of coarse sediment discharge to the ocean to date is that of Simons, Li, and Assoc. (1988); however, all river sediment discharge values are estimates. The range of estimates of sediment delivery to the coastal zone by the Santa Margarita and San Luis Rey Rivers is presented in Table 7-5.

b. Background. Six sets of aerial photographs were available to provide shoreline position measurements between March 1964 and January 1988. Historical shoreline positions were digitized at 100-ft intervals and were referenced to a baseline tied to the California state plane coordinate system. Data were analyzed over distances of 21,600 ft north and 21,600 ft south of Oceanside harbor to determine net change in shoreline position and average rates of change. During the period 1964 to 1974, the shoreline north of the harbor prograded an average 4.5 ft/yr. In the same period, the shoreline south of the harbor receded approximately 9.7 ft/yr, resulting in an average loss of 99.0 ft of beach. During this 10-year period, the only stretch of shore south of the harbor that exhibited progradation was between the south harbor jetty and the groin upcoast of the San Luis Rey River. This 10-year period selected was for examination because there are also wave hindcasts (WIS) available for the same period. These results were used to calibrate the shoreline change model.

(1) Erosion of the beaches south of the Oceanside Harbor complex and the accompanying accretion of sand in the entrance channel and harbor have been persistent problems since the construction of the Del Mar Boat Basin and the protective breakwaters in 1942-1943. Due to periodic sediment dredging and bypassing operations that transfer sand to Oceanside beaches, the harbor complex is a temporary sink in the middle of the littoral cell and traps sand moving in either direction (Figure 7-5). The northern breakwater acts as a partial barrier to southerly moving sand, trapping a portion of the sand on its north side until the shoreline realigns so that sand can move around the breakwater and into the entrance channel and harbor (Hales 1978). Sediment deposited in these areas is sheltered from wave action and littoral currents and cannot be transferred to the downdrift beaches except by mechanical means. Under conditions of northerly transport, the sand trapped north of the harbor tends to nourish the upcoast beaches (Hales 1978).

(2) Soon after construction of the north breakwater at the Del Mar Boat Basin in 1942, a large fillet of sand formed north of the harbor. Everts, Bertolotti, and Anderson (1989) observed that approximately 3,400,000 cu yd of sand accumulated north of the breakwater between 1942 and 1960. The shoreline advanced about 100 ft seaward along the reach from the breakwater to about 5.5 miles north of the structure. In the same period approximately 800,000 cu yd of material were
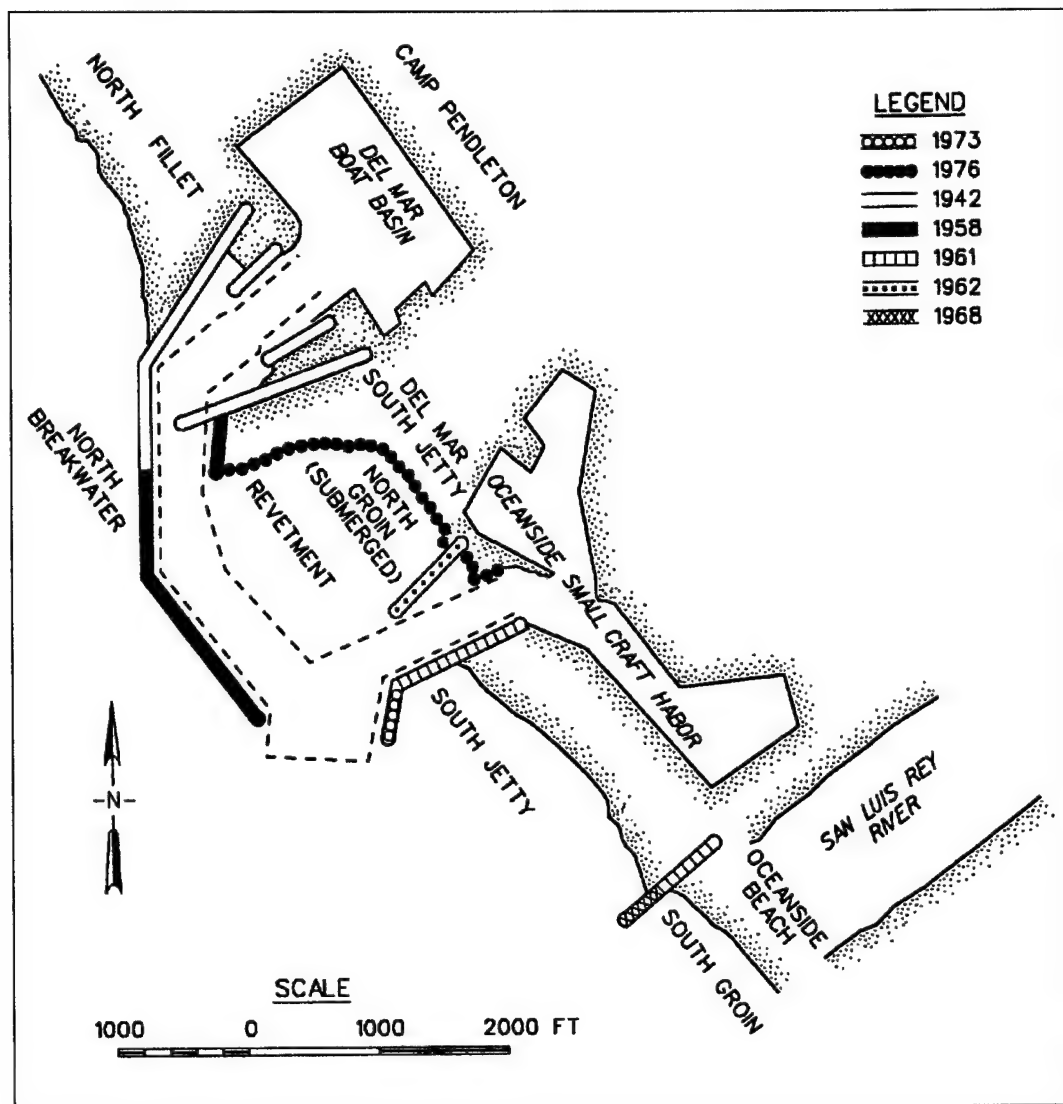
Figure 7-5. Del Mar Boat Basin and Oceanside Harbor

Table 7-5
Estimates of River Sediment Delivery, Oceanside, California, Littoral Cell

Investigator	Santa Margarita River cu yd/year	San Luis Rey River cu yd/year
DNOD (1977)	15,000	351,000
Brownlie and Taylor (1981)	11,300	12,500
Inman and Jenkins (1983)	24,000	37,000
Simons, Li and Assoc. (1988)	19,000	11,000

excavated from the harbor entrance channel and placed on Oceanside Beach. Also during this period, approximately 2,400,000 cu yd of sand were eroded from Oceanside Beach and the shoreface south of the harbor (in addition to the 800,000 cu yd of placed dredged material). Thus, a net 3,200,000 cu yd of sand was removed from Oceanside Beach. If all this material were lost after the breakwater was constructed, the rate of erosion at Oceanside Beach would be about 180,000 cu yd/year. The volume of sand accumulated and the rate of the fillet formation suggest the net longshore transport rate in the 1940s and 1950s averaged about 230,000 cu yd/year to the south (Everts, Bertolotti, and Anderson 1989).

(3) Since the mid-1960s, maintenance dredging of the entrance channel has been required on an almost annual basis. The average annual volume of material dredged from the entrance channel over the 17-year period between 1965 and 1982 is approximately 300,000 cu yd/year. Tekmarine, Inc. (1987) noted that two periods of distinctly different dredging rates appear to exist which constitute these average values. The dredging rate for the initial 6 years after the 1965 harbor expansion averaged 450,000 cu yd/year, but diminished by about one third to 293,000 cu yd/year for the succeeding 11 years. They believe the reason for such a substantial change in the dredging rate may be found in the change in disposal practices for beach nourishment operations beginning around 1971. As shown in Figure 7-6, until 1971 the disposal site was located relatively close to Oceanside Harbor, sometimes within 3,000 ft of the south jetty. The center of gravity of the disposed material was located about 7,000 ft from the south jetty. After 1971, the center of gravity of the disposed material was positioned about 11,000 ft from the south jetty.

c. Previous analyses. Three methods of estimating longshore sand transport rates for the Oceanside cell have been used in previous studies: fillet formation, beach erosion, and calculations of potential transport using either wave hindcasts or measurements and empirical predictive formulae. Marine Advisers (1961) developed a hindcast wave climate for Northern Hemisphere swell and local sea using weather maps from 1956-1958, and Southern Hemisphere swell using weather maps from 1948-1950. This data set was used to estimate potential longshore transport at Oceanside.

(1) Hales (1978) used a combination of Marine Advisers (1961) and California DNOD (1977) wave hindcast data. The DNOD (1977) statistics were considered quite reliable at that time. However, subsequent analysis has revealed their development suffered from computational limitations which may have introduced bias in the results. Hales (1978) calculated wave refraction to the break point and applied the Shore Protection Manual (1984) wave energy flux method to compute potential longshore transport. Island sheltering effects based on the work of Arthur (1951) were taken into consideration. Estimates using these hybrid deep water wave statistics produced an average annual transport to the south of 643,000 cu yd/year and a transport to the north of 541,000 cu yd/year for a net transport of 102,000 cu yd/year to the south.

(2) Inman and Jenkins (1983) produced the most complete estimate of potential longshore transport from

hindcast data for this region. They also used a combination of Marine Advisers (1961) and DNOD (1977) wave data, but utilized DNOD Station 5 which is more energetic and farther away from the coast than a hypothetical Station 5-1/2 (halfway between Station 5 and Station 6) used by Hales (1978). This decision resulted in a stronger southerly transport than that obtained by Hales (1978). Inman and Jenkins (1983) estimates resulted in an average annual transport to the south of 807,000 cu yd/year and a transport to the north of 553,000 cu yd/year for a net transport of 254,000 cu yd/year to the south.

(3) Seymour and Castel (1985) computed potential longshore transport rates using wave parameters derived from data collected by seven nearshore pressure sensor arrays for the period between 1980 and 1982. That analysis showed the episodic nature of the transport rates, characterized by extreme variability in direction and volume on a day-to-day basis. Although the absolute values of the rates obtained appear to be too small, nevertheless, they statistically confirm that seasonal transport can be several times larger than the annual net transport. In the vicinity of Oceanside, half of the annual gross transport was calculated to occur during only 10 percent of the time. According to Seymour and Castel, because of the extreme variability, missing one day of observations could result in a reversal of the estimated direction of longshore transport for the entire year at Oceanside.

(4) Estimates of the potential longshore sand transport in the vicinity of Oceanside are summarized in Table 7-6. The first three listed works used essentially the same methodology and wave data base to estimate potential transport rates, hence they cannot be considered independent. The latter two estimates result from independent methods and the net rates are within the range determined by the first three methods.

(5) It is important to draw a distinction between the potential longshore transport and the actual longshore transport. Potential longshore sediment transport is an estimate of the maximum capacity of the breaking waves to carry sand alongshore in the presence of an unlimited supply of movable material. Conditions often exist which prevent the actual transport of sand from achieving the potential rate. Examples of such limitations include an absence of sediment supply (rocky headland or littoral barrier) and an armored but otherwise sandy beach. The longest cobble beach region in southern California is found from Oceanside to Carlsbad. Many of the cobbles armoring this particular
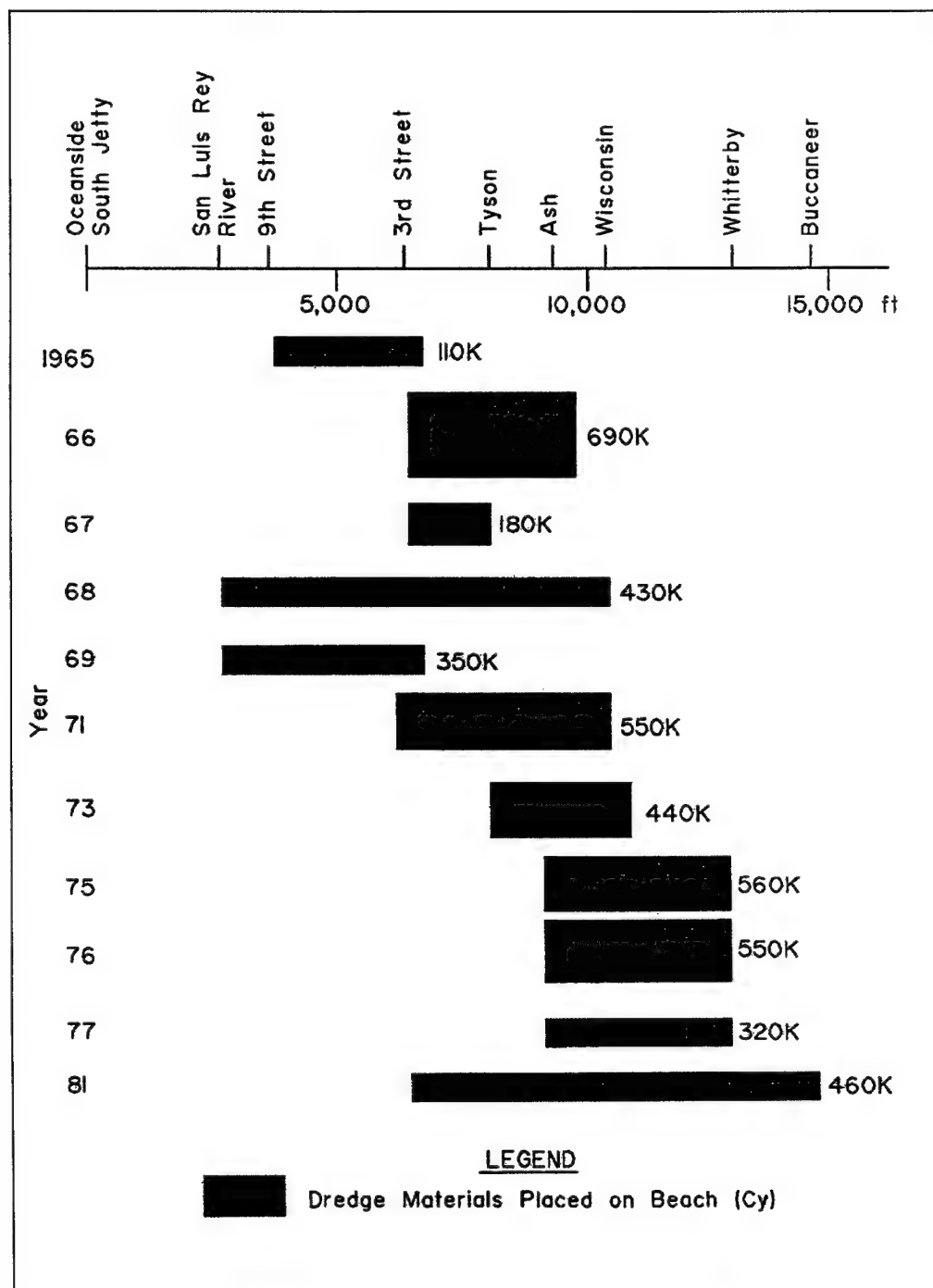
Figure 7-6. Beach nourishment placement locations (after Tekmarine 1987)

Table 7-6
Longshore Sand Transport Rate Estimates at Oceanside, California

Investigator	Method Used to Estimate Transport Rate	Transport Rate Estimates, cu yd/year		
		Northerly	Southerly	Net
Marine Advisers (1961)	Potential transport equation	545,000	760,000	215,000
Hales (1978)	Potential transport equation	541,000	643,000	102,000
Inman and Jenkins (1983)	Potential transport equation	553,000	807,000	254,000
Everts et al. (1989)	Fillet formation in 1950s			230,000
Everts et al. (1989)	Beach erosion, 1942-1960			180,000

area were apparently dredged from the Oceanside Small Craft Harbor development in 1963 and placed on the beach. No method exists for estimating the longshore sand transport rate in the presence of cobble and sand mixtures in the littoral zone. It is known that a cobble beach will significantly reduce the longshore sand transport due to the armoring of sand particles.

(6) Cobbles along the beaches at Oceanside tend to stabilize the shoreline position. After nourishment, fill material is removed by waves and currents exposing the cobbles. The apparent beach erosion rate is significantly reduced. Seemingly, whatever volume of beach nourishment material is placed on the susceptible beach area is removed, and the cobbles are again exposed.

(7) The longshore transport rate should depend only on the magnitude of the longshore wave energy flux. The fact that it also appears to depend on the distance of travel between the disposal site and the harbor entrance channel indicated to Tekmarine, Inc. (1987) that the prevailing longshore processes were functioning at less than the potential of the wave climate. Armoring by cobble was believed to have contributed to this phenomena. Everts, Bertolotti, and Anderson (1989) noted that the mid- to late-1960s was a period of abnormally high southern hemisphere swell, and the northerly component of longshore energy flux may have been larger between 1965-1971 than between 1971-1982. This would account for the larger volume of material transported into the harbor during this time interval, and the longshore processes might still be functioning near their potential.

(8) Everts, Bertolotti, and Anderson (1989) developed two sediment budgets each for two control volumes in the vicinity of Oceanside. The first sediment budget was for the period 1942 through 1958, and the second was for the period 1958 through 1987. A north control volume extended about 30,000 ft upcoast from the north breakwater to Las Flores Creek. A south control volume extended about 18,000 ft downcoast from the south jetty at the harbor entrance to near Buena Vista Lagoon. Results of these budget analyses are listed in Table 7-7.

(9) Everts, Bertolotti, and Anderson (1989) found that in excess of 2,200,000 cu yd of sediment were deposited outside, but adjacent to, the harbor between 1942 and 1971. The deposit formed in response to the interruption of littoral processes at the north breakwater. The shoreline prograded as the end of the north breakwater was extended. By 1971 the new subaqueous deposit extended for the entire length of the north breakwater and along the south jetty of Oceanside Harbor, being broken only in its form by the dredged entrance channel. This trend toward natural bypassing around the harbor would have encompassed the entire harbor had the entrance channel not been periodically dredged. Everts, Bertolotti, and Anderson (1989) believe that significant quantities of sediment are no longer being withdrawn from the littoral system outside the harbor. They deduced that a critical fill volume of approximately 390,000 cu yd/year is required to maintain a dynamically stable shoreline at Oceanside (one that fluctuates seasonally about a steady mean position).

d. Wave conditions.

(1) Determination of the wave conditions is an essential step in the application of the shoreline change model. Deep water hindcast wave estimates from the WIS (Corson et al. 1986) were used to generate wave information in 65 ft of water near Oceanside.

Table 7-7
Sediment Budget, Oceanside, California (Everts, Bertolotti, and Anderson 1989)

Component	North Control Volume cu yd/year 1942-1958	1958-1987	South Control Volume cu yd/year 1942-1958	1958-1987
Santa Margarita River	+20,000[1]	+20,000		
Santa Margarita Delta	+25,000	0		
San Luis Rey River			+11,000	+11,000
San Luis Rey Delta			+25,000	0
Sea cliffs	+3,000	0	+1,000	+2,000
Coastal terraces	+28,000	+28,000	0	
Shoreface	+16,000	-54,000	+10,000	-33,000
Beach fills	0	0	0	+82,000
Sand mining	-14,000	0	0	0
Bypassing	0	0	+50,000	+355,000
Volume change with shoreline effects	+156,000	-32,000	-110,000	-50,000
Volume change seaward of north breakwater			+50,000	+55,000

Note:
1. + indicates volume gain; - indicates volume loss.

Two-dimensional energy spectra from a position seaward of the offshore islands were applied as the outer boundary condition for the nearshore wave model. Propagation of North Pacific wave spectra to the 65-ft-depth contour at WIS Station 7 (Figure 7-7) included the effects of island shadowing of wave energy. In addition, local wind effects were incorporated to estimate local seas (Jensen, Vincent, and Reinhard 1989). Only 41 percent of local seas represented events directed onshore (within ±90 deg of shore normal). All offshore-directed wave events were assigned zero energy for the shoreline change modeling.

(2) Southern hemisphere swell data were obtained from measurements made at the Olympics buoy from April 1984 to September 1985. Measurements of January-March and October-December were repeated to create a full 2-year time series. Limitations of the measurement interval necessitated repetition of this 2-year time series of Southern Hemisphere swell throughout the simulation period. The Southern Hemisphere swell wave information also was propagated to WIS Station 7.

(3) The separate wave data were synchronously combined to produce a single time series consisting of the three wave components. Seven angle bands were used to summarize the distribution of the spectral peak periods of the northern swell, the southern swell, and the local seas. Table 7-8 summarizes the distribution of wave energy spectral peak periods and angle bands of average directions at 6-hr intervals for WIS Station 7.

These statistics include the three wave components for the period 1964-1974. This time period was selected, as previously mentioned, because both wave and historical shoreline position data were available.

(4) Northern swell is present for spectral peak periods between 5 and 20 sec, although the largest number of events occurs between 6 and 12 sec. In contrast, spectral peak periods for southern swell are typically 12 to 16 sec, with some as long as 20 sec. Directions of wave approach relative to the shoreline range from 55 deg north to 30 deg south of a line perpendicular to the coastline. Southern swell energy is more limited in direction, ranging only from 11 deg to 30 deg south of shore-normal.

(5) A statistical comparison of wave data calculated at 3- and 6-hr intervals for the 10-year period showed no significant difference in the distribution and magnitude of wave energy reaching the shoreline. In addition, the distribution of periods and angles was also nearly identical to that in the full 20-year time series. Thus, a time series of wave height, period, and angle at 6-hr intervals was selected as input for shoreline change modeling.

(6) To propagate the wave existing at the 65-ft contour onshore, it was necessary to develop a grid for the nearshore bathymetry. This information was obtained on magnetic media from the National Geophysical Data Center, Boulder, Colorado, and downloaded to disk for
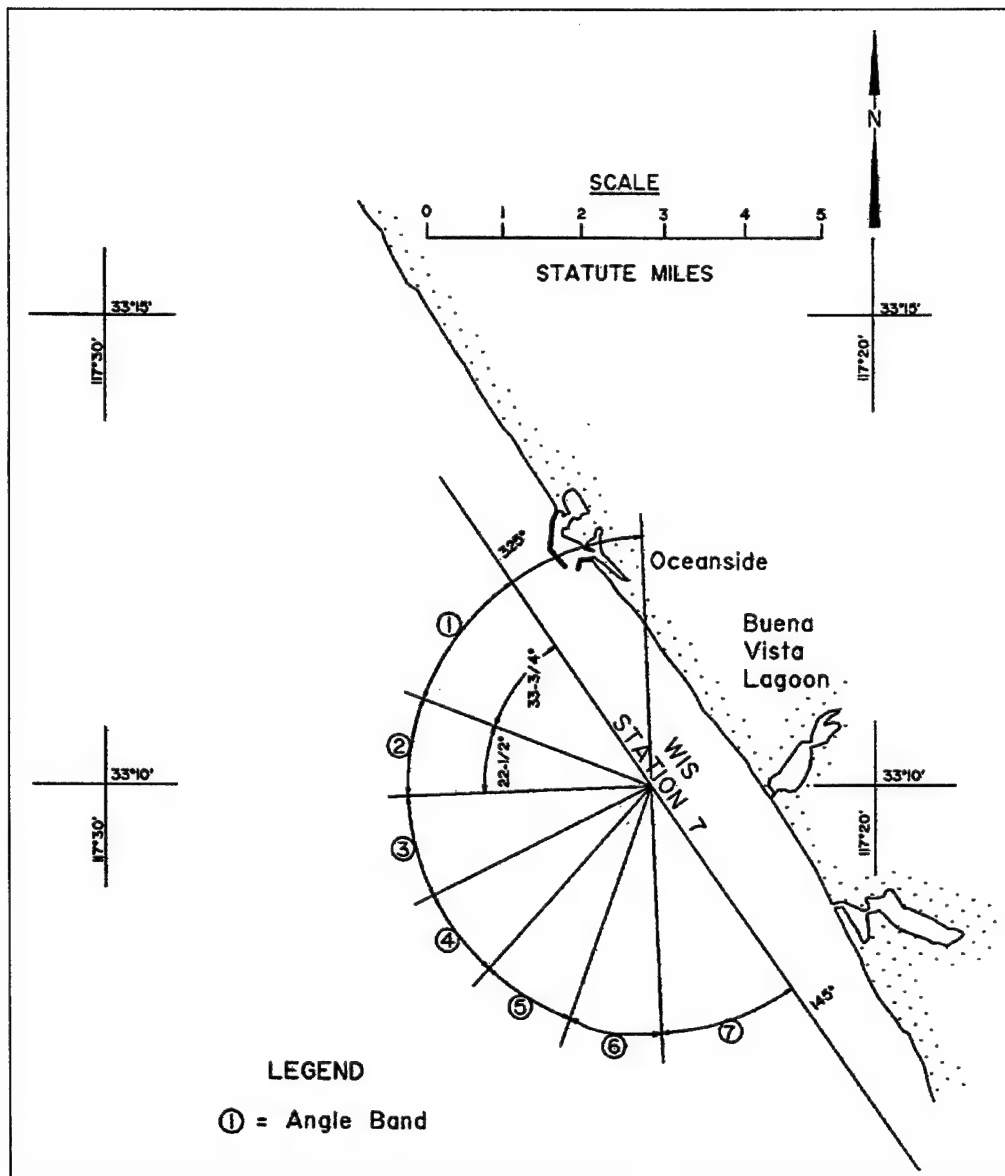
Figure 7-7. Orientation of wave angle bands at Oceanside

processing by a gridding software utility. A 3.2-mile by 10.3-mile rectangular grid was constructed for analysis of wave transformations. Over 9,800 data points were used to generate a 57- by 91-grid cell matrix of depths, with a 300-ft cross-shore dimension and a 600-ft long-shore dimension for each cell. The accuracy of this contour map was visually verified through comparison with National Oceanic and Atmospheric Administration (NOAA) Chart 18774 dated 1984.

(7) The wave transformation analysis over the grid of variable bathymetry was performed using the Regional Coastal Processes WAVE model (RCPWAVE) (Ebersole 1985; Ebersole, Cialone, and Prater 1986). The 46 wave period-wave angle conditions listed in Table 7-8 were transformed by RCPWAVE to approximately the 20-ft depth contour. Very little longshore variation in wave direction was present, a result of the relatively plane and parallel depth contours. The transformation

Table 7-8
Percent Occurrence of Waves by Period and Angle,
Oceanside, California

Period s	Angle Band 1	2	3	4	5	6	7
5	7.69	7.22	0.87	0.22	0.27	0.27	0.10
6	0.01	1.24	0.28	0.09	0.31	-	-
7	-	5.81	2.79	0.23	0.32	-	-
8	-	2.37	2.53	0.25	0.11	-	-
9	-	1.69	2.39	0.39	0.18	-	-
10	-	2.48	1.96	0.24	0.50	-	-
11	-	4.87	2.53	0.21	0.88	-	-
12	-	4.99	5.52	0.87	3.28	-	-
14	-	0.56	8.89	4.63	9.34	-	-
16	-	0.01	1.95	5.67	2.22	-	-
20	-	-	0.02	0.81	-	-	-

grid covered a broader area than the shoreline change model to place lateral boundary effects far from the region of interest. Transformed wave height and angle information are stored at positions corresponding to the nominal 20-ft-depth contour. This analysis provides the nearshore wave information required by the shoreline change model. Transport rates were calculated for each of three wave components (southern swell, northern swell, and local seas) every 6 hr.

e. Description of shoreline change model.

(1) The numerical shoreline change model GENESIS (Hanson 1989; Hanson and Kraus 1989; Gravens, Kraus, and Hanson 1991) was used in this study. It simulates long-term evolution of beach plan shape and provides a framework to perform a time-dependent sediment budget analysis. The model is versatile in that it can describe a broad range of conditions encountered in shore protection projects. GENESIS has been adapted to the personal computer environment for use in planning on a local scale.

(2) GENESIS is formulated through a control volume approach, as discussed in paragraph 6-10. A change in the sand volume is produced by either a spatial gradient in the longshore sand transport rate and/or sources and sinks within the control volume. This change in volume represents either a seaward (accretion) or landward (erosion) displacement of the profile. The beach profile is assumed to have a constant shape.

(3) Longshore variation in sand transport is the major cause of long-term shoreline change on an open

ocean coast. In GENESIS, the transport rate is calculated by Equations 6-22, 6-23, and 6-24.

(4) GENESIS is capable of simulating transport caused by multiple independent wave sources acting simultaneously. For example, in this study, northern swell, southern swell, and local seas are considered. At each 6-hr time step and at each model grid point along-shore, typically at 300-ft intervals, the volume transport rate $Q\ell$ in Equation 6-22 is determined as the vector sum of three independently calculated rates as

$$Q_\ell = Q_{NS} + Q_{SS} + Q_{LS} \qquad (7\text{-}1)$$

in which Q_{NS} is the transport rate produced by the northern swell, Q_{SS} is the transport rate produced by the southern swell, and Q_{LS} is the transport rate produced by locally generated seas.

(5) GENESIS is capable of representing a wide range of natural processes and coastal engineering activities that influence shoreline change. The principal capabilities and limitations of the model are summarized in Table 7-9. Nearshore waves can be input directly, computed from offshore conditions using a wave transformation model such as RCPWAVE or calculated from offshore conditions using an internal subroutine in GENESIS if the offshore bathymetry is very regular. Information such as structure locations and configurations, beach fill locations and volumes, and river sediment discharge volumes must be entered. Measured shoreline positions are needed to calibrate and verify the model. The main outputs of GENESIS are longshore sand transport rates and the resulting shoreline change.

f. Boundary conditions.

(1) The proper specification of boundary conditions is essential for the successful implementation of a shoreline change model. If the boundary conditions are incorrect, the calculated results will be wrong. This is particularly true for long simulations.

(2) The Oceanside Harbor jetties interrupt the continuity of longshore processes in the vicinity of Oceanside. These jetties form boundaries which separate the study area into a north reach (the shoreline north of the harbor) and a south reach (the shoreline south of the harbor). Since accurate dredging records are available, this is a good position to locate a boundary.

Table 7-9
Capabilities and Limitations of GENESIS

Capabilities

Almost arbitrary numbers of groins, jetties, detached breakwaters, seawalls, beach fills, and river discharges

Structures and beach fills in almost any combination

Compound structures such as T-shaped groins and spur groins

Bypassing of sand around and transmission through groins and jetties

Diffraction at detached breakwaters, jetties, and groins

Wave transmission through detached breakwaters

Coverage of wide spatial extent

Offshore input waves of arbitrary height, period, and direction

Multiple wave trains (as from independent wave sources)

Sand transport produced by oblique wave incidence and by a longshore gradient in wave height

Highly automated, numerically stable, and well tested

Limitations

No wave reflection from structures

No tombolo development in a strict sense (shoreline not allowed to touch a detached breakwater)

Slight restrictions on location, shape, and orientation of structures

Basic limitations of shoreline change modeling theory

(3) The other ends of the two reaches are more difficult to specify. Plots of shoreline positions from six measurements between March 1964 and January 1988 showed that the north reach shoreline was relatively stable at a location about 4.1 miles north of the harbor. Shoreline data for the south reach exhibited similar trends about 4.1 miles south of the harbor. These locations were designated as the two remaining model boundaries. Since the observed shoreline moved only slightly at these locations, there must exist a very small (assumed zero) gradient in the longshore transport. This type of open boundary condition is referred to as a pinned-beach boundary in GENESIS. It allows sand to freely pass through the boundary.

(4) The idealized north reach is shown in Figure 7-8. Essential features are an open or pinned-beach boundary at the north end, the Santa Margarita River near the south boundary, and a diffracting jetty at the south boundary. The GENESIS grid for the north reach consists of 72 cells, each 300 ft long, for a total shoreline distance of 21,600 ft. The shoreline position at the northern end of the north reach was fixed at an average of the measured shoreline positions from available surveys.

(5) The Santa Margarita River intermittently discharges sediment to the north reach model area. Sediment discharge by southern California coastal streams is episodic and difficult to estimate for any one year. For the purposes of long-term shoreline modeling, average annual sediment discharge input each year during the storm season provides a reasonable approximation of the historical process. The average annual volume of sand and gravel for the Santa Margarita River, 19,000 cu yd (Simons, Li, & Assoc. 1988), was introduced uniformly at the shoreline in cells 9 through 14 every year at a constant rate from December 1 through March 31.

(6) The Oceanside north jetty is the only shore structure in the north reach. It was designated as a wave-diffracting source at the location of the change in jetty alinement, approximately 500 ft from shore, and was assigned zero permeability. No beach fills are known to have been placed along the north reach.

(7) The south reach incorporates the features shown in Figure 7-9. A diffracting jetty is located at the north boundary, a long groin (considered to be non-diffracting) was constructed in 1968 immediately to the north of the mouth of the San Luis Rey River, and
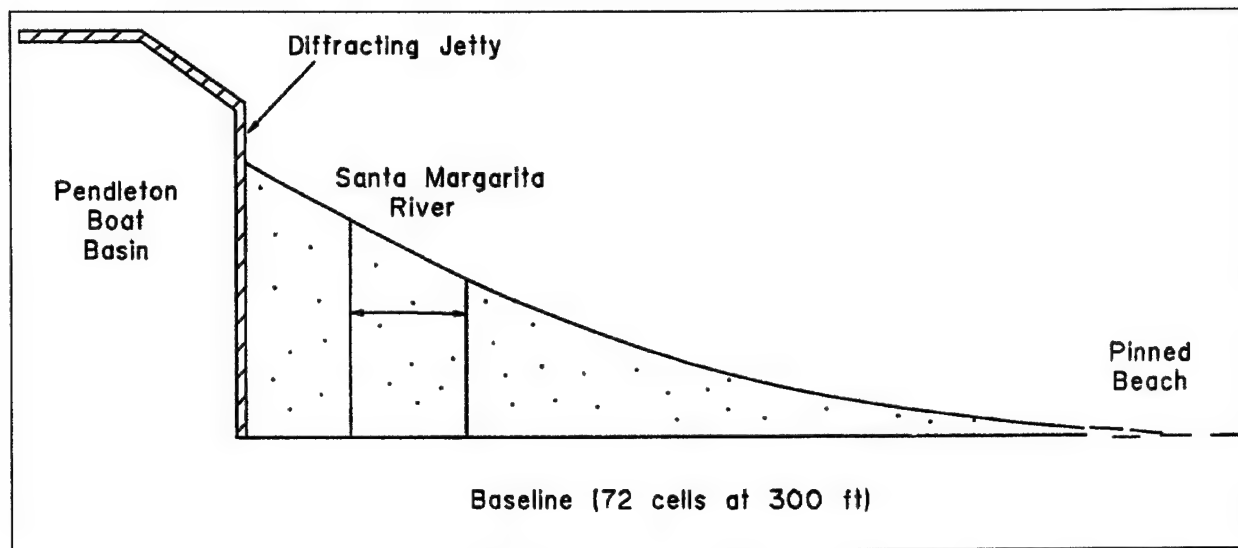
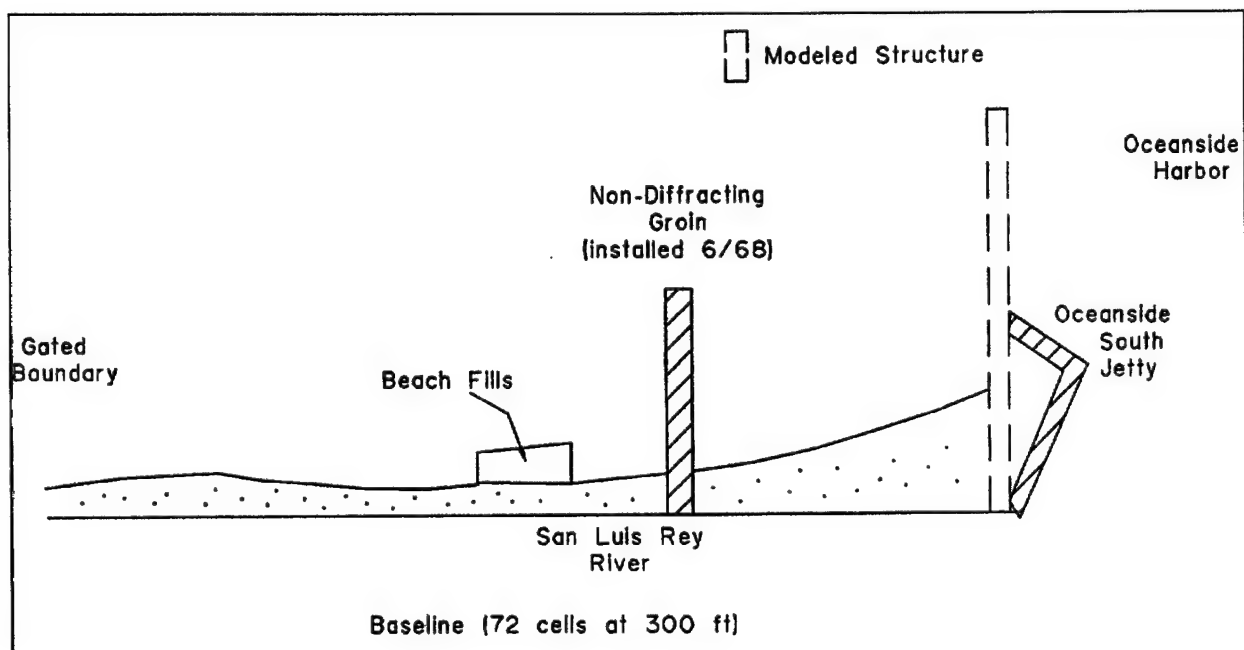Figure 7-8. Idealized features of Oceanside north reach

Figure 7-9. Idealized features of Oceanside south reach

several beach fills were placed to the south of the stream mouth. The south reach model grid also consists of 72 cells, each 300 ft long. At the south boundary, transport conditions were constrained to allow south-moving sand to move freely out of the study area, but to restrict north-moving sand onto the area (gated boundary). This represents the effects of the armored shoreline which existed during the calibration period south of the south reach (Hales 1978). Little sand was believed to be available for transport from Carlsbad to the shore at Oceanside.

(8) In the south reach, the San Luis Rey River input of sand and gravel was 11,000 cu yd annually at cells 63 through 65 from December 1 through March 31. This duration corresponds to the time in which winter storms are expected to cause the river to deliver sand to the coast.

(9) The south reach contains two structures. At the north boundary the end of the jetty was positioned to simulate the diffractive effects of the end of the outer breakwater at Oceanside Harbor. The groin at the San Luis Rey River mouth was incorporated in the model at the June 1968 simulation time-step. Zero permeability was assigned for both structures because the groin and south jetty have been grouted to prevent northerly sand movement through them. Shoreline surveys in the vicinity of the Oceanside pier indicate the pier has an insignificant effect on shoreline configuration, so it was not included in the model. Its location is shown on figures with model results for general orientation.

(10) A revetment was constructed in the area encompassed by the south reach prior to 1964 to harden the shoreline for upland protection. The revetment was implemented in the model as a seawall from cells 39 through 60 (extending approximately from 9th Street to Wisconsin Avenue).

(11) The shoreline in the south reach is an erosional shoreline and seven documented beach fills were placed in the reach during the calibration period. Initial placement volumes, alongshore extent of placement, and calculated berm widths are listed in Table 7-10. Experience with placing dredged material along this coast suggests modeling the placed volume by reducing the initial quantity by 20 percent to account for loss of fine material, and further reducing the remaining volume by 15 percent to account for losses from the system during profile adjustment. These volume adjustments were made before calculating berm widths listed in Table 7-10, which were then input to GENESIS.

Table 7-10
Beach Nourishment, Oceanside, California, 1965-1973

Date	Volume cu yd	Length ft	Effective Added Berm Width ft
1965	111,000	3000	16
1966	684,000	3600	79
1967	178,000	2100	35
1968	434,000	8100	22
1969	353,000	4200	35
1971	552,000	4200	55
1973	434,000	3000	45

(12) At Oceanside beach, the sea cliffs are protected by structures and the sediment yield from bluff erosion is negligible (Everts, Bertolotti, and Anderson 1989).

g. Beach profile

(1) Repetitive surveys were made at 12 transects in the Oceanside littoral cell between 1983 and 1988 as part of the Coast of California Storm and Tidal Wave Study (CCSTWS) field data collection program. Nine transects located in the study area were surveyed from three to eight times between 1983 and 1988. Profile characteristics were examined to evaluate parameters required in the shoreline change simulation.

(2) The closure depth defines the seaward limit of effective profile change. It is estimated by determining the depth at which significant profile changes cease to occur. To estimate closure depth, the standard deviation of depth was calculated as a function of mean depth at specified positions along each transect, following the procedure of Kraus and Harikai (1983). The depth of closure was determined to be the depth at which the variation in standard deviation decreased to a relatively constant amount and was estimated to be 30 ft in the Oceanside area. The berm height was determined from plotted profiles to be 14 ft relative to mean lower low water (MLLW). The zone of profile change extends from the berm crest to the closure depth, a total of 44 ft for the Oceanside model reaches.

(3) Another profile-related parameter required in GENESIS is the shape factor associated with the idealized equilibrium profile. The shape factor is calculated in GENESIS for a typical median grain diameter using an empirical formulation provided by Moore (1982). The effective grain size was obtained by comparing equilibrium profiles with mean nearshore profiles. The mean profile was calculated as the average of all surveys made at a transect. Equilibrium

profile curves generated for a range of sand sizes were compared with mean profiles. An effective median grain diameter of 0.28 mm was selected for input to GENESIS based on that comparison. Most sediment samples taken in water depths less than 15 ft in the study area from 1983 to 1988 had median grain sizes ranging from 0.16 to 0.50 mm. The input grain diameter determined from profile shape was, therefore, approximately the size determined statistically from samples.

h. Model calibration.

(1) The general calibration procedure for GENESIS requires determination of the longshore transport calibration parameters K_1 and K_2 in Equations 6-23 and 6-24 by reproducing measured shoreline changes that occurred in the study area. After initial model setup, calibration simulations were made in which the transport parameters and the passage of sand at the south boundary of the south reach model were varied. Computed shoreline change and longshore transport rates were optimized with $K_1 = 0.3$ and $K_2 = 0.2$.

(2) Simulated shoreline change for the calibration period is plotted for the north reach in Figure 7-10. Comparison of measured and calculated shoreline change near the harbor jetty shows reasonable agreement. The measured shoreline showed an advance over the entire reach length. The bulge in the middle of the reach could not be reproduced, degrading the quality of the simulation. The calculated average change in shoreline position was 2.5 ft/year advance, compared with a measured average of 4.5 ft/year advance.

(3) Only small variations in transport exist along the north reach because of the nearly plane and parallel offshore depth contours. The average net longshore transport rate was 430,000 cu yd/year to the south. At the south boundary of the north reach, the rate decreased to approximately 370,000 cu yd/year. This resulted in a shoreline advance and fillet formation near the north harbor jetty. Mean northerly and southerly sand transport rates averaged 100,000 cu yd/year and 530,000 cu yd/year, respectively. The magnitudes of the individual northerly and southerly sand transport rates differ somewhat from estimates presented in Table 7-6, but the net and the direction of net transport are consistent with previous estimates.

(4) The 1974 calculated south reach shoreline is plotted in Figure 7-11, along with the initial 1964 and the measured 1974 shorelines. Average simulated

shoreline recession was 5.9 ft/year as compared with a measured rate of 9.7 ft/year. Comparison of measured and calculated shoreline change trends again indicates good agreement. The largest deviations from measured trends in shoreline response occurred midway along the reach where a very large beach fill (3.8 million cu yd) was placed in 1963, one year before the date of the initial calibration shoreline. Profile adjustment was probably continuing during the early part of the calibration period and may have contributed to greater shoreline recession rates than those calculated by GENESIS.

(5) The calculated average annual transport rates were 100,000 cu yd/year to the north and 360,000 cu yd/year to the south for a net transport of 260,000 cu yd/year to the south. Greater impact of wave variability exists along the south reach where the mean net transport is relatively low and reverses from northerly at a position north of the San Luis Rey River mouth to southerly immediately south of the river mouth. The southerly transport increases with increasing distance south of the river mouth to a point about 10,000 ft south of the harbor. This spatial change in transport results from diffraction and sheltering of waves by the Oceanside breakwater. Along the southern 10,000 ft of the model reach, calculated net sand transport is uniformly 400,000 cu yd/year to the south, approximately equal to the net rate in the north reach.

(6) The calculated transport is predominantly to the south but at a rate somewhat greater than previously estimated (see Table 7-6). Although the direction of transport is consistent with earlier estimates, differences in magnitude may be related to the use of a complete time series of wave data in the present study rather than statistical wave summaries as done in previous studies. In addition, the method used to obtain breaking wave parameters for the transport calculations should provide more accurate results because wave transformation is modeled using the actual bathymetry and local shoreline orientation. Finally, by matching calculated and measured shorelines, net transport rates are potentially more realistic than estimates obtained without these constraints.

i. Sediment budget.

(1) Quantitative information on beach fill volumes, river discharges, and shoreline losses and gains were combined with calculated longshore sand transport rates to produce a sediment budget for the period 1964-1974 (Figure 7-12). The present analysis represents an optimal agreement between measured and calculated
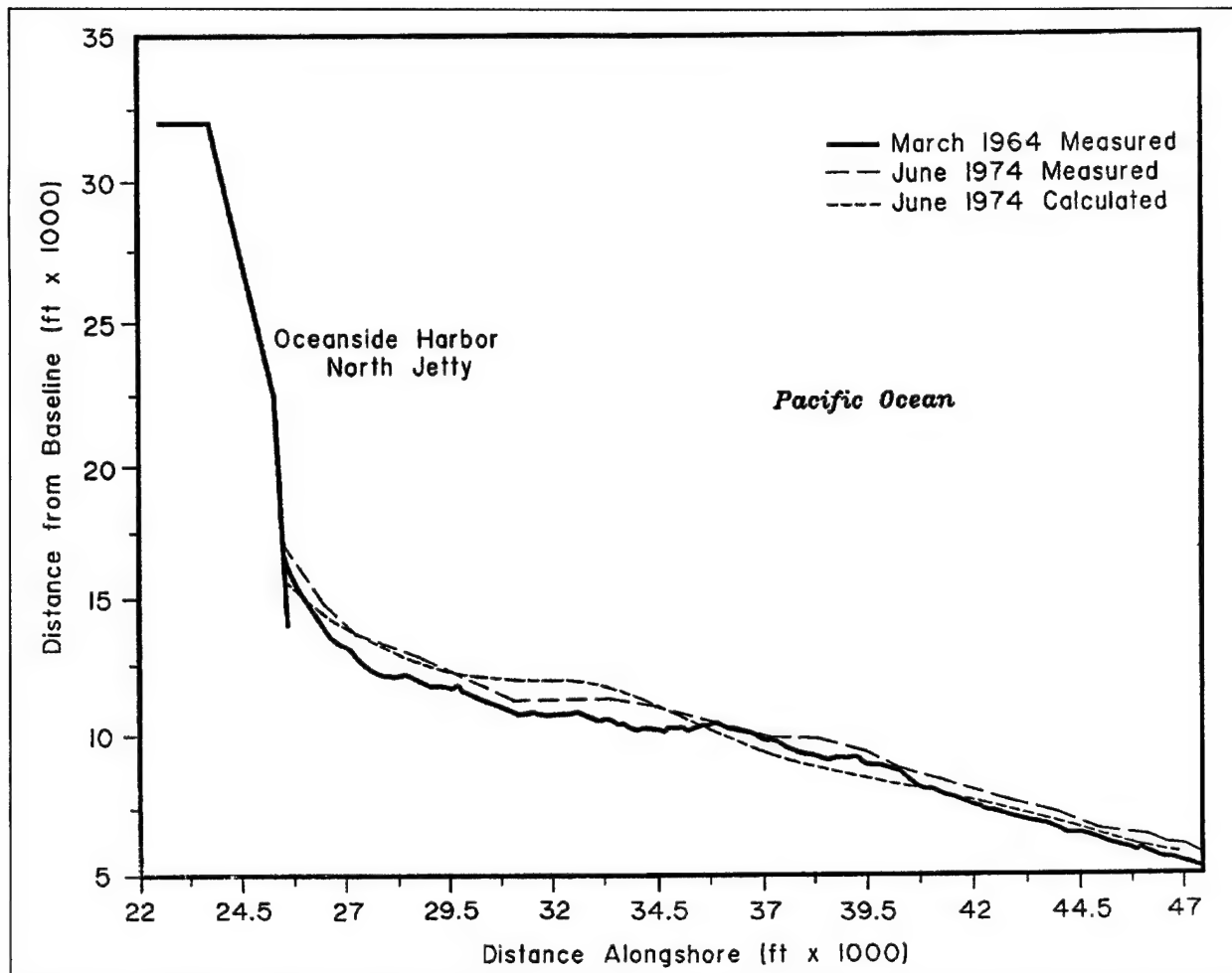
Figure 7-10. Oceanside north reach, 1964-1974

shoreline position and imposition of realistic boundary conditions. Volumes passing the lateral and shoreward sides of the control volume are known, whereas volumes passing the seaward boundary are derived by balancing the sediment budget. Estimated sediment exchange with the offshore was compared with amounts presented in other studies (Everts, Bertolotti, and Anderson 1989). For example, Weggel and Clark (1983) estimated that the amount of sediment lost to the offshore at the harbor ranged between 249,000 and 263,000 cu yd/year. Inman and Jenkins (1983) reported that about 48,000 cu yd/year were deflected offshore at the north jetty after it was extended in 1958.

(2) For the north reach, sand moves to the north out of the study area at an average rate of 90,000 cu yd/year and enters from the north at a rate of 540,000 cu yd/yr.

In addition, the Santa Margarita River adds 19,000 cu yd/year to the budget, and shoreline accretion removes 99,000 cu yd/year.   Although an estimated 210,000 cu yd/year of sand exits the north reach in a southerly direction, it does not bypass Oceanside Harbor but instead is deposited in the entrance channel and harbor complex. Some portion of this sand on the by-pass shoal will enter the harbor during periods or seasons of southerly waves, and appear to be sediment that has arrived from the south. Of the 210,000 cu yd/year estimated to arrive from the north reach, 50,000 cu yd/year was placed conceptually to arrive from the south reach, corresponding to the ratio of average annual transport rates to the north and to the south described in paragraph h (5). The volume estimated to deposit in the channel and harbor is the average annual volume of beach fill, less the fines fraction, that was placed along
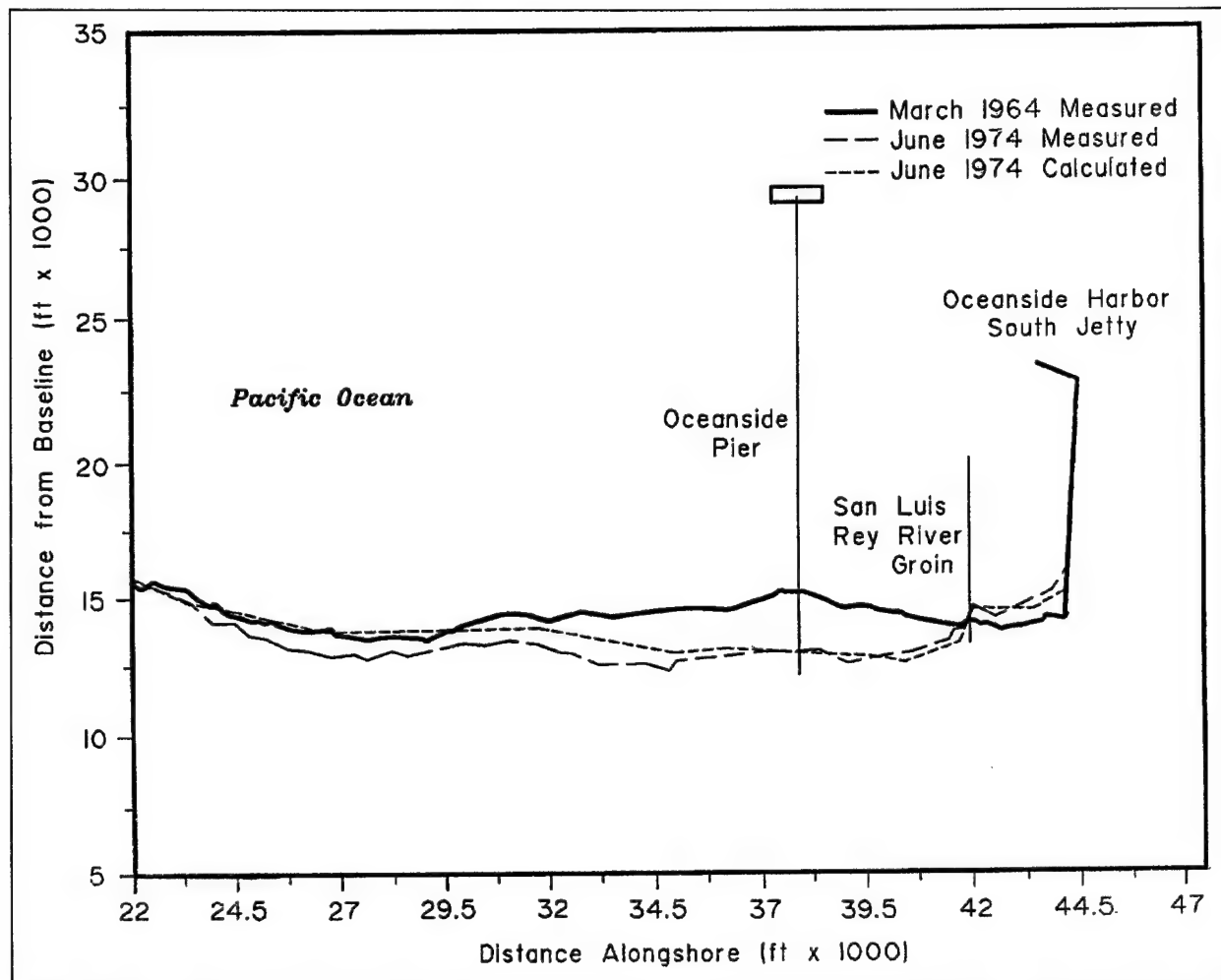
Figure 7-11. Oceanside south reach, 1964-7974

the south reach during this time interval. In closing the sediment budget to obtain the volume crossing the seaward boundary, approximately 160,000 cu yd/year were found to be lost from the system. It has been speculated that this offshore transport may be the source of sediment accretion observed in water depths up to 60 ft (Dolan et al. 1987). Because the shoreline change model uses a profile of fixed slope, a decrease in actual beach slope near the north jetty through sand impoundment is not represented. The associated portion of material accumulated inside the control volume would not appear in the budget and, therefore, would not be included in the seaward loss to balance the budget.

(3) Because of the recently completed grouting operations, the Oceanside Harbor complex is believed to

now completely block sediment movement in either direction at the north boundary of the south reach. If substantial sand were to move north and past the San Luis Rey River groin, it would be expected that the shoreline would advance on the south side of the groin. This has not been the case in the past several years. At the south boundary, 400,000 cu yd/year of sand are transported out of the reach, and sand transport to the north is nearly zero. The San Luis Rey River delivers about 11,000 cu yd/year of sand and gravel to the south reach (Simons, Li, & Assoc. 1988), and shoreline loss accounts for 209,000 cu yd/year. Historical records show that the rate of beach nourishment of the south reach was 265,000 cu yd/year during the simulation interval. It is assumed this volume came from the Oceanside harbor and channel and that all material

dredged from the harbor was placed as fill in the south reach. Approximately 30,000 cu yd/year of beach fill material were transported to the offshore during profile adjustment whereas 20 percent of the initial beach fill, or roughly 55,000 cu yd/year, were considered material finer than beach sand and removed from the south reach to the offshore. This fine sediment may be derived from the continuously suspended material in the surf one or the soil type into which the harbor was dredged.

(4) It is emphasized that the sediment budget shown in Figure 7-12 and similar figures represents a best estimate of average annual rates and trends over a long time period. It may not provide a good estimate of sediment transport for any one particular year. The significance of temporal variations in longshore sand transport on development of a sediment budget can be examined by noting the range in values calculated at the boundaries of the reaches. At the north boundary of the north reach, calculated annual southerly directed sand transport ranges from 333,000 cu yd to 840,000 cu yd. The standard deviation is ±160,000 cu yd or 30 percent of the average annual rate. Calculated annual transport of sand exiting the reach to the north ranges from

66,000 cu yd to 111,000 cu yd, with a standard deviation of ±22,000 cu yd/year. Greatest variability is associated with sand passing the south boundary of the south reach where the standard deviation (±140,000 cu yd/year) represents 35 percent of the average yearly transport rate.

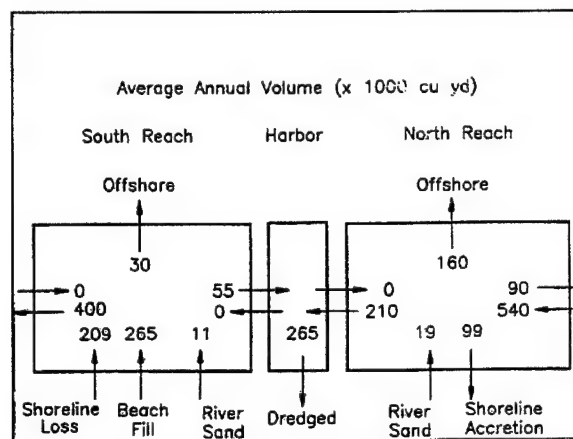Figure 7-12. Sediment budget for Oceanside

Appendix A
References

A-1. Required Publications

EM 1110-2-1414
EM 1110-2-1414. 1989 (7 July). Water Levels and Wave Heights for Coastal Engineering Design.

EM 1110-2-1614
EM 1110-2-1614. 1985 (30 April). Design of Coastal Revetments, Seawalls, and Bulkheads.

Ahrens 1977
Ahrens, J. P. 1977. "Prediction of Irregular Wave Overtopping," CETA 77-7, US Army Corps of Engineers, Coastal Engineering Research Center, Fort Belvoir, VA.

Ahrens and McCartney 1975
Ahrens, J. P., and McCartney, B. L. 1975. "Wave Period Effect of the Stability of Riprap," *Proceedings of Civil Engineering in the Oceans/III*, American Society of Civil Engineers, pp 1019-1034.

Ahrens and Titus 1985
Ahrens, J. P., and Titus, M. F. 1985. "Wave Runup Formulas for Smooth Slopes," *Journal of Waterway, Port, Coastal and Ocean Engineering*, American Society of Civil Engineers, Vol 111, No. 1, pp 128-133.

Airy 1845
Airy, G. B. 1845. "Tides and Waves," *Encyclopaedia Metropolitana*, Vol 192, pp 241-396.

Arthur 1951
Arthur, R. S. 1951. "The Effect of Islands on Surface Waves," *Bulletin of the Scripps Institution of Oceanography*, University of California, La Jolla, CA, Vol 6, No. 1.

Bagnold 1963
Bagnold, R. A. 1963. "Mechanics of Marine Sedimentation," in *The Sea*, M. N. Hill (Editor), Wiley-Interscience, New York, pp 507-582.

Bascom 1951
Bascom, W. H. 1951. "The Relationship Between Sand Size and Beach Face Slope," *Transactions of the American Geophysical Union*, Vol 32, pp 866-874.

Beach and Sternberg 1987
Beach, R. A., and Sternberg, R. W. 1987. "The Influence of Infragravity Motions on Suspended Sediment Transport in the Inner Surf Zone," *Proceedings of Coastal Sediments '87*, American Society of Civil Engineers, pp 913-928.

Berkoff 1972
Berkoff, J. C. W. 1972. "Computation of Combined Refraction-Diffraction," *Proceedings of the 13th International Conference on Coastal Engineering*, American Society of Civil Engineers, pp 471-490.

Blumenthal and O'Quinn 1981
Blumenthal, R. B., and O'Quinn, B. 1981. "The Coastal Environmental Reference Service," Reference Publication 35, Naval Oceanographic Office, NSTL Station, Bay St. Louis, MS.

Bodge and Dean 1987
Bodge, K. R., and Dean, R. G. 1987. "Short-Term Impoundment of Longshore Transport," *Proceedings of Coastal Sediments '87*, American Society of Civil Engineers, pp 468-483.

Booij 1981
Booij, N. 1981. "Gravity Waves on Water with Non-uniform Depth and Current," Doctoral dissertation, Technical University of Delft, the Netherlands.

Bowen 1969a
Bowen, A. J. 1969a. "The Generation of Longshore Currents on a Plane Beach," *Journal of Marine Research*, Vol 27, pp 206-215.

Bowen 1969b
Bowen, A. J. 1969b. "Rip Currents, 1. Theoretical Investigations," *Journal of Geophysical Research*, Vol 74, pp 5467-5478.

Bowen and Inman 1966
Bowen, A. J., and Inman, D. L. 1966. "Budget of Littoral Sands in the Vicinity of Port Arguello, California," US Army Corps of Engineers, Coastal Engineering Research Center, Technical Memorandum No. 19.

Bowen and Inman 1969
Bowen, A. J., and Inman, D. L. 1969. "Rip Currents, 2. Laboratory and Field Observations," *Journal of Geophysical Research*, Vol 74, pp 5479-5490.

Bowen and Inman 1971
Bowen, A. J., and Inman, D. L. 1971. "Edge Waves and Crescentic Bars," *Journal of Geophysical Research*, Vol 76, pp 8662-8671.

Brenninkmeyer 1976
Brenninkmeyer, B. M. 1976. "In Situ Measurements of Rapidly Fluctuating, High Sediment Concentrations," *Marine Geology*, Vol 20, pp 117-128.

Brownlie and Taylor 1981
Brownlie, W. R., and Taylor, B. D. 1981. "Sediment Management for Southern California Mountains, Coastal Plains, and Shorelines, Part C: Coastal Sediment Delivery by Major Rivers in Southern California," EQL Report No. 17-C, California Institute of Technology, Pasadena, CA.

Bruno and Gable 1976
Bruno, R. O., and Gable, C. G. 1976. "Longshore Transport at a Total Littoral Barrier," *Proceedings of the 15th International Conference on Coastal Engineering*, American Society of Civil Engineers, pp 1203-1222.

Bruno, Dean, and Gable 1980
Bruno, R. O., Dean, R. G., and Gable, C. G. 1980. "Littoral Transport Evaluations at a Detached Breakwater," *Proceedings of the 17th International Conference on Coastal Engineering*, American Society of Civil Engineers, pp 1453-1475.

Bruno et al. 1981
Bruno, R. O., Dean, R. G., Gable, C. G., and Walton, T. L. 1981. "Longshore Sand Transport Study at Channel Island Harbor, California," US Army Corps of Engineers, Coastal Engineering Research Center, Technical Paper No. 81-2, 48 p.

Caldwell 1956
Caldwell, J. M. 1956. "Wave Action and Sand Movement Near Anaheim Bay, California," US Army Corps of Engineers, Beach Erosion Board, Technical Memorandum No. 68, 21 p.

Caldwell 1966
Caldwell, J. M. 1966. "Coastal Processes and Beach Erosion," *Journal of the Boston Society of Civil Engineers*, Vol 53, pp 142-157.

California Department of Navigation and Ocean Development 1977
California Department of Navigation and Ocean Development. 1977. "Study of Beach Nourishment Along the Southern California Coastline," Sacramento, CA.

Chen and Houston 1986
Chen, H. A., and Houston, J. R. 1986. "Calculation of Water Oscillation in Coastal Harbors, HARBS and HARBD User's Manual," Instruction Report, US Army Engineer Waterways Experiment Station, Vicksburg, MS.

Cialone et al. 1992
Cialone, M. A., Mark, D. J., Chou, L. W., Leenknecht, D. A., Davis, J. E., Lillycrop, L. S., Jensen, R. E. 1992. "Coastal Modeling System (CMS) User's Manual," Instruction Report CERC-92-xx, US Army Engineer Waterways Experiment Station, Coastal Engineering Research Center, Vicksburg, MS.

Coakley and Skafel 1982
Coakley, J. P., and Skafel, M. G. 1982. "Suspended Sediment Discharge on a Non-Tidal Coast," *Proceedings of the 18th International Conference on Coastal Engineering*, American Society of Civil Engineers, pp 1288-1304.

Corson et al. 1986
Corson, W. D., Abel, C. E., Brooks, R. M., Farrar, P. D., Groves, B. J., Jensen, R. E., Payne, J. B., Ragsdale, D. S., and Tracy, B. A. 1986. "Pacific Coast Hindcast Deepwater Wave Information," WIS Report No. 14, US Army Engineer Waterways Experiment Station, Vicksburg, MS.

Corson et al. 1982
Corson, W. D., Resio, D. T., Brooks, R. M., Ebersole, B. A., Jensen, R. E., Ragsdale, D. S., and Tracy, B. A. 1982. "Atlantic Coast Hindcast, Phase II Wave Information," WIS Report No. 6, US Army Engineer Waterways Experiment Station, Vicksburg, MS.

Cross and Sollitt 1971
Cross, R., and Sollitt, C. 1971. "Wave Transmission by Overtopping," Technical Note No. 15, Massachusetts Institute of Technology, Ralph M. Parsons Laboratory.

Dally, Dean, and Dalrymple 1984
Dally, W. R., Dean, R. G., and Dalrymple, R. A. 1984. "Modeling Wave Transformation in the Surf Zone," Miscellaneous Paper CERC-84-8, US Army Engineer Waterways Experiment Station, Vicksburg, MS.

Dalrymple et al. 1984
Dalrymple, R. A., Kirby, J. T., and Hwang, P. A. 1984. "Wave Diffraction Due to Areas of Energy Dissipation," *Journal of Waterway, Port, Coastal, and Ocean Div.*, American Society of Civil Engineers, pp 67-79.

Dean 1973
Dean, R. G. 1973. "Heuristic Models of Sand Transport in the Surf Zone," *Proceedings of the 1st Australian Conference on Coastal Engineering*, Engineering Dynamics in the Surf Zone, Sydney, pp 208-214.

Dean 1983
Dean, R. G. 1983. "Principles of Beach Nourishment," in *Handbook of Coastal Processes and Erosion*, P. D. Komar (editor), CRC Press, Boca Raton, pp 217-231.

Dean and Dalrymple 1983
Dean, R. G., and Dalrymple, R. A. 1983. *Water Wave Mechanics for Engineers and Scientists*, Prentice-Hall, Inc., Englewood Cliffs, NJ.

Dean et al. 1987
Dean, R. G., Berek, E. P., Bodge, K. R., and Gable, C. G. 1987. "NSTS Measurements of Total Longshore Transport," *Proceedings of Coastal Sediments '87*, American Society of Civil Engineers, pp 652-667.

Dean et al. 1982
Dean, R. G., Berek, E. P., Gable, C. G., and Seymour, R. J. 1982. "Longshore Transport Determined by an Efficient Trap," *Proceedings of the 18th International Conference on Coastal Engineering*, American Society of Civil Engineers, pp 954-968.

Dolan 1971
Dolan, R. 1971. "Coastal Landforms; Crescentic and Rhythmic," *Geological Society of America Bulletin*, Vol 82, pp 177-180.

Dolan et al. 1987
Dolan, T. J., Castens, P. G., Sonu, C. J., and Egense, A. K. 1987. "Review of Sediment Budget Methodology: Oceanside Littoral Cell, California," *Proceedings of Coastal Sediments '87*, American Society of Civil Engineers, pp 1289-1304.

Downing 1984
Downing, J. P. 1984. "Suspended Sand Transport on a Dissipative Beach," *Proceedings of the 19th International Conference on Coastal Engineering*, American Society of Civil Engineers, pp 1765-1781.

Duane and James 1980
Duane, D. B., and James, W. R. 1980. "Littoral Transport in the Surf Zone Elucidated by an Eulerian Sediment Tracer Experiment," *Journal of Sedimentary Petrology*, Vol 50, pp 929-942.

Ebersole 1985
Ebersole, B. A. 1985. "Refraction-Diffraction Model for Linear Water Waves," *Journal of the Waterway, Port, Coastal, and Ocean Engineering Division*, American Society of Civil Engineers, Vol 111, pp 939-953.

Ebersole, Cialone, and Prater 1986
Ebersole, B. A., Cialone, M. A., and Prater, M. D. 1986. "Regional Coastal Processes Numerical Modeling System Report 1: RCPWAVE -- A Linear Wave Propagation Model for Engineering Use," Technical Report CERC-86-4, US Army Engineer Waterways Experiment Station, Vicksburg, MS.

Everts and Dill 1988
Everts, C. H., and Dill, C. E. 1988. "Sedimentation in Submarine Canyons in San Diego County, California," Coast of California Storm and Tidal Waves Study, Moffatt & Nichol Engineers, Long Beach, CA, prepared for US Army Engineer District, Los Angeles, CA.

Everts, Bertolotti, and Anderson 1989
Everts, C. H., Bertolotti, A., and Anderson, R. J. 1989. "Preliminary Sediment Budget, Mission Bay Littoral Cell," Moffatt and Nichol Engineers, prepared for Los Angeles District, US Army Corps of Engineers.

Fairchild 1972
Fairchild, J. C. 1972. "Longshore Transport of Suspended Sediment," *Proceedings of the 13th International Conference on Coastal Engineering*, American Society of Civil Engineers, pp 1069-1088.

Fairchild 1977
Fairchild, J. C. 1977. "Suspended Sediment in the Littoral Zone at Vetnor, New Jersey, and Nags Head, North Carolina," Technical Paper No. 77-5, US Army Corps of Engineers, Coastal Engineering Research Center, Fort Belvoir, VA.

Galvin 1979
Galvin, C. J. 1979. "Relation Between Immersed Weight and Volume Rates of Longshore Transport," Technical Paper 79-1, US Army Corps of Engineers, Coastal Engineering Research Center, Fort Belvoir, VA.

Goda 1969
Goda, Y. 1969. "Reanalysis of Laboratory Data on Wave Transmission," *Report of the Port and Harbour Research Institute*, Vol 18, No. 13.

Goda 1975
Goda, Y. 1975. "Irregular Wave Deformation in the Surf Zone," Coastal Engineering in Japan, Vol 18, pp 13-26.

Goda 1984
Goda, Y. 1984. *Random Seas and Design of Maritime Structures*, University of Toyko Press. pp 41-46.

Goda 1985
Goda, Y. 1985. Random Seas and Design of Maritime Structures, University of Tokyo Press, Tokyo.

Goda 1988
Goda, Y. 1988. "On the Methodology of Selecting Design Wave Height," *Proceedings, 21st Coastal Engineering Conference*, American Society of Civil Engineers, Costa del Sol-Malaga, Spain, pp 899-913.

Goda, Takeda, Moriya 1967
Goda, Y., Takeda, H., and Moriya, Y. 1967. "Laboratory Investigation of Wave Transmission over Breakwaters," Report of the Port and Harbour Research Institute, No. 13.

Gourley 1974
Gourley, M. R. 1974. "Wave Set-Up and Wave Generated Currents in the Lee of a Breakwater or Headland," *Proceedings of the 14th International Conference on Coastal Engineering*, American Society of Civil Engineers, pp 1976-1995.

Gourley 1976
Gourley, M. R. 1976. "Non-Uniform Alongshore Currents," *Proceedings of the 15th International Conference on Coastal Engineering*, American Society of Civil Engineers, pp 701-720.

Grant 1943
Grant, U. S. 1943. "Waves as a Transporting Agent," *American Journal of Science*, Vol 241, pp 117-123.

Gravens 1988
Gravens, M. B. 1988. "Use of Hindcast Wave Data for Estimation of Longshore Sediment Transport," *Proceedings of the Symposium on Coastal Water Resources*, American Water Resources Association, pp 63-72.

Gravens 1989
Gravens, M. B. 1989. "Estimating Potential Longshore Sand Transport Rates Using WIS Data," CETN-II-19, US Army Engineer Waterways Experiment Station, Vicksburg, MS.

Gravens 1991
Gravens, M. B. 1991. "Shoreline Modeling System (SMS) Version 1," Coastal Engineering Technical Note CETN-II-27, December 1991, US Army Engineer Waterways Experiment Station, Coastal Engineering Research Center, Vicksburg, MS.

Gravens, Kraus, and Hanson 1991
Gravens, M. B., Kraus, N. C., and Hanson, H. 1991. "GENESIS: Generalized Model for Simulating Shoreline Change," Instruction Report CERC-89-19, US Army Engineer Waterways Experiment Station, Vicksburg, MS.

Gravens, Scheffner, and Hubertz 1989
Gravens, M. B., Scheffner, N. W., and Hubertz, J. M. 1989. "Coastal Processes from Asbury Park to Manasquan, New Jersey," Miscellaneous Paper CERC-89-11, US Army Engineer Waterways Experiment Station Vicksburg, MS.

Griggs 1987
Griggs, G. B. 1987. "The Production, Transport, and Delivery of Coarse-Grained Sediment by California's Coastal Streams," *Proceedings of Coastal Sediments '87*, American Society of Civil Engineers, pp 1825-1838.

Guza and Thornton 1982
Guza, R. T., and Thornton, E. B. 1982. "Swash Oscillations on a Natural Beach," *Journal of Geophysical Research*, Vol 87, pp 483-491.

Hales 1978
Hales, L. Z. 1978. "Coastal Precesses Study of the Oceanside, California, Littoral Cell," Miscellaneous Paper H-78-8, US Army Engineer Waterways Experiment Station, Vicksburg, MS.

Hanes et al. 1988
Hanes, D. M., Vincent, C. E., Huntley, D. A., and Clarke, T. L. 1988. "Acoustic Measurements of Suspended Sand Concentration in the C^2S^2 Experiment at Stanhope Lane, Prince Edward Island," *Marine Geology,* Vol 81, pp 185-196.

Hanson 1989
Hanson, H. 1989. "GENESIS - A Generalized Shoreline Change Numerical Model," *Journal of Coastal Research,* Vol 5, No. 1, pp 1-27.

Hanson and Kraus 1989
Hanson, H., and Kraus, N. C. 1989. "GENESIS: Generalized Numerical Modeling System for Simulating Shoreline Change," Report 1, Technical Reference Manual, Technical Report CERC-89-19, US Army Engineer Waterways Experiment Station, Coastal Engineering Research Center, Vicksburg, MS.

Hardy and Kraus 1987
Hardy, T. A., and Kraus, N. C. 1987. "A Numerical Model for Shoaling and Refraction of Second-Order Cnoidal Waves Over an Irregular Bottom," Miscellaneous Paper CERC-87-9, US Army Engineer Waterways Experiment Station, Vicksburg, MS.

Hattori and Suzuki 1979
Hattori, M. and Suzuki, T. 1979. "Field Experiment on Beach Gravel Transport," *Proceedings,* 16th Coastal Engineering Conference, American Society of Civil Engineers, pp 1688-1704.

Hino 1974
Hino, M. 1974. "Theory of Formation of Rip-Current and Cuspidal Coast," *Proceedings, 14th Coastal Engineering Conference,* American Society of Civil Engineers, pp 901-919.

Holman 1983
Holman, R. A. 1983. "Edge Waves and the Configuration of the Shoreline," in *Handbook of Coastal Processes and Erosion,* P. D. Komar (editor), Boca Raton, Fla., CRC Press, pp 21-33.

Holman and Sallenger 1985
Holman, R. A., and Sallenger, A. H. 1985. "Set-Up and Swash on a Natural Beach," *Journal of Geophysical Research,* Vol 90, pp 945-953.

Hom-ma, Horikawa, and Kajima 1965
Hom-ma, M., Horikawa, K., and Kajima, R. 1965. "A Study of Suspended Sediment Due to Wave Action," *Coastal Engineering in Japan,* Vol 3, pp 101-122.

Hughes and Jensen 1986
Hughes, S. A., and Jensen, R. E. 1986. "A User's Guide to SHALWV: Numerical Model for Simulation of Shallow-Water Wave Growth, Propagation, and Decay," Instruction Report CERC-86-2, US Army Engineer Waterways Experiment Station, Vicksburg, MS.

Hunt 1979
Hunt, J. N. 1979. "Direct Solution of Wave Dispersion Equation," *Journal of the Waterways, Port, Coastal and Ocean Division,* No. WW4, American Society of Civil Engineers, pp 457-459.

Inman 1953
Inman, D. L. 1953. "Areal and Seasonal Variations in Beach and Nearshore Sediments at La Jolla, California," Technical Memorandum No. 39, Beach Erosion Board, Washington, D.C.

Inman 1976
Inman, D. L. 1976. "Summary Report of Man's Impact on the California Coastal Zone," Scripps Institution of Oceanography, University of California, La Jolla, CA, prepared for California Department of Navigation and Ocean Development, Sacramento, CA.

Inman and Bagnold 1963
Inman, D. L., and Bagnold, R. A. 1963. "Littoral Processes," in *The Sea,* M. N. Hill (Editor), Wiley-Interscience, New York, pp 529-553.

Inman and Frautschy 1966
Inman, D. L., and Frautschy, J. A. 1966. "Littoral Processes and the Development of Shorelines," *Proceedings of the Coastal Engineering Specialty Conference,* American Society of Civil Engineers, pp 511-536.

Inman and Jenkins 1983
Inman, D. L., and Jenkins, S. A. 1983. "Oceanographic Report for Oceanside Beach Facilities," La Jolla, California.

Inman et al. 1980
Inman, D. L., Zampol, J. A., White, T. E., Hanes, D. M., Waldorf, B. W., and Kastens, K. A. 1980. "Field Measurements of Sand Motion in the Surf Zone," *Proceedings of the 17th International Conference on Coastal Engineering*, American Society of Civil Engineers, pp 1215-1234.

Isobe 1985
Isobe, M. 1985. "Calculation and Application of First-Order Cnoidal Wave Theory," *Coastal Engineering*, Vol 9, pp 309-325.

James 1975
James, W. R. 1975. "Techniques in Evaluating Suitability of Borrow Material for Beach Nourishment," Technical Memorandum No. 60, US Army Engineer Waterways Experiment Station, Vicksburg, MS.

Jensen 1983a
Jensen, R. E. 1983a. "Mississippi Sound Wave-Hindcast Study," Technical Report HL-83-8, US Army Engineer Waterways Experiment Station, Vicksburg, MS.

Jensen 1983b
Jensen, R. E. 1983b. "Methodology for the Calculation of a Shallow-Water Wave Climate," WIS Report 8, US Army Engineer Waterways Experiment Station, Vicksburg, MS.

Jensen, Vincent, and Reinhard 1989
Jensen, R. E., Vincent, C. L., and Reinhard, R. D. 1989. "A Multifaceted Wind-Wave Hindcast Method to Describe a Southern California Wave Climate," *Proceedings of the 2nd International Workshop on Wave Hindcasting and Forecasting*, Vancouver, British Columbia, pp 161-170.

Johnson 1956
Johnson, J. W. 1956. "Dynamics of Nearshore Sediment Movement," *Bulletin of the American Society of Petroleum Geologists*, Vol 40, pp 2211-2232.

Johnson 1957
Johnson, J. W. 1957. "The Littoral Drift Problem at Shoreline Harbors," *Journal of the Waterways and Harbors Division*, American Society of Civil Engineers, Vol 83, pp 1-37.

Jones 1989
Jones, D. L. 1989. "Microcomputer Applications for Coastal Engineering (MACE)," Coastal Engineering Technical Note CETN-VI-16, US Army Engineer Waterways Experiment Station, Vicksburg, MS.

Jonsson 1966
Jonsson, I. G. 1966. "Wave Boundary Layers and Friction Factors," *Proceedings of the 10th Conference on Coastal Engineering*, American Society of Civil Engineers, pp 127-148.

Kamphuis 1975
Kamphuis, J. W. 1975. "Friction Factors Under Oscillatory Waves," *Journal of the Waterways, Harbors and Coastal Engineering Division*, American Society of Civil Engineers, Vol 101, pp 135-144.

Kamphuis et al. 1986
Kamphuis, J. W., Davies, M. H., Nairn, R. B., and Sayao, O. J. 1986. "Calculation of Littoral Sand Transport Rate," *Coastal Engineering*, Vol 10, pp 1-21.

Kana 1977
Kana, T. W. 1977. "Suspended Sediment Transport at Price Inlet, S.C.," *Proceedings of Coastal Sediments '77*, American Society of Civil Engineers, pp 366-382.

Kana 1978
Kana, T. W. 1978. "Surf Zone Measurements of Suspended Sediment," *Proceedings of the 16th International Conference on Coastal Engineering*, American Society of Civil Engineers, pp 1725-1743.

Katoh, Tanaka, and Irie 1984
Katoh, K., Tanaka, N., and Irie, I. 1984. "Field Observation on Suspended-Load in the Surf Zone," *Proceedings of the 19th International Conference on Coastal Engineering*, American Society of Civil Engineers, pp 1846-1862.

Kinsman 1965
Kinsman, B. 1965. *Wind Waves*, Prentice-Hall, Inc., Englewood Cliffs, New Jersey.

Kirby and Dalrymple 1986
Kirby, J. T., and Dalrymple, R. A. 1986. "Modelling Waves in Surf Zones and Around Islands," *Journal of*

Waterway, Port, Coastal, and Ocean Div., American Society of Civil Engineers, pp 78-93.

Knoth and Nummedal 1977
Knoth, J. S., and Nummedal, D. 1977. "Longshore Sediment Transport Using Fluorescent Tracer," *Proceedings of Coastal Sediments '77*, American Society of Civil Engineers, pp 383-398.

Kobayashi and Han 1988
Kobayashi, N., and Han, K.-S. 1988. "Erosion at Bend of Gravel Causeway Due to Waves," *Journal of the Waterway, Port, Coastal and Ocean Engineering Division*, American Society of Civil Engineers, Vol 114, pp 297-314.

Komar 1971
Komar, P. D. 1971. "Nearshore Cell Circulation and the Formation of Giant Cusps," *Geological Society of America Bulletin*, Vol 82, pp 2643-2650.

Komar 1973
Komar, P. D. 1973. "Computer Models of Delta Growth Due to Sediment Input from Waves and Long-shore Currents," *Geological Society of America Bulletin*, Vol 84, pp 2217-2226.

Komar 1975
Komar, P. D. 1975. "Nearshore Currents: Generation by Obliquely Incident Waves and Longshore Variations in Breaker Heights," in *Nearshore Sediment Dynamics and Sedimentation*, J. Hails and A. Carr (editors), John Wiley & Sons, London, pp 17-45.

Komar 1977
Komar, P. D. 1977. "Beach Sand Transport: Distribution and Total Drift," *Journal of the Waterway, Port, Coastal and Ocean Engineering Division*, American Society of Civil Engineers, Vol 103, pp 225-239.

Komar 1979
Komar, P. D. 1979. "Beach-Slope Dependence of Longshore Currents," *Journal of the Waterway, Port, Coastal and Ocean Engineering Division*, American Society of Civil Engineers, Vol 105, pp 460-464.

Komar 1983
Komar, P. D. 1983. "The Erosion of Siletz Spit, Oregon," in *Handbook of Coastal Processes and Erosion*, P. D. Komar (editor), CRC Press, Boca Raton, pp 65-76.

Komar 1988
Komar, P. D. 1988. "Environmental Controls on Littoral Sand Transport," *Proceedings of the 21st International Conference on Coastal Engineering*, American Society of Civil Engineers, pp 1238-1252.

Komar 1990
Komar, P. D. 1990. "Littoral Sediment Transport," in *Handbook on Coastal and Ocean Engineering*, J. B. Herbich (editor), Gulf Publishing Co., Galveston.

Komar and Holman 1986
Komar, P. D., and Holman, R. A. 1986. "Coastal Processes and the Development of Shoreline Erosion," *Annual Reviews Earth and Planetary Science*, Vol 14, pp 237-265.

Komar and Inman 1970
Komar, P. D., and Inman, D. L. 1970. "Longshore Sand Transport on Beaches," *Journal of Geophysical Research*, Vol 75, pp 5914-5927.

Kraus 1983
Kraus, N. C. 1983. "Applications of a Shoreline Prediction Model," *Proceedings of Coastal Structures '83*, pp 632-645.

Kraus 1991
Kraus, N. C. 1991. "ON_OFF: A PC-Based Computer Program for Predicting Beach Erosion and Accretion by Cross-Shore Wave-Induced Transport," Coastal Engineering Technical Note.

Kraus and Dean 1987
Kraus, N. C., and Dean, J. L. 1987. "Longshore Sand Transport Rate Distributions Measured by Trap," *Proceedings*, Coastal Sediments '87, ed., N. C. Kraus, American Society of Civil Engineers, pp 881-896.

Kraus and Harikai 1983
Kraus, N. C., and Harikai, S. 1983. "Numerical Model of the Shoreline Change at Oarai Beach," *Coastal Engineering*, Vol 7, pp 1-28.

Kraus and Larson 1991
Kraus, N. C., and Larson, M. 1991. "NMLONG: Numerical Model for Simulating the Longshore Current," Report 1: Model Development and Tests, Technical Report DRP-91-1, US Army Engineer Waterways Experiment Station, Coastal Engineering Research Center, Vicksburg, MS.

Kraus and Sasaki 1979
Kraus, N. C., and Sasaki, T. O. 1979. "Effect of Wave Angle and Lateral Mixing on the Longshore Current," *Coastal Engineering in Japan*, Vol 22, pp 59-74. (Also Mar. Sci. Commun., 1979, Vol 5, pp 91-126.)

Kraus et al. In preparation
Kraus, N. C., Byrnes, M. B., Hales, L. Z., Kadib, A. L., and Simpson, D. P. In preparation. "Coastal Processes Numerical Modeling: San Diego Region, Coast of California Storm and Tidal Waves Study," Miscellaneous Paper CERC-91-__, US Army Engineer Waterways Experiment Station, in press.

Kraus, Gingerich, and Rosati 1988
Kraus, N. C., Gingerich, K. J., and Rosati, J. D. 1988. "Toward an Improved Empirical Formula for Longshore Sand Transport," *Proceedings of the 21st International Conference on Coastal Engineering*, American Society of Civil Engineers, pp 1182-1196.

Kraus et al. 1989
Kraus, N. C., Gingerich, K. J., and Rosati, J. D. 1989. "DUCK85 Surf Zone Sand Transport Experiment," Technical Report CERC-89-5, US Army Engineer Waterways Experiment Station, Vicksburg, MS.

Kraus et al. 1982
Kraus, N. C., Isobe, M., Igarashi, H., Sasaki, T. O., and Horikawa, K. 1982. "Field Experiments on Longshore Transport in the Surf Zone," *Proceedings of the 18th International Conference on Coastal Engineering*, American Society of Civil Engineers, pp 969-988.

Kraus, Larson, and Kriebel 1991
Kraus, N. C., Larson, M., and Kriebel, D. 1991. "Critical Evaluation of Beach Erosion Predictors by Cross-Shore Transport," *Proceedings Coastal Sediments '91*, American Society of Civil Engineers, in prep.

Kriebel 1982
Kriebel, D. L. 1982. "Beach and Dune Response to Hurricanes," M.S. Thesis, Department of Civil Engineering, University of Delaware, Newark, DE.

Kriebel 1984a
Kriebel, D. L. 1984a. "Beach Erosion Model EBEACH User's Manual, Volume I: Description of Computer Model," Beach and Shores Technical Design Memorandum No. 84-5-I, Division of Beaches and Shores, Florida Department of Natural Resources, Tallahassee, FL.

Kriebel 1984b
Kriebel, D. L. 1984b. "Beach Erosion Model EBEACH User's Manual, Volume II: Theory and Background," Beach and Shores Technical Design Memorandum No. 84-5-II, Division of Beaches and Shores, Florida Department of Natural Resources, Tallahassee, FL.

Kriebel 1986
Kriebel, D. L. 1986. "Verification Study of a Dune Erosion Model," *Shore and Beach*, Vol 54, No. 3, pp 13-21.

Kriebel, Dally, and Dean 1987
Kriebel, D. L., Dally, W. R., and Dean, R. G. 1987. "Undistorted Froude Model for Surf Zone Sediment Transport," *Proceedings of the 20th International Conference on Coastal Engineering*, American Society of Civil Engineers, pp 1296-1310.

Larson and Kraus 1989
Larson, M., and Kraus, N. C. 1989. "SBEACH: Numerical Model for Simulating Storm-Induced Beach Change," Report 1, Empirical Foundation and Model Development, Technical Report CERC-89-9, US Army Engineer Waterways Experiment Station, Vicksburg, MS.

Larson and Kraus 1991
Larson, M., and Kraus, N. C. 1991. "Numerical Model of Longshore Current Over Bar and Trough Beaches," *Journal of Waterway, Port, Coastal and Ocean Engineering*, in press.

Larson, Hanson, and Kraus 1987
Larson, M., Hanson, H., and Kraus, N. C. 1987. "Analytical Solutions of the One-Line Model of Longshore Change," Technical Report CERC-87-15, US Army Engineer Waterways Experiment Station, Vicksburg, MS.

Larson, Kraus, and Byrnes 1990
Larson, M., Kraus, N. C., and Byrnes, M. R. 1990. "SBEACH: Numerical Model for Simulating Storm-Induced Beach Change," Report 2, Numerical Formulation and Model Tests, Technical Report CERC-89-9, US Army Engineer Waterways Experiment Station, Vicksburg, MS.

LeBlond and Tang 1974
LeBlond, P. H., and Tang, C. L. 1974. "On Energy Coupling Between Waves and Rip Currents," *Journal of Geophysical Research*, Vol 79, pp 811-816.

Leenknecht and Szuwalski 1988
Leenknecht, D. A., and Szuwalski, A. 1988. "Automated Coastal Engineering System: User Guide," US Army Engineer Waterways Experiment Station, Vicksburg, MS.

LeMehaute 1969
LeMehaute, B. 1969. "An Introduction to Hydrodynamics and Water Waves," *Water Wave Theories*, Vol II, TR ERL 118-POL-3-2, US Department of Commerce, ESSA, Washington, D.C.

Liu et al. 1986
Liu, P. L.-F., Boissevain, P. L., Ebersole, B. A., and Kraus, N. C. 1986. "Annotated Bibliography on Combined Wave Refraction and Diffraction," Miscellaneous Paper CERC-86-10, US Army Engineer, Waterways Experiment Station, Vicksburg, MS.

Longuet-Higgins 1952
Longuet-Higgins, M. S. 1952. "On the Statistical Distribution of the Heights of Sea Waves," *Journal of Marine Research*, Vol 11, pp 245-266.

Longuet-Higgins 1970a
Longuet-Higgins, M. S. 1970a. "Longshore Currents Generated by Obliquely Incident Waves, 1," *Journal of Geophysical Research*, Vol 75, pp 6778-6789.

Longuet-Higgins 1970b
Longuet-Higgins, M. S. 1970b. "Longshore Currents Generated by Obliquely Incident Waves, 2," *Journal of Geophysical Research*, Vol 75, pp 6790-6801.

Longuet-Higgins and Cokelet 1976
Longuet-Higgins, M. S., and Cokelet, E. D. 1976. "The Deformation of Steep Surface Waves on Water, I, a Numerical Method of Computation," *Proceedings of the Royal Society*, Vol 350, pp 1-25.

Madsen and White 1976
Madsen, O. S., and White, S. M. 1976. "Reflection and Transmission Characteristics of Porous Rubble-Mound Breakwaters," MR 76-5, US Army Corps of Engineers, Coastal Engineering Research Center, Fort Belvoir, VA.

Marine Advisers 1961
Marine Advisers. 1961. "A Statistical Survey of Ocean Wave Characteristics in Southern California Waters, La Jolla, CA," prepared for US Army Engineer District, Los Angeles.

Mark 1990
Mark, D. M. 1990. "Coastal Modeling System," CETN-VI-18, US Army Engineer Waterways Experiment Station, Vicksburg, MS.

Mase 1989
Mase, H. 1989. "Random Wave Runup Height on Gentle Slopes," *Journal of the Waterway, Port, Coastal, and Ocean Engineering Division*, American Society of Civil Engineers, Vol. 115, No. 5, pp 649-661.

Mase and Iwagaki 1984
Mase, H., and Iwagaki, Y. 1984. "Runup of Random Waves on Gentle Slope," *Proceedings of the 19th International Conference on Coastal Engineering*, Houston, TX, American Society of Civil Engineers, pp 593-609.

Mei and Liu 1977
Mei, C. C., and Liu, P. L.-F. 1977. "Effects of Topography on the Circulation in and Near the Surf Zone - Linear Theory," *Journal of Estuary and Coastal Marine Science*, Vol 5, pp 25-37.

Meyers, Holm, and McAllister 1969
Meyers, J. J., Holm, C. H., and McAllister, R. F. 1969. *Handbook of Ocean and Underwater Engineering*, McGraw-Hill Book Company, New York, pp 11.98-11.99.

Miller and Barcilon 1978
Miller, C., and Barcilon, A. 1978. "Hydrodynamic Instability in the Surf Zone as a Mechanism for the Formation of Horizontal Gyres," *Journal of Geophysical Research*, Vol 83, pp 4107-4116.

Moore 1982
Moore, B. D. 1982. "Beach Profile Evolution in Response to Changes in Water Level and Wave Height," unpub. M.S. Thesis, Department of Civil Engineering, University of Delaware, Newark, DE.

Moore and Cole 1960
Moore, G. W., and Cole, J. Y. 1960. "Coastal Processes in the Vicinity of Cape Thompson, Alaska," in *Geologic Investigations in Support of Project Chariot*

in the Vicinity of Cape Thompson, Northwestern Alaska - Preliminary Report, Kachadoorian et al. (editors), US Geological Survey Trace Elements Investigation Report 753, pp 41-55.

Noda 1974
Noda, E. K. 1974. "Wave-Induced Nearshore Circulation," *Journal of Geophysical Research*, Vol 79, pp 4097-4106.

Nolte 1973
Nolte, K. G. 1973. "Statistical Methods of Determining Extreme Sea States," *Proceedings of the 2nd International Conference on Port and Ocean Engineering under Arctic Conditions*, pp 705-742.

Peregrine and Svendsen 1978
Peregrine, D. H., and Svendsen, I. A. 1978. "Spilling Breakers, Bores, and Hydraulic Jumps," *Proceedings of the 16th International Conference on Coastal Engineering*, American Society of Civil Engineers, Vol 1, pp 540-550.

Perlin and Dean 1983
Perlin, M., and Dean, R. G. 1983. "A Numerical Model to Simulate Sediment Transport in the Vicinity of Coastal Structures," Miscellaneous Report No. 83-10, Coastal Engineering Research Center, US Army Corps of Engineers, Fort Belvoir, VA,

Petersen 1980
Petersen, M. S. 1980. "Recommendations for Use of SI Units in Hydraulics," *Journal of the Hydraulic Division*, American Society of Civil Engineers, Vol 106, pp 1981-1993.

Poole et al. 1977
Poole et al. 1977. "Minimal Resource Computer Program for Automatic Generation of Ocean Wave Ray or Crest Diagrams in Shoaling Waters," NASA Technical Memo 74076, National Aeronautics and Space Administration Langley Research Center, Hampton, VA.

Putman, Mink, and Traylor 1949
Putman, J. A., Mink, W. H., and Traylor, M. A. 1949. "The Prediction of Longshore Currents," Transactions of the American Geophysical Union, Vol 30, pp 337-345.

Resio and Tracy 1983
Resio, D. T., and Tracy, B. A. 1983. "A Numerical Model for Wind-Wave Predictions in Deep Water," WIS

Report 12, US Army Engineer Waterways Experiment Station, Vicksburg, MS.

Resio and Vincent 1977
Resio, D. T., and Vincent, C. L. 1977. "Estimation of Winds Over the Great Lakes," *Journal of the Waterway, Port, Coastal and Ocean Engineering Division*, American Society of Civil Engineers, Vol 103, pp 265-283.

Rosati and Kraus 1989
Rosati, J. D., and Kraus, N. C. 1989. "Development of a Portable Sand Trap for Use in the Nearshore," CERC Technical Report 89-11, US Army Engineer Waterways Experiment Station, Vicksburg, MS.

Sasaki 1975
Sasaki, T. 1975. "Simulation on Shoreline and Nearshore Current," *Proceedings of Civil Engineering in the Oceans, III*, American Society of Civil Engineers, pp 179-196.

Scheffner and Rosati 1987
Scheffner, N. W., and Rosati, J. D. 1987. "A Users Guide to the N-Line Model: A Numerical Model to Simulate Sediment Transport in the Vicinity of Coastal Structures," Instruction Report CERC-87-4, US Army Engineer Waterways Experiment Station, Vicksburg, MS.

Schneider 1981
Schneider, C. 1981. "The Littoral Environment Observation (LEO) Data Collection Program," CETA 81-5, US Army Engineer Waterways Experiment Station, Vicksburg, MS.

Seelig 1977
Seelig, W. N. 1977. "A Simple Computer Model for Evaluating Coastal Inlet Hydraulics," CETA 77-1, US Army Corps of Engineers, Coastal Engineering Research Center, Fort Belvoir, VA.

Seelig 1980
Seelig, W. N. 1980. "Two-Dimensional Tests of Wave Transmission and Reflection Characteristics of Laboratory Breakwaters," TR 80-1, US Army Corps of Engineers, Coastal Engineering Research Center, Fort Belvoir, VA.

Seelig, Harris, and Herchenroder 1977
Seelig, W. N., Harris, D. L., and Herchenroder, B. E. 1977. "A Spatially Integrated Numerical Model of Inlet

Hydraulics," GITI Report 14, US Army Corps of Engineers, Coastal Engineering Research Center, Fort Belvoir, VA.

Seymour and Castel 1985
Seymour, R. J., and Castel, D. 1985. "Episodicity in Longshore Sediment Transport," *Journal of the Waterway, Port, Coastal, and Ocean Engineering Division*, American Society of Civil Engineers, Vol 111, pp 542-551.

Shepard 1950
Shepard, F. P. 1950. "Beach Cycles in Southern California," Technical Memorandum No. 20, Beach Erosion Board, Washington, DC.

Shepard and Inman 1950
Shepard, F. P., and Inman, D. L. 1950. "Nearshore Circulation Related to Bottom Topography and Wave Refraction," *Transactions of the American Geophysical Union*, Vol 31, pp 555-565.

Sherlock and Szuwalski 1987
Sherlock, A. R., and Szuwalski, A. 1987. "A User's Guide to the Littoral Environment Observation Retrieval System," Instruction Report CERC-87-3, US Army Engineer Waterways Experiment Station, Vicksburg, MS.

Shore Protection Manual (SPM) 1973 and 1984
Shore Protection Manual (SPM). 1973 and 1984. Coastal Engineering Research Center, US Army Corps of Engineers, US Govt. Printing Office, Washington, D.C.

Simons, Li, and Associates 1988
Simons, Li, and Associates. 1988. "River Sediment Discharge Report," *Coast of California Storm and Tidal Waves Study*, Newport Beach, CA, prepared for US Army Engineer District, Los Angeles, CA.

Simpson, Kadib, and Kraus 1991
Simpson, D. P., Kadib, A. L., Kraus, N. C. 1991. "Sediment Budget at Oceanside, California, Calculated Using a Calibrated Shoreline Change Model," *Proceedings of Coastal Sediments '91 Conference*, American Society of Civil Engineers, in press.

Sonu 1972
Sonu, C. J. 1972. "Field Observation of Nearshore Circulation and Meandering Currents," *Journal of Geophysical Research*, Vol 77, pp 3232-3247.

Sternberg, Shi, and Downing 1984
Sternberg, R. W., Shi, N. C., and Downing, J. P. 1984. "Field Investigation of Suspended Sediment Transport in the Nearshore Zone," *Proceedings of the 19th International Conference on Coastal Engineering*, American Society of Civil Engineers, pp 1782-1798.

Tanimoto, Yagyu, and Goda 1982
Tanimoto, K., Yagyu, T., and Goda, Y. 1982. "Irregular Wave Tests for Composite Breakwater Foundations," *Proceedings of the 18th International Conference on Coastal Engineering*, American Society of Civil Engineers, pp 2144-2161.

Tekmarine, Inc. 1987
Tekmarine, Inc. 1987. "Oceanside Littoral Cell, Preliminary Sediment Budget Report," Coast of California Storm and Tidal Waves Study, Report No. CCSTWS 87-4, Sierra Madre, CA. Prepared for US Army Engineer District, Los Angeles, CA.

Thompson and Vincent 1985
Thompson, E. F., and Vincent, C. L. 1985. "Significant Wave Height for Shallow Water Wave Design," *Journal of the Waterway, Port, Coastal and Ocean Engineering Division*, American Society of Civil Engineers, Vol 111, pp 828-842.

Thornton 1970
Thornton, E. B. 1970. "Variations of Longshore Current Across the Surf Zone," *Proceedings of the 12th International Conference on Coastal Engineering*, American Society of Civil Engineers, pp 291-308.

Thornton 1972
Thornton, E. B. 1972. "Distribution of Sediment Transport Across the Surf Zone," *Proceedings of the 13th International Conference on Coastal Engineering*, American Society of Civil Engineers, pp 1049-1068.

Thornton and Guza 1983
Thornton, E. B., and Guza, R. T. 1983. "Transformation of Wave Height Distribution," *Journal of Geophysical Research*, Vol 88, pp 5925-5938.

Thornton and Morris 1977
Thornton, E. B., and Morris, W. D. 1977. "Suspended Sediments Measured Within the Surf Zone," *Proceedings of Coastal Sediments '77*, American Society of Civil Engineers, pp 655-668.

Trask 1952
Trask, P. D. 1952. "Source of Beach Sand at Santa Barbara, California, as Indicated by Mineral Grain Studies," US Army Corps of Engineers, Beach Erosion Board, Tech. Memo. No. 28.

Trask 1955
Trask, P. D. 1955. "Movement of Sand Around Southern California Promontories," US Army Corps of Engineers, Beach Erosion Board, Tech. Memo. No. 76.

US Army Material Development and Readiness Command (DARCOM) 1976
US Army Material Development and Readiness Command (DARCOM). 1976. *Engineering Design Handbook, Metric Conversion Guide*, DARCOM P 706-470, Washington, D.C.

US Department of Commerce 1990
US Department of Commerce. 1990. "Climactic Summaries for NDBC Buoys and Stations, Update 1," National Oceanic and Atmospheric Administration, NSTL, MS.

Watts 1953a
Watts, G. M. 1953a. "A Study of Sand Movement at South Lake Worth Inlet, Florida," US Army Corps of Engineers, Beach Erosion Board, Tech. Memo. No. 42.

Watts 1953b
Watts, G. M. 1953b. "Development and Field Test of a Sampler for Suspended Sediment in Wave Action," US Army Corps of Engineers, Beach Erosion Board, Tech. Memo. No. 34.

Weggel 1976
Weggel, J. R. 1976. "Wave Overtopping Equation," *Proceedings of the 15th Conference on Coastal Engineering*, American Society of Civil Engineers, pp 2737-2755.

Weggel and Clark 1983
Weggel, J. R., and Clark, E. R. 1983. "Sediment Budget Calculations, Oceanside, California," Miscellaneous Paper CERC-83-7, US Army Engineer Waterways Experiment Station, Vicksburg, MS.

Wiegel 1964
Wiegel, R. L. 1964. *Oceanographic Engineering*, Prentice-Hall, Englewood Cliffs, N.J.

Wright et al. 1984
Wright, L. D., May, S. K., Short, A. D., and Green, M. O. 1984. "Beach and Surf Zone Equilibria and Response Times," *Proceedings 19th Coastal Engineering 1 Conference*, American Society of Civil Engineers, pp 2150-2164.

Wright and Short 1983
Wright, L. D., and Short, A. D. 1983. "Morphodynamics of Beaches and Surf Zones in Australia," in *Handbook of Coastal Processes and Erosion*, P. D. Komar (editor), CRC Press, Boca Raton, pp 35-64.

Zenkovitch 1960
Zenkovitch, V. P. 1960. "Fluorescent Substances as Tracers for Studying the Movement of Sand on the Sea Bed, Experiments Conducted in the U.S.S.R.," *Dock and Harbor Authority*, Vol 40, pp 280-283.

A-2. Related Publications

Brebbia and Walker 1979
Brebbia, C. A., and Walker, W. 1979. *Dynamic Analysis of Offshore Structures*, Newnes-Butterworths, London.

Bruun 1985
Bruun, P. 1985. *Design and Construction of Mounds for Breakwaters and Coastal Protection*, Elsevier, Amsterdam.

Chakrabarti 1987
Chakrabarti, S. K. 1987. *Hydrodynamics of Offshore Structures*, Springer-Verlag Berlin, Heidelberg.

Gerwick 1986
Gerwick, B. C., Jr. 1986. *Construction of Offshore Structures*, John Wiley and Sons, New York.

Goda 1985
Goda, Y. 1985. *Random Seas and Design of Maritime Structures*, University of Tokyo Press, Tokyo.

Horikawa 1978
Horikawa, K. 1978. *Coastal Engineering*, John Wiley & Sons, New York.

Ippen 1966
Ippen, A. T. 1966. *Estuary and Coastline Hydrodynamics*, McGraw Hill Book Company, Inc., New York.

Kinsman 1965
Kinsman, B. 1965. *Wind Waves*, Prentiss Hall Inc., Englewood Cliffs.

Komar 1976
Komar, P. D. 1976. *Beach Processes and Sedimentation*, Prentiss Hall, Inc., Englewood Cliffs, NJ.

LeMehaute 1976
LeMehaute, B. 1976. *An Introduction to Hydrodynamics and Waterways*, Springer-Verlag, New York.

Mei 1983
Mei, C. C. 1983. *The Applied Dynamics of Ocean Surface Waves*, John Wiley and Sons, New York.

McCormic 1973
McCormic, M. E. 1973. *Ocean Engineering Wave Mechanics*, John Wiley and Sons, New York.

Muir Wood and Fleming 1981
Muir Wood, A. M., and Fleming, C. A. 1981. *Coastal Hydraulics*, Second Edition, John Wiley and Sons, New York.

peel Brahtz 1972
peel Brahtz, J. F. 1972. *Coastal Zone Managment: Multiple Use With Conservation*, John Wiley and Sons, Inc., New York.

Pilkey et al. 1983
Pilkey, O. H. Senior, Pilkey, W. D., Pilkey, O. H., Junior, and Neil, W.J. 1983. *Coastal Design - a Guide for Builders, Planners and Homeowners*, van Nostrand Reinhold Company, New York.

Sarpakya and Isaacson 1981
Sarpakya, T., and Isaacson, M. 1981. *Mechanics of Wave Forces on Offshore Structures*, van Nostrand Reinhold Company, New York.

Silvester 1974
Silvester, R. 1974. *Coastal Engineering, I, II*, Elsevier Scientific Publishing Company, Amsterdam.

Sleath 1984
Sleath, J. F. A. 1984. *Seabed Mechanics*, John Wiley & Sons, New York.

Sorensen 1978
Sorensen, Robert M. 1978. *Basic Coastal Engineering*, John Wiley & Sons, New York.

Wiegel 1964
Wiegel, R. L. 1964. *Oceanographical Engineering*, Prentiss Hall International Company Inc.

Appendix B
Notation

SYMBOL	DEFINITION	UNITS
A	Constant in longshore current profile	--
a	Numerical constant in JONSWAP spectrum	--
a	Slope of line for extreme value fitting	1/m
a	Constant in longshore current	--
a_c	Amplitude of the crest	m
a_n	Amplitude of wave n	m
a_t	Amplitude of the trough	m
B_1	Constant in longshore current profile	--
B_2	Constant in longshore current profile	--
b	Intercept for extreme value fitting	--
C	Wave celerity	m/sec
C_g	Group velocity	m/sec
C_{gb}	Group velocity at breaker line	m/sec
C_{go}	Deep water group velocity	m/sec
c	Critical slope coefficient	--
D	Duration of wave record	sec
D	Wave travel distance	km
D	Sediment grain size	mm
D_B	Elevation of berm	m
D_C	Closure depth	m
D_{50}	Median grain size	mm
d	Water depth	m
d_b	Breaker depth	m
E	Wave energy density	N/m
E_b	Wave energy density at breakerline	N/m
F	Fetch length	km
F_{min}	Minimum fetch length	km
f	Wave frequency	hz
f_f	Frictional drag coefficient	--
f_n	Frequency of wave n	hz
f_p	Peak frequency	hz
f_w	Drag coefficient for oscillatory wave motions	--
G	Spreading function	--
G_o	Beach face stability parameter	--
g	Gravitational acceleration	m/sec^2
H	Wave height	m
$\bar{H}$	Average wave height	m
H_b	Breaking wave height	m
H_{br}	Root mean square breaking wave height	m
H_{bs}	Significant breaking wave height	m
H_{max}	Maximum wave height	m
H_{m0}	Energy based significant wave height	m
H_{rms}	Root mean square wave height	m
H_s	Significant wave height	m
H_0	Deep water wave height	m
H_0'	Unrefracted deep water wave height	m
H_1	Mean wave height	m
$H_{1/3}$	Average highest of highest 1/3 waves	m
$H_{1/10}$	Average highest of highest 1/10 waves	m
$H_{1/100}$	Average highest of highest 1/00 waves	m
h	Dummy variable of integration	m
I_1	Immersed weight longshore transport rate	N/sec

SYMBOL	DEFINITION	UNITS
i	Immersed weight transport rate per unit cross-shore distance	N/m-sec
K	Longshore sediment transport coefficient	--
K'	Longshore sediment transport coefficient	--
K_D	Diffraction coefficient	--
K_F	Dissipation coefficient	--
K_R	Refraction coefficient	--
K_S	Shoaling coefficient	--
k	Wave number ($2\pi/L$)	1/m
k	Empirical longshore current coefficient	--
k_1	Longshore current coefficient	--
L	Prescribed time period for the encounter probability	yr
L	Wavelength	m
L_f	Length of fill	m
L_g	Length of groin	m
L_p	Length of peak period wave	m
L_0	Deep water wavelength	m
m	Rank of a wave height	
m	Beach slope	--
N	Mixing strength coefficient	--
N	Number of waves	--
n	Sediment porosity	--
P	Cumulative probability distribution function	--
P	Lateral mixing strength parameter	--
P_e	Encounter probability	--
P_1	Longshore component of wave energy flux	N/sec
p	Pressure	N/m^2
p_g	Pressure gradient across fetch	°Lat
p_1	Constant in longshore current profile	--
Q_G	Gross volumetric longshore transport rate	m^3/yr
Q_L	Left (facing the shoreline) volumetric longshore transport rate	m^3/yr
Q_1	Volumetric longshore transport rate	m^3/yr
Q_N	Net volumetric longshore transport rate	m^3/yr
Q_p	Spectral peakedness parameter	--
Q_o	Volumetric longshore transport for $\alpha_b = 45°$	m^3/sec
Q_R	Right (facing the shoreline) volumetric longshore transport rate	m^3/yr
q	Sediment sources and sinks	m^3/m-sec
R	Wave runup	m
R_G	Elevation correction for geostrophic wind speed	--
R_T	Temperature correction	--
r	Global shoreline coordinate	m
r	Time interval associated with each data point	yr
S_η	Wave energy density spectrum	m^2-sec
s	Global shoreline coordinate	m
s	Spreading function parameter	--
s	Isobar spacing on synoptic chart	mb

SYMBOL	DEFINITION	UNITS
T	Wave period	sec
T_a	Air temperature	°C
T_D	Decayed wave period	sec
T_F	Wave period at fetch	sec
T_p	Peak spectral period	sec
T_r	Return period	yr
T_s	Significant wave period	sec
T_s	Sea water temperature	°C
t	Time	sec
t	Storm duration	hr
U	Wind speed	m/sec
U_A	Wind stress factor	m/sec
U_g	Geostrophic wind speed	m/sec
u	Horizontal water particle velocity	m/sec
u_m	Maximum horizontal particle velocity	m/sec
V	Dimensionless longshore current velocity $(=v/v_o)$	--
v	Longshore current velocity	m/sec
V_ℓ	Midsurf longshore current velocity	m/sec
v_o	No-mixing longshore current velocity at the breakerline	m/sec
w	Vertical water particle velocity	m/sec
w	Fetch width	°Lat
w_s	Sediment settling velocity	m/sec
X	Dimensionless offshore distance $(= x/x_b)$	--
x	Abscissa scale for extreme value fitting	m
x	Offshore distance measured from the shoreline	m
x_b	Offshore distance to breaker line	m
y	Ordinate scale for extreme value fitting	--
y	Alongshore coordinate	m
z	Vertical coordinate	m
α	JONSWAP spectrum coefficient	--
α	Cumulative probability parameter	--
α_b	Angle between the breaking wave crest and the shoreline	rad
α_0	Angle between deep water wave angle	rad
α_p	Angle of refracted waves	rad

SYMBOL	DEFINITION	UNITS
α_{bg}	Breaker wave angle relative to global coordinate system	rad
α_{sg}	Shoreline angle relative to global coordinate system	rad
Γ	Gamma function	--
γ	Peak enhancement factor in JONSWAP spectrum	--
γ	Euler's constant (0.5722)	--
γ	Statistical distribution parameter	--
Δp	Pressure change across fetch	mb
ΔQ_1	Change in volumetric longshore transport rate	m³/sec
Δt	Time step	sec
Δx	Cross shore displacement of profile	m
Δy	Reach length	m
ε	Cumulative probability parameter	m
ζ	Constant in longshore current profile	--
η	Displacement of free surface relative to the still water level	m
Θ	Wave phase function	rad
Θ	Angle in directional spectrum	rad
$<$	Predominate angle of directional spectrum	rad
θ	Cumulative probability parameter	m
κ	Breaker index (H_b/d_b)	--
ξ	Surf similarity parameter	--
π	Constant 3.14159	--
ρ	Density of water	kg/m³
ρ_a	Density of air	kg/m³
ρ_{fw}	Density of fresh water	kg/m³
ρ_s	Density of sediment	kg/m³
σ	Numerical constant in JONSWAP spectrum	--
σ	Statistical distribution parameter	m
Φ	Depth function in TMA spectrum	--
Φ_n	Phase of wave n	rad
ϕ	Phi scale for grain size	--
ω	Circular wave frequency	rad/sec
ω_d	Coefficient in TMA spectrum	--

Appendix C
Glossary

ACCRETION. Natural or artificial buildup of land by the deposition of geologic material.

ALONGSHORE. In the shore parallel direction.

BACKRUSH. The seaward return of water following the uprush of waves.

BACKSHORE. The zone of the shore lying between the foreshore and coastline comprising the berm or berms acted upon by waves only during severe storms.

BACKWASH. Water or waves thrown back by an obstruction such as a ship, breakwater, or cliff.

BAR. A submerged or emerged embankment of sand, gravel, or other unconsolidated material built on the seafloor by waves and currents.

BATHYMETRY. The measurement of water depth in oceans, seas, and lakes.

BAYMOUTH BAR. A bar extending partially or entirely across the mouth of the bay.

BEACH. A zone of unconsolidated material that extends landward from the low water line to the place where there is a marked change in the material or physiographic form or to the line of permanent vegetation.

BEACH FACE. The section of the beach normally exposed to the action of the wave uprush.

BEACH FILL. Material placed on a beach to renourish eroding shores.

BEACH PROFILE. The intersection of the ground surface with a vertical plane.

BEACH RIDGE. A nearly continuous mound of beach material that has been shaved by wave or other action.

BEACH WIDTH. The horizontal dimension of the beach measured normal to the shoreline.

BED FORMS. Any deviation from a flat bed that is readily detectable by eye and higher than the largest sediment size present in the parent bed material.

BED LOAD. That fraction of the total sediment transport load that moves by rolling, sliding, or bouncing on the bed.

BENCH. A level or gently sloping erosion plane inclined seaward on a beach or structure.

BENCHMARK. A permanently fixed point of known elevation.

BERM. A nearly horizontal part of the beach or backshore formed by the deposit of materials by wave action. Some beaches have no berms, others have one or more.

BERM CREST. The seaward limit of a berm.

BREAKER. A wave which is breaking. Breakers are commonly classified into four types.

SPILLING - Bubbles and turbulent water spill down the face of the wave. The upper 25% of the front face may become vertical before breaking. Breaking generally occurs over a distance.

PLUNGING - Crest curls over air pocket; breaking is usually with a crash. Smooth splash often follows.

COLLAPSING - Breaking occurs over lower half of wave with minimal air pocket and usually no splash-up. Bubbles and foam present.

SURGING - Wave peaks up, but bottom rushes forward from under wave and wave slides up on beach face with little or no bubble formation. Water surface remains almost plane except where ripples may be produced on the beach face during runback.

BREAKER DEPTH. The water depth at the point where the wave breaks. Also called breaking depth.

BREAKWATER. A structure protecting a shore area, harbor, anchorage, or basin from waves.

BYPASSING. Hydraulic or mechanical movement of sand from the accreting updrift side to the eroding downdrift side of an inlet or harbor entrance. The hydraulic movement may be natural or mechanical.

CANYON. A relatively narrow, deep depression with steep slopes, the bottom which grades continuously downward. May be underwater (submarine) or on land (subaerial).

CELERITY. Wave speed.

CONTINENTAL SHELF. The zone bordering a continent and extending from the low water line to the depth (usually about 180 m) where there is a marked or rather steep descent toward a greater depth.

CONTOUR. A line on a map or chart representing points of equal elevation with respect to a datum.

CURRENT

COASTAL. One of the offshore currents flowing generally parallel to the shoreline in deeper water beyond the surf zone. These are usually related to tides, winds, the earth's rotation, or density variations.

DRIFT. A broad shallow slow-moving ocean or lake current.

EBB. The tidal current which occurs on falling tide.

FEEDER. Any of the parts of the nearshore current system that flow parallel to the shore before converging to form the neck of a rip current.

FLOOD. The tidal current during the rising tide.

LITTORAL. Any current in the littoral zone caused primarily by wave action.

LONGSHORE. The current flowing essentially parallel to the shoreline, usually generated by waves breaking at an angle to the shoreline.

RIP. A strong current flowing seaward from the shore. It usually appears as a visible band of turbid water.

CUSP. A low mound of beach material often in series separated by crescent-shaped troughs spaced more or less at regular intervals along the beach face.

CUSPATE BAR. A crescentic shaped bar uniting with a shore at each end.

CUPSATE SPIT. A spit that forms in the lee of a shoal or offshore feature (breakwater, island, rock outcrop) by waves that are refracted and/or diffracted around the offshore feature. It may eventually grow into a tombolo linking the feature to the mainland.

DECAY DISTANCE. The distance that waves travel after leaving the generating area.

DEEP WATER. Water so deep that surface waves are unaffected by the presence of the bottom. Generally water depths deeper than one half the surface wavelength are considered deep water.

DEFLATION. The removal of loose material by wind action.

DELTA. An alluvial deposit, roughly triangular or digitate in shape formed at a river mouth.

DEPTH. The vertical distance from a specified datum to the sea or lake floor.

DIFFRACTION. The phenomena by which wave energy is transmitted laterally along the wave crest.

DOWNDRIFT. The predominant direction of littoral materials alongshore.

DRIFT. (1) A short form for littoral drift. (2) The speed at which the current runs. (3) Floating material deposited on a beach. (4) A deposit of a continental ice sheet.

DUNES. Hills or mounds of windblown material, usually sand.

DURATION. The length of time that the wind blows in nearly the same direction with nearly the same intensity over the fetch.

DURATION, MINIMUM. The smallest time necessary for steady state wave conditions to develop for a given wind speed and fetch length.

EDGE WAVE. A low frequency gravity wave traveling parallel to the shore line trapped by refraction. The amplitude decreases with offshore distance across the shore and the waves may be standing or progressive.

EMBAYMENT. An indentation in the shoreline forming an open bay.

EOLIAN. Sediments which have been transported by winds.

EROSION. The removal of sediment by the action of natural forces.

C-2

ESCARPMENT. A line of cliffs or steep slopes facing in one general direction which are caused by erosion or faulting.

ESTUARY. The part of a river which is affected by tides, or the region near a river mouth in which the fresh water of the river mixes with the salt water of the sea.

FATHOM. A unit of measure used in soundings equal to 1.83 m or 6 ft.

FATHOMETER. The copyrighted trademark for an echo sounder.

FETCH. The area in which seas are generated by the wind having a fairly constant direction and speed. Sometimes used synonymously with fetch length.

FOAM LINE. The front of the wave as it advances shoreward, after it is broken.

FOREDUNE. The front dune immediately behind the backshore.

FORERUNNER. A low, long ocean swell which commonly precedes the main swell from a distant storm.

FORESHORE. The area that is ordinarily traversed by the uprush and the backwash of the waves as the tides rise and fall.

GRAVITY WAVE. A water wave whose velocity of propagation is controlled primarily by gravity.

GROIN. A shore protection structure usually built perpendicular to the shoreline to trap littoral drift or retard erosion of the shore.

GROIN SYSTEM. A series of groins acting together to protect a section of beach. Commonly called a groin field.

GROUP VELOCITY. The velocity of a wave group; the speed at which energy propagates.

HINDCASTING. The use of historic synoptic wind charts to calculate characteristics of waves that probably occurred at some past time.

JETTY. Structure extending into a body of water which is designed to prevent shoaling of a channel by littoral materials and to direct and confine the stream or tidal flow.

KNOT. The unit of speed used in navigation equal to one nautical mile per hour (one nautical mile equals 6,076 ft or 1,852 m).

LEE. Sheltered or turned away from the wind or waves.

LEEWARD. The direction toward which the wind is blowing; the direction toward which the waves are traveling.

LITTORAL. Of or pertaining to a shore, especially the sea.

DEPOSITS. Deposits of littoral drifts.

DRIFT. The sedimentary material moved in the littoral zone under the influence of waves and currents.

TRANSPORT. The movement of littoral drift in the littoral zone by waves and currents. Includes movement parallel (longshore transport) and perpendicular (onshore-offshore transport).

TRANSPORT RATE. Rate of transport of sedimentary material parallel or perpendicular to the shore in the littoral zone.

ZONE. In beach terminology, an indefinite zone extending seaward from the shoreline to just beyond the breaker zone.

LOAD. The quantity of sediment transported by a current, including both the suspended load and bed load.

LONGSHORE. Parallel to the shoreline.

LONGSHORE CURRENT. See current, longshore.

LONGSHORE TRANSPORT RATE. The rate of transport of sedimentary material parallel to the shoreline.

MEDIAN DIAMETER. The diameter which marks the division of a grain-size sample into two equal parts by weight.

MONOCHROMATIC WAVES. A series of waves in which each wave has the same characteristics (height and period).

NAUTICAL MILE. The length of a minute of arc on the equator of the earth. (1 mi = 1,852 m = 6,076 ft)

NEARSHORE. The indefinite zone extending seaward from the shoreline well beyond the breaker zone.

NOURISHMENT. The process of replenishing a beach. It may be brought about by natural longshore transport or artificially by the deposition of materials.

OFFSHORE. The zone extending from the breaker line to the seaward edge of the continental shelf.

PERCHED BEACH. A beach or buildup of sediment retained above an otherwise normal profile level by a submerged dike.

PROGRESSIVE WAVE. An oscillatory wave in which the wave form propagates at the wave celerity.

PROTOTYPE. In laboratory usage, the full-scale structure concept or phenomenon used as a basis for constructing a scale model or copy.

REFLECTED WAVE. That part of an incident wave which is returned seaward when the wave impinges on a steep beach, barrier, or the reflecting surface.

REFRACTION. A wave transformation in which the direction and height are modified due to the change in wave phase speed as the water depth changes.

REVETMENT. A facing of stone or concrete built to protect a scarp, embankment, or shore structure against erosion by wave action or currents.

RIPRAP. A protective barrier or facing of randomly placed quarrystone to prevent erosion and scour of an embankment or bluff.

RUBBLE-MOUND STRUCTURE. A mound of randomly placed stones or concrete armor units placed to provide stability against waves.

RUNUP. A rush of water up the face of a structure or beach.

SCOUR. Removal of underwater material by waves or currents.

SEA STATE. Description of the sea surface with regard to the intensity of wave action.

SEAWALL. A structure separating land and water areas, primarily designed to prevent erosion and other damage due to wave action.

SIGNIFICANT WAVE HEIGHT. The average height of the highest one-third waves in a wave group.

SIGNIFICANT WAVE PERIOD. Generally taken as the period of the one-third highest waves in a wave group.

SPIT. A small point of land or a narrow shoal projecting into a body of water from the shore.

STILL-WATER LEVEL (SWL). The elevation of the free surface if all wave action were absent.

STORM SURGE. A rise above the normal water level on the open coast due to the wind stress and low barometric pressure.

SURF. The wave activity in the area between the shoreline and the outermost limit of the breakers.

SURF ZONE. The area between the outermost breaker and the limit of wave uprush.

SUSPENDED LOAD. The portion of the total sediment load which is moving primarily in suspension in the fluid.

SWASH. The rush of water onto the beach face following the breaking of the wave.

SWELL. Wind-generated waves that have traveled out of their generating area and characteristically exhibit a more regular and longer period.

SYNOPTIC CHART. A chart showing a distribution of meteorological conditions over a given area at a given time. Popularly called a weather map.

TIDE

DIURNAL. A tide with one high water and one low water in a tidal day.

EBB. The period of tide between high water and the succeeding low water, a falling tide.

HIGHER HIGH WATER (HHW). The higher of the two high waters of any tidal day.

HIGHER LOW WATER (HLW). The higher of two low waters of any tidal day.

HIGH-WATER LINE (HWL). The intersection of the plane of mean high water with the shore. The shoreline delineated on nautical charts from NOAA is an approximation of the high-water line.

LOW TIDE. The minimum elevation reached by each falling tide.

LOW-WATER LINE. The intersection of the low tide datum plane with the shore.

LOWER HIGH WATER (LHW). The lower of the two high waters of any tidal day.

LOWER LOW WATER (LLW). The lower of the two low waters of any tidal day.

MEAN HIGH WATER (MHW). The average height of the high waters over a 19-year period.

MEAN HIGHER HIGH WATER (MHHW). The average height of the higher high waters over a 19-year period. For shorter periods of observation, corrections are applied to eliminate known variations and reduce the results of the equivalent of a 19-year value.

MEAN LOW WATER (MLW). The average height of the low waters over a 19-year period.

MEAN LOWER LOW WATER (MLLW). The average height of the lower low waters over a 19-year period.

MEAN SEA LEVEL. The average height of the surface of the sea for all stages of the tide over a 19-year period. Usually determined from hourly heights readings. Not necessarily equal to the equal tide level.

MIXED TIDES. A type of tide in which the presence of a diurnal tide is conspicuous by a large inequality in either the high or low water heights with two high waters and two low waters usually occurring each day.

NEAP TIDE. A tide occurring near the time of quaditure of the moon with the sun.

TIDAL PERIOD. The interval of time between two consecutive like phases of the tide.

TIDAL RANGE. The difference in height between consecutive high and low tides.

TIDAL INLET. A natural inlet maintained by tidal flow.

TOMBOLO. A bar or spit that connects or ties an island or offshore structure to the mainland or an other island.

TROUGH. The lowest part of the waveform between successive crests.

UPDRIFT. The direction opposite to that of the predominant movement of littoral materials.

UPRUSH. The rush of water up onto the beachface following the breaking of a wave.

WAVE DECAY. The reduction of wave height and the increase in wave period after they leave the generating area and pass through a calm or region of lighter winds.

WAVELENGTH. The horizontal distance between similar points on two successive waves.

WAVE SETUP. Superelevation of the water surface over normal surge elevation due to the onshore gradient of wave momentum.

Appendix D
Conversions

In 1975, the Deputy Secretary of Defense established policies which encouraged a gradual changeover to the use of the metric system of measurement. At present, this impacts the Corps of Engineers primarily in the preparation of technical reports, feasibility studies, and design aids. The primary reference used in the preparation of this appendix is Engineering Design Handbook - Metric Conversion Guide (DARCOM 1976). A more common reference is Petersen (1980). The metric system being adopted throughout the United States is the "International System of Units," commonly referred to as *SI Units*. This is the most widely used system for scientific and technical data and specifications.

Multiply	By	To Obtain
Length, Area, and Volume		
inches	25.4* 2.54*	millimeters centimeters
feet	30.48* 0.3048*	centimeters meters
yards	0.9144*	meters
fathoms	1.8288*	meters
statute miles (U.S.)	1609.344* 1.609344*	meters kilometers
nautical miles (internat.)	1852.0* 1.852*	meters kilometers
square inches	6.4516*	square centimeters
square feet	919.030 0.092903	square centimeters square meters
square yards	0.836127	square meters
acres	0.404686 4046.86	hectares square meters
square miles (U.S. statute)	2.58999	square kilometers
cubic inches	16.3871	cubic centimeters
cubic feet	0.0283168	cubic meters
cubic yards	0.764555	cubic meters
cubic yards per foot	2.50838	cubic meters per meter
acre-feet	1233.48	cubic meters
Mass and Density		
slugs	14.5939029*	kilograms
slugs per cubic foot	515.379	kilograms per cubic meter
Force, Stress, and Specific Weight		
pounds	4.44822	newtons
kips (1000 lb)	4.44822	kilonewtons
short tons (2000 lb)	8.89644	kilonewtons
long tons (2240 lb)	9.96401	kilonewtons
pounds per foot	14.5939	newtons per meter
kips per foot	14.5939	kilonewtons per meter
millibar	100.0*	pascals
pounds per square inch	6.89476	kilopascals
pounds per square foot	47.8803	pascals

Multiply	By	To Obtain
Force, Stress, and Specific Weight (Continued)		
short tons per square foot	95.7605	kilopascals
pounds per cubic inch	271.447	kilonewtons per cubic meter
pounds per cubic foot	157.087	newtons per cubic meter
Velocity and Acceleration		
feet per second	0.3048*	meters per second
miles per hour (statute)	0.44704* 1.609344*	meters per second kilometers per hour
knots (international)	0.514444 1.852*	meters per second kilometers per hour
feet per second	0.3048*	meters per second
Volume Discharge		
cubic feet per second	0.028317*	cubic meters per second
cubic yards per year	0.764555	cubic meters per year
Energy and Power		
foot-pounds	1.35582	joules
kilowatt hours	3.60*	megajoules
British thermal units (Btu)	1055.06	joules
horsepower	745.700	watts
Btu per hour	0.293071	watts
foot-pound-force per second	1.35582	watts

* Values are exact conversion values.

Appendix E
Computer Programs

MACE PROGRAMS

MACE (Micro Computer Applications for Coastal Engineering) programs are described in CETN-VI-16 (Jones 1989), and may be obtained from the Engineering Computer Programs Library Section, Technical Information Center, US Army Engineer Waterways Experiment Station, 3909 Halls Ferry Road, Vicksburg, MS, 39180-6199.

BWCOMP calculates breakwater volumes and costs, demonstrating the effect of varying breakwater slopes on wave transmission, the choice of armor size and shape, and overall volume.

BWDAMAGE estimates expected damage and life cycle costs of related maintenence and repairs of a rubblemound breakwater.

BWLOSS1 estimates economic losses due to wave attack as a function of wave height. The program optionally provides an estimate of expected annual economic losses due to wave probability distribution of significant wave heights.

BWLOSS2 fits a long-term cumulative probability distribution to transmitted wave height data and estimates expected annual economic losses due to wave attack after a protective breakwater has been built.

DUNE predicts storm-induced dune erosion given an initial profile shape, storm surge level, sediment size, and a wave height.

FWAVOCUR determines how frequently extreme wave conditions are expected over a specified time period.

HURWAVES estimates the maximum gradient wind speed, the maximum sustained wind speed, the maximum significant wave height, and the maximum significant wave period for slow-moving hurricanes.

TIDEC estimates the tidal current speed at any time based on the predictions of the National Oceanic and Atmospheric (NOAA) tidal current tables.

TIDEHT estimates the elevation of the water surface at any time or the time at increments of elevation based on the predictions of NOAA tide tables.

WAVDIS1 estimates the parameters of the three commonly used extremal probability distributions for prediction of extreme wave conditions.

WAVDIS2 is an alternate version of WAVDIS1 that estimates the parameters by the method of moments.

ACES PROGRAMS

ACES (Automated Coastal Engineering System) is a microcomputer-based design and analysis system in the field of coastal engineering. The contents range from simple algebraic expressions both theoretical and empirical in origin, to numerically intense algorithms spawned by the increasing power and affordability of computers. ACES is described in CETN-VI-20 and by Leenknecht and Szuwalski (1988). Copies of ACES programs may be obtained from US Army Engineer Waterways Experiment Station, ATTN: CEWES-IM-MI-S, 3909 Halls Ferry Road, Vicksburg, MS 39180-6199.

Windspeed Adjustment and Wave Growth
The methodologies represented in this ACES application provide quick and simple estimates for wave growth over open-water and restricted fetches in deep and shallow water. Also, improved methods (over those given in the Shore Protection Manual (SPM) 1984) are included for adjusting the observed winds to those required by wave growth formulas.

Beta-Rayleigh Distribution
This application provides a statistical representation for a shallow water wave height distribution. The Beta-Rayleigh distribution is expressed in familiar wave parameters: the energy-based wave height, peak spectral wave period, and water depth. After constructing the distribution, other statistically based wave height estimates such as the root-mean-square height, mean wave height, and average of the highest one-tenth wave heights can be easily computed.

Extremal Significant Wave Height Analysis
This application provides significant wave height estimates for various return periods. Confidence intervals are also provided. The approach developed by Goda (1988) is used to fit five candidate probability distributions to an input array of extreme significant wave heights.

Constituent Tide Record Generation
This application predicts a tide elevation record at a specific time and locale using known amplitudes and epochs for individual harmonic constituents.

Linear Wave Theory
This application yields first-order approximations for various parameters of wave motion as predicted by the wave theory bearing the same name (also known as small amplitude, sinusoidal, or Airy theory). It provides estimates for common items of interest such as water surface elevation, general wave properties, particle kinematics, and pressure as functions of wave height and period, water depth, and position in the wave form.

Cnoidal Wave Theory
This application yields various parameters of wave motion as predicted by first-order (Isobe 1985) and second-order (Hardy and Kraus 1987) approximations for Cnoidal wave theory. It provides estimates for common items of interest such as water surface elevation, general wave properties, kinematics, and pressure as functions of wave height and period, water depth, and position in the wave form.

Linear Wave Theory with Snell's Law
This application provides a simple estimate for the transformation of monochromatic waves. It considers two common processes of wave transformation: refraction (using Snell's law) and shoaling using wave properties predicted by linear wave theory (Airy 1845). Given wave properties and a crest angle at a known depth, it predicts the values in deep water and at a subject location specified by a new water depth. An important assumption is that all depth contours are assumed to be straight and parallel.

Combined Diffraction and Reflection by a Vertical Wedge
This application estimates wave height modification due to combined diffraction and reflection near jettied harbor entrances, quay walls, and other such structures. Jetties and breakwaters are approximated as a single straight, semi-infinite breakwater by setting the wedge angle equal to 90 degrees. Additionally, such natural diffracting and reflecting obstacles as rocky headlands can be approximated by setting a particular value for the wedge angle.

Irregular Wave Transformation (Goda's method)
This application yields cumulative probability distributions of wave heights as a field of irregular waves propagate from deep water through the surf zone. The application is based on two random-wave theories by Goda (1975, 1984). The application combines the two theories, by shoaling and refracting random waves over a plane bottom with straight and parallel contours. The

theories assume a Rayleigh distribution of wave heights in the nearshore zone and a Bretscheneider-Mitsuyasu incident directional spectrum. The processes modeled include: wave refraction, wave shoaling, wave breaking, wave setup, and surf beat.

Breakwater Design Using Hudson and Related Equations
This application provides estimates for the armor weight, minimum crest width, armor thickness, and the number of armor units per unit area of a breakwater using Hudson and related equations.

Toe Protection Design
This application determines armor stone size and width of a toe protection apron for vertical face structures such as seawalls, bulkheads, quay walls, breakwaters, and groins. Apron width is determined by the geotechnical and hydraulic guidelines specified in EM 1110-2-1614. Stone size is determined by a method (Tanimoto, Yagyu, and Goda 1982) whereby a stability equation is applied to a single rubble unit placed at a position equal to the width of the toe apron and subjected to standing waves.

Nonbreaking Wave Forces at Vertical Walls
This application provides the pressure distribution and resultant force and moment loading on a vertical wall caused by normally incident, nonbreaking, regular waves. The results can be used to design vertical structures in protected or fetch-limited regions when the water depth at the structure is greater than about 1.5 times the maximum expected wave height. The application provides the same results as found using the design curves given in Chapter 7 of the SPM (1984).

Rubble Mound Revetment Design
Quarrystone is the most commoly used material for protecting earth embankments from wave attack because, where high-quality stone is available, it provides a stable and unusually durable revetment armor material at relatively low cost. This ACES application provides estimates for revetment armor and bedding layer stone sizes, thicknesses, and gradation characteristics. Also calculated are two values of runup on the revetment, an expected extreme and a conservative runup value.

Irregular Wave Runup on Beaches
This application provides an approach to calculate runup statistical parameters for wave runup on smooth slope linear beaches. To account for permeable and rough

slope natural beaches, the present approach needs to be modified by multiplying the results for the smooth slope linear beaches by a reduction factor. However, there is no guidance for such a reduction due to the sparsity of good field data on wave runup. The approach used in this ACES application is based on existing laboratory data on irregular wave runup (Mase and Iwagaki 1984, and Mase 1989).

Wave Runup and Overtopping on Impermeable Structures

This application provides estimates of wave runup and overtopping on rough and smooth slope structures which are assumed to be impermeable. Runup heights and overtopping rates are estimated independently or jointly for monochromatic or irregular waves specified at the toe of the structure. The empirical equations suggested by Ahrens and McCartney (1975), Ahrens and Titus (1985), and Ahrens and Burke (1987) are used to predict runup, and Weggel (1976) to predict overtopping. For irregular wave conditions the runup caused by these conditions is assumed to have a Rayleigh distribution (Ahrens 1977). The overtopping rate is estimated by summing the overtopping contributions from the individual runups.

Wave Transmission on Impermeable Structures

This application provides estimates of wave runup and transmission on rough and smooth slope structures. It also addresses wave transmission over impermeable vertical walls and composite structures. In all cases, monochromatic waves are specified at the toe of a structure that is assumed to be impermeable. For sloped structures, a method suggested by Ahrens and Titus (1985) and Ahrens and Burke (1987) is used to predict runup, while the method of Cross and Sollitt (1971) as modified by Seelig (1980) is used to predict overtopping. For vertical wall and composite structures, a method proposed by Goda, Takeda, and Moriya (1967) and Goda (1969) is used to predict wave transmission.

Wave Transmission Through Permeable Structures

This application determines wave transmission coefficients and transmitted wave heights for permeable breakwaters with crest elevations at or above the still-water level. This application can be used with breakwaters armored with stone or artificial armor units. The application uses a method developed for predicting wave transmission by overtopping coefficients using the ratio of breakwater freeboard to wave runup (suggested by Cross and Sollitt 1971). The wave transmission by overtopping prediction method is then combined with

the model of wave reflection and wave transmission through permeable structures of Madsen and White (1976).

Longshore Sediment Transport

This application provides estimates of the potential longshore transport rate under the action of waves. The method used is based on the empirical relationship between the longshore component of wave energy flux entering the surf zone and the immersed weight of sand moved (Galvin 1979). Two methods are available to the user depending on whether available input data are breaker wave height and direction or deep water wave height and direction.

Numerical Simulation of Time-Dependent Beach and Dune Erosion

This application is a numerical beach and dune erosion model that predicts the evolution of an equilibrium beach profile from variations in water level and breaking wave height as occur during a storm. The model is one-dimensional (only onshore-offshore sediment transport is represented). It is based on the theory that an equilibrium profile results from uniform wave energy dissipation per unit volume of water in the surf zone. The general characteristics of the model are based on a model described by Kriebel (1982, 1984a, 1984b, 1986). Because of the complexity of this methodology and the input requirements, familiarization with the references listed is strongly recommended.

Calculation of Composite Grain Size Distributions

The major concern in the design of a sediment sampling plan for beach fill purposes is determining the composite grain size characteristics of both the native beach and the potential borrow site. This application calculates a composite grain size distribution that reflects textural variability of the samples collected at the native beach or the potential borrow area.

Beach Nourishment Overfill Ratio and Volume

This application provides two approaches to the planning and design of beach nourishment projects. The first approach is the calculation of the overfill ratio, which is defined as the volume of actual borrow material required to produce a unit volume of usable fill. The second approach is the calculation of a renourishment factor which is germane to the long-term maintenance of a project, and addresses the basic question of how often renourishment will be required if a particular borrow source is selected that is texturally different from the native beach sand. The methods described can be found in James (1975) and the SPM (1984).

A Spatially Integrated Numerical Model of Inlet Hydraulics
This application is a numerical model which estimates coastal inlet velocities, discharges, and bay levels as functions of time for a given time-dependent sea level fluctuation. Inlet hydraulics are predicted in this model by simultaneously solving the time-dependent momentum equation for flow in the inlet and the continuity equation relating the bay and sea levels to inlet discharge. The model is designed for cases where the bay water level fluctuates uniformly throughout the bay and the volume of water stored in the inlet between high and low water is negligible compared to the prism of water that moves through the inlet. The model has been previously described by Seelig (1977) and Seelig, Harris, and Herchenroder (1977) for use on large computers.

CMS

The Coastal Modeling System (CMS) is a user-friendly, supercomputer-based system of models and supporting software packages described in CETN VI-18 (Mark 1990) and by Cialone et al. 1992. CMS incorporates models that are computationally and memory intensive for transfer to the Corps elements. Software packages for supporting the CMS models include grid generation software, post-processing software to display model results, utility software to supplement data used by the models, and automated Job Control Language (JCL) procedures to execute these functions.

WIFM (Cialone et al. 1992). The US Army Corps of Engineers Waterways Experiment Station (WES) Implicit Flooding Model (WIFM) solves the vertically integrated Navier-Stokes equations in stretched Cartesian coordinates. The model simulates shallow-water, long wave hydrodynamics such as tidal elevations and currents, storm surges, and tsunami propagation. WIFM contains many useful features for studying phenomena such as moving boundaries to simulate flooding/drying of low-lying areas and subgrid flow boundaries to simulate small barrier islands, jetties, dunes, or other structural features. The model may be driven at the outer boundary by tide elevation, flow velocities, uniform flux, or inverted barometer effects. WIFM also accepts wind fields for including the effects of wind stress during hurricanes or other strong storm systems.

SPH (Cialone et al. 1992). The Standard Project Hurricane (SPH) numerical model represents wind and atmospheric pressure fields generated by hurricanes. It is based on the Standard Project Hurricane criteria

developed by the National Oceanic and Atmospheric Administration (NOAA), and the model's primary output are hurricane-generated wind fields which can be used in storm surge modeling. It can be run separately, or invoked from within the model WIFM.

RCPWAVE (Ebersole, Cialone, and Prater 1986). The Regional Coastal Processes Wave (RCPWAVE) propagation model is a two-dimensional, steady state, short wave model for solving wave propagation problems over an arbitrary bathymetry. The governing equations solved in the model are the "mild slope" equation for linear, monochromatic waves, and the equation specifying irrotationality of the wave phase function gradient. These equations account for shoaling, refraction, and bottom-induced diffraction within a study area, and also contain a wave breaking scheme.

CLHYD (Cialone et al. 1992). The Curvilinear Longwave Hydrodynamic (CLHYD) model is a two-dimensional, depth-averaged model for computing tidal circulation and storm surge propagation. It is a finite difference model developed in boundary-fitted (curvilinear) coordinates. The model solves finite difference approximations of the Navier-Stokes (continuity and horizontal momentum) equations for the water surface displacement and the unit flow rate components. CLHYD can simulate flow fields induced by wind fields, river inflows/outflows, and tidal forcing. The model should be used where shallow-water wave theory applies (water depth is sufficiently small when compared with wavelength).

HARBD (Chen and Houston 1986). The Harbor-Deep (HARBD) model is a two-dimensional, steady state, finite element model for studying wave oscillations in and around harbors, and is applicable to harbors having arbitrary depths and geometric configurations. This model is based on linear wave theory, and solves a boundary value problem of harbor resonance and wave scattering which includes the effects of bottom friction. The model may also be applied to weakly nonlinear waves, though great care must be exercised while interpreting results.

SHALWV (Hughes and Jensen 1986, Cialone et al. 1992). The Shallow Wave (SHALWV) model is a two-dimensional, pseudo-discrete, time dependent spectral wave model for simulating wave growth, decay, and transformation. Developed in a rectangular Cartesian coordinate system, the model is based on the solution of the inhomogeneous energy balance equation via finite

difference methods. This equation accounts for several mechanisms, including wind-wave growth, refraction, shoaling, nonlinear wave-wave interaction, high frequency energy dissipation, surf zone breaking and decomposition of energy into wind-sea and swell wave components. Model output includes one-dimensional frequency and two-dimensional frequency directional spectrums.

STWAVE (Cialone et al. 1992). The numerical model STWAVE is a nearcoast, time-independent spectral wave energy propagation model. The model solves the spectral energy balance equation (including refraction, shoaling, and wave breaking) using finite-difference methods. This steady-state model simulates wave prop-agation over a spatial area assuming wave conditions vary sufficiently slowly. The variation of waves at a given point may be neglected relative to the time re-quired for waves to pass across the computational grid if the model is limited to nearcoast applications in which waves move quickly across the grid (within 30 minutes).

SMS

The Shoreline Modeling System (SMS) is a microcom-puter-based software package that contains a collection of generalized computer programs assembled to enable the user to perform complete longshore sediment trans-port processes and shoreline evolution assessments (Gravens 1991). The SMS contains two major coastal process numerical models: GENESIS and RCPWAVE (see discussion in CMS section); twelve system-support programs for data preparation, analysis, and numerical model input generation; one general purpose graphics program; and two special purpose editors for generation or modification of model configuration input files. The system-support programs were specifically developed to automate and standardize the typical data preparation and analysis tasks encountered in the course of conduct-ing a shoreline evolution study, beginning with the user's original data source and concluding with input data sets (files) for GENESIS.

GENESIS (Hanson and Kraus 1989; Gravens, Kraus, and Hanson 1991). The Generalized Model of Shoreline Change (GENESIS) model was developed to assess impact of shoreline structures or determine littoral budgets. The model can include an arbitrary number of groins, jetties, detached breakwaters, seawalls, beach fills and river discharges; diffraction at detached breakwaters, jetties and groins; multiple wave trains from independent sources; and sand transport due to

oblique wave incidence and longshore gradient in wave height.

RCPWAVE (see previous discussion under CMS heading).

CORPS OF ENGINEERS NUMERICAL MODELS

Other Corps of Engineers numerical mainframe and personal computer models which may be of use in coastal planning and engineering studies are described below.

NMLONG (Kraus and Larson 1990, Larson and Kraus 1991). The Numerical Model of the Longshore current (NMLONG) calculates the distribution of the longshore current for almost arbitrary wave and beach conditions. Both the wave and wind-induced longshore current and wave height distribution for multiple bar and trough bathymetry and given wave conditions are computed, and a plot is generated to show results.

ON_OFF (Kraus 1991). ON_OFF is a personal com-puter program that determines the likelihood for erosion or accretion given a beach with a given grain size, under certain wave height and period conditions. The program predicts erosion or accretion in terms of "highly probable" and "probable" qualifiers.

SBEACH (Larson and Kraus 1989; Larson, Kraus, and Byrnes 1990). The Storm-Induced model of Beach Change (SBEACH) is an empirically based two-dimensional model that simulates cross-shore sediment transport due to storm events, and post-storm profile recovery. It was developed for sandy beaches with uniform representative grain sizes in the range of 0.20 to 0.42 mm. SBEACH accepts as input varying water level as produced by storm surge and tide, varying wave height and period, and arbitrary grain size in the fine to medium sand range. The model simulates bar formation during storms, and subsequent beach recovery with berm buildup.

WISTRT (Gravens 1989). WISTRT provides calcula-tions of potential longshore sand transport rates using Wave Information Study (WIS) Phase III hindcast wave estimates. Refraction and shoaling of incident linear waves are calculated using Snell's law and conservation of wave energy flux. A shallow-water wave breaking criterion defines wave properties at the break point, and potential longshore sand transport rates are calculated by means of the energy flux method in the SPM (1984).

REF/DIF (Kirby and Dalrymple 1986, Dalrymple et al. 1984). REF/DIF is a combined refraction/diffraction monochromatic wave propagation model based on Booij's (1981) parabolic approximation for Berkoff's (1973) mild slope equation, where reflected waves are neglected. The model is valid for waves propagating within 60 degrees of the input direction, and is based on Stokes perturbation expansion. In order to have a model that is valid in shallow water outside the Stokes range of validity, a dispersion relationship which accounts for the nonlinear effects of amplitude is used. Wave breaking is simulated using Kirby and Dalrymple's (1986) dissipation scheme, and boundaries such as coastlines and islands are modeled using the thin film approximation where the surface piercing feature is replaced by shoals with very shallow depth (less than 0.1 depth units).